



Ministério da Saúde
Instituto Nacional do Câncer
Coordenação de Pós-graduação

INSTITUTO NACIONAL DO CÂNCER
Pós-Graduação em Oncologia

RICARDO CORTEZ CARDOSO PENHA

ANÁLISE DE ALTERAÇÕES EPIGENÉTICAS EM CÉLULAS
DA TIREOIDE APÓS A EXPOSIÇÃO À RADIAÇÃO X

Orientadores: Prof. Dr. Alfredo Fusco
Prof. Dr. Luis Felipe Ribeiro Pinto

Rio de Janeiro

2019



Ministério da Saúde
Instituto Nacional do Câncer
Coordenação de Pós-graduação

INSTITUTO NACIONAL DO CÂNCER
Pós-Graduação em Oncologia

RICARDO CORTEZ CARDOSO PENHA

**ANÁLISE DE ALTERAÇÕES EPIGENÉTICAS EM CÉLULAS
DA TIREOIDE APÓS A EXPOSIÇÃO À RADIAÇÃO X**

Tese de Doutorado apresentada ao Instituto Nacional de Câncer como parte dos requisitos para a obtenção do título de Doutor em Oncologia.

Orientadores: Prof. Dr. Alfredo Fusco
Prof. Dr. Luis Felipe Ribeiro Pinto

Rio de Janeiro

2019

FICHA CATALOGRÁFICA

P399a Penha, Ricardo Cortez Cardoso

Análise de alterações epigenéticas em células da tireóide após a exposição à radiação X / Ricardo Cortez Cardoso Penha. - Rio de Janeiro, 2019.

171 f. : il. color.

Tese (Doutorado em Oncologia) – Instituto Nacional de Câncer José Alencar Gomes da Silva, 2019.

Orientadores: Alfredo Fusco; Luis Felipe Ribeiro Pinto.

1. Neoplasias da Glândula Tireoide. 2. Radiação Ionizante. 3. Epigenômica.
4. MicroRNAs. I. Fusco, Alfredo (Orient.). II. Pinto, Luis Felipe Ribeiro (Orient.). III. Instituto Nacional de Câncer José Alencar Gomes da Silva.
IV. Título.

CDD 616.99444

À minha mãe e irmã amadas,
meu porto seguro.

AGRADECIMENTOS

Primeiramente, agradeço a DEUS por conceder-me o dom da vida e, sobretudo, pela permissão de cumprir a minha missão ao lado de pessoas tão queridas e iluminadas, que contribuem, dia a dia, para o meu progresso moral, espiritual e intelectual. A cada dia que desvendo os mistérios da natureza e aproximo-me da verdade, tenho a certeza de Sua existência.

Aos meus orientadores, Luis Felipe Ribeiro Pinto e Alfredo Fusco por acreditarem no meu potencial, guiando-me na jornada acadêmica por meio de críticas sempre construtivas e conselhos sábios e paternais, fortalecendo as bases do pensamento científico. Vocês, meus “pais científicos”, foram peças chaves para o meu crescimento profissional e pessoal e ensinaram-me que ser cientista é uma profissão nobre e, como tal, deve ser exercida com muita seriedade e dedicação. Que a prática da ciência transforma uma sociedade e oferece a possibilidade de nos libertarmos do medo irracional do desconhecido.

A base familiar é um dos pilares da construção do meu caráter, pautado no respeito ao próximo, união, resiliência e determinação para não esmorecer e continuar a sonhar. Sou profundamente grato à minha família pelo amor incondicional, os conselhos valiosos, os gestos sinceros de carinho e afeto e, claro, pelo apoio financeiro que foi crítico durante a minha formação acadêmica. Em particular, agradeço à minha querida mãe, Maria Andréa, a quem dedico essa tese, a minha mais pura gratidão. Amiga confidente e mãe exemplar, você foi o elemento essencial para a realização desse trabalho. Em especial, sou grato à minha irmã pela amizade verdadeira, que transcende o tempo e os laços dessa vida, pela união de almas, ensinando-me o real significado do amor ao próximo. Também agradeço ao Luis Fernando, meu padrasto e amigo, pelos conselhos, carinho e o apoio irrestrito aos meus sonhos e projetos.

Acredito que o verdadeiro significado de família extrapola os laços de sangue e, por isso, também agradeço o carinho da minha “família napolitana”, cujo amor acalentou o meu coração e o respeito às tradições familiares e à própria terra reafirmou as minhas próprias raízes.

Agradeço aos meus caros amigos pelo companheirismo, o ombro amigo, o respeito mútuo e as boas risadas. A amizade se constrói nos gestos, palavras e sentimentos que deixam pegadas no nosso coração que nem o tempo apaga. Amigos que estão distantes, amigos que estão mais próximos, devo dizer que é um privilégio partilhar da companhia de vocês. Muito obrigado por me acolherem em suas vidas, contribuindo para a construção de um Ricardo melhor. A cada dia, com o apoio de amigos, tenho a certeza que a amizade é uma das maiores riquezas desse mundo.

Enfim, agradeço a todos que contribuíram para a realização desse trabalho. A minha jornada acadêmica foi árdua, repleta de reveses e percalços. Contudo, na dificuldade encontrei a força para vencer os obstáculos, superar os meus limites e expectativas. Muito obrigado pelo apoio dos familiares, amigos e colegas de trabalho. Não acredito no acaso. Acredito na certeza que vivemos com um propósito concedido por DEUS, e seja lá qual for o meu, vocês são peças fundamentais. **MUITO OBRIGADO.**



Ministério da Saúde
Instituto Nacional do Câncer
Coordenação de Pós-graduação

INSTITUTO NACIONAL DO CÂNCER

Pós-Graduação em Oncologia

RICARDO CORTEZ CARDOSO PENHA

ANÁLISE DE ALTERAÇÕES EPIGENÉTICAS EM CÉLULAS DA TIREOIDE APÓS A EXPOSIÇÃO À RADIAÇÃO X

Orientadores: Prof. Dr. Alfredo Fusco
Prof. Dr. Luis Felipe Ribeiro Pinto

Aprovada em ____/____/_____.

BANCA EXAMINADORA

Profª. Doutora Patrícia Cristina Lisboa da Silva
Universidade do Estado do Rio de Janeiro (UERJ)

Prof. Doutor Rodrigo Soares Fortunato
Universidade Federal do Rio de Janeiro (UFRJ)

Profª. Doutora Patrícia Abrão Possik
Instituto Nacional de Câncer José de Alencar Gomes da Silva (INCA)

Prof. Doutor Fernando Luiz Dias
Instituto Nacional de Câncer José de Alencar Gomes da Silva (INCA)

Prof. Doutor Hector Nicolas Seuáñez Abreu – Suplente I
Instituto Nacional de Câncer José de Alencar Gomes da Silva (INCA)

Prof. Doutor Egberto Gaspar de Moura- Suplente II
Universidade do Estado do Rio de Janeiro (UERJ)

Rio de Janeiro

2019

SUMÁRIO

LISTA DE TABELAS	x
LISTA DE FIGURAS	xi
LISTA DE SIGLAS E ABREVIATURAS	xii
RESUMO	xiv
ABSTRACT	xv
1 INTRODUÇÃO	1
1.1 CÂNCER	1
1.2 O CÂNCER DA TIREOIDE	2
1.3 SUBTIPOS HISTOLÓGICOS DO CÂNCER DE TIREOIDE	5
1.3.1 CARCINOMA PAPILÍFERO DA TIREOIDE (CPT).....	5
1.3.2 CARCINOMA FOLICULAR DA TIREOIDE (CFT).....	6
1.3.3 CARCINOMA ANAPLÁSICO DA TIREOIDE (CAT).....	8
1.4 OS MODELOS DE PROGRESSÃO TUMORAL NA TIREOIDE	8
1.5 RADIAÇÃO IONIZANTE E CARCINOMA PAPILÍFERO DA TIREOIDE	12
1.6 EPIGENÉTICA	17
1.6.1 METILAÇÃO DO DNA.....	17
1.6.2 MODIFICAÇÃO DE HISTONAS.....	19
1.6.3 MICRORNA (MIRNA OU MIR).....	19
1.7 MIRNA E TIREOIDE	23
2 JUSTIFICATIVA	26
3 OBJETIVO GERAL	27
3.1 OBJETIVOS ESPECÍFICOS	27
4 RESULTADOS	29
4.1 CAPÍTULO I	30
4.1.1 DADOS SUPLEMENTARES DO ARTIGO 1.....	44

4.2 CAPÍTULO II	47
4.2.1 DADOS NÃO PUBLICADOS DO CAPÍTULO II	64
4.3 CAPÍTULO III	72
4.3.1 DADOS SUPLEMENTARES DO ARTIGO 3	82
4.3.2 DADOS NÃO PUBLICADOS DO CAPÍTULO III	83
4.4 CAPÍTULO IV	85
5 DISCUSSÃO	104
6 CONCLUSÕES	115
7 REFERÊNCIA BIBLIOGRÁFICA	118
8 ANEXOS	149
8.1 ANEXO I- REVISÃO SISTEMÁTICA SOBRE RADIAÇÃO IONIZANTE	149
8.2 ANEXO II- ARTIGO SOBRE OS RNAS LONGOS NÃO CODIFICANTES NO CPT	1536

LISTA DE TABELAS

Tabela 1: Vias de sinalização alvo dos miRNAs alterados pela radiação X na linhagem FRTL-5 CL2.....	67
--	----

LISTA DE FIGURAS

Figura 1: As principais vias de sinalização alteradas no câncer de tireoide.....	9
Figura 2: Modelos de progressão tumoral da tireoide.....	11
Figura 3: Vias de reparo da quebra-dupla do DNA (DSB).....	14
Figura 4: Biogênese dos miRNAs.....	21
Figura 5: Expressão basal dos miR-10b-5p e miR-199a-3p nas linhagens celulares de tireoide e os seus efeitos sobre a maquinaria de reparo por recombinação homóloga (HR).....	69
Figura 6: O miR-10b-5p sensibiliza a linhagem de CAT, 8505c, à RI.....	71
Figura 7: Efeito de <i>DICER1</i> sobre o ciclo celular das células PCCI 3.....	84
Figura 8: Principais achados da tese de doutorado.....	116

LISTA DE SIGLAS E ABREVIATURAS (padronizar)

AMPc – 3', 5'- adenosina monofosfato cíclico
ATM- serina/ treonina quinase mutada na ataxia-telangiectasia (“*Serine/Threonine Ataxia Telangiectasia Mutated Kinase*”)
ATR- Proteína mutada na ataxia telangiectasia e relacionada à Rad3 (“*Ataxia Telangiectasia And Rad3-Related Kinase*”)
AUC- Área sob a curva (“*Area Under The Curve*”)
BRAF-AKAP9- Rearranjo entre o gene BRAF e o que codifica a proteína âncora de quinase A
BRAV600E- Substituição de uma valina por um ácido glutâmico no códon 600 do gene BRAF
CAT- Carcinoma anaplásico da tireoide
cDNA - Ácido desoxirribonucléico complementar
CDT- Carcinomas diferenciados da tireoide
CFT- Carcinoma folicular da tireoide
CMT- Carcinoma medular da tireoide
CpG- 5'—Citosina—fosfato—Guanina—3'
CPT- Carcinoma papilífero da tireoide
CREB - Proteína que se liga ao elemento responsivo a AMPc (“*Cyclic AMP-Responsive element-Binding Protein*”)
CTNNB1- Gene que codifica a proteína beta catenina-1 (“*Catenin Beta 1*”)
DNMT- DNA metiltransferase
dNTP- Desoxirribonucleotídeo trifosfato
DSB- Quebra dupla do DNA (“*Double-strand DNA Breaks*”)
EDTA - Ácido etilenodinitrilotetra acético
EGFR- Receptor do fator de crescimento epidermal
FRTL-5 CL2- Linhagem de tireócito normal de rato Fisher jovem- 3 semanas
GNAS- Gene que codifica a subunidade estimulatória S acoplada à proteína G (“*Guanine Nucleotide Binding Protein (G Protein), Alpha Stimulating Activity Polypeptide*”)
H3K36- Lisina 36 da histona H3
HDAC- Histonas desacetilases
HEK293 – Linhagem embrionária de rim humano
HeLa - Linhagem humana de carcinoma cervical (Henrietta Lacks)
Hhex – Proteína homeobox hematopoiética
RH-Recombinação homóloga
HSA- Homo sapiens
HT – Hormônios tireoidianos
KiKi- Oncogene v-ras-Ki
LINEs- Elementos nucleares longos intercalados (“*Long interspersed nuclear elements*”)
MAPK- Proteína quinase ativada por mitógenos (“*Mitogen-Activated Protein Kinase 1*”)
MCF-7- Linhagem humana de câncer de mama
MiR/ miRNA- MicroRNA
MRN- Complexo multimérico formado pelas proteínas MRE11, RAD50 e NBS1
MTT- brometo de 3-(4,5-dimetiltiazol-2-il)-2,5-difeniltetrazólio
NADPH – Nicotinamida adenina dinucleotídeo-fosfato”)
NHEJ- Junção terminal de cromossomos não homólogos (“*Non-homologous end joining*”)

NIS - Cotransportador Na⁺/I
 NTRK1- Receptor neurotrófico de tirosina quinase tipo 1 (“*Neurotrophic Receptor Tyrosine Kinase 1*”)
 PAF- Punção por agulha fina
 PAX8 - homeoproteína codificada pelo gene PAX8 (“*Paired box gene 8*”)
 PCC1 3 - Linhagem de tireócito normal de rato Fisher adulto- 18 meses
 PET- Tomografia por emissão de pósitrons
 pH – Potencial hidrogeniônico
 PI3K – Fosfatidil inositol 3 cinase
 PKA – Proteína quinase A
 PKC - Proteína quinase C
 PPAR γ - Receptor ativado por proliferador de peroxissoma (“*Peroxisome Proliferator Activated Receptor Gamma*”)
 pre-miRNA- MicroRNA precursor
 pri-miRNA- MicroRNA primário
 qRT-PCR – Reação em cadeia da polimerase quantitativa
 RAI- iodo radioativo (“*radioactive iodide*”)
 RAS- Nome derivado do vírus do sarcoma de rato (“*Rat Sarcoma Viral Oncogene*”)
 RET/PTC- Rearranjo cromossômico entre o gene que codifica o domínio tirosino-quinase e um promotor constitutivamente ativo
 RI- Radiação ionizante
 RISC- Complexo de silenciamento induzido por RNA (“*RNA-induced silencing complex*”)
 RNAm – Ácido ribonucleico mensageiro
 RPL4 - Proteína ribossomal L4, componente da subunidade maior ribossômica
 ROC- “*Receiver Operating Characteristics*”
 SDS- Dodecil sulfato de sódio
 SINES- Elementos nucleares curtos intercalados (“*Short Interspersed Nuclear Elements*”)
 T3 – 3,5,3’-triodotironina
 T4 – 3,5,3’,5’-tetraiodotironina ou tiroxina
 Tg - Tireoglobulina
 TNM- sistema onde T= tamanho do tumor, N e M, a presença/ausência de metástase em linfonodos regionais e à distância
 TP53- Gene supressor tumoral que codifica uma proteína de massa molecular 53 kDa
 TPO - Tireoperoxidase
 TSH – Hormônio estimulador da tireóide ou tireotrofina
 TSHR - Receptor de tireotrofina
 TTF1 – Fator de transcrição tireóide específico 1 (“*Thyroid Transcription Factor 1*”)
 TTF2 - Fator de transcrição tireóide específico 2 (“*Thyroid Transcription Factor 2*”)
 UTR- Regiões não-traduzidas (“*untranslated region*”)
 VEGFR- Receptor do fator de crescimento vascular endotelial (“*Vascular Endothelial Growth Factor Receptor*”)
 γ H2AX- Fosforilação da serina 39 da variante de histona H2AX



Ministério da Saúde
Instituto Nacional do Câncer
Coordenação de Pós-graduação
INSTITUTO NACIONAL DO CÂNCER

ANÁLISE DE ALTERAÇÕES EPIGENÉTICAS EM CÉLULAS DA TIREOIDE APÓS A EXPOSIÇÃO À RADIAÇÃO X

RESUMO

TESE DE DOUTORADO

Ricardo Cortez Cardoso Penha

A radiação ionizante (RI) é o principal fator de risco para o desenvolvimento do carcinoma papilífero da tireoide (CPT), devido à perda gradual dos genes de reparo e ao acúmulo de lesões no DNA. As vias de reparo do DNA por recombinação homóloga (HR) e por junção terminal de cromossomos não homólogos (NHEJ) são ativadas em resposta à quebra dupla do DNA (DSB), induzida pela RI, para manter a integridade genômica. As modificações epigenéticas como a metilação aberrante do DNA e a desregulação da expressão dos microRNAs vêm sendo associadas à carcinogênese da tireoide e à resposta terapêutica. Portanto, o objetivo principal dessa tese foi o de investigar as alterações epigenéticas nos tireócitos expostos à radiação X. A tese foi dividida em quatro capítulos. No primeiro capítulo, foi demonstrado que RI promove a parada do ciclo celular na fase G₂/M nas linhagens celulares de tireócito normais de rato, sem afetar a viabilidade celular. As células FRTL-5 CL2 exibiram uma cinética de reparo das DSB mais lenta e menores níveis globais de metilação (Line-1) do que as PCC1 3. A RI não acarretou em nenhuma alteração nos níveis de metilação global e da região promotora, e na expressão dos genes de reparo do DNA, exceto pela diminuição da expressão de *Brcal*. A expressão de todos os genes de reparo foi induzida nas células senescentes. No segundo capítulo, foi realizada o perfil global dos microRNAs nas células FRTL-5 CL2 irradiadas, identificando-se os miR-199a-3p e miR-10b-5p com as expressões mais alteradas. Validou-se *LIN28B* como alvo de miR-199a-3p (perda de estabilidade do RNAm) e *DICER1* como de miR-10b-5p (repressão da tradução). O miR-10b-5p aumenta a proliferação celular enquanto o miR-199a-3p a atenua. Ambos os microRNAs regulam negativamente a eficiência do reparo por HR. A superexpressão de miR-10b-5p diminuiu a viabilidade e proliferação das células irradiadas. No terceiro capítulo, foi demonstrado que os níveis proteicos de *DICER1* estão subexpressos no CPT. A superexpressão de *DICER1* estimulou a proliferação enquanto o seu silenciamento comprometeu a diferenciação dos tireócitos. Além disso, a expressão de *DICER1* mutada (c.5438A>G; E1813G) comprometeu o processamento dos microRNAs e a proliferação celular mediada por *DICER1* selvagem. No quarto capítulo, a expressão de hsa-miR-34a e hsa-miR-1249 discriminou os pacientes portadores do CPT expostos à RI (sensibilidade=73.3%, especificidade=75.5%, AUC=77.6%). Os hsa-let-7c, hsa-let-7d, hsa-miR-127 e hsa-miR-377 identificaram os rearranjos relacionados à RI (sensibilidade=88.9%, especificidade=77.6%, AUC=84.2%). Em suma, a metilação aberrante do DNA não parece estar envolvida nas etapas iniciais da carcinogênese tireóidea no nosso modelo. Os microRNAs são desregulados pela RI, afetando a eficiência do reparo do DNA por HR nas células irradiadas. A superexpressão de miR-10b-5p poderia ser uma abordagem terapêutica inovadora para o tratamento do CAT ao promover a radiosensibilidade. Os níveis proteicos de *DICER1* estão subexpressos no CPT e afetam a proliferação e diferenciação dos tireócitos enquanto a mutação (c.5438A>G; E1813G) no seu gene compromete o processamento dos microRNAs e a proliferação celular induzidos por *DICER1* selvagem. Além disso, os miRNAs poderiam ser usados para a identificação de CPT relacionados à RI.



**Ministério da Saúde
Instituto Nacional do Câncer
Coordenação de Pós-graduação
INSTITUTO NACIONAL DO CÂNCER**

ANALYSES OF EPIGENETIC ALTERATIONS IN THYROID CELLS EXPOSED TO X-RAY RADIATION

ABSTRACT

DOCTORATE THESIS

Ricardo Cortez Cardoso Penha

Ionizing radiation (IR) is the main risk factor for papillary thyroid cancer (PTC), due to gradual inactivation of DNA repair genes and DNA damages. The homologous recombination (HR) and non-homologous end joining (NHEJ) DNA repair pathways are triggered to efficiently repair the IR-induced DNA double-strand breaks (DSB) and safeguard genome integrity. Epigenetic mechanisms such as aberrant DNA methylation and microRNA expression deregulation have been associated with thyroid carcinogenesis and therapeutic response. Thus, this thesis aimed at studying the epigenetic mechanisms in thyroid cells exposed to X-ray. The thesis is divided into four chapters. In the first chapter, it was demonstrated that X-ray exposure promoted a G₂/M arrest in normal thyroid cell lines, without any effect in cellular viability. FRTL-5 CL2 cells displayed a slower kinetics of DSB repair and a lower global methylation (Line-1) than the PCCl 3 cells. Neither global and DNA repair genes' promoter methylation profiles nor the expression of genes involved in HR and NHEJ pathways was altered by acute X-ray exposure, apart from *Brcal* downregulation. DNA repair gene was overexpressed in radiation-induced senescent thyroid cells. In the second chapter, the global microRNA expression profile of irradiated FRTL-5 CL2 cells identified miR-10b-5p and miR-199a-3p as the most pronounced alterations in expression. We validated *LIN28B* as target of miR-199a-3p (mRNA instability) and miR-10b-5p targeting *DICER1* (repression of translation). MiR-10b-5p increases the growth rate of FRTL-5 CL2 cells, while miR-199a-3p inhibits their proliferation. Moreover, both of these microRNAs negatively affect HR efficiency. The overexpression of miR-10b-5p decreases the viability of the irradiated cells. In the third chapter, it was shown that *DICER1* is downregulated, at protein level, in PTC. *DICER1* overexpression positively regulates thyroid cell proliferation, whereas its silencing impairs thyroid cell differentiation. The expression of *DICER1* gene mutation (c.5438A>G; E1813G) negatively affects the microRNA machinery and cell proliferation, as well as upregulates endogenous *DICER1* protein levels of thyroid cells. In the fourth chapter, it was demonstrated that the expression of the hsa-miR-34a and hsa-miR-1249 could predict radiation exposure status (sensitivity=73.3%, specificity=75.5%, AUC=77.6%) Our proposed model was also able to identify IR-related fusion genes in PTC samples using the expressions of four miRNAs (hsa-let-7c, hsa-let-7d, hsa-miR-127 and hsa-miR-377) (sensitivity=88.9%, specificity=77.6%, AUC=84.2%) In conclusion, our data suggest that DNA methylation might not be the epigenetic mechanism involved in early steps of thyroid carcinogenesis in our study model. The IR exposure deregulates microRNA expression, affecting the DSB repair efficiency of irradiated thyroid cells, and our data suggests that miR-10b-5p overexpression may be an innovative approach for anaplastic thyroid cancer therapy by increasing cancer cell radiosensitivity. *DICER1* protein levels are downregulated in PTC and affect thyroid proliferation and differentiation, while *DICER1* gene mutation (c.5438A>G; E1813G) compromises the *DICER1* wild-type-mediated microRNA processing and cell proliferation. Besides, miRNA-based model might help screening PTC patients with radiation history background.

1 INTRODUÇÃO

1.1 CÂNCER

O câncer foi responsável por 9,6 milhões de mortes no mundo em 2018, sendo que 70% destas ocorreram em países em desenvolvimento (WHO, 2018). É bastante comum nesses países a apresentação da doença em estágios avançados devido ao diagnóstico e tratamento inacessíveis, o que contribuem para esse cenário preocupante (WHO, 2018). A Organização Mundial de Saúde estima que o número anual de óbitos por câncer aumente em 50% até 2030 no mundo (WHO, 2018). O impacto econômico gerado pelo câncer está aumentando, correspondendo a 1,16 trilhões no ano de 2010 em todo o mundo (WHO, 2018). No Brasil, as estimativas apontam cerca de 640 mil novos casos de câncer, onde os tipos mais prevalentes são em homens o de próstata (31,7%) e em mulheres o de mama (29,5%) (INCA, 2017). É inquestionável que o câncer seja um problema de saúde pública e, portanto, é fundamental o melhor entendimento da biologia dos tumores.

Apesar dos relatos da doença serem milenares, o termo “câncer” foi originalmente empregado por Aristóteles a partir das semelhanças entre os vasos sanguíneos que alimentam a massa tumoral e a forma do caranguejo (Mukherjee, 2012). A ideia do câncer como uma doença genética surgiu somente no século passado por Boveri & Boveri (1929), quando sugeriram uma associação entre cromossomos aberrantes e tumores.

Atualmente, o modelo que explica o surgimento do câncer é o de evolução clonal, baseado no sistema de evolução Darwiniana (Greaves & Maley, 2012). Este modelo preconiza que a evolução clonal é um processo dinâmico entre a aquisição de mutações fundadoras e alterações epigenéticas por uma única célula (clone) e a pressão seletiva do tecido que se encontram, garantindo uma vantagem seletiva para a sua expansão clonal. Esse equilíbrio é afetado pelas interações do tecido e inclusive das próprias células tumorais com os fatores sistêmicos (hormônios, nutrientes) e células inflamatórias, assim como o ambiente que cerca o indivíduo (estilo de vida e exposição aos fatores de risco), contribuindo para a progressão tumoral. Cada clone sofre ondas de replicação clonal concomitante ao acúmulo de novas mutações e instabilidade cromossômica, gerando populações de subclones. Nesse sentido, as

análises mutacionais de célula única revelaram que a trajetória evolutiva dos clones ancestrais é complexa e ramificada, indo ao encontro da heterogeneidade genética intra e intertumoral, característica comum a diversos tipos de tumores, incluindo o da tireoide, e associada ao potencial invasivo, metastático e à resistência terapêutica (Greaves & Maley, 2012).

1.2 O CÂNCER DA TIREOIDE

A tireoide é a primeira glândula endócrina humana, começando seu desenvolvimento na terceira semana de gestação, quando os fatores de diferenciação tireoideos *TTF1*, *PAX8*, *TTF2*, *HHEX* e *FOXE1* começam a ser expressos (De Felice & Di Lauro, 2004) e, pesa entre 15-25 g no homem adulto. Quanto a sua estrutura, a glândula consiste em dois lobos lateralizados, direito e esquerdo, cobertos por músculos esterneioide e esternotireoide e unidos por um istmo do parênquima glandular apoiado sobre a traqueia anterior na altura da cartilagem cricoide. Sua histologia é caracterizada por milhões de unidades aproximadamente esféricas denominadas folículos, ricamente vascularizados por capilares provenientes dos ramos da carótida e veias tireoideas. Cada folículo é formado por uma única camada de células foliculares (tireócitos, 95%), cuja morfologia é regulada pelo hormônio tireotrófico (TSH) hipofisário. O TSH é o principal modulador da função tireóidea. Sintetizado e secretado pelos tireotrofos da adenohipófise, atua na glândula tireoide via receptor de TSH (TSHR) acoplado à proteína G, presente na membrana basolateral do tireócito. Ao ligar ao seu receptor acoplado à proteína Gs, o TSH ativa a cascata intracelular com a ativação da adenilato ciclase, que leva ao aumento da geração de AMP cíclico que, por sua vez, ativa a proteína quinase A (PKA). Desse modo, desencadeia uma cascata responsável pela fosforilação de proteínas, levando ao aumento da biossíntese dos hormônios da tireoide. Por outro lado, quando ligado ao seu receptor acoplado à proteína Gq, ativa a via do fosfatidil-inositol e da proteína quinase C. Como resultado, estimula a produção hormonal e a proliferação dos tireócitos (Nunes e cols., 2008). O interior do folículo, o lúmen, é preenchido pelo coloide mucoproteico, composto em sua grande parte por tireoglobulina (Tg), na qual os hormônios tireoideos (HT) tiroxina (T4) e triiodotironina (T3) permanecem armazenados até se iniciar o processo de secreção hormonal (Nunes e cols., 2008).

As células C (5%), incorporadas ao parênquima tireoidiano, produzem o hormônio calcitonina (Nunes e cols., 2008).

O câncer da tireoide é o tipo de tumor mais comum do sistema endócrino (DeLellis e cols., 2004). A sua incidência mundial média é de 8,6 casos a cada 100.000 habitantes (GLOBOCAN, 2018). No Brasil, são estimados 1.570 casos novos para o sexo masculino e 8.040 para o sexo feminino para 2018, ocupando a décima quarta e quinta posição, respectivamente, entre os tumores mais incidentes do país (INCA, 2017).

A maior parte dos carcinomas da tireoide resulta da transformação neoplásica das células foliculares (95%) e são classificados pelo padrão histopatológico em carcinomas diferenciados da tireoide (CDT) (85-95%), pouco diferenciados (0-7%) e indiferenciados/ anaplásicos (2%) (Kondo e cols., 2006). O CDT é subdividido em dois subtipos histológicos: o carcinoma papilífero da tireoide (CPT) e o carcinoma folicular da tireoide (CFT) (Kondo e cols., 2006). A diferenciação do CDT permite que, de maneira geral, o tumor seja sensível ao TSH, capte iodo e produza Tg e, dessa forma, viabiliza as intervenções diagnósticas e terapêuticas com os radioisótopos I^{123} e I^{131} (Dohán e cols., 2003). Apesar da maior parte dos CDT ser esporádica, 5-15% é familiar (Nosé, 2011). Já o carcinoma medular da tireoide (CMT), originado das células C, representa 3% dos casos dos tumores da tireoide (Kondo e cols., 2006). Além disso, as taxas de incidência do câncer da tireoide são próximas às de prevalência, sendo o CPT o mais prevalente (60-95%), seguido do CFT (10-20%), CMT (5-10%) e o anaplásico (1-5%) (GLOBOCAN, 2018).

Nas últimas décadas, a taxa de incidência do câncer da tireoide vem crescendo em todo o mundo (aproximadamente 1% ao ano), sendo este fenômeno proporcional ao nível de desenvolvimento do país (GLOBOCAN, 2018). Um bom exemplo é o avanço da taxa de incidência do câncer de tireoide registrada nos Estados Unidos (6%) impulsada pela elevação do número de casos de CPT em detrimento da estabilização (CMT e CAT) ou queda (CFT) das taxas de incidência dos outros subtipos histológicos (Cramer e cols., 2010). Tal fato poderia ser parcialmente explicado pelas melhorias no diagnóstico durante as últimas décadas e pelo aumento do uso de exames de imagens, como tomografias computadorizadas, ressonância magnética e tomografia por emissão de pósitrons (PET) nos países desenvolvidos, levando à

descoberta de nódulos tireoidianos de maneira acidental (Cramer e cols., 2010; Schonfeld e cols., 2011). Vale ressaltar que o método de base para a detecção destes nódulos (5% malignos) é a ecografia, um sistema baseado no ultrassom e mais simples quando comparado às técnicas mais complexas de imagem descritas acima, seguido da punção por agulha fina (PAF) para o diagnóstico final (Mazzaferrri, 1999). Contudo, a explicação para esse aumento ainda é controversa. Vários trabalhos mostraram o aumento de aproximadamente 50 % dos microcarcinomas da tireoide (< 2 cm) diagnosticados nos Estados Unidos entre 1978-2011 embora em torno de 70% dos mesmos não apresentem qualquer relevância clínica, o que vai ao encontro da teoria do excesso de diagnóstico (Pellegreti e cols., 2013). Por outro lado, a elevação da incidência dos casos de tumores maiores (> 4 cm) e de todos os estadiamentos clínicos (Pellegreti e cols., 2013), quase exclusivamente do subtipo histológico CPT sugerem que outros fatores poderiam estar influenciando no aumento da incidência dos tumores da tireoide.

O câncer da tireoide possui evolução clínica indolente e excelente prognóstico, com sobrevida global de 95% para o CPT, de 77% para o CFT e 85% para os CMT em 10 anos. Em contrapartida, os carcinomas pouco diferenciados e anaplásicos possuem sobrevida global de 15% e 2%, respectivamente, em 5 anos. As taxas de mortalidade do câncer da tireoide diminuíram na maioria dos países, incluindo o Brasil, provavelmente, devido à melhoria do tratamento (GLOBOCAN, 2018).

O principal fator de risco para o câncer da tireoide é a radiação ionizante (RI) (tópico discutido adiante). Contudo, outros fatores parecem impactar no risco do desenvolvimento desse tumor: 1) ser do sexo feminino visto que a proporção de casos em mulheres e homens é de 3:1 no CDT (de Castro e cols., 2016); 2) o aporte de iodo, uma vez que a deficiência na ingestão de iodo foi associada ao maior risco de desenvolvimento dos carcinomas anaplásicos e foliculares (Zimmermann & Galetti, 2015); 3) a doença autoimune tireoidite de Hashimoto foi associada ao maior risco de desenvolver CPT (Replinger e cols., 2008); 4) predisposição genética (Nosé, 2011); 5) obesidade/ índice de massa corporal (Kitahara e cols., 2011).

As diferenças étnicas e geográficas impactam nas taxas de incidência do câncer de tireoide. Mundialmente, as suas maiores taxas de incidência são nas ilhas do Pacífico, principalmente na etnia melanesiana de Nova Caledônia (>25 casos por 100.000 habitantes) seguido dos filipinos no Havaí (>20 casos por 100.000 habitantes), da Polinésia Francesa (>15

casos por 100.000 habitantes) e dos melanesianos de Fiji (>10 casos por 100.000 habitantes) (Blots e cols., 1997). Além disso, a incidência do câncer de tireoide é maior nos imigrantes chineses, japoneses e filipinos que vivem nos Estados Unidos do que nos seus descendentes e os nativos brancos do país (Rossing e cols., 1995), sugerindo que fatores ambientais nos países de origem estariam contribuindo para o maior risco de desenvolvimento do câncer de tireoide nessas populações. Nesse sentido, alguns estudos atribuem esse fenômeno ao consumo excessivo de vegetais crucíferos nas mulheres melanesianas (moderadamente deficiente em iodo) (Truong e cols., 2010), à dieta pobre em iodo nos residentes da Polinésia Francesa (Cléro e cols., 2012) e à alta frequência de sobrepeso e obesidade nas populações das ilhas do Pacífico (Cléro e cols., 2010). Nenhuma associação com o risco de desenvolvimento do câncer de tireoide e a exposição à radiação foi encontrada nessas populações.

As principais alterações genéticas envolvidas na transformação neoplásica das células foliculares da tireoide estão relacionadas à via de sinalização de MAPK (Kondo e cols., 2006). No CPT esporádico, as alterações genéticas mais frequentes são *BRAF*^{V600E} (29-69%), *RET/PTC* (13-43%), *RAS* (0-21%) e *NTRK1* (5-13%). Por outro lado, os rearranjos *RET/PTC* (50-90%) são os mais frequentes no CPT com histórico prévio de exposição à RI. No CFT, o gene *RAS* (40-53%) e o rearranjo *PPARγ-PAX8* (25-63%) são predominantes. Já no CAT, as principais mutações encontram-se nos genes *CTNNB1* (66%) e *TP53* (67-88%), seguido de *RAS* (20-60%) e *BRAF*^{V600E} (10-35%).

1.3 SUBTIPOS HISTOLÓGICOS DO CÂNCER DE TIREOIDE

1.3.1 CARCINOMA PAPILÍFERO DA TIREOIDE (CPT)

O CPT, derivado das células foliculares, é o subtipo mais frequente de câncer da tireoide (80%) e o seu diagnóstico e a classificação histopatológica são feitas pela morfologia nuclear, usando a técnica de H&E: núcleos claros, superposição nuclear, pseudoinclusão nuclear e sulcos nucleares embora sejam os aspectos citoplasmáticos e a arquitetura tecidual que contribuam para a classificação dos seus subtipos, denominados variantes (clássica, folicular, células altas, oncócítica, células claras e difusas, esclerosante e a sólida) (Al-Brahim & Asa, 2006; Lloyd e cols., 2011). Dentre as variantes, a clássica é a predominante (65-74%), apresentando estruturas

papilares bem definidas (Lloyd e cols., 2011). Por outro lado, a variante sólida é a mais frequente em populações expostas à RI (>30%), como observado após o acidente nuclear de Chernobyl (Lloyd e cols., 2011).

O estadiamento do CPT é determinado pelo sistema TNM, onde o T significa o tamanho do tumor/ extensão extratireoidiana, N e M, a presença/ausência de metástase em linfonodos regionais e à distância, respectivamente (Tuttle e cols., 2017, TNM 8ª edição). Nesse sentido, alguns fatores impactam no prognóstico dos pacientes portadores do CPT: sexo masculino, idade avançada (> 65 anos), tamanho do tumor (> 2 cm), multicentricidade, extensão extratireoidiana, presença de células altas, extensão linfonodal, invasão vascular e não responsividade à radioiodoterapia (RAI) (Passler e cols., 2004; Guo & Wang, 2014; de Castro e cols., 2016; Shi e cols., 2016).

A disseminação para linfonodos locais é frequente nas etapas iniciais da doença (> 50%) (LiVolsi, 2011). Em contrapartida, a doença metastática à distância, principalmente pulmão e osso, decorrente da disseminação hematogênica, é pouco frequente (5- 7%) (LiVolsi, 2011). Mesmo na presença de metástase à distância, a sobrevida global dos pacientes com CPT é razoável, 65% e 45 % em 5 e 10 anos, respectivamente, especialmente quando responsivos à RAI (Sugitani e cols., 2008).

O tratamento do CPT é cirúrgico (tireoidectomia parcial ou total), seguido ou não da ablação com I^{131} dos remanescentes tireoidianos e/ou terapêutica adjuvante com o uso de levotiroxina (LT4) em dose supressiva para o TSH (Mazzaferri, 1999).

1.3.2 CARCINOMA FOLICULAR DA TIREOIDE (CFT)

O CFT, também oriundo das células foliculares, é o segundo subtipo mais frequente de câncer da tireoide (6,5 – 9,7 %) e os seus principais achados histológicos são a diferenciação (foliculos contendo coloide), as invasões vasculares e a exclusão das atipias nucleares características do CPT (Sobrinho-Simões e cols., 2011). Dessa forma, o CFT apresenta três subtipos histológicos, baseado no encapsulamento e invasividade vascular: o minimamente

invasivo (encapsulado e pouca invasão vascular), o angioinvasivo encapsulado (invasivo) e o amplamente invasivo (parcialmente ou não encapsulado com ampla penetração vascular) (Sobrinho-Simões e cols., 2011). O maior desafio é o diagnóstico diferencial entre a variante folicular do CPT, o CFT e o adenoma folicular (Sobrinho-Simões e cols., 2011), apontando a necessidade da busca por biomarcadores moleculares.

A deficiência de iodo é um importante fator de risco para o desenvolvimento do CFT (Zimmermann & Galetti, 2015). Essa informação se baseia em estudos epidemiológicos onde foi observada uma associação entre a diminuição dos casos de CFT e a reposição de iodo na dieta nas áreas endêmicas para o bócio (Zimmermann & Galetti, 2015). Estes dados foram confirmados a partir de estudos em animais que mostraram a carência de iodo atuando na promoção dos tumores da tireoide (Zimmermann & Galetti, 2015). Os possíveis mecanismos de ação propostos seriam: 1) pela estimulação crônica da produção de TSH, levando ao aumento da proliferação celular e, logo, à hiperplasia e à aneuploidia; 2) pelo estresse oxidativo induzido pela deficiência de iodo, resultando em danos ao DNA e mutações.

Assim como o CPT, o estadiamento do CFT também é determinado pelo sistema TNM (Tuttle e cols., 2017, TNM 8ª edição) e apresentam, de maneira geral, os mesmos fatores que influenciam no prognóstico dos pacientes (Passler e cols., 2004; Sobrinho-Simões e cols., 2011). Além disso, a invasividade (o CFT minimamente invasivo exibe melhor prognóstico do que o amplamente invasivo) e a diferenciação (a variante oncocítica e CFT com estrutura insular/trabecular exibem pior resposta à RAI) parecem impactar no prognóstico dos pacientes (Sobrinho-Simões e cols., 2011). Ao contrário do observado no CPT, a disseminação para linfonodos locais não é comum (cerca de 10%) e as metástases à distância, predominante pulmão e ossos, são mais frequentes (19%) (Ruegemer e cols., 1988).

O tratamento do CFT também é o cirúrgico, tireoidectomia parcial ou total, seguido da ablação com I^{131} dos remanescentes tireoidianos e/ou terapêutica adjuvante com o uso de levotiroxina (LT4) em dose supressiva para o TSH (Mazzaferrri, 1999). A tireoidectomia total e a dissecação dos linfonodos do compartimento central são recomendadas para as variantes com piores prognósticos, a oncocítica e a insular/trabecular (Schmidbauer e cols., 2017).

1.3.3 CARCINOMA ANAPLÁSICO DA TIREOIDE (CAT)

O CAT é raro (< 2%) e altamente agressivo. Histologicamente, exibe um fenótipo indiferenciado, com células gigantes, inúmeras figuras mitóticas, mitoses atípicas, necrose extensiva e abundante infiltrado inflamatório. A maior parte dos pacientes portadores do CAT é maior de 60 anos e possuem longo histórico de bócio. A mediana de sobrevida é de 5 meses e apenas 20% dos pacientes permanecem vivos após o primeiro ano do diagnóstico. Devido à sua agressividade, o CAT é considerado estágio IV pelo Comitê Americano Misto para o Câncer (Keutgen e cols., 2015). Os fatores que influenciam no pior prognóstico dos pacientes são a idade avançada (≥ 70 anos), leucocitose, tamanho do tumor (> 5 cm), estadiamento (IVa vs. IVb) e metástase à distância (Sugitani e cols., 2012).

A invasão de tecidos adjacentes (90%), linfonodos cervicais (43%) e metástases à distância (20-50%), principalmente pulmão, osso e cérebro, são comuns nas etapas iniciais da doença (O'Neill & Shaha, 2013). Dessa forma, o tratamento do CAT deve ser rápido e multimodal: radioterapia neoadjuvante pré-operativa combinada com a ressecção cirúrgica completa, seguido de quimioterapia (uso dos radiosensibilizadores cisplatina, doxorubicina e paclitaxel) e radioterapia adjuvantes, ressaltando que a preservação das vias aéreas deve ser sempre a prioridade (Keutgen e cols., 2015). Contudo, como o CAT é refratário a todas as terapias, incluindo a radioterapia (Sugitani e cols., 2012), nenhuma abordagem terapêutica ainda foi capaz de melhorar efetivamente a sobrevida e a qualidade de vida dos pacientes, revelando a necessidade da busca por novos alvos moleculares.

1.4 OS MODELOS DE PROGRESSÃO TUMORAL DA TIREOIDE

As principais mutações fundadoras do câncer de tireoide pertencem à via de sinalização MAPK (74,8 %) e são mutuamente exclusivas (Cancer Genome Atlas Research Network, 2014) (Figura 1). A mutação $BRAF^{V600E}$ ocorre no aminoácido da posição 600 codificada pelo proto-oncogene *B-RAF* - substituição do aminoácido valina (V) pelo ácido glutâmico (E) – levando à ativação constitutiva da via de MAPK, independente da regulação por *RAS* e insensível a sinais antiproliferativos. A presença dessa mutação exerce um efeito pleiotrópico nas células tumorais,

como a proliferação (Hanly e cols., 2014), a perda de diferenciação e a transição epitélio-mesenquimal (Watanabe e cols., 2007; Durante e cols., 2007). O gene *RAS* codifica uma proteína que atua como um transdutor de sinais entre as tirosino-quinases e os receptores acoplados à proteína G e os seus efetores das vias de MAPK e PI3K-Akt. A sua atividade é regulada por GTP, de tal forma que é ativado quando ligado ao GTP e inativado quando ligado ao GDP (Nikiforov & Nikiforova, 2011). Mutações pontuais nos códons 12 e 13 (aumento de afinidade por GTP) ou a inibição da atividade autocatalítica do GTP (códon 61) acarretam em sua ativação aberrante (Suárez e cols., 1988). Os rearranjos *RET/PTC* serão discutindo no próximo tópico. O proto-oncogene *NTRK1* (receptor tirosino-quinase neutrófico) codifica um receptor transmembranar tirosino-quinase e é expresso estritamente em células da crista neural em condições normais, exercendo um papel crítico na sobrevivência celular. O rearranjo *ETV6-NTRK3* têm ação análoga a dos *RET/PTC*, disparando cascatas de sinalização envolvendo os efetores das vias de MAPK e PI3K-Akt (Kondo e cols., 2006).

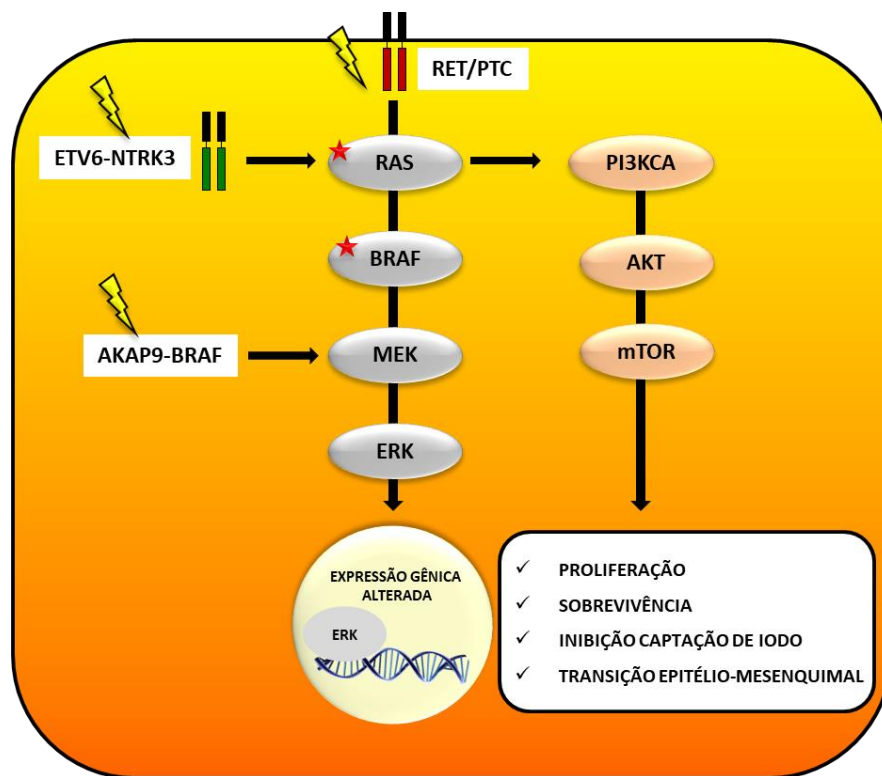


Figura 1 As principais vias de sinalização alteradas no câncer de tireoide. As alterações genéticas, mutuamente exclusivas, na via de MAPK ($BRAF^{V600E}$, *RAS*, *RET/PTC*) levam à

ativação constitutiva das vias de MAPK e PI3K-Akt e, conseqüentemente, à expressão gênica alterada. Particularmente, as mutações *BRAF*^{V600E} e em *RAS* são frequentes em tumores bem diferenciados da tireoide (destacados com a estrela vermelha). A exposição à radiação ionizante (raio amarelo) induz a formação de rearranjos cromossômicos (*RET/PTC*, *AKAP9-BRAF* e *ETV6-NTRK3*) que, por sua vez, ativam as vias descritas anteriormente. Os efeitos promovidos por esses oncogenes nos tireócitos são o aumento da proliferação e sobrevivência celular, assim como maior capacidade invasiva e menor diferenciação celular. *RET/PTC*= rearranjo entre a sequência de DNA que codifica o receptor tirosino-quinase *RET* e a região promotora de genes heterólogos; *ETV6-NTRK3*= fusão gênica entre o domínio hélice-volta-hélice de *ETV6* e o domínio tirosino-quinase de *NTRK3*; *AKP9-BRAF*= fusão gênica entre os éxons 1-8 de *AKAP9* e os éxons 9-18 de *BRAF* que codificam o domínio serina/ treonina quinase. (Baseado em Kondo e cols., 2006; Agrawal e cols., 2014).

O modelo mais aceito para explicar a carcinogênese da tireoide é o de evolução clonal (Kondo e cols., 2006; Parameswaran e cols., 2010; Cancer Genome Atlas Research Network, 2014; Costa e cols., 2015) (Figura 2). Primeiramente, as células foliculares adquirem mutações mutuamente exclusivas em proto-oncogenes que ativam a cascata de sinalização de MAPK (*BRAF*, *RAS*, *RET*, *NTRK1*), o que garante uma vantagem seletiva para a proliferação destas células (clones) e, acarreta na formação de adenomas foliculares e carcinomas. A exposição aos fatores de risco (RI, por exemplo) também está diretamente associada ao aparecimento das mutações fundadoras e à instabilidade cromossômica. Em seguida, a ativação da via de MAPK promove à aquisição de novas alterações genéticas como o rearranjo *PPAR γ* (receptor ativado por proliferador de peroxissoma)-*PAX8* presente no CFT bem como a inibição de p27 e a superexpressão da ciclina D1 no CPT, contribuindo para a progressão tumoral. A aquisição de mutações nos genes *CTNNB1* (acúmulo de β -catenina no núcleo) e *TP53* (inativação) estão relacionadas à desdiferenciação dos CDT pré-existent em CAT. No caso dos adenomas benignos, a presença de mutações nos genes *TSHR* e *GNAS* (codifica a subunidade estimulatória S acoplada à proteína G) induz o estímulo mitogênico nas células foliculares pela via do AMP cíclico- PKA e, leva à formação dos nódulos hiperfuncionantes (95% benignos).

Outra teoria que tem ganhado força na última década é a da carcinogênese pelas células progenitoras tireoidianas (Takano & Amino, 2005; Takano, 2014) (Figura 2). A principal diferença dessa teoria seria o fato de que o processo de transformação neoplásica não seria sequencial e sim direto pela aquisição de mutações fundadoras pelas células progenitoras presentes na tireoide, que diferem entre si pelo grau de diferenciação: progenitora indiferenciada (células tronco) que daria origem ao CAT; 2) tireoblastos (expressa Tg) ao CDT; 3) pró-tireócitos (não produzem HT) ao adenoma folicular. Essa teoria baseia-se no comportamento dos carcinomas da tireoide e as características das células progenitoras da qual seriam originados. O CDT progride lentamente e a disseminação linfática e à distância são frequentes, o que é compatível com a baixa proliferação e alta capacidade migratória dos tireoblastos. Em contrapartida, o CAT apresenta alta taxa de crescimento, o que vai ao encontro da capacidade ilimitada de crescimento das células tronco.

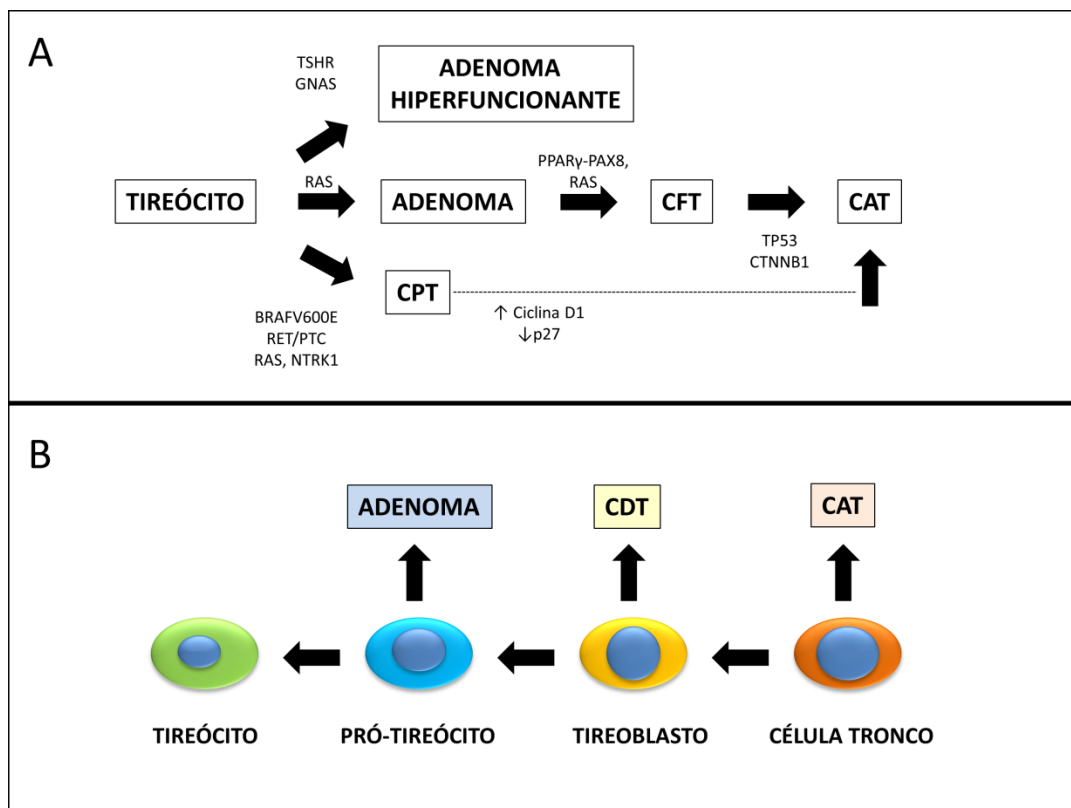


Figura 2 Modelos de progressão tumoral da tireoide. A) Modelo de evolução clonal. Os tireócitos adquirem mutações mutuamente exclusivas em genes da via de MAPK (*BRAF*, *RAS*,

RET/PTC, *NTRK1*) que levam ao aparecimento de adenomas ou o CPT. Alterações genéticas adicionais como *PPAR γ* (receptor ativado por proliferador de peroxissoma)-*PAX8* acarretam na formação do CFT enquanto a superexpressão de ciclina D1 e inibição de p27 contribuem para a progressão do CPT. A aquisição de mutações nos genes *TP53* e *CTNNB1* (codifica β -catenina) contribuem para a progressão dos CDT em CAT. Por outro lado, mutações nos genes *TSHR* (codifica o receptor de TSH) e *GNAS* (codifica a subunidade estimulatória S da proteína G) levam ao desenvolvimento de adenomas hiperfuncionantes (benignos). B) Modelo de carcinogênese fetal da tireoide. As células progenitoras da tireoide (células tronco, tireoblasto e pró-tireócito) adquirem as mutações fundadoras descritas acima, o que levaria ao desenvolvimento de carcinomas e adenomas. CPT = carcinoma papilífero da tireoide; CFT= carcinoma folicular da tireoide; CMT= carcinoma medular da tireoide; CAT= carcinoma anaplásico da tireoide; CDT= carcinoma diferenciado da tireoide. (Baseado em Kondo e cols., 2006; Takano, 2014).

1.5 RADIAÇÃO IONIZANTE E CARCINOMA PAPILÍFERO DA TIREOIDE

A radiação ionizante (RI) é o fator de risco mais bem estabelecido para o desenvolvimento do CPT (Ron e cols., 1995). As maiores evidências advêm dos estudos epidemiológicos usando populações expostas à RI (Ron e cols., 1995): os sobreviventes dos acidentes nucleares de Hiroshima e Nagasaki em 1945, os moradores do arquipélago próximo à área dos testes nucleares nas ilhas Marshall entre 1946-1958 (Land e cols., 2010), as coortes de pacientes portadores de tumores pediátricos e cervicais, os tratados por radioterapia para *tinea capitis* e, sobretudo, as crianças e adolescentes que viveram na região de Belarus e Ucrânia após o acidente nuclear de Chernobyl em 1986 (Pacini e cols., 1997; Cardis e cols., 2006). A partir dos dados destes estudos, foi possível estabelecer uma relação linear entre a dose de exposição à RI e o risco relativo do desenvolvimento do CPT (7,7 x/ Gy).

Os mecanismos de ação da RI podem ser diretos (60-70%) ou indiretos (30-40%) (Okuno & Yoshimura, 2010). Quando diretos, a RI interage diretamente com as moléculas do corpo, como o DNA. Quando indiretos, a RI promove a quebra das moléculas de água (radiólise da água) que compõem o corpo, gerando radicais livres e, estes, por sua vez, interagem com o DNA

causando danos. Dessa forma, os efeitos carcinogênicos associados à RI podem ser atribuídos aos danos provocados no DNA: danos de bases (3,000/ Gy), quebras de fita simples do DNA (1,000/ Gy) e, principalmente, as quebras da fita dupla do DNA (DSB) (40/ Gy) (Ward e cols., 1994; Sarasin e cols., 1999), predispondo ao aparecimento de mutações, deleções e rearranjos cromossômicos em células eucarióticas (Little, 2000). O acúmulo das DSB está particularmente associado à formação do rearranjo cromossômico *RET/PTC*, alteração genética fundadora do CPT (Kondo e cols., 2006). O rearranjo cromossômico *RET/PTC*, produto da fusão entre a sequência que codifica o receptor tirosino-quinase e um gene heterólogo, foi originalmente extraído das amostras de DNA do CPT e tem atividade oncogênica (Fusco e cols., 1987). Vale ressaltar que embora não seja expresso nos tireócitos normais, o gene *RET* selvagem é expresso nas células parafoliculares C, derivadas da crista neural (Fusco & Santoro, 2007).

Para corrigir as DSB e manter a estabilidade genômica, ocorre a ativação coordenada de sensores e transdutores de sinais nos sítios lesados (Figura 3). Destes, a serina/ treonina quinase mutada na ataxia-telangiectasia (ATM) é primariamente ativada pela sua associação ao complexo multimérico MRN (MRE11, RAD50 e NBS1) e BRCA1/2, no sítio de quebra, o que permite seu recrutamento e ativação completa. ATM, por sua vez, fosforila uma série de substratos: a variante de histona γ H2AX, TP53, 53BP1 e a quinase de checagem Chk2 (Shiloh, 2003). A proteína ataxia telangiectasia relacionada à Rad3 (ATR), por sua vez, fosforila Chk1. Enquanto ATM atua preferencialmente no reparo das DSB, ATR age no reparo dos erros de parada da forquilha de replicação e quebras simples do DNA (Yan e cols., 2014). Em conjunto, essas proteínas coordenam a parada do ciclo celular, o reparo do DNA, a transcrição gênica, a apoptose e a senescência celular. Após o reconhecimento do sítio de lesão, duas vias de reparo do dano ao DNA, em resposta à DSB, são preferencialmente ativadas: a de junção terminal de cromossomos não homólogos (NHEJ) e a de recombinação homóloga (HR). Enquanto a primeira, mais sujeita a erros, funde dois terminais livres de um cromossomo quebrado além de ser mais ativa na fase G0/G1 do ciclo celular, a segunda utiliza a cromátide-irmã como molde e desempenha um papel importante na fase S/G2 (Weterings & Chen, 2007; Bunz, 2008). A falha no reparo destas lesões e o acúmulo dos danos resultantes levam à morte celular imediatamente após a irradiação ou à inativação celular após algumas divisões celulares (Willers & Held, 2006).

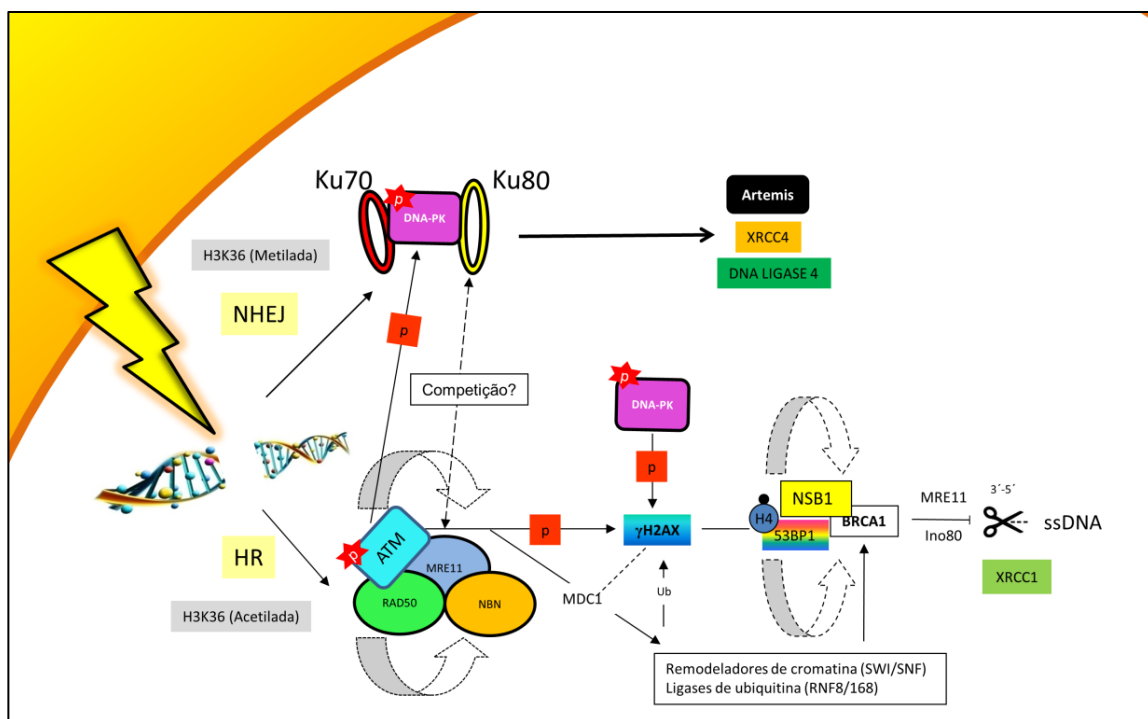


Figura 3. Vias de reparo da quebra-dupla do DNA (DSB). Após a exposição à radiação ionizante (representado por um raio) ocorre a formação de DSB e, em resposta a estas lesões, uma série de sensores e transdutores de sinais são ativados pelas vias de reparo por recombinação homóloga (HR) e junção terminal de cromossomos não homólogos (NHEJ). As modificações na lisina 36 da histona H3 (H3K36) podem contribuir para o direcionamento do tipo de reparo do DNA. Posteriormente, as quinases DNA-PK e ATM são primariamente ativadas próximo ao sitio lesado e, fosforilam diversos substratos como γ H2AX, 53BP1 e BRCA1/2. ATM pode interagir com a DNA-PK, levando à fosforilação e ativação de ambas as quinases e, como resultado, à competição pelos mesmos substratos como a γ H2AX. A fosforilação da variante de histona H2AX além de flanquear o sítio lesado, também amplifica a cascata de sinalização, levando ao recrutamento de remodeladores da cromatina (complexo SWI/SNF) e ao reparo do DNA. p= fosforilação; Ub= ubiquitinação. (Baseado em Bartkova e cols., 2005; Pai e cols., 2014).

Os CPT esporádicos e os relacionados à radiação possuem perfis moleculares distintos (Port e cols., 2007). Os CPT relacionados à radiação possuem maior frequência de *RET/PTC1* (*RET_CCDC6*) e *RET/PTC3* (*RET_NCOA4*) como descrito nos tumores de sobreviventes da

bomba atômica no Japão (22 %) (Hamatani e cols., 2008), pós-Chernobyl (63,8 %) (Rabes e cols., 2000) e tratados com radiação externa para condições benignas e malignas (84 %) (Bounacer e cols., 1997). Já nos esporádicos, sem histórico prévio de exposição à RI, a frequência destes rearranjos é menor (13-43%) (Bounacer e cols., 1997; Kondo e cols., 2006; Tronko e cols., 2010). Além disso, a formação de *RET/PTC* é induzida diretamente pela RI, de maneira dose-dependente (Caudil et al., 2006). Recentemente, a fusão gênica *ETV6-NTRK3* foi identificada com maior frequência em tumores pós-Chernobyl (14,5 % vs. 2 %) e a sua formação foi induzida pela exposição à RI (Leeman-Neill e cols., 2014). Enquanto a mutação *BRAF*^{V600E} está presente em 46 % dos CPT esporádicos e apenas 12 % dos relacionados à radiação (Lima e cols., 2004), a translocação cromossômica *AKAP9-BRAF* é frequente em 11 % dos CPT relacionados à radiação e 1 % dos esporádicos (Ciampi e cols., 2005), revelando o importante papel da ativação da via de MAPK para a carcinogênese da tireoide. Além disso, os CPT relacionados à radiação exibem um comportamento mais agressivo (por exemplo, maior frequência de extensão extratireoidiana e linfonodal) do que os esporádicos (Pacini e cols., 1997), o que foi correlacionado ao aumento da expressão das metaloproteinases MMP-1, 9 e 13 nestes tumores em relação aos esporádicos (Boltze e cols., 2009).

Os efeitos da RI foram divididos em agudo e crônico. O primeiro foi definido como o fenótipo horas ou dias após uma única dose de exposição, quando é realizada a maior parte dos experimentos em células e animais. O último, como as consequências após meses ou anos da exposição à RI, abrangendo os estudos epidemiológicos.

As respostas à RI variam de acordo com o tipo celular, a dose e o tempo. Em baixas doses (62 mGy), a radiação X estimula a proliferação das células normais da tireoide enquanto o efeito oposto é observado nas células tumorais, positivas para *RET/PTC* (Abou-El-Ardat e cols., 2012). Em altas doses (4 Gy), a via canônica de *TGFβ* é ativada nas células normais e a de *TP53* nas células tumorais (Abou-El-Ardat e cols., 2012). Estes dados foram recapitulados em camundongos tratados com I¹³¹ (Rudqvist e cols., 2015). As radiações gama e X induzem a formação preferencial de *RET/PTC1* em células tireoideas, usando modelos *in vivo* e *in vitro*, de maneira tempo dependente (Mizuno e cols., 2000; Caudill e cols., 2005).

A exposição crônica às doses baixas (≤ 100 mSv) e altas (> 100 mSv) de RI exercem impactos distintos nas células da tireoide (UNSCEAR, 2016). Quando em baixas doses, o modelo linear, que assume o risco de câncer proporcional à dose de radiação, falha ao prever os riscos das incidências de câncer devido às flutuações dos resultados observados, limitando as análises estatísticas (Suzuki e cols., 2012). Dados obtidos a partir da otimização do modelo linear usando o método de Monte Carlo, algoritmo computacional baseado na probabilidade matemática que calcula as doses efetivas de RI a partir de suas interações pelo efeito Compton no corpo humano, indicaram que a exposição à dose efetiva de 1,48 mSV poderia já potencializar os riscos de câncer da tireoide (Seo e cols., 2015). Dessa forma, vários estudos correlacionaram o número de tomografias e a dose de radiação com o maior risco do desenvolvimento do câncer da tireoide em crianças e adolescentes (Schonfeld e cols., 2011; Su e cols., 2014; Boice e cols., 2015), apontando o problema mundial do aumento da exposição à radiação médica (0,62 mSv/ ano) e sua influência em órgãos radiosensíveis como a tireoide. Recentemente, os primeiros dados sobre o desastre nuclear ocorrido em Fukushima em 2011 foram publicados e não foi observada qualquer associação entre a dose de exposição à radiação e o risco do desenvolvimento dos tumores da tireoide (Yamashita e cols., 2018). A principal diferença da população afetada em Fukushima e a de Chernobyl em 1986 são: 1) baixa dose efetiva de radiação na tireoide (< 20 mSV); 2) a faixa etária dos indivíduos na época do acidente nuclear que, posteriormente foram diagnosticados com câncer de tireoide, é maior (10-15 anos), não havendo registros de tumores na faixa de 0-5 anos na época do acidente, quando há maior susceptibilidade do desenvolvimento de tumores da tireoide induzidos pela radiação; 3) os tumores são menores (14 mm *vs.* 40 mm) e as metástases à distância são menos frequentes (2 % *vs.* 19%); 4) enquanto as alterações genéticas mais frequentes nos tumores de Chernobyl são os rearranjos cromossômicos, os de Fukushima são as mutações de bases simples (Yamashita e cols., 2018).

Enquanto as alterações genéticas foram bem caracterizadas nos CPT esporádicos e nos relacionados à RI, as alterações epigenéticas ainda carecem de mais estudos. Inúmeros relatos vêm indicando a participação de tais alterações em todas as etapas da carcinogênese da tireoide, bem como na resposta terapêutica, o que será discutido detalhadamente nos próximos tópicos.

1.6 EPIGENÉTICA

O termo “epigenética” é uma evolução da palavra “epigênese”, cunhado pelo médico e fisiologista William Harvey (1650) para descrever o conceito do desenvolvimento como um processo de aumento gradual da complexidade a partir do material genético homogêneo, o zigoto. Posteriormente, esse termo foi introduzido na biologia moderna pelo embriologista e geneticista britânico Conrad Hal Waddington (1940) para descrever o processo de desenvolvimento (Holliday, 2006). Atualmente, este mesmo termo se refere a modificações herdáveis que resultam em alterações de expressão gênica sem modificar a sequência de bases do DNA. Os mecanismos epigenéticos descritos são a metilação do DNA, as modificações de histonas e os RNAs não codificantes, como os microRNAs (Holliday, 2006). Estes mecanismos desempenham papéis cruciais na biologia celular e, portanto, sua desregulação pode levar ao aparecimento de doenças, como o câncer.

1.6.1 METILAÇÃO DO DNA

Desde a última década, um conjunto de trabalhos vem mostrando que o câncer é uma doença que surge não só de alterações na sequência de bases do DNA, mas também de alterações epigenéticas (Feinberg & Tycko, 2004; Baylin & Ohm, 2006; Baylin & Jones, 2011). Dentre estas alterações, a mais estudada é a metilação dos resíduos de citosina posicionadas 5' em relação às guaninas no DNA, chamadas dinucleotídeos CpG, reação catalisada pelas DNA metiltransferases (DNMTs) (Adams e cols., 1979; Herceg, 2007). A DNMT1 é a metiltransferase de manutenção responsável pela preservação do perfil de metilação durante a divisão celular enquanto as DNMT3a/b realizam a metilação *de novo* do DNA (Denis e cols., 2011).

Os sítios CpG não estão distribuídos de maneira homogênea no genoma, localizando-se principalmente nas sequências repetitivas LINEs (*Long Interspersed Nuclear Elements*) e SINEs (*short interspersed nuclear elements*), bem como nas regiões promotoras de aproximadamente 50% dos genes (Lopez e cols., 2009; Bird, 2000). Em células normais, os sítios CpG das regiões repetitivas estão geralmente metilados, enquanto os das ilhotas CpG encontram-se normalmente

desmetilados, com exceção daquelas ilhotas dos genes imprintados e genes localizados no cromossomo X inativo (Lopez e cols., 2009).

Por outro lado, o genoma de células tumorais apresenta, simultaneamente, um padrão de hipometilação global e hipermetilação de regiões promotoras específicas. Particularmente, essas modificações ocorrem com maior frequência nos estágios iniciais da doença (Feinberg & Tycko, 2004; Baylin & Ohm, 2006; Baylin & Jones, 2011; Lima e cols., 2011). O mesmo fenômeno foi observado após a exposição à RI (Weidman e cols., 2007; Antwi e cols., 2013). A hipometilação global, promovida indiretamente pela RI, foi associada à ativação de elementos de transposição, elevada quebra cromossômica, aneuploidia e maior taxa mutacional, gerando instabilidade genômica, característica comum a diversos tipos de tumores, incluindo o CPT (Ellis e cols., 2014).

A metilação do DNA está, geralmente, associada à cromatina inativa e, na maioria dos casos, à repressão gênica, afetando a expressão de genes importantes para a homeostase celular, como os supressores de tumor (Weber & Schuebeler, 2007; Denis e cols., 2011). A hipermetilação induz o silenciamento da expressão gênica por dois mecanismos: 1) o bloqueio da ligação dos fatores de transcrição pelos grupamentos metil, o que impede o acesso da RNA polimerase ao gene (Molloy & Watt, 1990); 2) proteínas que possuem domínio de ligação aos sítios CpG metilados (MDSB) e histonas desacetilases competem com os fatores de transcrição pelos seus sítios de ligação ao DNA, tornando a cromatina menos acessível (Nan, e cols., 1998).

No contexto do câncer da tireoide, a hipermetilação das regiões promotoras dos genes supressores tumorais *RASSF1A* (inibidor da via de MAPK) e *PTEN*, bem como os de reparo do DNA *ATM* e *MLH1* estão diretamente associados à menor expressão dos mesmos e ao pior prognóstico dos pacientes (Xing e cols., 2004; Smith e cols., 2007; Guan e cols., 2008; Xing, 2010). A caracterização molecular do CPT revelou a metilação aberrante da região promotora de alguns genes envolvidos no reparo do DNA (Cancer Genome Atlas Research Network, 2014) e, portanto, a hipermetilação da região promotora poderia ser um mecanismo plausível para a perda de expressão e atividade dos genes de reparo nas etapas precoces da carcinogênese, contribuindo para a menor eficiência do reparo e o acúmulo de lesões, o que poderia diretamente e/ ou indiretamente induzir a carcinogênese tireoidea.

1.6.2 MODIFICAÇÃO DE HISTONAS

As histonas são proteínas responsáveis pela organização do DNA, empacotando-o em estruturas octoméricas denominadas nucleossomos. De maneira geral, as histonas regulam negativamente a transcrição gênica por obstrução física, impedindo a ligação dos fatores de transcrição e, portanto, tornando a cromatina menos acessível. As caudas das histonas, localizadas na sua região amino terminal, são passíveis de modificações pós-traducionais que interferem na sua afinidade pelo DNA e, assim, impactam diretamente na compactação e acessibilidade da cromatina. As principais modificações são acetilação, metilação, fosforilação, ubiquitinação, sumoilação, ribosilação e desaminação (Lawrence e cols., 2016). Os exemplos clássicos de regulação da expressão gênica por essas modificações são a acetilação da lisina 16 da histona H4 afrouxando a cromatina e, dessa forma, estimulando a transcrição gênica *in vitro* e *in vivo* (Akhtar & Becker, 2000), enquanto a di ou trimetilação da lisina 20 da histona H4 exerce o efeito oposto (Lu e cols., 2008). Além da cauda, a região central das histonas, especificamente a região lateral externa com contato direto com o DNA, também sofre modificações. Estas modificações também impactam de maneira distinta na expressão gênica (Lawrence e cols., 2016).

As alterações na atividade das histonas desacetilases (HDAC) vêm sendo descritas em células neoplásicas e o efeito antitumoral dos inibidores de HDAC foi reportado em diversos tipos de tumor, incluindo o de tireoide (Allis & Jenuwein, 2016). Nesse sentido, foi demonstrado que o tratamento com os inibidores de HDAC e os de proteassomo induzem sinergicamente a apoptose nas linhagens celulares oriundas do CAT (Borbone e cols., 2010). Além disso, o domínio EZH2 do complexo Polycomb, que possui a atividade metiltransferase para as lisinas de histonas, está superexpressa no CAT e promove o silenciamento da expressão gênica de *PAX8* e, logo, a desdiferenciação celular (Borbone e cols., 2011).

1.6.3 MICRORNA (MIRNA OU MIR)

Os miRNAs são pequenas sequências endógenas de RNAs não-codificantes de fita simples (20-23 nucleotídeos), envolvidos na regulação da expressão gênica, que são expressos,

de maneira tecido-específica, ao longo do desenvolvimento. Como ilustrada na figura 4, a sua biogênese é iniciada pela transcrição do miRNA primário (pri-miRNA) - que possui o formato de grampo e rico em estruturas secundárias, capeamento 5' e cauda poliA 3' - pela RNA polimerase II. O pri-miRNA, por sua vez, é metilado pela metiltransferase-like 3, auxiliando no seu reconhecimento e clivagem pela ação da endonuclease DROSHA, gerando o precursor de miRNA (pre-miRNA). O pre-miRNA é exportado do núcleo para o citoplasma pela proteína Exportina-5 e, posteriormente, processado pela RNase III DICER1 e membros da família Argonauta e TRBP, como descrito acima. Particularmente, o gene que codifica *DICER1* humana está localizado no cromossomo 14q32.13 e contém 27 éxons que codificam uma proteína de 220 kDa. Estruturalmente, possui os domínios: N-terminal com atividade DExD/H box helicase, PAZ (Piwi-Argonaute-Zwille), DUF283, RNase IIIa e IIIb, bem como o domínio de ligação a dsRNA (dsRBD) (Foulkes e cols., 2014). *DICER1* desempenha um papel central na biogênese dos miRNAs. Canonicamente, o domínio PAZ auxiliado pelo domínio dsRBD reconhece o pre-miRNA (50-70 nucleotídeos) que, por sua vez, é clivado em miRNA maduro pela ação catalítica dos dois domínios RNase III. Após o processamento, *DICER1* catalisa o carregamento do duplex de miRNA maduro à proteína Argonauta II (AGO2) do complexo RISC (complexo de indução de silenciamento de RNA). Posteriormente, a fita de menor estabilidade termodinâmica é degradada pela ação de AGO2 e a outra (fita guia) é incorporada ao complexo RISC que, direciona o complexo ao RNAm alvo. Ao se ligarem em seus elementos responsivos nas regiões não-traduzidas (UTR) 3' e 5' e, na região codificante de transcritos-alvos, o silenciamento da expressão gênica dá-se pela degradação do RNAm (pareamento perfeito entre as sequências por complementaridade Watson-Crick) e/ ou repressão de sua tradução em proteína (Ambros & Chen, 2007; Kurzynska-Kokorniak e cols., 2015; Peng & Croce, 2016). De fato, análises *in silico* demonstraram que pelo menos 50 % do RNAm de humanos podem ser regulados por miRNA (Friedman e cols., 2009).

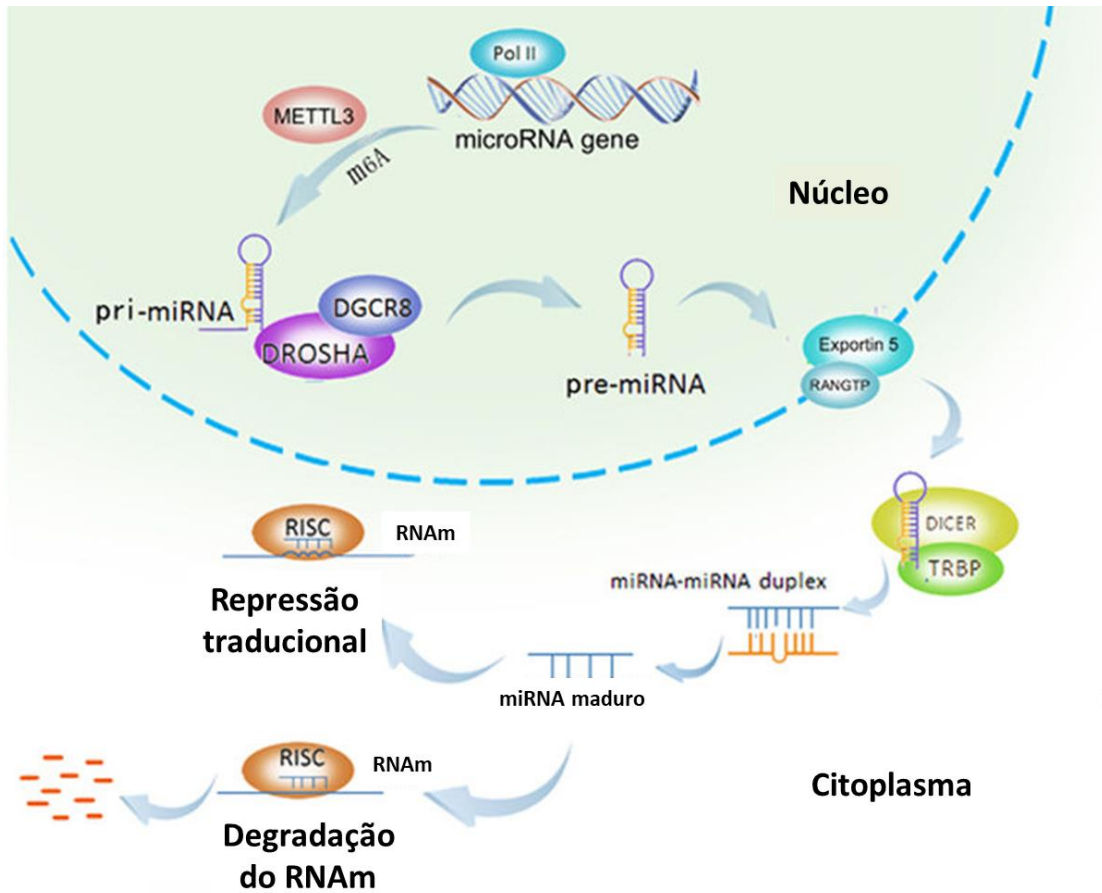


Figura 4. Biogênese dos miRNAs. Os miRNAs primários (pri-miRNA) são transcritos pela RNA polymerase II (Pol II) e, posteriormente metilados pela enzima metiltransferase-like 3 (METTL3) para o seu reconhecimento e clivagem pelo complexo composto pela proteína ligante de RNA DGCR8 e a endonuclease DROSHA em uma estrutura de grampo de ~85 nucleotídeos, chamado de miRNA precursor (pre-miRNA). Em seguida, o pre-miRNA é exportado do núcleo para o citoplasma pela Exportina 5, num processo ativo dependente de GTP. No citoplasma, o pre-miRNA é processado pela endonuclease DICER num duplex de miRNA (uma cópia é a passageira e a outra é a guia) de aproximadamente 22 nucleotídeos. Posteriormente, esse duplex é separado e a fita guia de miRNA é ligada ao complexo de silenciamento induzido por RNA (RISC), guiando o complexo RISC ao RNAm alvo. A inibição da expressão gênica ocorre pela degradação do RNAm ou pela repressão da tradução do RNAm (Adaptado de Peng & Croce, 2016).

Os miRNAs desempenham um papel crucial no desenvolvimento e na regulação de diversos processos fisiológicos como diferenciação, proliferação, reparo do DNA, apoptose, sobrevivência, crescimento, senescência e migração celular (Wahid e cols., 2010). Dessa forma, o uso de modelos *knockout* condicional para *DICER1* em camundongos revelou a sua importância para o desenvolvimento normal de diversos tecidos como cerebelo (Zindy e cols., 2015), sistema reprodutivo feminino (Hong e cols., 2008), fígado (Chen & Verfaillie, 2014), rins (Chu e cols., 2014) e, sobretudo, a tireoide (Frezzetti e cols., 2011; Rodriguez e cols., 2012). No contexto da tireoide, os autores mostraram que a perda de *DICER1* leva ao hipotireoidismo severo, culminando na morte dos animais logo após o nascimento caso não haja a reposição do T4. Além disso, com o passar da idade, os animais mutados para *DICER1* apresentam claros sinais de alterações neoplásicas, como a perda dos marcadores de diferenciação (*NIS*, *TPO*, *TG*, *PAX8* e *FOXE1*) e desorganização da estrutura folicular da tireoide.

A expressão aberrante de *DICER1* está associada às diversas patologias, como o câncer. Quanto à sua expressão, os dados na literatura variam com o tipo de tumor. A perda de *DICER1* é associada à progressão e ao pior prognóstico dos pacientes portadores de câncer de mama (Khoshnaw e cols., 2012), pulmão (Karube e cols., 2005), ovário (Faggad e cols., 2010), cervical (Zhao e cols., 2014) e adrenocortical (de Sousa e cols., 2015). Por outro lado, *DICER1* é superexpressa no câncer de próstata (Ambs e cols., 2008), colorretal (Faber e cols., 2011) e laringe (Gao e cols., 2014). No câncer de tireoide, de acordo com Cancer Genome Atlas Research Network e cols., (2014), os níveis de expressão de *DICER1* estão diminuídos nos CPT em comparação ao tecido normal e, esta desregulação foi associada ao pior prognóstico dos pacientes (Erler e cols., 2014).

Quanto ao perfil mutacional, já foram identificadas mutações germinativas e somáticas no gene de *DICER1* humana (Foulkes e cols., 2014). Quando germinativas, as mutações resultam em proteínas truncadas na proximidade do domínio catalítico RNase III (por exemplo, c.3579_3580delCA) e estão associadas à síndrome de DICER (penetrância de 15%), que leva ao aumento do risco do desenvolvimento de neoplasias benignas (bócio multinodular) e malignas (exemplo, CPT) (de Kock e cols., 2014). Quando somáticas, as mutações são mais frequentes nos éxons 24 e 25, que codificam o domínio RNase IIIb. Essas alterações genéticas ocorrem

particularmente no sítio de ligação aos íons metálicos (c.5438A>G, c.5429A>T e c.5429A>G). De maneira interessante, essas alterações são do tipo *missense* e resultam em não transcrição do éxon 25 (Foulkes e cols., 2014). Recentemente, o nosso grupo identificou a presença da mutação c.5438A>G (E1813G) no gene de *DICER1* (1/18) numa análise em amostras de pacientes portadores de CPT (Costa e cols., 2015). Além disso, o perfil mutacional das amostras de CPT revelou uma correlação positiva entre a presença das mutações E1705Q, D1810H, E1813G e E1813Q na região codificante de *DICER1* e a sua superexpressão nos casos analisados (Yoo e cols., 2016).

De maneira geral, os miRNAs estão localizados em regiões genômicas associadas ao câncer. Análises sistemáticas do genoma e transcriptoma de diferentes linhagens e tecidos tumorais revelaram profundas alterações nos genes não codificantes. Em especial, rearranjos como amplificação, deleção, inversão e translocação cromossômica (Stratton e cols., 2009; Beroukhim e cols., 2010). Ainda mais, os miRNAs estão sujeitos à regulação por oncogenes, supressores tumorais e mecanismos epigenéticos (Calin & Croce, 2006). O oncogene *HMGA1* regula negativamente os miR-1, miR-196a-2, miR-101b, miR-331 e miR-29a em fibroblastos embrionários de camundongo, ligando-se à região a montante do início do sítio de transcrição desses miRNAs (De Martino e cols., 2009). Além disso, STAT3 regula positivamente a expressão de miR-21 e miR-181 na linhagem celular normal de mama MCF-10A, contribuindo para a transformação neoplásica mediada por IL-6 (Iliopoulos e cols., 2010). A hipometilação de let-7a-3 nos casos de adenocarcinoma de pulmão está associada à sua reativação e à progressão tumoral (Brueckner e cols., 2007). Já a associação entre a hipermetilação do DNA dos supressores de tumor miR-137 e miR-193a e o silenciamento da expressão dos mesmos foi descrita durante o processo de carcinogênese oral (Kozaki e cols., 2008).

1.7 MIRNA E TIREOIDE

A expressão dos miRNAs é fundamental para a diferenciação e proliferação das células normais da tireoide (Frezzetti e cols., 2011; Rodriguez e cols., 2012). A tireoide expressa um conjunto de miRNAs, importante para a manutenção da diferenciação: por exemplo, os membros

da família let-7 que possuem como alvos preditos *TTF-1*, *PAX8* e *FOXE1*; o cluster miR-15/16 e *SLC5A5* (*NIS*), *DuOx2* e *TTF-1*; membros da família do miR-30 e *Tg* e *TTF-1*; miR-33-5p e *SLC5A5* (*NIS*), *Tg*, *TSHR* e *SLC26A4* (*pendrina*), miR-125b-5p e *DuOx1*; miR-99-5p e *TPO* (Fuziwara & Kimura, 2017). Nesse sentido, o TSH, hormônio fundamental para a função tireoideia, regula negativamente um conjunto de miRNAs, miR-1, miR-28a, miR-290-5p, miR-296-3p e miR-297a que, por sua vez, possuem como alvo comum o gene *CREB1*, um fator de transcrição ativado pela via de AMP cíclico e necessário para a proliferação e diferenciação do tireócito (Leone e cols., 2011).

Os miRNAs são cruciais nas diferentes etapas da tumorigênese. De acordo com a sua expressão no tumor, podem atuar como supressores tumorais ou oncogenes (Spizzo e cols., 2009). Geralmente, quando superexpressos, regulam negativamente os genes supressores tumorais. Por outro lado, quando inibidos, contribuem para a superexpressão dos oncogenes. Além disso, os miRNAs dirigem as células neoplásicas na aquisição progressiva do fenótipo de malignidade (Santarpia e cols., 2010). Na tireoide, a indução do *cluster* miR-221/222 parece estar envolvida nos estágios iniciais da carcinogênese ao aumentar a proliferação celular pela diminuição dos níveis proteicos de p27 kip1 e levando ao aumento da transição G1/S do ciclo celular (Pallante e cols., 2010). Além disso, estes miRNAs regulam negativamente a expressão dos membros da família let-7 em carcinomas diferenciados e não diferenciados da tireoide, favorecendo a progressão tumoral pela indução de reguladores do ciclo celular e oncogenes, incluindo *RAS*, *HMGAI* e *HMGGA2*, *MYC*, *CCNB1* e *CCNE2* (Pallante e cols., 2010; Palante e cols., 2014). Embora os miR-221/222/181b/146 não sejam detectados na linhagem de tireócito normal (PCCI 3) e no tecido paranodular de pacientes com CPT, os mesmos são expressos em altos níveis no mesmo modelo após a transformação com os oncogenes *v-ras-Ha*, *v-ras-Ki*, *v-raf*, *RET/PTC1* e *RET/PTC3* (He e cols., 2005).

O perfil de expressão de alguns miRNAs está correlacionado com a mutação encontrada nos CPT. Nos tumores *RET/PTC* positivos, miR-187 está superexpresso enquanto nos tumores com mutações em *BRAFV600E* e *RAS*, é frequente a superexpressão de miR-221/222 (Nikiforova e cols., 2008). Além disso, a transformação das células normais da tireoide pelo oncogene *RET/PTC* acarreta na redução da expressão dos membros da família let-7, importantes

para expressão dos marcadores de diferenciação tireoideos *TTF1* e *Tg* e a proliferação celular e, a sua reintrodução em células tumorais de CPT, *RET/PTC* positivas, reverte esses efeitos (Ricarte-Filho e cols., 2009). Assim, estes dados indicam que a perda de *let-7* é importante para a transformação neoplásica induzida por *RET/PTC*.

A população dos miRNAs alterados na tireoide consegue diferir as principais neoplasias benignas (adenomas) e malignas da tireoide, os carcinomas papilífero, folicular e anaplásico (Pallante e cols., 2010). Nesse sentido, os miR-221-/222, miR-181 e miR-146 são superexpressos no CPT em relação aos nódulos tireoidianos hiperplásicos (Pallante e cols., 2010, Pallante e cols., 2014). Os miRNAs miR-187, miR-221/222, miR-224 e miR-155 estão superexpressos nos CFT clássicos e os miR-187, miR-221/222, miR-339, miR-183 e miR-197 nas variantes oncócicas e, sobretudo, não foi observada alteração da expressão destes miRNAs nos nódulos hiperplásicos da tireoide (Nikiforova e cols., 2008). Por fim, a regulação negativa da expressão dos miR-30d, miR-125b, miR-26a e miR-30a-5p é característica dos CAT (Visone e cols., 2007). Dessa forma, o perfil de expressão dos miRNAs parece ser uma valiosa ferramenta no diagnóstico de neoplasias tireoideas.

A resposta ao estresse induzida nas células irradiadas está intimamente associada à expressão diferencial dos miRNAs. A utilização de ferramentas de bioinformática permitiu a identificação das vias de sinalização que são alvos dos miRNAs e suas consequências fisiopatológicas (Lhaxhang & Chaudhry, 2012; Methetrairut & Slack, 2013). Nesse contexto, os membros da família *let-7* são desregulados pela RI e regulam negativamente a expressão de *RAS* e, logo, a ativação da via de MAPK, promovendo radiosensibilidade e diminuindo a proliferação celular em diversas linhagens celulares, incluindo as da tireoide (Dent e cols., 2003; Perdas e cols., 2016). A expressão de miR-34 é rapidamente induzida por *TP53* e *ATM* em resposta ao dano do DNA, levando à inibição da proliferação celular e apoptose (Salzman e cols., 2016). O aumento da expressão de miR-21, promovido pela RI, tem sido demonstrado consistentemente em diversos modelos celulares (Methetrairut & Slack, 2013) e este miRNA tem como alvo direto genes da via de apoptose como *PTEN* e *BCL2* (Buscaglia & Li, 2011). Além disso, miR-21 promove radiorresistência ao otimizar o reparo do DNA pelas vias NHEJ e HR (Hu e cols., 2017).

2 JUSTIFICATIVA

A RI é o principal fator de risco para o desenvolvimento do CPT, atuando nas etapas de iniciação e promoção da doença. Apesar dos CPT esporádicos serem na maior parte dos casos indolentes, os relacionados à RI apresentam maior agressividade ao diagnóstico com progressão rápida, acarretando no pior prognóstico dos pacientes. Enquanto as alterações genéticas são bem caracterizadas em tumores da tireoide relacionados à RI, as epigenéticas ainda precisam ser mais bem elucidadas. Nesse sentido, já foi demonstrado que as alterações na metilação do DNA e na expressão dos miRNAs podem levar à perda de expressão de genes da maquinaria de reparo do DNA durante a progressão do CPT. Dessa forma, investigar as alterações epigenéticas induzidas pela RI em células da tireoide podem ajudar na melhor compreensão da biologia do tumor, principalmente nas etapas iniciais da carcinogênese da tireoide, e na identificação de potenciais alvos terapêuticos.

3 OBJETIVO GERAL

Investigar alterações epigenéticas induzidas pela radiação X que podem contribuir para o câncer de tireoide.

3.1 OBJETIVOS ESPECÍFICOS

CAPÍTULO I:

- Caracterizar o papel da radiação X na proliferação, viabilidade e ciclo celular das células diferenciadas de tireócito de rato, FRTL-5 CL2 e PCCI 3;
- Analisar a cinética de reparo das DSB através de alterações de alguns de seus efetores (ATM, ATR, γ H2AX e 53BP1) nas células FRTL-5 CL2 e PCCI 3 irradiadas;
- Investigar os níveis globais de metilação do DNA (Line-1) nas células FRTL-5 CL2 e PCCI 3 irradiadas;
- Correlacionar os níveis de metilação da região promotora dos genes de reparo do DNA das vias de HR e NHEJ com a expressão gênica por q-RT-PCR nas células FRTL-5 CL2 irradiadas;
- Avaliar a expressão dos genes das vias de HR e NHEJ das células FRTL-5 CL2, em senescência celular induzida pela exposição crônica à radiação X.

CAPÍTULO II:

- Estudar o perfil de expressão diferencial dos microRNAs nas células FRTL-5 CL2 irradiadas;
- Validar os alvos de miR-199a-3p (*LIN28B*) e miR-10b-5p (*DICER1*);
- Correlacionar a expressão destes microRNAs a dos seus respectivos alvos moleculares nas células FRTL-5 CL2 irradiadas;
- Avaliar os efeitos dos miR-199a-3p e miR-10b-5p sobre a proliferação, viabilidade e reparo do DNA por recombinação homóloga;

- Analisar o impacto de miR-10b-5p sobre a radiosensibilidade nas linhagens celulares FRTL-5 CL2, FRTL KiKi e 8505c.

CAPÍTULO III:

- Caracterizar a expressão de *DICER1* em amostras de CPT, CAT, tireoide normal e linhagens celulares de carcinoma da tireoide (TPC-1, B-CPAP, FRO, 8505c);
- Avaliar o papel de *DICER1* sobre a proliferação, diferenciação e ciclo celular, bem como o processamento do microRNAs em linhagens normais da tireoide e de CPT;
- Identificar o papel da mutação c.5438A>G; E1813G no gene de *DICER1* sobre os mesmos parâmetros, citados acima.

CAPÍTULO IV:

- Investigar se os miRNAs regulados pela RI poderiam ser usados como marcadores de exposição à radiação em amostras de CPT do banco de dados TCGA;
- Avaliar se os miRNAs regulados pela RI poderiam identificar os rearranjos relacionados à RI;
- Identificar as vias de sinalização alteradas pelos miRNAs dos modelos propostos.

4 RESULTADOS

Os resultados desta tese estão dispostos na forma de artigos científicos e dados não publicados e foram divididos em quatro capítulos. Os resultados não publicados que compõem os capítulos 2 e 3 estão imediatamente após os respectivos artigos. Um resumo sobre cada capítulo, escrito em português, encontra-se antes dos trabalhos publicados ou submetidos.

4.1 CAPÍTULO I

A hipometilação de *LINE-1* e a baixa expressão de *Brcal* estão associadas ao reparo tardio do DNA em células normais da tireoide expostas à radiação ionizante

A radiação ionizante (RI) é o fator de risco mais bem estabelecido para o desenvolvimento do carcinoma papilífero da tireoide (CPT), especialmente durante a infância (<5 anos de idade), principalmente devido à perda gradual dos genes de reparo do DNA e ao acúmulo de mutações. Recentemente, a caracterização molecular das amostras de CPT revelou a metilação aberrante dos genes das vias de reparo do DNA e a diminuição da expressão destes genes nas amostras analisadas. Dessa forma, o silenciamento gênico por metilação do DNA poderia ser um mecanismo plausível para a perda dos genes de reparo em tumores induzidos pela RI na tireoide. Nesse capítulo, caracterizou-se a resposta de células normais da tireoide de rato (FRTL-5 CL2 e PCCI 3) à RI, focando nas alterações de metilação global e na região promotora dos genes das vias de reparo do DNA ativadas em resposta às quebras de fita dupla (DSB), a recombinação homóloga (HR) e a junção terminal de cromossomos não homólogos (NHEJ), bem como seus efeitos sobre a expressão gênica. Nossos dados mostraram que embora a exposição à RI não tenha comprometido a viabilidade celular, observou-se a diminuição da proliferação e a parada das células irradiadas na fase G₂/M do ciclo celular. Quanto ao reparo das DSB, as linhagens celulares utilizadas nesse estudo exibiram uma cinética de reparo similar à cultura primária de tireócitos humanos, demonstrando a robustez do modelo utilizado para o estudo de dano ao DNA. A RI induziu a rápida fosforilação na serina 139 da variante de histona H2AX (γ H2AX) nas células tireoidianas irradiadas, uma das respostas celulares mais precoces à DSB, apresentando um pico de indução uma hora após o insulto. Particularmente, as células FRTL-5 CL2 reparam as DSB mais lentamente do que as PCCI 3. Dentre todos os genes das vias de HR e NHEJ analisados, somente *Brcal* teve sua expressão reduzida nas células irradiadas e foi diferencialmente expresso entre as linhagens celulares. O nível de metilação global basal foi menor nas células FRTL-5 CL2 do que nas células nas PCCI 3 e nos tecidos de rato testados (tireoide, mama, fígado e rim). A RI não foi capaz de alterar os níveis de metilação global das células tireoidianas normais, mesmo após a sincronização das mesmas na fase G₀/G₁ do ciclo celular. A região promotora dos genes das vias de HR e NHEJ apresentaram ausência ou baixos

níveis de metilação e não parecem se correlacionar com a expressão gênica. Em seguida, foi construído o modelo de exposição crônica à RI, baseado no esquema de radioterapia empregado no tratamento de pacientes com tumores pediátricos. Os níveis de metilação global e na região promotora dos genes das vias de reparo do DNA não foram alterados no modelo crônico de irradiação. Por outro lado, todos os genes destas vias foram induzidos pela RI nas células senescentes. Portanto, a alteração da metilação do DNA não parece ser o mecanismo epigenético que contribua para etapas iniciais da transformação neoplásica induzida pela RI no nosso modelo. Além disso, os nossos dados sugerem que as células FRTL-5 CL2 possuam uma maquinaria de reparo das DSB menos eficiente do que as PCCI 3.

Intrinsic *LINE-1* Hypomethylation and Decreased *Brca1* Expression are Associated with DNA Repair Delay in Irradiated Thyroid Cells

Ricardo Cortez Cardoso Penha,^{1,a} Sheila Coelho Soares Lima,^a Mariana Boroni,^a Renata Ramalho-Oliveira,^a João P. Viola,^a Denise Pires de Carvalho,^c Alfredo Fusco^{a,b} and Luis Felipe Ribeiro Pinto^{a,2}

^a Instituto Nacional de Câncer - INCA, Rio de Janeiro, Brazil; ^b Istituto di Endocrinologia ed Oncologia Sperimentale - CNR c/o Dipartimento di Medicina Molecolare e Biotecnologie Mediche, Università degli Studi di Napoli "Federico II", Naples, Italy; and ^c Instituto de Biofísica Carlos Chagas Filho - CCS, Universidade Federal do Rio de Janeiro, Rio de Janeiro, Brazil

Penha, R. C. C., Lima, S. C., Boroni, M., Ramalho-Oliveira, R., Viola, J. P., de Carvalho, D. P., Fusco, A. and Pinto, L. F. R. Intrinsic *LINE-1* Hypomethylation and Decreased *Brca1* Expression are Associated with DNA Repair Delay in Irradiated Thyroid Cells. *Radiat. Res.* 188, 144–155 (2017).

Exposure to ionizing radiation greatly increases the risk of developing papillary thyroid carcinoma (PTC), especially during childhood, mainly due to gradual inactivation of DNA repair genes and DNA damages. Recent molecular characterization of PTC revealed DNA methylation deregulation of several promoters of DNA repair genes. Thus, epigenetic silencing might be a plausible mechanism for the activity loss of tumor suppressor genes in radiation-induced thyroid tumors. Herein, we investigated the impact of ionizing radiation on global methylation and CpG islands within promoter regions of homologous recombination (HR) and non-homologous end joining (NHEJ) genes, as well as its effects on gene expression, using two well-established normal differentiated thyroid cell lines (FRTL5 and PCCL3). Our data reveal that X-ray exposure promoted G₂/M arrest in normal thyroid cell lines. The FRTL5 cells displayed a slower kinetics of double-strand breaks (DSB) repair and a lower long interspersed nuclear element-1 (*LINE-1*) methylation than the PCCL3 cells. Nevertheless, acute X-ray exposure does not alter the expression of genes involved in HR and NHEJ pathways, apart from the downregulation of *Brca1* in thyroid cells. On the other hand, HR and NHEJ gene expressions were upregulated in radiation-induced senescent thyroid cells. Taken together, these data suggest that FRTL5 cells intrinsically have less efficient DNA DSB repair machinery than PCCL3 cells, as well as genomic instability, which could predispose the FRTL5 cells to unrepaired DSB lesions and, therefore, gene mutations. © 2017 by Radiation Research Society

INTRODUCTION

Thyroid carcinoma is the most frequently diagnosed malignancy of the endocrine system (1), and papillary thyroid carcinoma (PTC) accounts for approximately 80–85% of the cases (2). Exposure to ionizing radiation increases the risk of developing PTC, especially during childhood (3). Carcinogenic effects of radiation could be attributed to base damages, single-strand breaks and, above all, double-strand breaks (DSB), involved on *RET/PTC* rearrangement formation (4).

In response to DSB, a coordinated activation of sensors (γ -H2AX and 53BP-1), signal transducers and effectors, mostly homologous repair (HR) and non-homologous end joining (NHEJ) partners, is triggered (5). Defects in this machinery predispose to genomic instability and cancer (6).

Cancer arises from genetic and epigenetic alterations (7). Of these, CpG methylation is one of the most common mechanisms of gene expression regulation at the transcriptional level, usually associated with inactive chromatin when in the promoter region. Genomes from cancer cells simultaneously exhibit global hypomethylation and hypermethylation in promoters of specific tumor suppressor genes. These events frequently occur during the early stages of tumorigenesis (7, 8). The same phenomena have also been observed after radiation exposure (9, 10). Radiation could indirectly promote global hypomethylation and, therefore, genomic instability, a common feature observed in a variety of tumors, including PTC (11). On the other hand, hypermethylation of *MLH1* (12) and *ATM* (13) promoters has also been reported in PTC samples when compared to normal surrounding tissues and inversely associated with their expression and patient prognosis. Recent molecular characterization of PTC revealed a DNA methylation deregulation of several DNA repair gene promoters (14). Thus, early aberrant methylation of DNA repair genes could be a plausible mechanism of their silencing in radiation-induced thyroid tumors.

In this study, we investigated the effect of radiation on long interspersed nuclear element-1 (*LINE-1*) methylation, an

Editor's note. The online version of this article (DOI: 10.1667/RR14532.1) contains supplementary information that is available to all authorized users.

¹ Ricardo Cortez Cardoso Penha is "Bolsista da CAPES, Programa PVE".

² Address for correspondence: Instituto Nacional de Câncer - INCA, Rua André Cavalcanti, 37-Centro, Rio de Janeiro, CEP 20231-050 RJ, Brazil; email: lfrpinto@inca.gov.br.

indicator of global methylation, and CpG islands within promoter regions of HR and NHEJ genes, as well as its effects on gene expression, using two well-established normal differentiated thyroid cell lines (FRTL5 and PCCL3). Our data reveal that FRTL5 displayed slower DSB repair kinetics and a lower *LINE-1* methylation than PCCL3 cells. Radiation did not appear to modify the expression of genes involved in HR and NHEJ pathways apart from the downregulation of *Brcal* in the thyroid cells. On the other hand, radiation-induced senescence promoted upregulation of HR and NHEJ gene expression in thyroid cells.

MATERIALS AND METHODS

Cell Culture and Irradiation

Rat thyroid cells, PCCL3 and FRTL5, derived from 18-month-old and 3–4-week-old normal Fisher rats, respectively (15), were grown in Coon's modified Ham's F-12 media (HiMedia Laboratories, Mumbai, India), supplemented with 5% fetal bovine serum and a six-hormone mixture [1 mU/ml thyrotropin (TSH), 10 μ g/ml insulin, 5 μ g/ml transferrin, 10 nM hydrocortisone, 10 ng/ml somatostatin and 10 ng/ml glycyl-L-histidyl-L-lysine acetate-complete media].

Acute irradiations were performed as single 1–10 Gy X-ray doses (X-RAD 320; Precision X-ray Inc., North Branford, CT) for 1–48 h. In parallel, 20 μ m of H₂O₂ (Sigma-Aldrich® LLC, St. Louis, MO) was used as a positive control of water radiolysis (indirect effect of radiation) (16). Synchronization of 97% of FRTL5 cells on G₀/G₁-phase cell cycle was performed, as previously described by Degrassi *et al.* (17). Briefly, cells were starved from TSH for 72 h, then TSH was added to the media and cells were monitored for three days.

For chronic exposures, five X-ray treatments of 5 Gy were performed to reach a maximum dose of 25 Gy (X-RAD 320; Precision X-Ray) with intervals of two or three days between each treatment. This protocol was based on a childhood cancer cohort in which the estimated mean thyroid dose was 12.50 Gy (18).

Cytotoxicity and Cell Cycle

As an index of cell viability, we used the commercially available MTT assay (Sigma-Aldrich), according to the manufacturer's instructions. All measurements were performed in triplicate and the results were expressed as relative to nonirradiated control cells or irradiated cells at the initial time (1 h). Trypan blue was used to evaluate cell proliferation at 1, 6 and 24 h postirradiation.

Cell cycle profile was evaluated using propidium iodide (2 μ g/ml) on a FACSCalibur™ cytometer (Becton Dickinson and Co., Franklin, NJ) and analyzed on CELL-FIT software (Becton Dickinson).

Western Blot

Cells were homogenized in lysis buffer containing 135 mM NaCl, 1 mM MgCl₂, 2.7 mM KCl, 20 mM Tris, pH 8.0, 1% Triton™, 10% glycerol and protease and phosphatase inhibitors (0.5 mM Na₃VO₄, 10 mM NaF, 1 mM leupeptin, 1 mM pepstatin, 1 mM okadaic acid and 0.2 mM phenylmethylsulfonyl fluoride) and then syringed five times. An aliquot was used to determine the protein concentration by BCA protein assay kit (Pierce™ Biotechnology/Thermo Fisher Scientific Inc., Rockford, IL), according to the manufacturer's instructions. Cell lysate proteins (30–100 μ g) were then subjected to SDS/PAGE electrophoresis, transferred to polyvinylidene fluoride (PVDF) microporous membranes, and probed with the indicated antibodies: anti- γ -H2AX, 1:1,000 (EMD Millipore, Billerica, MA); anti- β -actin, 1:10,000 (Sigma-Aldrich); anti-BRCA1, 1:1,000 (Novus Biologicals, Oakville, Canada); anti-phospho-ATM, 1:2000 (Rockland); anti-ATR, 1:2,000 (Novus

Biologicals); anti-Vinculin, 1:1,000 (Santa Cruz Biotechnology® Inc., Dallas, TX); anti-rabbit, 1:2,000 (Abcam, Cambridge, UK); anti-mouse, 1:3,000 (Santa Cruz Biotechnology); anti-goat, 1: 3,000 (SouthernBiotech, Birmingham, AL). The detection of the proteins was performed using ECL (Pierce Biotechnology/Thermo Fisher Scientific).

Immunofluorescence of γ -H2AX and 53BP-1

Irradiated and control cells were fixed in methanol-acetone solution (70:30) at –20°C for 7 min, permeabilized with 0.5% Triton X-100 solution for 30 min and dried. After rehydration in phosphate-buffered saline and blocking with 1% bovine serum albumin for 1 h, cells were stained with the anti- γ -H2AX (1:500; EMD Millipore) for 90 min and Alexa Fluor® 488 anti-mouse (1:250, Invitrogen™, Carlsbad, CA) as secondary antibody for 1 h. The same procedure was performed for 53BP1 (1:500; Novus Biologicals) with Alexa Fluor 594 anti-rabbit (1:250; Invitrogen). Nuclei were counterstained with 40,6-diamidino-2-phenylindole (DAPI). Coverslips were mounted using Vectashield® mounting media (Vector® Laboratories, Burlingame, CA). Fluorescence images were obtained using an Olympus FV10i confocal microscope (Olympus, Tokyo, Japan). To determine the average total number of foci per cell, per field, for three independent experiments, we counted the number of γ -H2AX foci per cell used NIH ImageJ software, v.38.

Pyrosequencing

Lesion-specific DNA repair pathway genes (HR and NHEJ), involved on DNA damage response, were selected due to CpG island presence on their promoter regions using UCSC Genome Browser (University of California, Santa Cruz, CA) (Table 1). To access the *LINE-1* methylation pattern of the cell line genomes, we used two sets of primers designed by Hamm *et al.* (19). We obtained the rat genome sequence (m4/v. 3.4, November 2004) and annotation for repetitive elements from the UCSC Genome Database. Based on the provided data, 899,092 *LINE-1* sequences were subjected to *in silico* bisulfite treatment and 8,460 L1 elements with length over 6,000 bp were identified and aligned to generate LINE nucleotide base matrix. The sets of primers for pyrosequencing analysis were designed within L1 elements with dense CpG dinucleotides. An electronic PCR was performed and the consensus sequence was visualized using WebLogo (20). A total of 1,285 PCR products with 117 pb mean length were generated. The two sets of primers allowed us to assess 7 CpG dinucleotides within each L1 sequence, generating data from a minimum of 8,995 CpG sites. The DNA was eluted to reach a final concentration of 25 ng/ μ l. To quantify the percentage of methylated cytosines in individual CpG sites, bisulfite-converted DNA was sequenced using a pyrosequencing system (PSQTM 96MA, QIAGEN, Hilden, Germany), as previously described (8).

Real-Time PCR

A total of 1,500 ng of RNA was used in the reverse transcription reaction (RT) using SuperScript II® (Invitrogen), following the manufacturer's protocol. The oligonucleotides for real-time PCR, comprising exon-exon junctions, were purchased from Integrated DNA Technologies® (San Diego, CA), designed with Primer-BLAST software (National Center for Biotechnology Information, Bethesda, MD) and are listed in Table 2. We used the Rotor-Gene® Q system and QuantiFast® reagent SYBR Green PCR Kit (both from QIAGEN®, Valencia, CA). Each reaction contained 5 μ l of QuantiFast SYBR Green buffer 2X (QIAGEN), 0.5 μ l of specific oligonucleotides at a final concentration of 0.25 μ M, 3 μ l of cDNA (diluted 10 \times) and sterile deionized water to complete the final volume of 10 μ l. The amplification reaction was performed as follows: 5 min of pre-denaturation at 95°C, followed by 40 cycles of denaturation for 5 s at 95°C and an annealing and extension step for 10 s at 60°C. Relative gene expression was determined using comparative C_t method (21) and *RPLA* was used as a housekeeping gene.

TABLE 1
Pyrosequencing Primers Used in this Study Selected According to the Signaling Pathways

Signaling pathways	Genes	Region (CpG)	Sequences	Product (bp)	Sequence to analyze
HR	<i>Atm</i>	Promoter (80)	F: AGTAAAGAAGGGTAAGAGG	267	AGTTYGAGYGTYYGTTTTTYGTTTTTAT
			R: ACTCAAATAAATTCCTCTATA		
			S: TTTGATGAGAATTTTTTTATAGA		
	<i>Brcal</i>	Promoter (23)	F: GGAGAGGAGGAGTAAGTTGA	317	TYGGAATYGTATTGAGGYG GAATATGAGYGTAAAGGTAGTGTTA
			R: CTTCCACAATCCTCTATTACC		
<i>Mre11</i>	Promoter (47)	F: AGGATTGGTTTTGTGAGTTATT	232	TTTTYGYGAGAAGTAYG GATGYGTTTTTTTTYGYGTTAAATTTAGGTTT	
		R: CCTAAATACCCCAACCTAAACTTAT			
<i>Rad50</i>	Promoter (16/37)	F: GGGAAAGTGGATGAAGTGGATGATTA	203	GGTTTTYAGGTTTAYGTATTATAAGGYGATATTTTAAATTTTTTGGGGTTT	
		R: TCTCAACCCCTCACAAATTT			
NHEJ	<i>Lig4</i>	Promoter (44)	F: GGTGGATTGGGATTTATAGG	154	TAATAGGTAYGTAGGTTTATTTYGTTGAGYGTTTTTGAAAGTTGTGATAAT
			R: TTCAAATACCTAAATCCAAACACACTCT		
			S: GTTTAGGTAAGTAAAGTATTAATG		
	<i>Xrcc6</i>	Promoter (66)	F: GGGTTAGGTTTTGGATAGGT	264	TYGTGGYGYGTTAYGATGGTTTTYGGGTATT
			R: CTCTCTATCACCTCACATAATC		
<i>Xrcc4</i>	Promoter (38)	F: AAGGGTATGGTGGATTAG	243	YGGGYGTGTGGGGYGYGGGAGTTTTGGTTTTAGTGTGATTTT	
		R: ACTCTTCTAAATCTATTAACCTAATACTC			
Retrotransposon	<i>Line-1</i>	5'-UTR	F: TTGGTGAGTTGGGATAT R: AAATCTAAAAACAAAACTACTAC S1: TAGAATTTTTTAGGAT S2: ATAGGAAGTTTATATT	117	S1: YGGGTAYGTTTTGTGTTTAYGGAAGTT S2: YGYGGATTTYGTTYGTAGTAG

Notes. This table encompasses: CpG island's length and region, sequence, PCR set of primers and the sequence analyzed by pyrosequencing. HR = homologous recombination repair; NHEJ = non-homologous end joining; retrotransposon = *LINE-1* (long interspersed nuclear element-1).

Beta-Galactosidase Activity

Total proteins of 2×10^5 cells were extracted using RIPA buffer (25 mM Tris-HCl pH 7.6, 150 mM NaCl, 1% NP-40, 0.1% SDS, 1% sodium deoxycholate, 50 mM NaF, 1 mM EDTA) and protease inhibitors (0.2 mM PMSF, 1 mM pepstatin and 80 mM

aprotinin). Nonirradiated control and irradiated whole cell lysates (10 μ l) were incubated with 40 μ l of buffer Z (60 mM $\text{Na}_2\text{HPO}_4 \cdot 7\text{H}_2\text{O}$, 40 mM $\text{NaH}_2\text{PO}_4 \cdot \text{H}_2\text{O}$, 10 mM KCl, 1 mM $\text{MgSO}_4 \cdot 7\text{H}_2\text{O}$ and 0.3% 2-mercaptoethanol) containing 1 mg/ml X-Gal (Sigma-Aldrich) for 3 h (pH 7). Absorbance was measured at 595 nm.

TABLE 2
qPCR Primers Used in this Study Selected According to the Signaling Pathways

Signaling pathways	Gene	Sequences	Amplicon (bp)
HR	<i>Rad50</i>	F: 5'-GGCTGGGGAGGATGATTGAG-3' R: 5'-TGCTTAGTTCACGTTCCGCT-3'	156
	<i>Atm</i>	F: 5'-GACATGCCAGGGTGAAGGAA-3' R: 5'-TTCCAGTTCTCCGACTGCC-3'	108
	<i>Mre11</i>	F: 5'-TCTGTACGGCTTAGGGTCCA-3' R: 5'-TGAAGTTGGTGCTTCCGTGT-3'	155
	<i>Brcal</i>	F: 5'-CTGTGGTGAAGGAGCTTCCA-3' R: 5'-CCCAATATCAGGGCAGTCGTT-3'	107
	<i>Xrcc1</i>	F: 5'-GGAACAGTCAGAAGGACGGG-3' R: 5'-GAATTGGCAGGTCAGCCTCT-3'	191
NHEJ	<i>Lig4</i>	F: 5'-CAGTTGCTTAGTTAAAACCGGAG-3' R: 5'-GAGCACAAAGTCTGCAAAGGG-3'	103
	<i>Xrcc6</i>	F: 5'-TTGGTCAACGGGAGCTCAAC-3' R: 5'-GGGAGACATTCTTCCGGCT-3'	103
	<i>Xrcc4</i>	F: 5'-GGAGACACCGAATGCAGACA-3' R: 5'-GCCAAGCCTTTCTTCTCTCT-3'	86
L4E family of ribosomal proteins	<i>Rpl4</i>	F: 5'-GGCCTTCAGAAACATCCCTG-3' R: 5'-CCATACAACCTCACTCCCG-3'	138

Note. HR = homologous recombination repair; NHEJ = non-homologous end joining; L4E family of ribosomal proteins = housekeeping gene.

Statistical Analysis

All results were expressed as mean \pm SD. Basal gene expression, global methylation, cell viability, cell cycle and β -galactosidase activity were analyzed by the nonparametric Kruskal-Wallis test followed by Dunnett's multiple comparison test. Data regarding promoter methylation, gene expression and γ -H2AX foci were analyzed by two-way analysis of variance (ANOVA) followed by Bonferroni post-hoc test. Statistical analyses were performed using Prism v. 5 (Graphpad Software Inc., San Diego) and differences were considered statistically significant at $P < 0.05$.

RESULTS

High X-Ray Doses do not Compromise Cell Viability and Promote G₂/M Arrest

To evaluate the effects of X rays on a normal thyrocyte cell cycle, FRTL5 and PCCL3 cells were X irradiated with 1–10 Gy or treated with 20 μ M H₂O₂ (water radiolysis), and cell viability and cycle were evaluated (Fig. 1). Both cell lines remained viable after 48 h in all conditions (Fig. 1A and B). As expected, irradiation blocked cell proliferation up to 24 h (Fig. 1C and D). Cells were arrested in G₂/M phase, in a dose-dependent manner, at 24 h postirradiation compared to paired nonirradiated controls, and these events were earlier (12 vs. 24 h) and more pronounced in FRTL5 than PCCL3 after 10 Gy X-ray irradiation (PCCL3: 33% vs. 21%; FRTL5: 45% vs. 22%; $P < 0.05$) (Fig. 1E and F). In addition, exposure also diminished the percentage of cells in G₀/G₁ and S phases, with such proportions being normalized 48 h postirradiation, compared to their respective nonirradiated controls (Fig. 1E and F).

FRTL5 Cells Display a Slower Kinetics of DSB Repair than PCCL3

Since γ -H2AX and 53BP-1 are early DSB sensors (5), they were used as an indirect measure of DSB lesions. Both cell lines exhibited a peak of γ -H2AX at 1 h postirradiation, but PCCL3 restored control levels sooner than FRTL5 (6 vs. 12 h) (Fig. 2A and Supplementary Fig. S1; <http://dx.doi.org/10.1667/RR14532.1.S1>). No γ -H2AX signal was detected in PCCL3 cells at 6 h postirradiation (Supplementary Fig. S1). Accordingly, in FRTL5, γ -H2AX foci per cell reached the maximum number at 1 h postirradiation compared to the respective control (104 vs. 5), 68% repaired after 6 h (33 vs. 6), and the control levels were restored after 24 h, although few damage sites remained unrepaired (10 vs. 5) (Fig. 2). Interestingly, in PCCL3, a peak of γ -H2AX foci per cell was induced at 1 h postirradiation compared to the respective control (131 vs. 1) and the control levels were restored after 6 h (3 vs. 1) (Fig. 2). 53BP1 and γ -H2AX displayed similar expression kinetics with strong colocalization (Pearson's coefficient = 0.93) (Fig. 2C). Concerning upstream targets of the DSB-response pathway, radiation induced ATR expression and ATM (p-ATM) activation in both cell lines (Fig. 2D).

FRTL5 Cells Have Lower Basal LINE-1 Methylation than PCCL3

Since global hypomethylation is associated with genomic instability and DNA damage (9), we evaluated the *LINE-1* methylation profile of rat thyroid cells, an indirect indicator of global methylation (22), through the interrogation of seven CpG sites within a consensus region of L1 elements by pyrosequencing. Our data revealed that, compared to PCCL3, FRTL5 cells have lower *LINE-1* methylation levels (71.18 vs. 82.93%) and the latter levels were similar in different rat tissues (thyroid, breast, liver and kidney) (Fig. 3A). Surprisingly, exposure to 10 Gy did not have an effect on the *LINE-1* methylation profile of either thyroid cell line (Fig. 3C and E), even when 97% of the cells were synchronized in G₀/G₁ phase of cell cycle with TSH deprivation (Fig. 3B).

FRTL5 Cell Line Expresses Lower Basal Brcal mRNA Levels than PCCL3

We investigated the expression of DNA repair genes involved on DSB response pathways (HR and NHEJ). FRTL5 and PCCL3 cell lines showed different *Brcal* mRNA levels, which were more abundant in PCCL3 than FRTL5 cells (Fig. 4B). Conversely, no changes were observed in the expression of the other selected genes, such as *Atm*, *Rad50*, *Mre11*, *Xrcc1*, *Xrcc4*, *Xrcc6* and *Lig4* (Fig. 4A and C–H). Interestingly, DNA methylation levels of their CpG-rich promoters were null or low (0–6.5%) (Table 3).

Ionizing Radiation Affects Brcal Expression Regardless of DNA Methylation of its Promoter Region on the FRTL5 Cell Line

We investigated whether radiation could influence DNA methylation and expression of DNA repair genes. Radiation induced a decrease of up to 50% of the *Brcal* mRNA and protein levels in FRTL5 cells compared to paired-controls (1, 6 and 24 h postirradiation) (Fig. 5A and C). In PCCL3 cells, the downregulation of *Brcal* (for approximately 50%), at protein level, was also observed during the first 6 h postirradiation (Fig. 5D), although no significant differences were found at mRNA levels (Fig. 5B). No modulation of the expression of the DNA repair genes (*Atm*, *Rad50*, *Mre11*, *Xrcc1*, *Xrcc4*, *Xrcc6* and *Lig4*) was observed, at least at the transcriptional level (Supplementary Fig. S2; <http://dx.doi.org/10.1667/RR14532.1.S1>). Moreover, the CpG sites within the promoter region of all the selected genes were not altered by radiation (Supplementary Table S1; <http://dx.doi.org/10.1667/RR14532.1.S1>), even when FRTL5 cells were synchronized at the G₀/G₁ phase of the cell cycle (Supplementary Table S2; <http://dx.doi.org/10.1667/RR14532.1.S1>). These results suggest that DNA methylation of the promoter region of HR and NHEJ genes is not influenced by radiation.

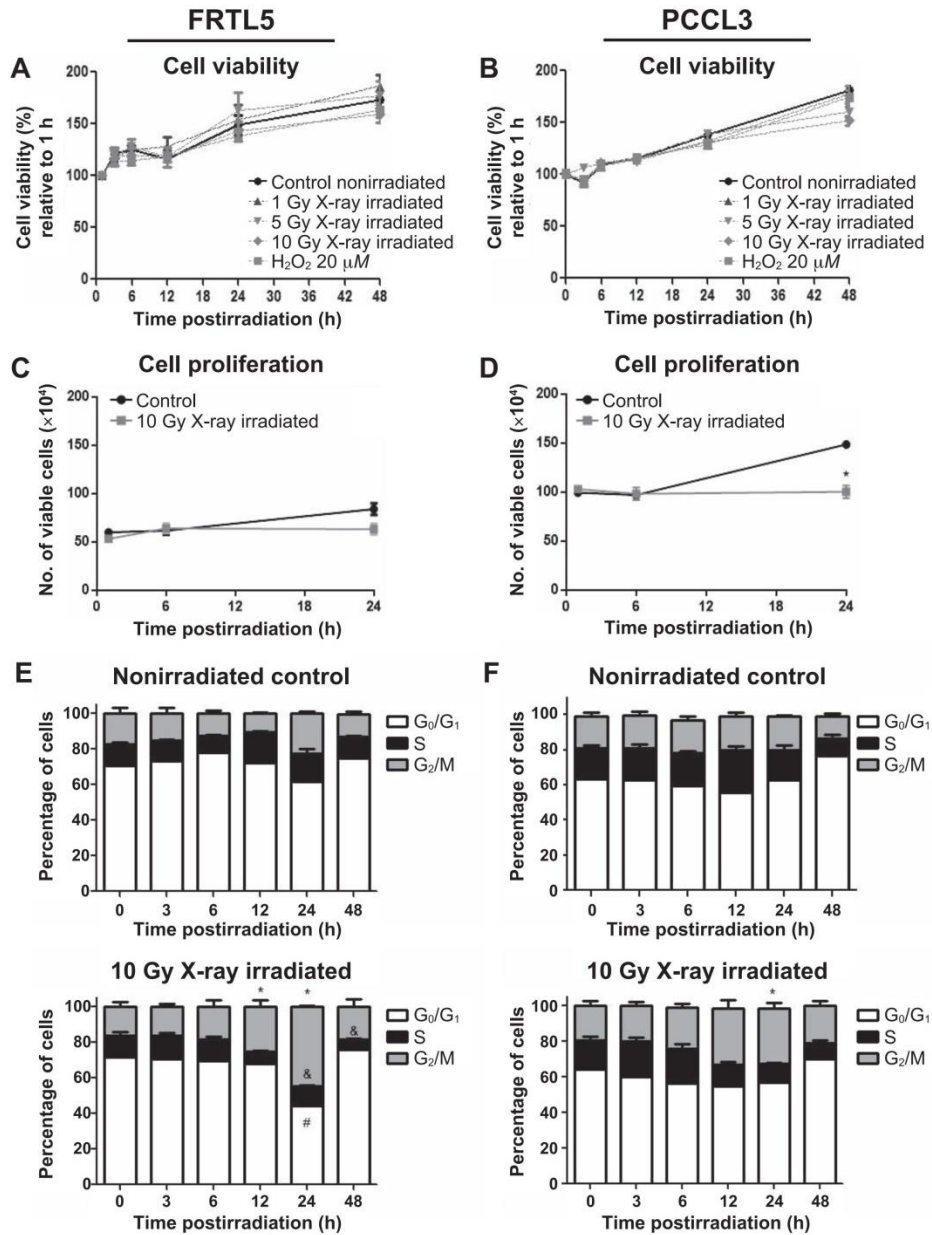


FIG. 1. Cytotoxicity and cell cycle profile of FRTL5 and PCCL3 cell lines after X-ray irradiation. FRTL5 and PCCL3 cell lines were X-ray irradiated with 1–10 Gy or treated with 20 μM H₂O₂ (water radiolysis), and cell viability and proliferation, as well as cell cycle, were evaluated. Panels A and B: Cell viability of FRTL5 and PCCL3, respectively. Panels C and D: Cell proliferation of FRTL5 and PCCL3, respectively. Panels E and F: Cell cycle of FRTL5 and PCCL3, respectively. All determinations were made in triplicates of three independent experiments and the results were expressed as: relative to nonirradiated control cells (black line) or irradiated in initial time (1 h) (dotted gray lines) for cell viability; number of viable cells ($\times 10^4$) cells for cell proliferation; percentage of cells in G₀/G₁ (white bar), S (black bars) and G₂/M (gray bars) compared to their respective nonirradiated controls for each cell cycle. * $P < 0.05$ compared to G₂/M phase for nonirradiated control; # $P < 0.05$ compared to S phase for nonirradiated control, & $P < 0.05$ compared to G₀/G₁ phase for nonirradiated control.

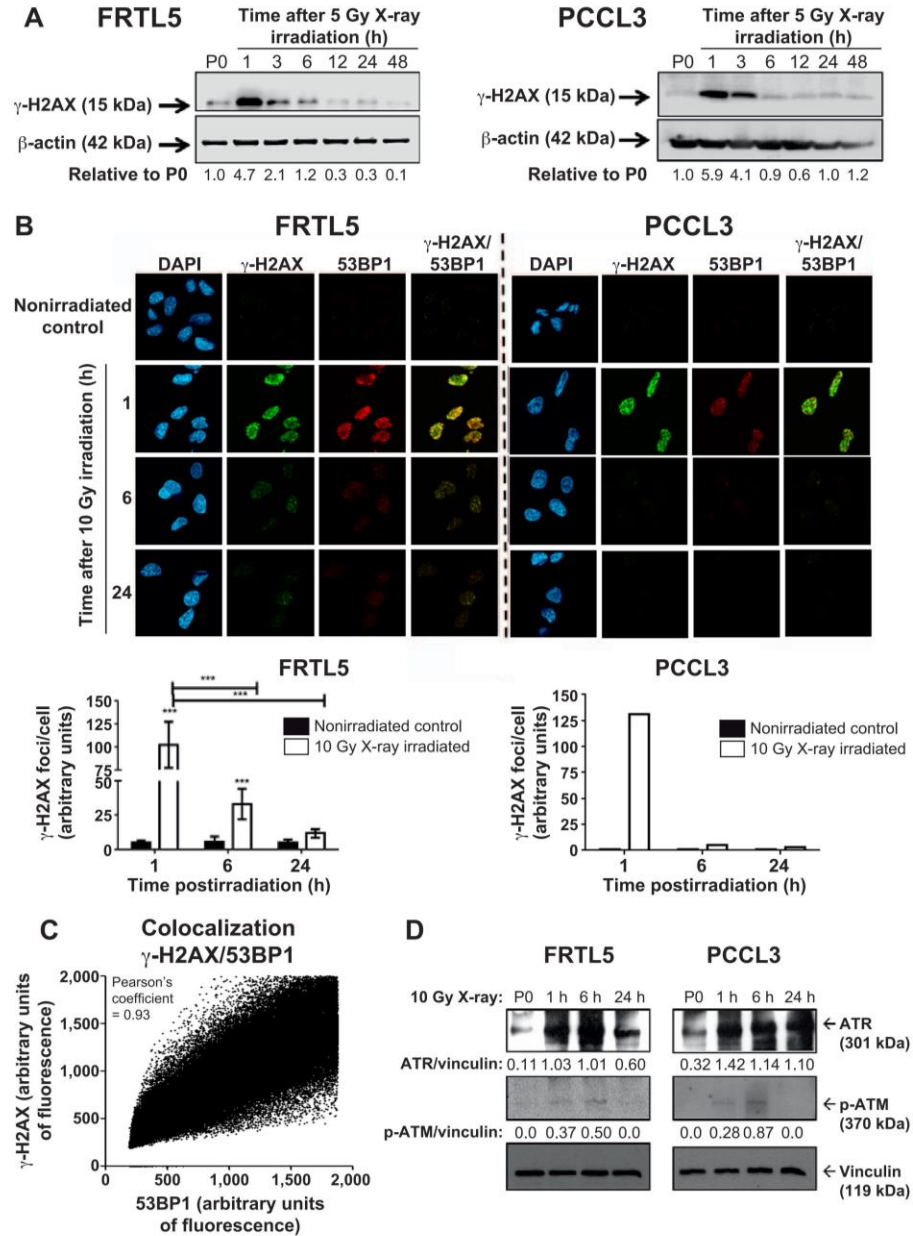


FIG. 2. Double-strand break (DSB) repair kinetics of FRTL5 and PCCL3 cells. Panel A: Representative γ -H2AX immunoblots of irradiated thyroid cells at 1–48 h postirradiation. Intensity quantification was relative to the starting point (0 h) (P0). Panel B: Immunofluorescence of nonirradiated control and irradiated FRTL5 and PCCL3 cells stained with anti- γ -H2AX (green) and 53BP1 (red). Nuclei were counterstained with DAPI (blue). In parallel, the number of γ -H2AX foci per cell was determined as an average of the total foci number per cell per field. Panel C: Foci colocalization of γ -H2AX and 53BP1. Panel D: Representative p-ATM and ATR immunoblots of irradiated thyroid cells at 1, 6 and 24 h postirradiation. Absolute intensity quantification was calculated as ratio target: vinculin. Beta-actin and vinculin were used as loading control. *** $P < 0.001$ compared to nonirradiated control.

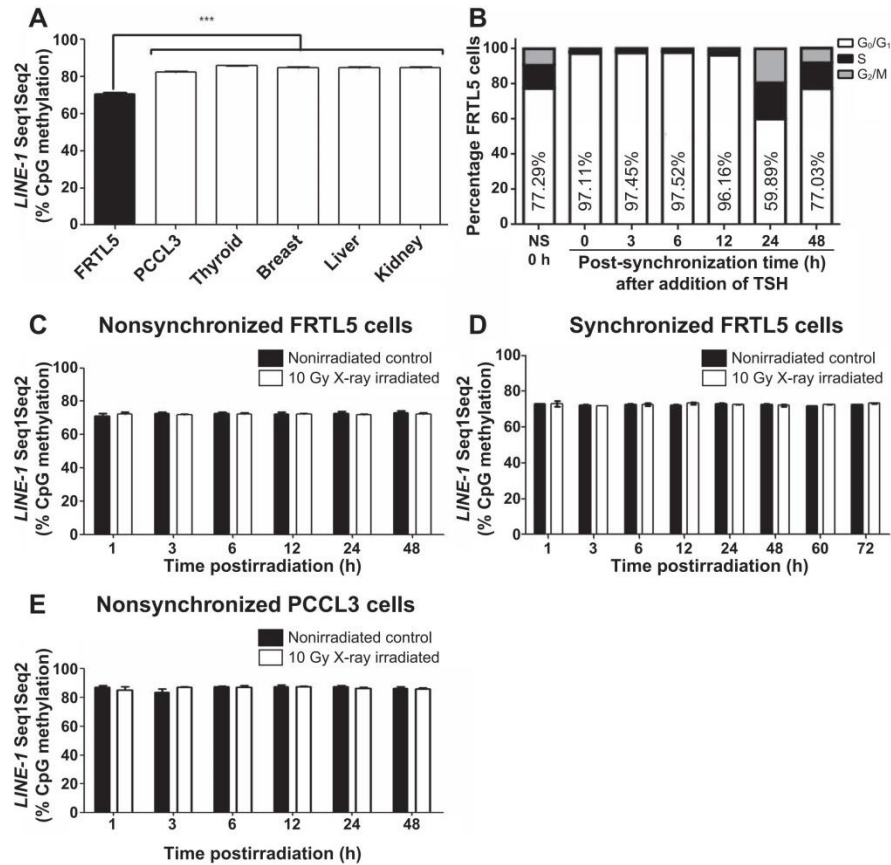


FIG. 3. Global methylation of thyroid cell lines. Panel A: *LINE-1* pyrosequencing of FRTL5 and PCCL3 cell lines. Rat tissues (thyroid, breast, liver and kidney) were used as control. Panel B: Synchronization of FRTL5 cells in G₀/G₁-phase cell cycle was performed by starving cells of thyrotropin (TSH) for 72 h, and then adding TSH to the media, after which the cells were monitored for three days. NS = nonsynchronized. Panels C–E: *LINE-1* pyrosequencing. Nonsynchronized and synchronized FRTL5 cell lines (panels C and D, respectively), and nonsynchronized PCCL3 cell lines (panel E) are shown for both nonirradiated paired control and 10 Gy X-ray irradiated cells. The results are expressed as percentage of cells that displayed methylation on seven selected CpG sites within L1 elements. *** $P < 0.001$.

Chronic Exposure caused Senescent Phenotype to occur in FRTL5 Cells

We established a chronic exposure model with the FRTL5 cell line. Figure 6 shows that the number of viable irradiated cells reached a plateau after the second radiation treatment, while the number of viable paired nonirradiated control cells increased with time (Fig. 6A). Accordingly, radiation induced a gain in β -galactosidase activity (Fig. 6B) and promoted morphological changes (flattened, elongated and enlarged cell shape) (Fig. 6C), suggesting a radiation-inducible senescence phenotype. Moreover, no *LINE-1* methylation changes were observed in irradiated cells (Fig. 6D).

Chronic Radiation Exposure Promotes Upregulation of HR and NHEJ Genes in the FRTL5 Cell Line

When assessing the long-term effect of exposure on DNA repair gene expression, we observed an upregulation of all HR and NHEJ DNA repair genes, selected for this study, after the fifth radiation treatment (25 Gy) (Fig. 7). In addition, a transient increment of mRNA levels of *Brcal*, *Mre11*, *Xrcc1* and *Xrcc4* was also detected after the third radiation treatment (15 Gy) (Fig. 7B, D–F, H). These data indicate that radiation-induced senescence elicits an activation of HR and NHEJ genes in the FRTL5 cell line.

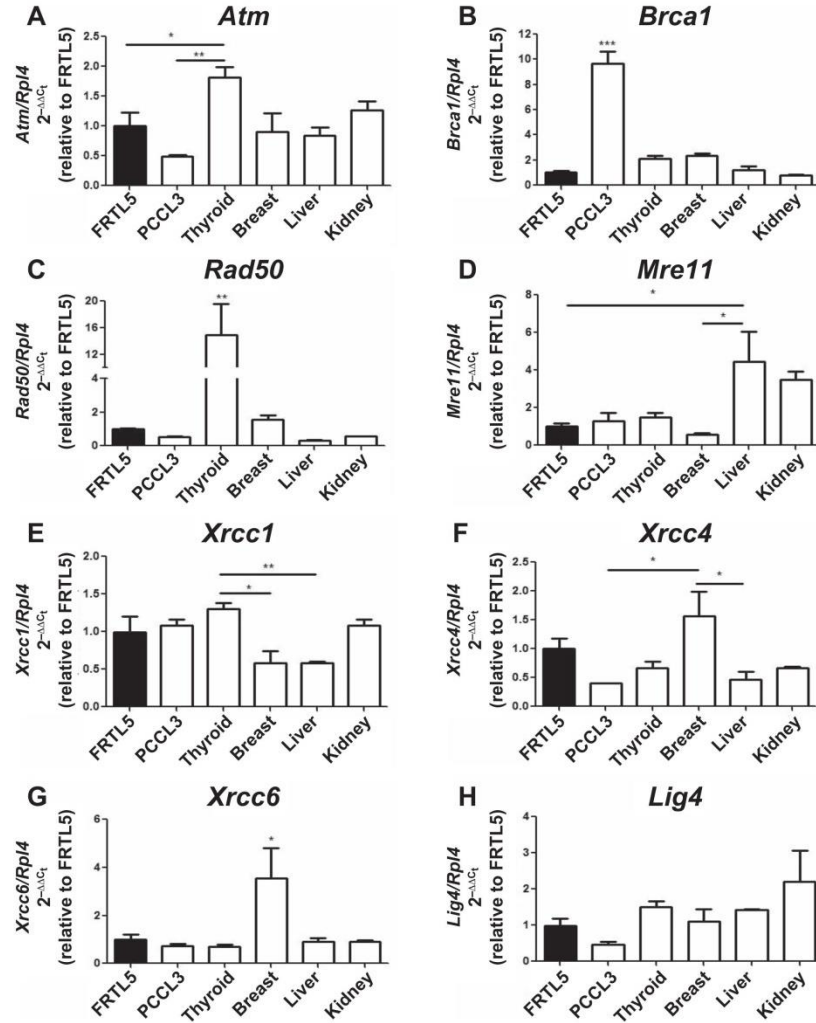


FIG. 4. Basal expression of double-strand break (DSB) genes in thyroid cell lines. Relative mRNA expression levels are shown according to DNA repair pathways of FRTL5 and PCCL3 cell lines: HR (panels A–E) and NHEJ (panels F–H). Expression levels are relative to the FRTL5 cell line. Rat tissues (thyroid, breast, liver and kidney) were used as control. * $P < 0.05$; ** $P < 0.01$.

TABLE 3
Basal Promoter Methylation Profiles of HR and NHEJ Genes

	Percentage CpG methylation (average)							
	<i>Atm</i>	<i>Brca1</i>	<i>Rad50</i>	<i>Mre11</i>	<i>Xrcc1</i>	<i>Xrcc4</i>	<i>Xrcc6</i>	<i>Lig4</i>
FRTL5	0.00 ± 0.0	2.10 ± 2.1	1.05 ± 0.9	0.00 ± 0.0	4.36 ± 1.9	0.00 ± 0.0	0.61 ± 0.5	6.5 ± 0.5
PCCL3	2.59 ± 0.5	0.92 ± 0.9	0.44 ± 0.8	0.00 ± 0.0	0.95 ± 0.3	0.00 ± 0.0	3.08 ± 0.4	2.00 ± 0.0
Thyroid	1.31 ± 1.3	1.83 ± 0.4	3.88 ± 0.7	0.00 ± 0.0	1.09 ± 0.5	0.00 ± 0.0	0.00 ± 0.0	2.00 ± 0.0
Breast	0.00 ± 0.0	1.42 ± 1.3	2.66 ± 0.0	0.00 ± 0.0	1.03 ± 0.2	0.00 ± 0.0	0.44 ± 0.8	3.50 ± 1.5
Liver	0.00 ± 0.0	2.83 ± 1.1	2.11 ± 1.00	0.00 ± 0.0	0.75 ± 0.3	0.00 ± 0.0	0.50 ± 0.9	2.17 ± 0.3
Kidney	1.57 ± 2.7	1.75 ± 0.3	3.11 ± 1.3	0.00 ± 0.0	0.98 ± 0.5	0.00 ± 0.0	0.00 ± 0.0	4.50 ± 0.9

Notes. Pyrosequencing of HR (*Atm*, *Brca1*, *Rad50*, *Mre11* and *Xrcc1*) and NHEJ genes (*Xrcc4*, *Xrcc6* and *Lig4*) were performed on nonexposed thyroid cell lines (FRTL5 and PCCL3) and rat tissues (thyroid, breast, liver and kidney). The results were expressed as percentage of cells that displayed methylation on selected CpG sites ±SD.

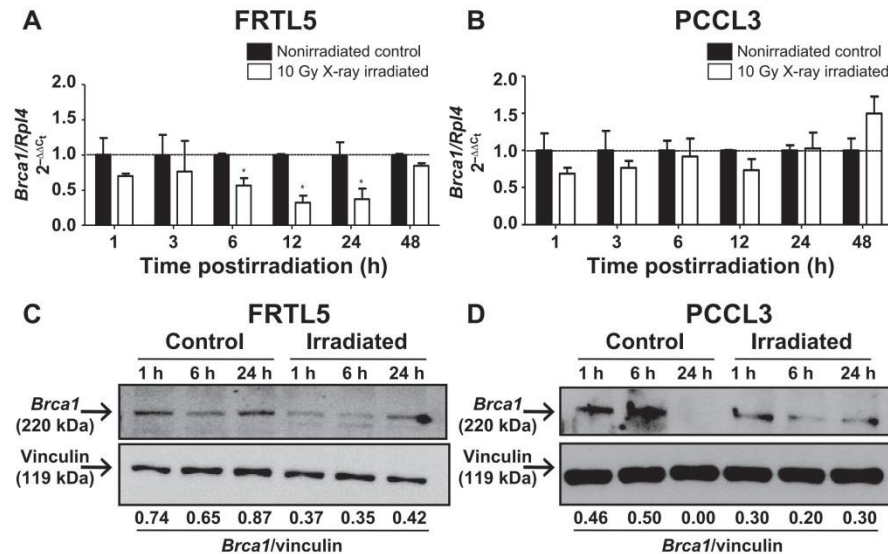


FIG. 5. Expression of *Brca1* gene after acute 10 Gy X-ray irradiation in FRTL5 and PCCL3 cell lines. Cells were irradiated (white bars) and *Brca1* mRNA levels evaluated in FRTL5 and PCCL3 cell lines (panels A and B, respectively). Expression levels were relative to paired nonirradiated controls (black bars). Representative *Brca1* immunoblots are shown for irradiated FRTL5 and PCCL3 thyroid cells (panels C and D, respectively) at 1, 6 and 24 h postirradiation. Vinculin was used as a loading control. Absolute intensity quantification was calculated as ratio *Brca1*/vinculin. * $P < 0.05$.

DISCUSSION

In this study, we demonstrate that radiation exposure promotes G_2/M arrest in two differentiated thyroid cell lines, in agreement with what has been previously reported by Green *et al.* (23), using the FRTL5 cell line. However, radiation-induced cell cycle arrest was more pronounced in the FRTL5 than PCCL3 cell line, which may be explained by the higher proliferation rate of FRTL5 (24) with respect to PCCL3. Our data also reveal that normal rat thyroid cells respond quickly to radiation insults, and repair them within a few hours, in agreement with previously reported results in human primary thyrocytes (25). Therefore, FRTL5 and PCCL3 are potentially suitable models for elucidating DNA repair in the thyroid. Above all, FRTL5 cells repaired radiation-induced DSB later than PCCL3 and, as a result, these cells are prone to accumulate DNA damages.

As for upstream targets of the DSB-response pathway, the expression of ATR and p-ATM revealed significant differences in the capacity for DNA repair between these two cell lines. In PCCL3 cells, ATM phosphorylation was much higher than FRTL5 cells at 6 h postirradiation, while ATR expression was higher in FRTL5 than PCCL3 cells at 1–6 h postirradiation. These kinases play an essential role in the maintenance of genomic integrity as well as act as barriers during early tumorigenesis (26). Interestingly, even though ATM and ATR share some downstream effectors, they are activated in response to different types of lesions (26). While ATM is primarily involved in double-strand

break pathways, ATR responds to a broader spectrum of DNA damages, especially those that interfere with DNA replication. Thus, these data could be linked to the delayed DSB repair in FRTL5 cells and to the differential *Brca1* expression in the thyroid cell lines.

Our findings also demonstrate that FRTL5 cells have a lower *LINE-1* methylation level compared to PCCL3 and thyroid tissue. *LINE-1* methylation levels have been widely used as a surrogate marker for global methylation status in cancer, not only due to the abundance of such elements, but also due to its ability to distinguish normal tissue from tumor tissue (22). In addition, it has been shown that decreased *LINE-1* methylation levels can already be observed in early stages of tumor development (27) and associated with an increased risk of cancer development (28). Global hypomethylation is commonly related to genomic instability and transformation of normal cells into cancer cells (9, 29), and is also crucial in thyroid cancer progression (11). Therefore, FRTL5 cells appear to be more susceptible to genomic instability and malignant transformation than PCCL3 cells, as previously reported (15). Since radiation was not capable of modulating *LINE-1* methylation levels in FRTL5 and PCCL3 cells, even when cells were synchronized, we could hypothesize a protective mechanism was in place to maintain cell viability. In fact, treatment with the demethylating agent 5-aza-2'-deoxycytidine compromises human thyroid cancer cell viability (30). Interestingly, FRTL5 cells express lower *Brca1* levels than PCCL3, and irradiation caused a drastic decrease in the

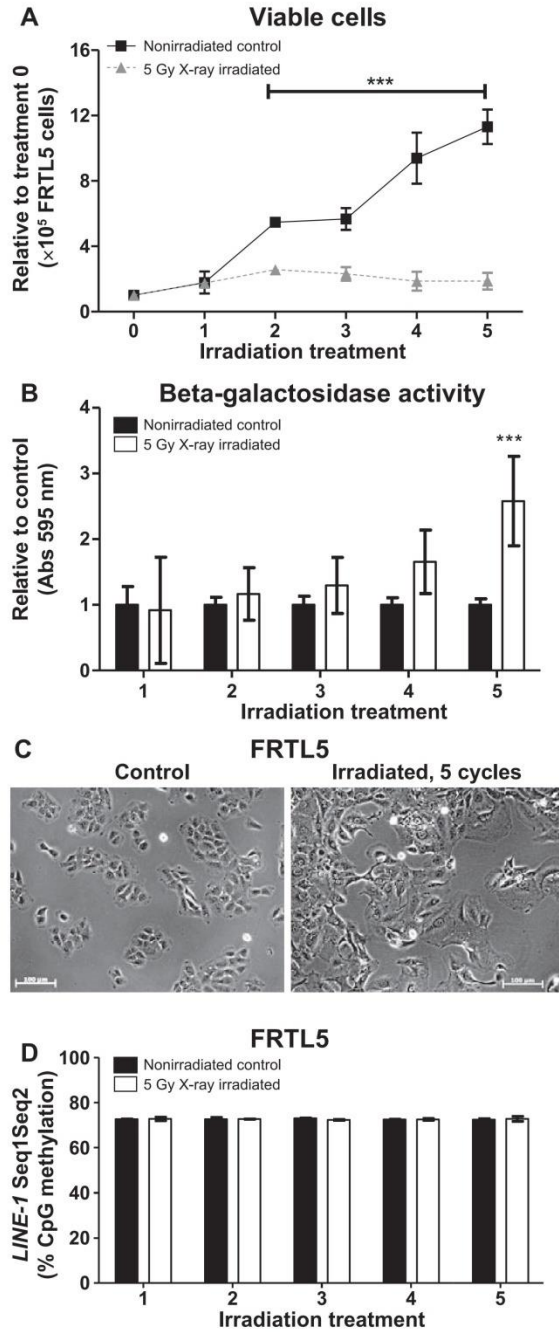


FIG. 6. Characterization of the chronic X-ray exposure model in a FRTL5 cell line. Cells received five treatments of 5 Gy with 2–3 day intervals between each exposure and assessed for cell viability (panel A), β -galactosidase activity (panel B), morphology (panel C) and *LINE-1* methylation (D). *** $P < 0.001$.

expression of this gene in FRTL5 cells. In fact, the transient inhibition of *Brcal* expression could cause premature inactivation of the mitotic checkpoint, which exerts an important role on genomic integrity, in MCF7 cells (31). Taking into account that *Brcal* is fundamental for homologous recombination repair (32), we might expect that FRTL5 cells intrinsically have less efficient DNA DSB repair machinery. Indeed, gradual loss of DNA repair genes and the accumulation of DNA damages are early steps of the carcinogenesis process in several solid tumors (6), including PTC (33).

We established a chronic radiation exposure model using the FRTL5 cell line to investigate the effects of chronic exposure on thyrocytes. In contrast to our observations with acute exposure, when FRTL5 cells were chronically exposed to radiation, a transcription activation of DNA repair genes was triggered. The striking difference between these models is that in the first one, cells maintain the capacity to proliferate, while in the latter, they become senescent. In fact, unrepaired damage and, consequently, DNA damage signaling persistence result in senescence (34). Evasion of senescence, in turn, could give rise to post-senescent transformed and mutated precancerous cells (35). Since radiation exposure is the most important risk factor for PTC (18), we hypothesize that there is a mechanism by which the upregulation of DNA repair machinery maintains the viability of senescent thyroid cells and, therefore, favors the accumulation of mutations that would cause cells to become susceptible to senescence evasion and transformation.

In conclusion, we report a differential HR and NHEJ gene expression in response to exposure in thyroid cells, depending on the proliferation and senescence status. Our results also suggest that intrinsic *LINE-1* hypomethylation and decreased expression of *Brcal* after acute radiation exposure, as well as the upregulation of DSB repair machinery in radiation-induced senescent cells, could lead to the accumulation of gene mutations and favor thyroid cell transformation. However, further studies are required to more fully elucidate the biological relevance of HR and NHEJ genes to thyroid carcinogenesis.

SUPPLEMENTARY INFORMATION

Fig. S1. Double-strand break repair kinetics of PCCL3. PCCL3 cells X-ray irradiated with 1, 5 and 10 Gy, and after 1, 3 and 6 h, γ -H2AX and total H2AX immunoblots were performed on nonirradiated control and irradiated cells. As a positive DSB damage control, cells were treated with 20–500 μ M H_2O_2 . Intensity quantification was relative to control (panel C). Beta-actin was used a loading control.

Fig. S2. Expression of HR and NHEJ genes after 10 Gy X-ray irradiation in a FRTL5 cell line. At 1–48 h postirradiation (white bars), mRNA levels of DSB DNA repair genes were evaluated. Expression levels were relative to paired nonirradiated control (black bars). * $P < 0.05$.

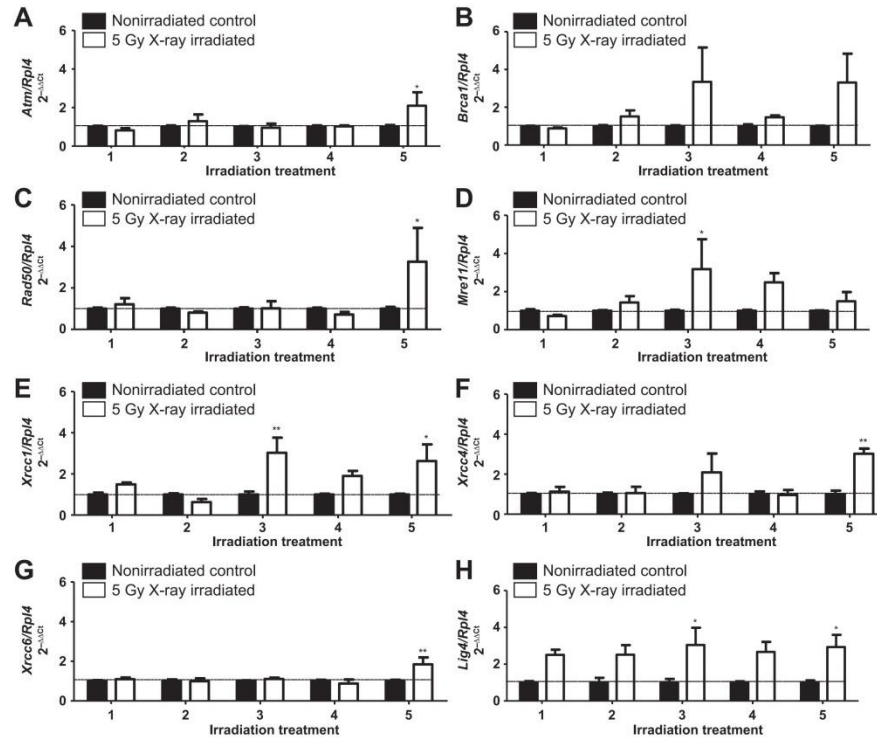


FIG. 7. HR and NHEJ gene expression in FRTL5 cell line after chronic X-ray exposure. Cells received five treatments of 5 Gy (white bars) with 2–3 h intervals between each exposure and relative mRNA expression levels according to DNA repair pathways were evaluated: HE (panels A–E) and NHEJ (panels F–H). Expression levels were relative to paired nonirradiated controls (black bars). * $P < 0.05$; ** $P < 0.01$.

Table S1. Promoter methylation profiles of HR and NHEJ genes in an irradiated FRTL5 cell line. Pyrosequencing of HR (*Atm*, *Bcl2l1*, *Rad50*, *Mre11* and *Xrcc1*) and NHEJ genes (*Xrcc4*, *Xrcc6* and *Lig4*) was performed on a 10 Gy X-ray irradiated and paired nonirradiated control FRTL5 cell line. The results were expressed as percentage of cells that displayed methylation on selected CpG sites \pm SD. * $P < 0.05$ (time).

Table S2. Promoter methylation profiles of HR and NHEJ genes in a synchronized FRTL5 cell line. Pyrosequencing of HR (*Atm*, *Bcl2l1*, *Rad50*, *Mre11* and *Xrcc1*) and NHEJ genes (*Xrcc4*, *Xrcc6* and *Lig4*) was performed on a 10 Gy X-ray irradiated and paired nonirradiated control FRTL5 cell line, previously synchronized on G₀/G₁ cell cycle phase. The results were expressed as percentage of cells that displayed methylation on selected CpG sites \pm SD.

ACKNOWLEDGMENTS

This study was supported by CAPES, CNPQ and FAPERJ. AF is “Bolsista Capes”.

Received: May 31, 2016; accepted: April 28, 2017; published online: June 2, 2017

REFERENCES

- DeLellis RA, Lloyd RV, Heitz PU. World Health Organization Classification of Tumours. Pathology and genetics of tumours of endocrine organs. Lyon (France): IARC Press; 2004.
- LiVolsi VA. Papillary thyroid carcinoma: an update. *Mod Pathol* 2011; 24:S1–9.
- Pacini F, Vorontsova T, Demidchik EP, Molinaro E, Agate L, Romei C, et al. Post-Chernobyl thyroid carcinoma in Belarus children and adolescents: comparison with naturally occurring thyroid carcinoma in Italy and France. *J Clin Endocrinol Metab* 1997; 82:3563–9.
- Caudill CM, Zhu Z, Ciampi R, Stringer JR, Nikiforov YE. Dose-dependent generation of RET/PTC in human thyroid cells after in vitro exposure to gamma-radiation: a model of carcinogenic chromosomal rearrangement induced by ionizing radiation. *J Clin Endocrinol Metab* 2005; 90:2364–9.
- Grabarz A, Barascu A, Guirouilh-Barbat J, Lopez BS. Initiation of DNA double strand break repair: signaling and single-stranded resection dictate the choice between homologous recombination, non-homologous end-joining and alternative end-joining. *Am J Cancer Res* 2012; 2:249–68.
- Bartkova J, Horejsí Z, Koed K, Krämer A, Tort F, Zieger K, et al. DNA damage response as a candidate anti-cancer barrier in early human tumorigenesis. *Nature* 2005; 434:864–70.
- Baylin SB, Jones PA. A decade of exploring the cancer epigenome - biological and translational implications. *Nat Rev Cancer* 2011; 11:726–34.

8. Lima SC, Hernández-Vargas H, Simão T, Durand G, Kruel CD, Le Calvez-Kelm F, et al. Identification of a DNA methylome signature of esophageal squamous cell carcinoma and potential epigenetic biomarkers. *Epigenetics* 2011; 6:1217–27.
9. Weidman JR, Dolinoy DC, Murphy SK, Jirtle RL. Cancer susceptibility: epigenetic manifestation of environmental exposures. *Cancer J* 2007; 13:9–16.
10. Antwih DA, Gabbara KM, Lancaster WD, Ruden DM, Zielske SP. Radiation-induced epigenetic DNA methylation modification of radiation-response pathways. *Epigenetics* 2013; 8:839–48.
11. Ellis RJ, Wang Y, Stevenson HS, Boufraqech M, Patel D, Nilubol N, et al. Genome-wide methylation patterns in papillary thyroid cancer are distinct based on histological subtype and tumor genotype. *J Clin Endocrinol Metab* 2014; 99:E329–37.
12. Guan H, Ji M, Hou P, Liu Z, Wang C, Shan Z, et al. Hypermethylation of the DNA mismatch repair gene hMLH1 and its association with lymph node metastasis and T1799A BRAF mutation in patients with papillary thyroid cancer. *Cancer* 2008; 113:247–55.
13. Smith JA, Fan CY, Zou C, Bodenner D, Kokoska MS. Methylation status of genes in papillary thyroid carcinoma. *Arch Otolaryngol Head Neck Surg* 2007; 133:1006–11.
14. Agrawal N, Akbani R, Aksoy BA, Ally A, Arachchi H, Asa SL, et al. Integrated genomic characterization of papillary thyroid carcinoma. *Cell* 2014; 159:676–90.
15. Fusco A, Berlingieri MT, Di Fiore PP, Portella G, Grieco M, et al. One- and two-step transformations of rat thyroid epithelial cells by retroviral oncogenes. *Mol Cell Biol* 1987; 7:3365–70.
16. Ameziane-El-Hassani R, Boufraqech M, Lagente-Chevallier O, Weyemi U, Talbot M, Métivier D, et al. *Cancer Res* 2010; 70:4123–32.
17. Degrassi A, Monaco MC, Lisignoli G, Belvedere O, Toneguzzi S, Malangone W, et al. Cell cycle synchronization of FRTL5 cells. A physiological model system. *J Exp Clin Cancer Res* 1998; 17:527–32.
18. Ron E, Lubin JH, Shore RE, Mabuchi K, Modan B, Pottern LM, et al. Thyroid cancer after exposure to external radiation: a pooled analysis of seven studies. *Radiat Res* 1995; 141:259–77.
19. Hamm CA, Xie H, Costa FF, Vanin EF, Sefter EA, Sredni ST, et al. Global demethylation of rat chondrosarcoma cells after treatment with 5-aza-2'-deoxycytidine results in increased tumorigenicity. *PLoS One* 2009; 4:e8340.
20. Crooks GE, Hon G, Chandonia JM, Brenner SE. WebLogo: A sequence logo generator. *Genome Res* 2004; 14:1188–90.
21. Schmittgen TD, Livak KJ. Analyzing real-time PCR data by the comparative C(T) method. *Nat Protoc* 2008; 3:1101–08.
22. Nüsgen N, Goering W, Dauksa A, Biswas A, Jamil MA, Dimitriou I, et al. Inter-locus as well as intra-locus heterogeneity in LINE-1 promoter methylation in common human cancers suggests selective demethylation pressure at specific CpGs. *Clin Epigenetics* 2015; 7:17.
23. Green LM, Murray DK, Bant AM, Kazarians G, Moyers MF, Nelson GA, et al. Response of thyroid follicular cells to gamma irradiation compared to proton irradiation. I. Initial characterization of DNA damage, micronucleus formation, apoptosis, cell survival, and cell cycle phase redistribution. *Radiat Res* 2001; 155:32–42.
24. Kimura T, Van Keymeulen A, Golstein J, Fusco A, Dumont JE, Roger PP. Regulation of thyroid cell proliferation by TSH and other factors: a critical evaluation of in vitro models. *Endocr Rev* 2001; 22:631–56.
25. Galleani J, Miranda C, Pierotti MA, Greco A. H2AX phosphorylation and kinetics of radiation-induced DNA double strand break repair in human primary thyrocytes. *Thyroid* 2009; 19:257–64.
26. Maréchal A, Zou L. DNA damage sensing by the ATM and ATR kinases. *Cold Spring Harb Perspect Biol* 2013; 5:a012716.
27. Park SY, Seo AN, Jung HY, Gwak JM, Jung N, Cho NY, Kang GH. Alu and LINE-1 hypomethylation is associated with HER2 enriched subtype of breast cancer. *PLoS One* 2014; 9:e100429.
28. Kamiyama H, Suzuki K, Maeda T, Koizumi K, Miyaki Y, Okada S, et al. DNA demethylation in normal colon tissue predicts predisposition to multiple cancers. *Oncogene* 2012; 31:5029–37.
29. Kovalchuk O, Baulch JE. Epigenetic changes and non-targeted radiation effects – is there a link? *Environ Mol Mutagen* 2008; 49:16–25.
30. Dom G, Galdo VC, Tarabichi M, Tomás G, Hébrant A, Andry G, et al. 5-aza-2'-deoxycytidine has minor effects on differentiation in human thyroid cancer cell lines, but modulates genes that are involved in adaptation in vitro. *Thyroid* 2013; 23:317–28.
31. Chabaliere C, Lamare C, Racca C, Privat M, Valette A, Larminat F. BRCA1 downregulation leads to premature inactivation of spindle checkpoint and confers paclitaxel resistance. *Cell Cycle* 2006; 5:1001–7.
32. Caestecker KW, Van de Walle GR. The role of BRCA1 in DNA double-strand repair: past and present. *Exp Cell Res* 2013; 319:575–87.
33. Leprat F, Alapetite C, Rosselli F, Ridet A, Schlumberger M, Sarasin A, et al. Impaired DNA repair as assessed by the “comet” assay in patients with thyroid tumors after a history of radiation therapy: a preliminary study. *Int J Radiat Oncol Biol Phys* 1998; 40:1019–26.
34. Klement K, Goodarzi AA. DNA double strand break responses and chromatin alterations within the aging cell. *Exp Cell Res* 2014; 329:42–52.
35. Nassour J, Martien S, Martin N, Deruy E, Tomellini E, Malaquin N, et al. Defective DNA single-strand break repair is responsible for senescence and neoplastic escape of epithelial cells. *Nat Commun* 2016; 7:10399.

4.1.1 DADOS SUPLEMENTARES DO ARTIGO 1

(PENHA *ET AL.* RADIATION RESEARCH, V. 188, N. 2, P. 144-155, AUG 2017)

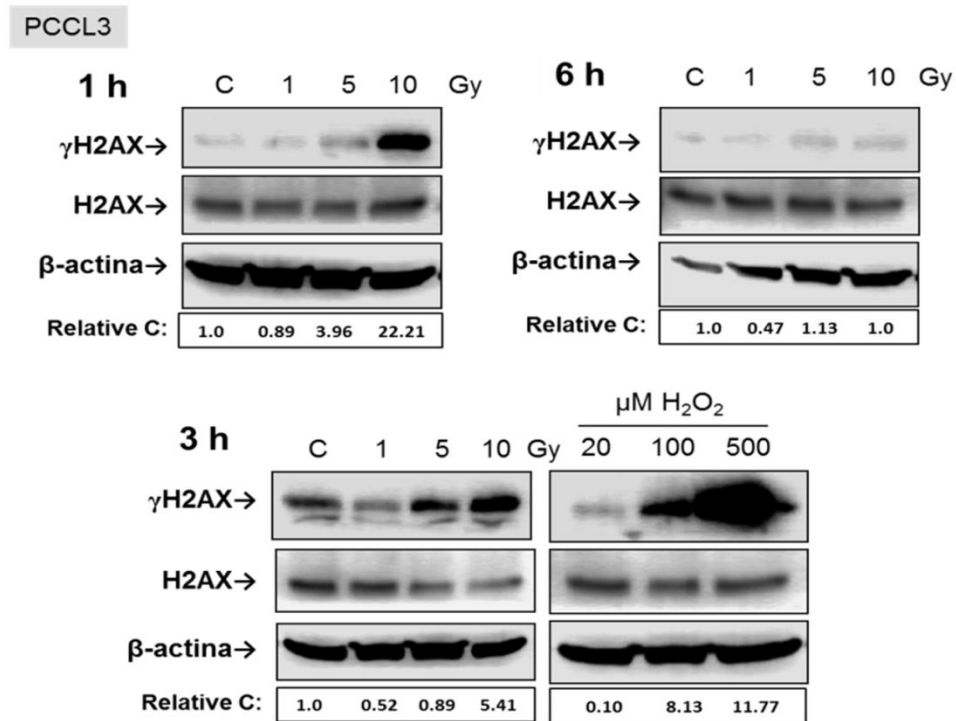


Fig. S1. Double-strand break repair kinetics of PCCL3. PCCL3 cells X-ray irradiated with 1, 5 and 10 Gy, and after 1, 3 and 6 h, γ H2AX and total H2AX immunoblots were performed on nonirradiated control and irradiated cells. As a positive DSB damage control, cells were treated with 20–500 μ M H₂O₂. Intensity quantification was relative to control (panel C). Beta-actin was used a loading control.

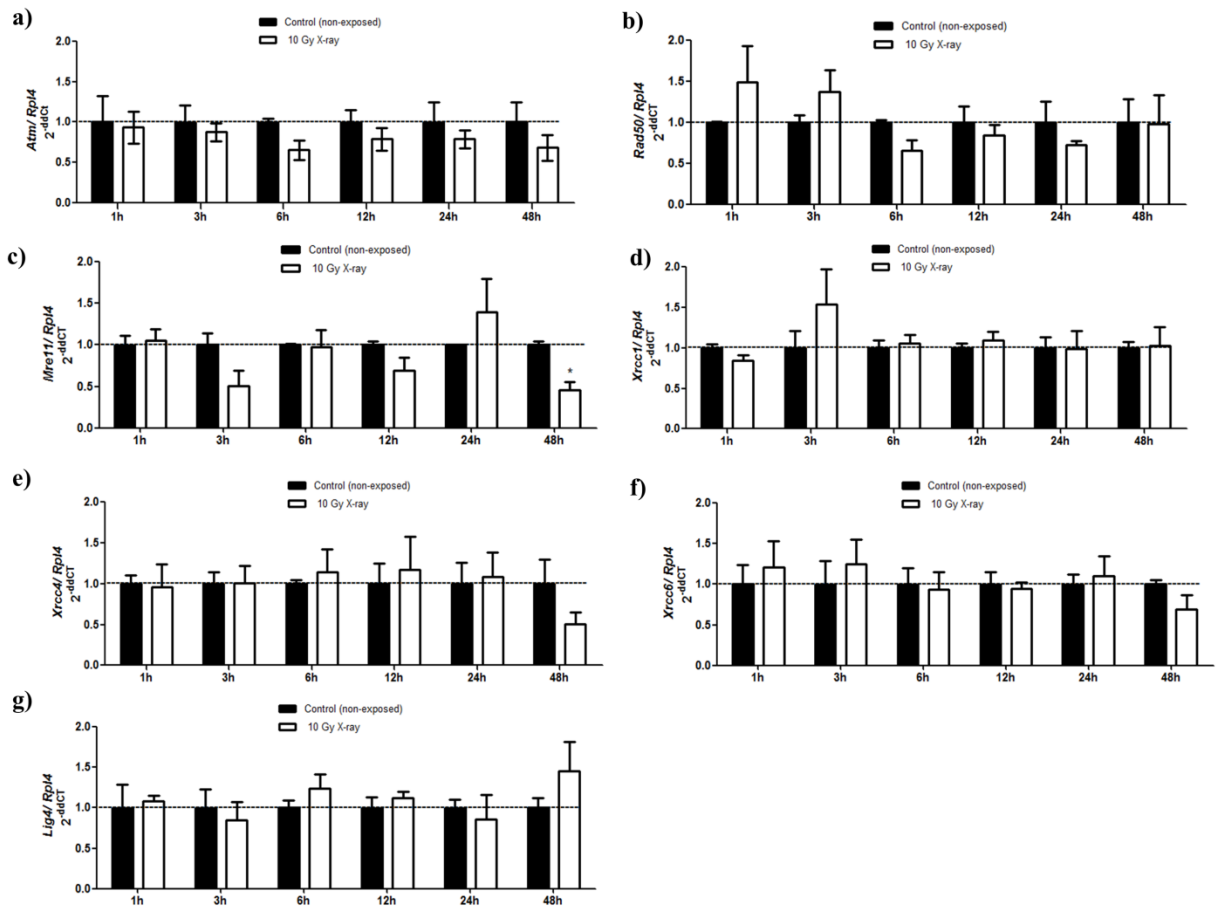


Fig.S2. Expression of HR and NHEJ genes after 10 Gy X-ray irradiation in a FRTL5 cell line. At 1–48 h postirradiation (white bars), mRNA levels of DSB DNA repair genes were evaluated. Expression levels were relative to paired nonirradiated control (black bars). *P < 0.05.

Table S1. Promoter methylation profiles of HR (homologous repair) and NHEJ (non-homologous end joining repair) genes in irradiated FRTL5 cell line.

*p < 0.5	% CPG METHYLATION (AVERAGE)															
	Atm*		Brca1*		Rad50*		Mre11		Xrcc1*		Xrcc4		Xrcc6*		Lig4*	
	Control	10 Gy	Control	10 Gy	Control	10 Gy	Control	10 Gy	Control	10 Gy	Control	10 Gy	Control	10 Gy	Control	10 Gy
1H	2.32 ± 0.77	2.01 ± 1.16	0.93 ± 0.91	2.19 ± 2.11	1.56 ± 1.62	5.51 ± 4.87	0.00 ± 0.00	0.00 ± 0.00	0.73 ± 0.37	1.92 ± 2.10	0.90 ± 1.45	0.96 ± 0.93	2.85 ± 0.42	4.91 ± 2.65	7.54 ± 1.54	9.39 ± 2.70
3H	2.11 ± 0.56	1.24 ± 1.25	1.24 ± 0.73	0.66 ± 0.93	1.57 ± 1.49	2.36 ± 1.67	0.00 ± 0.00	0.00 ± 0.00	0.22 ± 0.50	0.33 ± 0.45	0.32 ± 0.72	0.00 ± 0.00	2.72 ± 0.40	2.14 ± 1.34	7.48 ± 0.71	7.74 ± 0.52
6H	1.68 ± 1.00	2.02 ± 1.08	1.27 ± 0.79	1.19 ± 0.74	1.43 ± 1.47	1.37 ± 1.46	0.00 ± 0.00	0.00 ± 0.00	0.10 ± 0.22	0.33 ± 0.31	0.00 ± 0.00	0.40 ± 0.60	2.96 ± 0.63	3.17 ± 1.11	7.82 ± 1.03	8.09 ± 0.75
12H	2.06 ± 1.69	2.15 ± 0.16	2.62 ± 1.27	0.77 ± 1.07	4.85 ± 4.21	0.83 ± 1.14	0.00 ± 0.00	0.00 ± 0.00	2.13 ± 2.13	0.33 ± 0.45	0.80 ± 1.12	0.00 ± 0.00	3.98 ± 1.14	3.12 ± 0.50	9.61 ± 2.52	8.40 ± 1.25
24H	2.91 ± 1.55	1.48 ± 0.62	2.53 ± 1.75	0.55 ± 0.76	6.41 ± 3.38	0.95 ± 1.33	0.00 ± 0.00	0.00 ± 0.00	2.46 ± 1.85	0.29 ± 0.42	1.40 ± 1.64	0.30 ± 0.68	5.85 ± 2.49	3.31 ± 0.69	10.65 ± 1.96	7.86 ± 0.64
48H	3.10 ± 1.30	1.66 ± 1.32	1.95 ± 1.48	0.77 ± 0.76	5.79 ± 2.99	1.90 ± 1.17	0.00 ± 0.00	0.00 ± 0.00	2.68 ± 1.58	0.44 ± 0.61	1.07 ± 0.98	0.00 ± 0.00	5.18 ± 2.42	2.69 ± 0.56	10.43 ± 2.06	8.53 ± 0.62

Table S2. Promoter methylation profiles of HR (homologous repair) and NHEJ (non-homologous end joining repair) genes in synchronized FRTL5 cell line.

	% CPG METHYLATION (AVERAGE)															
	Atm		Brca1		Rad50		Mre11		Xrcc1		Xrcc4		Xrcc6		Lig4	
	Control	10 Gy	Control	10 Gy	Control	10 Gy	Control	10 Gy	Control	10 Gy	Control	10 Gy	Control	10 Gy	Control	10 Gy
1H	1.09 ± 0.49	0.61 ± 0.86	2.13 ± 0.18	1.38 ± 1.94	1.34 ± 0.47	3.84 ± 0.23	0.63 ± 0.18	0.00 ± 0.00	0.60 ± 0.85	1.30 ± 0.14	0.00 ± 0.00	0.00 ± 0.00	3.50 ± 0.71	2.63 ± 0.18	10.75 ± 1.06	9.50 ± 0.00
3H	0.71 ± 1.00	0.00 ± 0.00	1.00 ± 1.41	1.00 ± 0.00	1.34 ± 0.94	2.00 ± 0.00	0.38 ± 0.53	0.00 ± 0.00	0.10 ± 0.14	1.20 ± 0.00	0.00 ± 0.00	0.00 ± 0.00	3.38 ± 1.59	3.75 ± 0.00	16.00 ± 0.00	0.00
12H	1.42 ± 0.26	0.62 ± 0.88	1.75 ± 1.06	1.63 ± 0.88	2.83 ± 0.71	3.33 ± 0.00	0.00 ± 0.00	0.00 ± 0.00	1.00 ± 0.00	0.90 ± 0.42	0.00 ± 0.00	0.00 ± 0.00	2.63 ± 0.88	2.00 ± 0.71	13.00 ± 0.71	9.50 ± 2.12
24H	0.62 ± 0.88	2.25 ± 1.22	2.13 ± 0.18	1.00 ± 0.35	1.34 ± 0.47	2.83 ± 0.71	0.00 ± 0.00	0.00 ± 0.00	0.60 ± 0.85	1.30 ± 0.14	0.00 ± 0.00	0.00 ± 0.00	3.13 ± 0.53	2.75 ± 0.35	9.75 ± 1.77	10.25 ± 0.35
36H	0.61 ± 0.86	0.73 ± 1.03	0.63 ± 0.88	3.38 ± 2.65	2.33 ± 1.41	4.00 ± 0.47	0.00 ± 0.00	0.00 ± 0.00	1.60 ± 0.00	1.30 ± 0.71	0.00 ± 0.00	0.00 ± 0.00	2.88 ± 0.88	2.25 ± 0.00	11.50 ± 2.12	10.25 ± 3.18
48H	0.56 ± 0.78	0.59 ± 0.83	1.50 ± 0.71	2.00 ± 2.83	2.17 ± 1.18	3.84 ± 1.18	0.38 ± 0.53	0.00 ± 0.00	1.50 ± 0.14	1.10 ± 0.14	0.00 ± 0.00	0.00 ± 0.00	3.75 ± 0.35	2.13 ± 0.88	9.75 ± 1.06	8.00 ± 0.71
60H	1.17 ± 0.13	0.00 ± 0.00	0.63 ± 0.88	2.50 ± 1.41	3.67 ± 0.47	2.17 ± 0.71	0.00 ± 0.00	0.00 ± 0.00	1.70 ± 0.14	1.00 ± 0.57	0.00 ± 0.00	0.00 ± 0.00	2.63 ± 0.18	2.25 ± 0.35	9.75 ± 0.35	10.50 ± 0.71
72H	1.23 ± 0.11	0.68 ± 0.95	2.13 ± 1.24	1.13 ± 1.59	3.50 ± 0.24	3.00 ± 1.41	0.00 ± 0.00	0.00 ± 0.00	1.30 ± 0.14	1.50 ± 0.14	0.00 ± 0.00	0.00 ± 0.00	1.38 ± 1.94	1.63 ± 2.30	12.75 ± 3.18	9.25 ± 0.35

4.2 CAPÍTULO II

A exposição à radiação ionizante desregula o perfil de expressão dos microRNAs em células diferenciadas da tireoide

A radiação ionizante (RI) é o principal fator de risco para o desenvolvimento do CPT e tem sido reportado que a exposição à RI pode alterar a expressão dos microRNAs, pequenos RNAs não codificantes importantes para a carcinogênese da tireoide. Portanto, nesse capítulo, foi investigado o impacto da RI sobre o perfil de expressão dos microRNAs numa linhagem celular de tireoide normal (FRTL-5 CL2), bem como o efeito dos microRNAs sobre a radiosensibilidade de células da tireoide, especialmente as oriundas do CAT (8505c), refratário a todas as terapias convencionais, incluindo a radioterapia. Para tanto, foi realizado o perfil global da expressão dos microRNAs nas células FRTL-5 CL2 irradiadas (dose de 5 Gy de raio-X) e os dados do sequenciamento foram confirmados por qRT-PCR pela expressão dos rno-miR-10b-5p, rno-miR-33-5p, rno-miR-128-1-5p, rno-miR-199a-3p, rno-miR-296-5p, rno-miR-328a-3p e rno-miR-541-5p. Focou-se nos miR-199a-3p e miR-10b-5p porque foram os únicos microRNAs diferencialmente expressos em todos os tempos analisados, já foram descritos previamente com papéis importantes para a carcinogênese da tireoide e possuem alvos preditos *in silico* com relevância biológica para tireoide. Os alvos destes microRNAs foram validados por qRT-PCR, western blot e ensaio de luciferase. Os efeitos dos miR-199a-3p e miR-10b-5p sobre o reparo do DNA foram determinados pela: 1) ativação das quinases mutadas na ataxia-telangiectasia (ATM e ATR) e a fosforilação da serina 39 da variante de histona H2AX (γ H2AX) nas células FRTL-5 CL2 irradiadas; 2) atividade da maquinaria de reparo do DNA por recombinação homóloga (HR) nas células HeLa. O impacto do miR-10b-5p sobre a radiosensibilidade foi analisada pela contagem do número de células e o ensaio de viabilidade celular MTT nas linhagem celulares FRTL-5 CL2, FRTL-5 CL2 transformada pelo oncogene *RAS-ki* (FRTL KiKi) e 8505c. Nossos dados demonstraram que o miR-10b-5p reprime a tradução de *DICER1* (redução dos níveis proteicos sem afetar o RNAm) ao se ligar na região 3'-UTR do gene. Por outro lado, o miR-199a-3p diminuiu a estabilidade do RNAm que codifica *LIN28B* (diminuição dos níveis de RNAm e proteína) pela ligação na região 3'-UTR do gene, levando à diminuição do oncogene *HMGA2* pela indução de *Let-7b*. A superexpressão de miR-10b-5p aumentou a proliferação celular enquanto a de miR-199a-3p a atenuou. Ambos os

microRNAs regularam negativamente a eficiência do reparo por HR. Os nossos resultados sugerem que tal efeito seria devido à menor ativação de ATM e expressão de ATR, o que estaria levando ao acúmulo de quebras duplas do DNA. A superexpressão de miR-10b-5p diminuiu a viabilidade e proliferação das células FRTL-5 CL2 e 8505c irradiadas. De forma consistente, a sua inibição nas células FRTL-5 CL2 transformadas com o oncogene v-ras-Ki (FRTL KiKi), que expressam altos níveis basais de miR-10b-5p, levam ao efeito oposto. Em suma, a RI desregula a expressão dos microRNAs, afetando a eficiência da maquinaria de reparo das células irradiadas da tireoide e, sugere que a superexpressão de miR-10b-5p poderia ser uma abordagem terapêutica inovadora para o tratamento do CAT ao promover o aumento da radiosensibilidade destas células.

Ionizing Radiation Deregulates the MicroRNA Expression Profile in Differentiated Thyroid Cells

Ricardo Cortez Cardoso Penha,^{1,2} Simona Pellicchia,¹ Roberto Pacelli,³
Luis Felipe Ribeiro Pinto,² and Alfredo Fusco^{1,2}

Background: Ionizing radiation (IR) is a well-known risk factor for papillary thyroid cancer, and it has been reported to deregulate microRNA expression, which is important to thyroid carcinogenesis. Therefore, this study investigated the impact of IR on microRNA expression profile of the normal thyroid cell line (FRTL-5 CL2), as well as its effect on radiosensitivity of thyroid cancer cell lines, especially the human anaplastic thyroid carcinoma cell line (8505c).

Methods: The global microRNA expression profile of irradiated FRTL-5 CL2 cells (5 Gy X-ray) was characterized, and data were confirmed by quantitative real-time polymerase chain reaction evaluating the expression of rno-miR-10b-5p, rno-miR-33-5p, rno-miR-128-1-5p, rno-miR-199a-3p, rno-miR-296-5p, rno-miR-328a-3p, and rno-miR-541-5p in irradiated cells. The miR-199a-3p and miR-10b-5p targets were validated by quantitative real-time polymerase chain reaction, Western blot, and luciferase target assays. The effects of miR-199a-3p and miR-10b-5p on DNA repair were determined by evaluating the activation of the protein kinases ataxia-telangiectasia mutated, ataxia telangiectasia, and Rad3-related and the serine 39 phosphorylation of variant histone H2AX as an indirect measure of double-strand DNA breaks in irradiated FRTL-5 CL2 cells. The impact of miR-10b-5p on radiosensitivity was analyzed by cell counting and MTT assays in FRTL-5 CL2, *Kras*-transformed FRTL-5 CL2 (FRTL KiKi), and 8505c cell lines.

Results: The results reveal that miR-10b-5p and miR-199a-3p display the most pronounced alterations in expression in irradiated FRTL-5 CL2 cells. *Dicer1* and *Lin28b* were validated as targets of miR-10b-5p and miR-199a-3p, respectively. Functional studies demonstrate that miR-10b-5p increases the growth rate of FRTL-5 CL2 cells, while miR-199a-3p inhibits their proliferation. Moreover, both of these microRNAs negatively affect homologous recombination repair, reducing activated ataxia-telangiectasia mutated and Rad3-related protein levels, consequently leading to an accumulation of the serine 39 phosphorylation of variant histone H2AX. Interestingly, the overexpression of miR-10b-5p decreases the viability of the irradiated FRTL5-CL2 and 8505c cell lines. Consistent with this observation, its inhibition in FRTL KiKi cells, which display high basal expression levels of miR-10b-5p, leads to the opposite effect.

Conclusions: These results demonstrate that IR deregulates microRNA expression, affecting the double-strand DNA breaks repair efficiency of irradiated thyroid cells, and suggest that miR-10b-5p overexpression may be an innovative approach for anaplastic thyroid cancer therapy by increasing cancer cell radiosensitivity.

Keywords: thyroid cells, ionizing radiation, microRNA, DNA repair, radiosensitivity, anaplastic thyroid carcinoma

Introduction

MICRORNAs (miRNAs or miRs) are small non-coding RNA sequences of 20–24 nucleotides that are involved in the regulation of protein expression levels by binding to target sequences in mRNAs, thereby resulting in reduced

protein levels via repression of translation and/or mRNA decay (1).

Several studies have shown that deregulated miRNA expression contributes to thyroid carcinogenesis, contributing to the development and the progression of the malignant phenotype (2–4). For example, overexpression of the miR-

¹Istituto di Endocrinologia ed Oncologia Sperimentale—CNR c/o Dipartimento di Medicina Molecolare e Biotecnologie Mediche;

³Dipartimento di Diagnostica per Immagini e Radioterapia; Università degli Studi di Napoli “Federico II,” Naples, Italy.

²Instituto Nacional de Câncer—INCA, CPQ, Rio de Janeiro, Brazil.

221/222 cluster in papillary thyroid carcinomas (PTC) increases thyroid cell proliferation by downregulating p27 kip1 protein levels and subsequent enhancement of the G1/S transition (3,4), whereas downregulation of *let-7* family members in differentiated and undifferentiated thyroid carcinomas favors cancer progression due to their ability to modulate cell cycle regulators and oncogenes, including *RAS*, *HMGA1* and *HMGA2*, *MYC*, *CCNB1*, and *CCNE2* (4).

Moreover, miRNA expression also has a critical role in the differentiation and proliferation of normal thyroid cells. For example, it has previously been reported that thyrotropin (TSH) stimulation of rat thyroid cells leads to the downregulation of miR-1, miR-28a, miR-290-5p, miR-296-3p, and miR-297a that target *CREB1*, a transcription factor activated by the cAMP pathway and required for thyroid cell proliferation and differentiation (5).

Ionizing radiation (IR) is one of the critical risk factors for PTC (6–8). This is illustrated by several studies analyzing the effect of the Chernobyl accident, which have documented a significant increase of the PTC incidence (7.7×) in the children living in Ukraine and Belarus due to the carcinogenic effects of beta and gamma radiation after exposure to the radioactive ¹³¹I isotope (7,8). Data on the nuclear explosions in Japan, exposure to X-ray therapy for conditions such as tinea capitis and cervical and childhood tumors also illustrate that radiation is a risk factor for thyroid carcinogenesis (6). It has also been shown that radiation can induce *RET/PTC1* rearrangements in human normal thyroid tissues transplanted into SCID mice (9), a gene fusion that represents the driving genetic alteration in 13–43% of PTCs (10).

The carcinogenic effects of IR can be attributed to DNA damage, especially, double-strand breaks (DSB), which can for example generate *RET/PTC* rearrangements (11). DSB repair signaling, in turn, mostly homologous recombination (HR) and non-homologous end joining (NHEJ), are triggered to maintain genomic integrity (12). In this context, alterations in the miRNA expression profile have been reported as fundamental in radiation-induced response (13). Several miRNAs, such as miR-421 and miR-182, which are regulated by IR, also target HR genes such as *ATM* and *BRCA1*, thereby sensitizing cells to IR (13).

Anaplastic thyroid carcinoma (ATC) is a rare (1–2%) and highly aggressive and lethal type of cancer (median survival time of five to six months) that is largely refractory to all conventional therapies, including radiotherapy (14). Global miRNA analysis revealed several deregulated miRNAs in ATC samples (15), which have been previously reported to be important for radioresistance, including miR-146 that targets *BRCA1* (16), miR-30 that regulates the PI3K pathway (17), and *let-7*, which is important for thyroid differentiation and radiosensitivity (18).

The identification of IR-induced changes in miRNA expression in thyroid cells and their impact on DNA repair efficiency, as well as the characterization of potential targets that sensitize tumor cells to IR, represent an important issue, and was therefore the aim of this study. Consequently, the global miRNA profile in irradiated differentiated rat thyroid cells was analyzed. Among the IR-deregulated miRNAs, attention was focused on miR-10b-5p and miR-199a-3p, which are upregulated and downregulated, respectively, by IR. The study demonstrates that miR-10b-5p and miR-199a-3p target *Dicer1* and *Lin28b*, respectively. Moreover, miR-

10b-5p overexpression stimulates thyroid cell proliferation and favors thyroid cell radiosensitivity, whereas miR-199a-3p shows the opposite effect.

Material and Methods

Small RNA sequencing

Small RNA sequencing experiments were performed on four samples: FRTL-5 CL2 non-exposed (control) and irradiated samples at 1 and 6 hours post 5 Gy X-ray exposure by Genomix4Life (Salerno, Italy). Prior to further analysis, a RNA quality check was performed on sequencing data using Agilent 4200 TapeStation System (Agilent Technologies). Then, indexed libraries of the samples were sequenced (1×50, ~30,000,000 total reads/sample) on a HiSeq2500 Illumina platform. Mature miRNA identification was performed on all four samples using the online tools sRNA-toolbox (19). The analysis was performed by aligning the reads on the *Rattus norvegicus* genome using the MiRBase v21 database. Differential expression probability for each one of the miRNA ($p \geq 0.7$) and fold change (>2) were calculated using NOISeq (20), comparing irradiated with paired control samples (Table 1).

Cell culture, irradiation, and transfection

FRTL-5 CL2 thyroid cells, derived from three-week-old Fischer rats, were cultured in Coon's modified Ham's F-12 medium (Euroclone), supplemented with 5% calf serum, 1% L-glutamine 10 mM, 1% penicillin/streptomycin (Life Technologies), and a six-hormone mixture (1 mIU/mL of TSH, 10 µg/mL of insulin, 5 µg/mL of transferrin, 10 nM of hydrocortisone, 10 ng/mL somatostatin, and 10 ng/ml glycy-

TABLE 1. DIFFERENTIAL MICRORNAs DEREGULATED BY X-RAY EXPOSURE AT 1 AND 6 HOURS POST IRRADIATION

miR	Fold-change	Probability
FRTL-5 CL2 IR versus control (1 hour)		
rno-miR-541-5p	-8.54	0.72
rno-miR-199a-3p	-7.00	0.73
rno-miR-434-3p	-6.37	0.70
rno-miR-127-3p	-5.05	0.70
rno-miR-411-5p	-4.41	0.70
rno-miR-33-5p	-2.55	0.70
rno-miR-10b-5p	-2.41	0.70
FRTL-5 CL2 IR versus control (6 hours)		
rno-miR-10a-5p	2.02	0.79
rno-miR-328a-3p	2.05	0.83
rno-miR-1249	2.21	0.74
rno-miR-30c-2-3p	2.23	0.89
rno-miR-193b-3p	2.28	0.77
rno-miR-451-5p	2.63	0.75
rno-miR-296-5p	2.78	0.73
rno-miR-128-1-5p	3.28	0.75
rno-miR-10b-5p	4.28	0.91
rno-miR-199a-3p	10.04	0.92

The values indicate the fold change comparing irradiated with paired control samples. Probability means the differential expression probability for each miRNA. The microRNAs highlighted in bold are those validated by quantitative real-time polymerase chain reaction. miR or miRNA, microRNA.

L-histidyl-L-lysine acetate- 6H; Sigma–Aldrich) (21–23). *Kras*-transformed FRTL-5 CL2 cells (FRTL KiKi) were grown in Coon’s modified Ham’s F-12 medium (Euroclone), supplemented with 10% calf serum, 1% L-glutamine 10 mM, and 1% penicillin/streptomycin (Life Technologies) and without 6H (22,23). Both FRTL-5 CL2 and FRTL KiKi cell lines were generated at the Dipartimento di Medicina Molecolare e Biotecnologie Mediche, Università degli Studi di Napoli Federico II, Naples, Italy. The human papillary thyroid carcinoma cell lines, TPC-1 (*RET/PTC1* rearrangement) and BCPAP (*BRAF*^{V600E} mutation), the ATC cell lines, FRO (*p53*-null) and 8505c (*BRAF*^{V600E} mutation), and the human embryonic kidney cell line (HEK293) were grown in Dulbecco’s modified Eagle’s medium (Life Technologies) supplemented with 10% fetal bovine serum, 1% L-glutamine 10 mM, and 1% penicillin/streptomycin (Life Technologies). The Short Tandem Repeat (STR) profile of the human thyroid carcinoma cell lines used in this study was carried out on the samples of each provided cell line using nine highly polymorphic STR loci plus amelogenin (Cell IDTM System; Promega) by IRCCS Azienda Ospedaliera Universitaria San Martino—IST (Genoa, Italy). Detection of amplified fragments was obtained using a ABI PRISM 3100 Genetic Analyzer (Thermo Fisher Scientific). Data analysis was performed with GeneMapper software v4.0 (Thermo Fisher Scientific). The STR profile of all the tested human thyroid carcinoma cell lines did not show any difference when compared to the profiles published by one or more of the international databases.

Cells were exposed to a single X-ray dose of 5 Gy (1 Gy/min at 320 KV, 12.5 mA, 50 cm source to surface distance; X-RAD 320; Precision X-Ray) at about 70% confluence and collected after 1–48 hours. As an index of cell viability, the commercially available MTT assay was used (Sigma–Aldrich). Briefly, cells (2×10^3 cells/well) were seeded in 96-well plates and incubated for one hour with MTT reagent, diluted at final concentration of 0.5 mg/mL in cell medium, and then solubilized in 100 μ L of dimethyl sulfoxide. Measures were performed at 570 nm using an ELx800 microplate reader (BIO-TEK).

For transient overexpression of miR-199a-3p and miR-10b-5p and miR-10b-5p inhibition, cells were transfected with 50 nM pre-miRNA precursors (pre-miR-10b-5p, PM10133; pre-miR-199a-3p, PM11779; Anti-miR-10b-5p, AM17000; Ambion) or control no-targeting scramble (#1, AM17110; Ambion) using Lipofectamine 2000 (Life Technologies) following the manufacturer’s instructions.

Quantitative real-time polymerase chain reaction

Total RNA was extracted from cells (2×10^5 cells/60 cm² culture dish) using the Trizol reagent (Life Technologies). Total RNA (1 μ g) of each sample was used to obtain single-strand cDNA with the QuantiTect Reverse Transcription Kit (Qiagen). Quantitative real-time polymerase chain reaction (qRT-PCR) was performed with the CFX96 thermocycler (Bio-Rad) in 96-well plates. Each PCR reaction included 10 μ L of $2 \times$ Sybr Green (Bio-Rad), 200 nM of each primer, and 20 ng of the previously generated cDNA. The oligonucleotides for qRT-PCR, comprising exon–exon junctions, were purchased from Integrated DNA Technologies and designed with Primer-BLAST software (*Dicer1*: Fw CAC ATG CCT CCT ACC ACT ACA AT, Rv TGC TTG GTT ATG

AGG TAG TCC A; *Lin28b*: Fw AGC CCC TTGG ATA TTC CAG TC, Rv AAT GTG AAT TCC ACT GGT TCT CCT; *Rpl4*: Fw GAT GAA TTG TAC GGC ACT TGG, Rv TCT TTG GAT CTC TGG GCT TTT TC). Relative gene expression was determined using the comparative C(T) method (24). *Rpl4* was used as the housekeeping gene.

To assess miRNA expression, 1 μ g of total RNA of each sample was reverse transcribed with the miScript reverse transcription Kit (Qiagen) according to the manufacturer’s instruction. The cDNA served as the template for qRT-PCR. qRT-PCR analysis was performed using a miRNA-specific miScript Primer Assay (forward primer) (Qiagen), as described above, and the miScript SYBR Green PCR Kit (Qiagen), which contains the miScript Universal Primer (reverse primer) and QuantiTect SYBR Green PCR Master. The following miScript Primers used for this work were: miR-10b-5p (MS00033194), miR-33-5p (MS00033439), miR-128-1-5p (MS00026656), miR-199a-3p (MS00013195), miR-296-5p (MS00016457), miR-328a-3p (MS00027349), miR-541-5p (MS00013720), and *Let-7b* (MS00000007). RNU6 (MS00033740) was used for normalization.

Western blot

Cells (1×10^6 cells) were homogenized in RIPA lysis buffer (20 mM of Tris-HCl, pH 7.5, 5 mM of EDTA, 150 mM of NaCl, 1% Nonidet P40, and a mix of protease inhibitors). Cell lysate proteins (50 μ g) were then subjected to sodium dodecyl sulfate polyacrylamide gel electrophoresis and transferred onto Immobilon-P Transfer membranes (Millipore). The membranes were blocked with 5% non-fat milk proteins and probed with the indicated antibodies at the appropriate dilutions: Dicer1 (1:1000; sc-136981; Santa Cruz Biotechnology), Lin28b (1:1000; #5422; Cell Signaling Technology), γ -tubulin (1:1000; sc-8035; Santa Cruz Biotechnology), HMG2 (1:500; α 939, polyclonal antibody raised against a synthetic peptide located in the NH₂-terminal region), Vinculin (1:1000; sc-7649; Santa Cruz Biotechnology), p-ATM (1:1000; Rockland), ATM (1:1000; ab91; Abcam), ATR (1:2000; Novus Biological), γ H2AX (1:1000; #05-636; Upstate), and Gapdh (1:3000; sc-32233; Santa Cruz Biotechnology). Membranes were then incubated with a horseradish peroxidase-conjugated secondary antibody (1:3000) for 60 minutes at room temperature, and the signals were detected by a Western blot detection system (Thermo Fisher Scientific).

Flow cytometry

FRTL-5 CL2 cells (2×10^5 cells/well) were seeded in six-well culture plates, and 24 hours later, the cells were exposed to 5 Gy X-ray, as mentioned above. After 24 hours, cell pellets were re-suspended in 500 μ L of propidium iodide solution (0.1% Triton X-100, 0.1% RNase, and 2 μ g/mL propidium iodide) and incubated on ice for five minutes. Cell cycle analysis was conducted on a FACScan flow cytometer (Becton Dickinson) and analyzed with CELL-FIT software (Becton Dickinson).

Plasmids and luciferase target assay

Predicted targets of miR-10b-5p and miR-199a-3p were searched for using the online software packages TargetScan

(www.targetscan.org/vert_71) and miRBase (www.mirbase.org). Potential targets that contain at least two conserved miRNA binding sites, the highest prediction scores, and that were present in both databases were selected. The 3'-UTR regions of *Dicer1* (963 bp) and *Lin28b* (945 bp), including miRNA binding sites for miR-10b-5p and miR-199a-3p, respectively, were amplified by PCR using the following primers: *Dicer1* (3'-UTR_Fw: aat ttc tag att tgc tgc agt tgt caa gcc; 3'-UTR_Rv: aat ttc tag agc tca gcg tgc tga aac ttc) and *Lin28b* (3'-UTR_Fw: aat tgc tag cgt cag tgt tct ctt cac c; 3'-UTR_Rv: aat tgc tag ctc tga gga ctc ttg atg gga). The amplified fragments were single digested with restriction enzymes (3 IU/ μ g DNA) for three hours using *XbaI* (R0145S; New England BioLabs) for *Dicer1* and *NheI* (R0131L; New England BioLabs) for *Lin28b* and then cloned into the pmirGLO Dual-Luciferase miRNA Target Expression Vector (Promega) using the *XbaI* cloning sites for the *Dicer1* 3'-UTR region and *NheI* sites for the *Lin28b* 3'-UTR region, immediately downstream of the stop codon of the luciferase gene, generating vectors that contain the correct 3'-UTR region (sense) or the inverted 3'-UTR region sequence (antisense), which compromises the microRNA binding site. The vectors were sequenced by Eurofins Genomics (Luxemburg). HEK293 cells (1×10^5 cells/well) were seeded in a 12-well culture plate. After 24 hours, 500 ng of each vector and 50 nM of pre-miRNA precursors or control no-targeting scramble were co-transfected using Lipofectamine 2000, as described above. After 48 hours, cells were harvested and collected for the determination of luciferase and renilla luciferase activities using the Dual-Luciferase reporter assay system (Promega). Luciferase activity was normalized by renilla luciferase activity. Luminescence was measured in a microplate reader (Synergy HT; BIO-TEK). Results are expressed as the percentage of relative luciferase activity, compared to scramble, of three independent experiments.

Growth curve assay

Cells (2×10^5 cells) were plated in 60 cm² dishes, and 24 hours later, cells were transfected or irradiated as described above. A time course at 0, 1, 6, 12, 24, and 48 hours was performed using trypan blue to evaluate cell growth rate.

Statistical analysis

Results are expressed as mean \pm standard deviation and were analyzed by the nonparametric Mann-Whitney test (when comparing two groups) or by the nonparametric Kruskal-Wallis test followed by Dunn's multiple comparison tests (when comparing three or more groups). Statistical analyses were performed using the software Graphpad Prism v6.0 (GraphPad Software, Inc.), and the difference was considered significant when $p < 0.05$.

Results

Effects of IR on FRTL-5 CL2 cells

First, rat thyroid FRTL-5 CL2 cells, which maintain markers of thyroid differentiation *in vitro* (21), were exposed to 5 Gy X-ray. Then, cell proliferation, viability, and cycle were assessed (Fig. 1). Regarding the dose of exposure, a dose curve (1–10 Gy X-ray) was previously performed, and no cytotoxicity was observed in this cell line (25). The de-

cision to proceed with the 5 Gy dose is based on the linear-exponential model (cancer relative risk and radiation dose to thyroid curve) based on studies analyzing the thyroid cancer risk after exposure to external radiation in several cohorts in children (6). IR-exposed FRTL-5 CL2 cells exhibited a reduced growth rate compared to non-exposed paired control cells (Fig. 1A), whereas no changes were observed in cell viability up to 48 hours after irradiation (Fig. 1B). Moreover, irradiated cells accumulated in the G₂/M phase of the cell cycle, 24 hours after the exposure, in comparison with controls (34.64% vs. 23.84%; $p < 0.05$; Fig. 1C). In parallel, IR led to a decrease of the percentage of cells in the S phase (10.48% vs. 20.93%; Fig. 1C).

Differential miRNA expression profile of irradiated FRTL-5 CL2 cells

Next, the miRNA expression profile was analyzed by small RNA sequencing in the irradiated FRTL-5 CL2 cell line. A list of differentially expressed miRNAs in irradiated FRTL-5 CL2 cells and paired non-exposed control cells was obtained, one and six hours post irradiation (fold change ≥ 2.0 ; differential expression probability ≥ 0.70 ; reads > 20 ; Table 1). Seven miRNAs that were significantly downregulated one hour post irradiation and 10 miRNAs that were upregulated six hours after exposure were found (Table 1).

Then, the sequencing results were validated by assessing the expression of miR-10b-5p, miR-33-5p, miR-128-1-5p, miR-199a-3p, miR-296-5p, miR-328a-3p, and miR-541-5p in irradiated cells in comparison with paired non-exposed control cells at 1, 6, 12, and 24 hours post irradiation by qRT-PCR (Fig. 2). As shown in Figure 2, the expression of these miRNAs is downregulated one hour post irradiation and then upregulated after six hours, returning to non-exposed control expression levels 24 hours after irradiation. Subsequently, the study focused on miR-10b-5p and miR-199a-3p because of their previously shown role in thyroid carcinogenesis (23,26) and the biological relevance of their predicted targets for thyroid cancer.

miR-199a-3p targets *Lin28b*

Bioinformatic algorithms predicted several targets for miR-199a-3p. Among them, the study focused on *Lin28b* because it has the highest target score in the miRDB and TargetScan software analyses and also contains two conserved binding sites for miR-199a-3p. To validate *Lin28b* as target of miR-199a-3p, miR-199a-3p in FRTL-5 CL2 cells were overexpressed (Fig. 3A). A reduction of 48% and 63% of *Lin28b* protein levels was observed at 48 and 72 hours, respectively, in the miR-199a-3p-transfected cells in comparison with the scrambled oligonucleotide (Fig. 3B). *Lin28b* mRNA levels were also downregulated in the cells expressing miR-199a-3p (Fig. 3C), indicating that miR-199a-3p decreases *Lin28b* protein levels by affecting, at least partially, mRNA stability.

Since it is known that *Lin28a* and *Lin28b* selectively block the expression of *let-7* miRNAs (27) that in turn target *HMG2A*, an important protein involved in thyroid cancer progression (28,29), the *HMG2A* protein levels in the miR-199a-3p-transfected cells were also evaluated. In agreement with the ability of miR-199a-3p to target *Lin28b*, a reduction of *HMG2A* protein levels by 53% and 33% at 48 and 72 hours

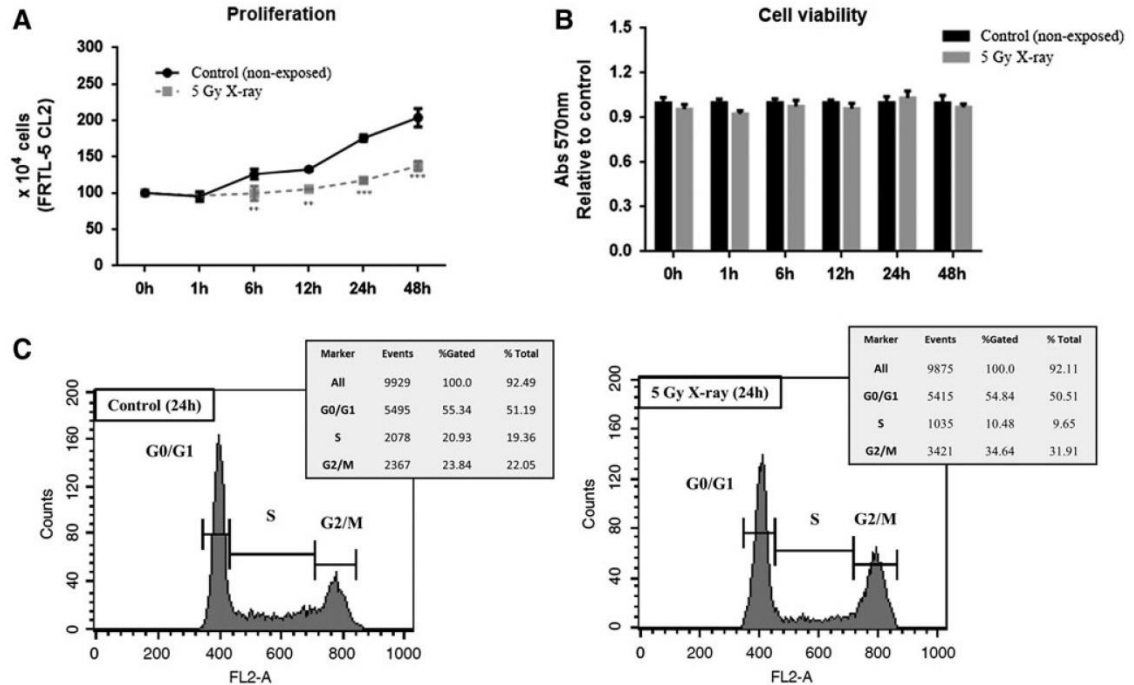


FIG. 1. Effects of ionizing radiation (IR) on FRTL5 cell line. FRTL-5 CL2 cells were exposed to 5 Gy X-ray, and the following parameters were evaluated. (A) Growth curve of control (non-exposed) or irradiated FRTL-5 CL2 cells at 0, 1, 6, 12, 24, and 48 hours post irradiation. (B) Cell viability of control (non-exposed) or irradiated cells were assessed by MTT assay in the same conditions. All determinations were made from three independent experiments, and the results are expressed relative to controls (non-exposed cells; black bars) \pm standard deviation (SD). (C) Representative cell cycle profile of FRTL-5 CL2 cells control (non-exposed) or irradiated (5 Gy X-ray) 24 hours after IR exposure. Results are reported as the percentage of cells in G0/G1, S, and G2/M. $**p < 0.01$; $***p < 0.001$.

Downloaded by Mary Ann Liebert, Inc., publishers from www.liebertpub.com at 03/20/18. For personal use only.

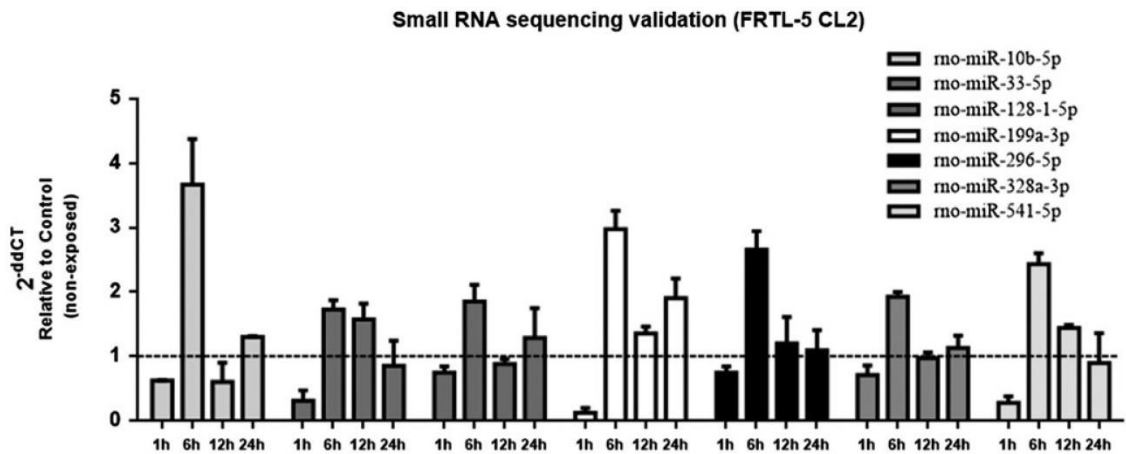


FIG. 2. Validation of small RNA sequencing. Samples of control (non-exposed) and irradiated (5 Gy X-ray) FRTL-5 CL2 cells used for array sequencing (1 and 6 hours), as well as additional samples at 12 and 24 hours after IR exposure were selected to validate the small RNA sequencing, evaluating the expression of the following mature miRNAs by quantitative real-time polymerase chain reaction (qRT-PCR): rno-miR-10b-5p, rno-miR-33-5p, rno-miR-128-1-5p, rno-miR-199a-3p, rno-miR-296-5p, rno-miR-328a-3p, and rno-miR-541-5p. Results are expressed as relative to paired non-exposed control. *U6* was used to normalize miRNA levels. Data are represented as the mean value \pm SD from two independent experiments, including the samples used for the small RNA sequencing. miR or miRNA, microRNA.

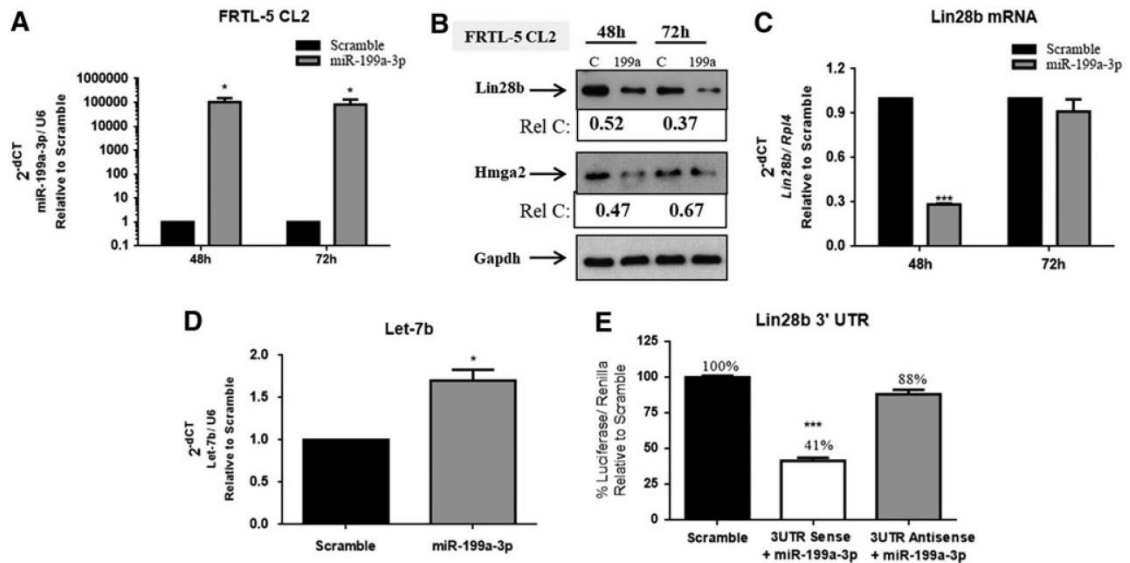


FIG. 3. Lin28b is a target of miR-199a-3p. FRTL-5 CL2 cells were transfected with miR-199a-3p or no-targeting scramble oligonucleotide precursors and 48 and 72 hours after transfection the following parameters were evaluated. (A) The expression of miR-199a-3p by qRT-PCR. (B) The protein levels of Lin28b and HMGA2 by Western blot. Densitometric analyses were relative to paired controls of the representative Western blot. Gapdh was used to normalize the protein levels. (C) The mRNA levels of *Lin28b* by qRT-PCR. (D) The expression of *let7-b* by qRT-PCR 72 hours after transfection. Data are expressed relative to control (C, scramble). *Rpl4* and *U6* were used as the housekeeping genes for mRNA and miRNA levels, respectively. (E) Relative luciferase activity in HEK293 cells transiently transfected with the 3'-UTR of *Lin28b*, in sense (3'-UTR sense) or inverted orientation (3'-UTR antisense) along with miR-199a-3p or no-targeting scramble (scramble) oligonucleotide precursors. The relative activity of firefly luciferase expression was normalized with Renilla luciferase activity. Data are expressed as the percentage of luciferase activity with respect to cells transfected with 3'-UTR sense/antisense + scramble. Each bar represents the mean value \pm SD from three independent experiments. * $p < 0.05$; *** $p < 0.001$.

after transfection, respectively, was observed compared to the control (Fig. 3B) and was associated with an increase in *let-7b* expression (Fig. 3D). It is noteworthy that the overexpression of miR-199a-3p caused no changes in *let-7a/e* expression. These results indicate that miR-199a-3p also regulates *HMGA2* expression and suggest that the *Lin28b-let-7b* pathway could be involved in this phenomenon.

To determine whether the direct interaction between miR-199a-3p and *Lin28b* mRNA is responsible for the attenuation of Lin28b protein levels, 3'-UTR of *Lin28b*, comprising the two conserved binding sites for miR-199a-3p in sense and antisense orientation, was inserted downstream of the luciferase ORF. The luciferase activity of *Lin28b* 3'-UTR in sense orientation, evaluated in HEK293 cells, was significantly diminished (59%) compared to the scrambled oligonucleotide-transfected cells, whereas only a slight decrease in the luciferase activity was observed when cells were transfected with the antisense construct (Fig. 3E). Therefore, these results indicate that miR-199a-3p directly regulates *Lin28b* expression by binding to the 3'-UTR of *Lin28b*, leading to a decrease of its expression.

miR-10b-5p targets *Dicer1*

Potential targets of miR-10b-5p were also searched for using the online software TargetScan, which predicts miRNA

binding sites within 3'-UTRs of mRNAs (30). Among the predicted targets, our attention was concentrated on *Dicer1* because it has two conserved binding sites for miR-10b-5p, plays a central role in miRNA processing (31), and has been reported to be critical for thyroid cell proliferation and differentiation (32,33). To validate the influence of miR-10b-5p on *Dicer1* expression, the *Dicer1* protein levels in FRTL-5 CL2 cells transfected with miR-10b-5p oligonucleotide precursor or control-no-targeting oligonucleotide were evaluated by Western blot analysis. A significant decrease by 59% and 36% levels at 48 and 72 hours, respectively, of the *Dicer1* protein was found in the miR-10b-5p precursor-transfected cells in comparison with the control cells (Fig. 4A and B). Conversely, no changes were detected in *Dicer1* mRNA levels after transfection with miR-10b-5p (Fig. 4C), indicating that post-transcriptional mechanisms might be responsible for the downregulation of *Dicer1* mediated by miR-10b-5p.

To investigate whether miR-10b-5p could interact with *Dicer1* mRNA, the 3'-UTR sequence of *Dicer1*, containing the predicted miR-10b-5p binding site, was inserted downstream of the luciferase ORF, in sense or antisense orientation. The luciferase activity of *Dicer1* 3'-UTR in sense orientation was reduced after transfection of miR-10b-5p when compared to scramble (33%; $p < 0.001$), while a weak change was observed with the *Dicer1* 3'-UTR antisense

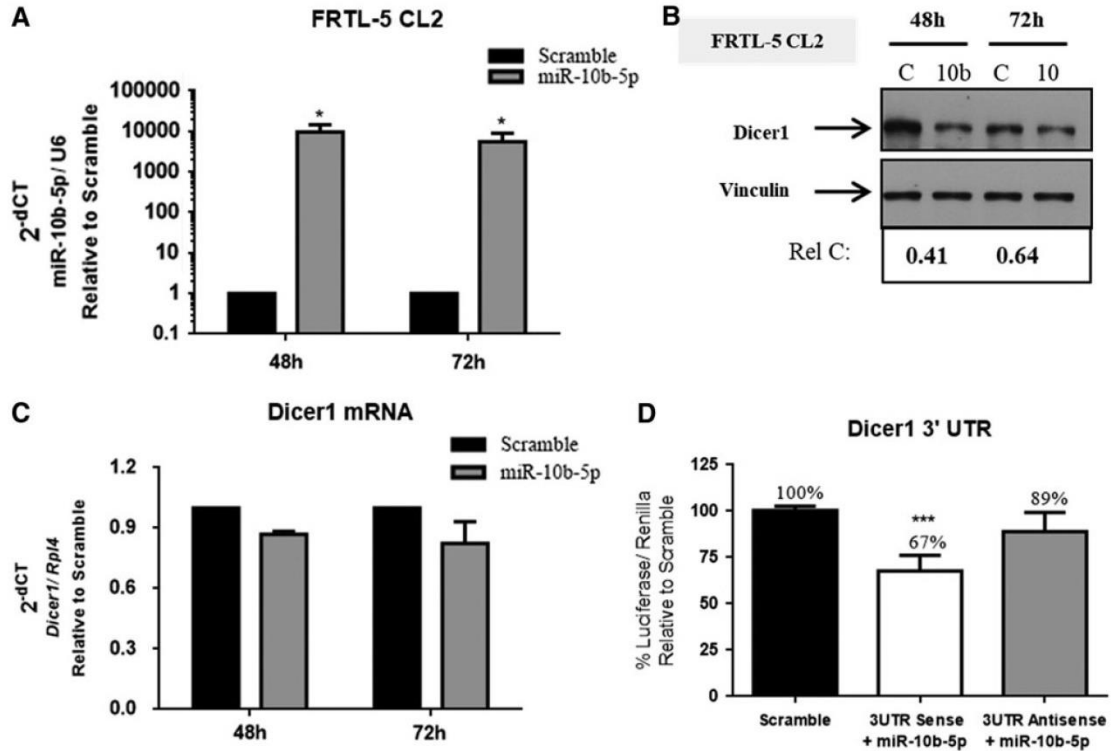


FIG. 4. Dicer1 is a target of miR-10b-5p. FRTL-5 CL2 cells were transfected with miR-10b-5p or no-targeting scramble oligonucleotide precursors, and 48 and 72 hours after transfection the following parameters were evaluated. (A) The expression of miR-10b-5p by qRT-PCR. (B) The protein levels of Dicer1 by Western blot. Densitometric analyses are relative to paired controls of the representative Western blot. Vinculin was used to normalize the protein levels. (C) The mRNA levels of *Dicer1* by qRT-PCR. Data are relative to control (C, scramble). *Rpl4* and *U6* were used as the house-keeping genes for mRNA and miRNA levels, respectively. (D) Relative luciferase activity in HEK293 cells transiently transfected with 3'-UTR of *Dicer1*, in sense (3'-UTR sense), or inverted orientation (3'-UTR antisense), along with miR-10b-5p or no-targeting scramble (scramble) oligonucleotide precursors. The relative activity of firefly luciferase expression was normalized with Renilla luciferase activity. Data are expressed as the percentage of luciferase activity with respect to cells transfected with 3'-UTR sense/antisense + scramble. Each bar represents the mean value \pm SD from three independent experiments. * $p < 0.05$; *** $p < 0.001$.

vector (11%; Fig. 4D). The validation of the miR-10b-5p binding sites within the 3'-UTR region of *Dicer1* mRNA and the decreased protein levels of Dicer1 by miR-10b-5p without affecting its mRNA levels strongly suggest that repression of its translation is the responsible post-transcriptional mechanism.

Lin28b and *Dicer1* protein levels correlate with miR-199a-3p and miR-10b-5p expression in the IR-exposed FRTL-5 CL2 cells

Having demonstrated that *Lin28b* and *Dicer1* are the targets of miR-199a-3p and miR-10b-5p, respectively, the next step was to verify the presence of a correlation between the expression of these miRNAs and their respective targets in FRTL-5 CL2 irradiated cells by performing qRT-PCR and Western blot analyses. The data unravel that IR induces a biphasic increment in *Lin28b* mRNA levels (around 2 \times), 1 and 12 hours post irradiation (Fig. 5A). Consistently, IR increased *Lin28b* protein levels one hour after exposure (2 \times)

when compared to non-exposed control cells, returning to control levels after six hours (1.0 \times ; Fig. 5B). It is noteworthy that IR also induced HMGA2 protein levels one hour after exposure (1.6 \times), which correlates with IR-mediated *Lin28b* expression at this point (Fig. 5B). No correlation was observed between HMGA2 and *Lin28b* protein levels, 6 and 24 hours after IR exposure (Fig. 5B).

As far as *Dicer1* expression is concerned, its protein levels increase one hour post irradiation (1.77 \times), then decrease after six hours (0.50 \times), returning to control levels 24 hours after irradiation (0.90 \times ; Fig. 5C). Nevertheless, no alteration in *Dicer1* mRNA levels was observed after IR exposure (Fig. 5D).

Role of miR-10b-5p and miR-199a-3p in thyroid cell proliferation and DSB repair machinery

Then, the study considered whether the overexpression of miR-10b-5p and miR-199a-3p could influence cell proliferation and DSB-damage response induced by IR in the FRTL-5 CL2 cell line. First, FRTL-5 CL2 cells were transfected

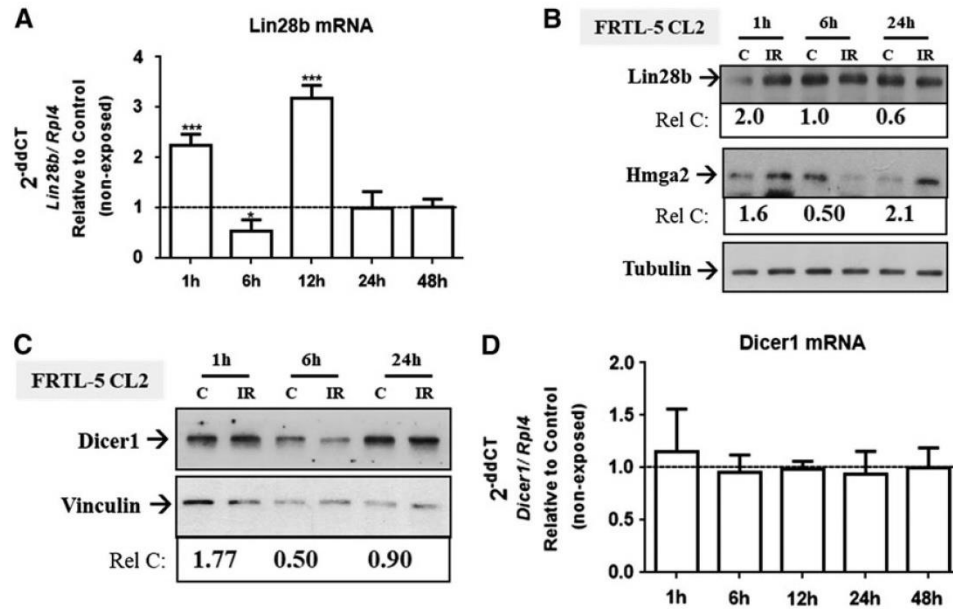


FIG. 5. IR modulates Lin28b and Dicer1 expression in the FRTL-5 CL2 cell line. Cells were exposed to 5 Gy X-ray, and (A) *Lin28b* mRNA levels were assessed by qRT-PCR at 1, 6, 12, 24, and 48 hours post irradiation, and (B) Lin28b and HMG2 protein levels were evaluated by Western blot at 1, 6, and 24 hours after IR exposure. Dicer1 protein and mRNA levels were evaluated by (C) Western blot and (D) qRT-PCR, respectively, in the same conditions. Data are relative to paired non-exposed controls. Densitometric analyses are relative to paired controls of the representative Western blot. *Rpl4* was used as the housekeeping gene for the normalization of mRNA levels. Tubulin and vinculin expression were used to normalize Western blot data. Results are expressed as the mean value \pm SD from three independent experiments. * $p < 0.05$; ** $p < 0.01$; *** $p < 0.001$.

with miR-10b-5p, miR-199a-3p, or no-targeting scramble oligonucleotide precursors to evaluate the impact of these miRs on the proliferation of FRTL-5 CL2 cells. The results demonstrate that miR-10b-5p increases the growth rate of FRTL-5 CL2 cells compared to cells transfected with scrambled oligonucleotides (Fig. 6A). Conversely, the overexpression of miR-199a-3p attenuates cell proliferation (Fig. 6A). To investigate whether these miRNAs could modify the effects of IR on thyroid cell proliferation, FRTL-5 CL2 cells were irradiated 48 hours after the transfection with scramble, miR-10b-5p, or miR-199a-3p oligonucleotide precursors (the start point, P0) because at that point, miR-10b-5p and miR-199a-3p have the highest expression levels compared to scramble and efficiently downregulate their respective targets, *Dicer1* and *Lin28b*. Since miR-10b-5p increases and miR-199a-3p decreases the growth rate of thyroid cells (Fig. 6A), the start point has different cell numbers for each condition. It was observed that the growth rate of miR-10b-5p-overexpressing cells was severely compromised by IR up to 24 hours post irradiation (Fig. 6B). In contrast, IR slightly reduced the number of cells transfected with the scrambled oligonucleotide or miR-199a-3p six hours after exposure, but cells recovered the ability to proliferate after 24 hours (Fig. 6B). Moreover, cell viability was evaluated with an MTT assay that showed a decrease in the relative number of viable miR-10b-5p-overexpressing cells (20%) compared to controls 24 hours post irradiation, while cells

transfected with miR-199a-3p displayed increased viability (30%; Fig. 6C). Taken together, these results indicate that miR-10b-5p induces radiosensitivity in FRTL-5 CL2 cells, whereas miR-199a-3p acts in the opposite way.

Subsequently, the efficiency of the DSB repair machinery was analyzed by Western blot analysis. FRTL-5 CL2 cells were transfected with miR-10b-5p and miR-199a-3p or scramble, and 48 hours after transfection, cells were exposed to 5 Gy X-ray (Fig. 6D). Cells overexpressing miR-10b-5p have lower levels of activated ATM (p-ATM; 1 h: 0.7 vs. 1.0; 6 h: 0.6 vs. 1.0) and ATR (1 h: 0.7 vs. 1.0; 6 h: 0.6 vs. 1.0), one and six hours post irradiation compared to scramble. As far as the cells transfected with miR-199a-3p are concerned, they have lower basal protein levels of ATR when compared to scramble, and its relative expression was progressively induced by IR, with a peak six hours after irradiation (1.5 vs. 1.0). However, no relative changes of p-ATM levels were observed in miR-199a-3p-transfected cells.

Modification of γ H2AX was used as an indirect measure of DSB lesions, since it is an early DSB sensor (34). The results show that γ H2AX levels are higher in cells transfected with miR-10b-5p than scramble at one (1.4 vs. 1.0) and six hours (1.2 vs. 1.0) after irradiation (Fig. 6D). Interestingly, even though no relative alteration in γ H2AX levels was noticed in miR-199a-3p-overexpressing cells in comparison with scramble in the first hour after irradiation, an accumulation of γ H2AX levels was observed six hours later compared to

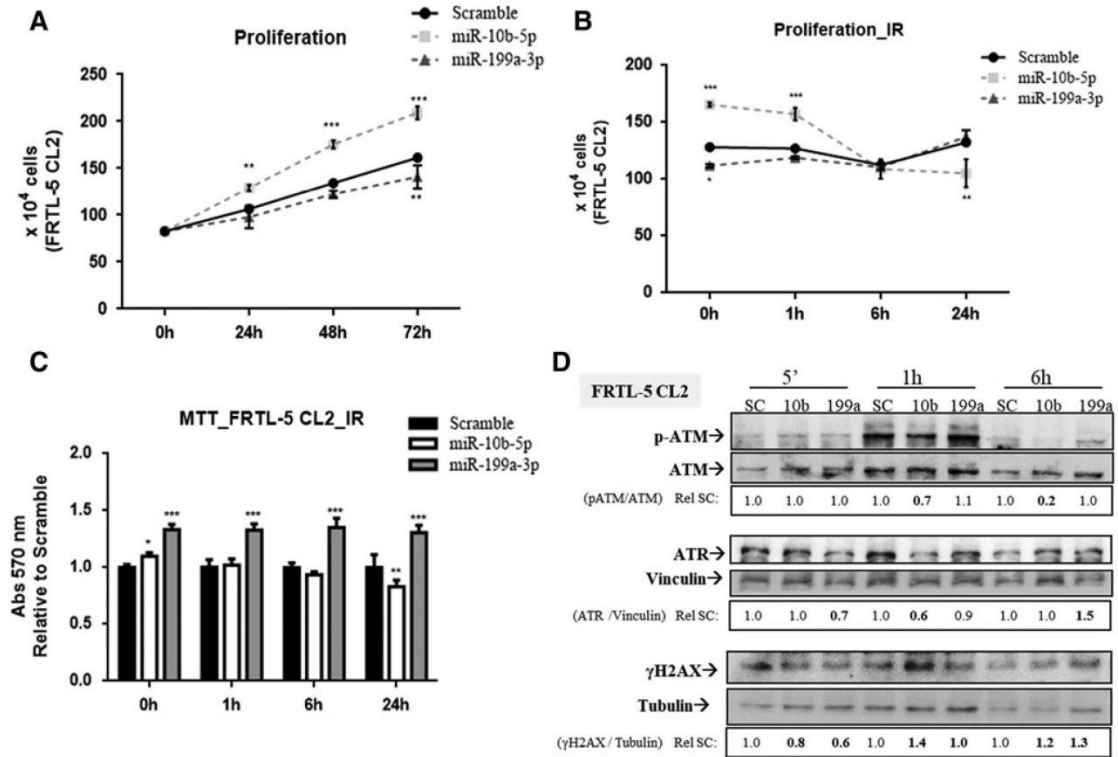


FIG. 6. Role of miR-199a-3p and miR-10b-5p in proliferation and double-strand break (DSB) repair of the FRTL-5 CL2 cell line. (A) Growth curve of cells transfected with miR-199a-3p or miR-10b-5p or scramble oligonucleotide precursors at 0, 24, 48, and 72 hours post transfection. (B) Forty-eight hours after the transfection with the mentioned miRNA precursors, cells were exposed to 5 Gy X-ray (IR), and cell counting was performed at a time course of 0, 1, 6, and 24 hours. (C) Cell viability was assessed by MTT assay in the same conditions. Results are expressed as relative to paired control (scramble). (D) Representative Western blot of DSB repair proteins, p-ATM, ATM, ATR, and γ H2AX at 5 minutes and 1 and 6 hours after irradiation. Results of densitometric analyses are relative to paired scramble (SC) of the representative Western blot. Vinculin and tubulin were used to normalize protein levels. Results are expressed as the mean value \pm SD from three independent experiments. * p < 0.05; ** p < 0.01; *** p < 0.001.

scramble (1.3 vs. 1.0; Fig. 6D). Therefore, these results suggest that miR-10b-5p and miR-199a-3p decrease DSB repair efficiency of irradiated FRTL-5 CL2 cells.

Effects of miR-10b-5p inhibition on irradiated Kras-transformed FRTL-5 CL2 cells

Next, the effects of IR on *Kras*-transformed FRTL-5 CL2 (FRTL KiKi) cells were analyzed. This choice was motivated by previous studies showing miR-10b-5p overexpression in these cells (23). First, it was confirmed that FRTL KiKi cells have higher basal levels of miR-10b-5p than FRTL-5 CL2 cells (around 25 \times ; Fig. 7A). Further, FRTL KiKi cells were exposed to 5 Gy X-ray in order to evaluate the expression of miR-10b-5p. As shown in Figure 7B, IR upregulates miR-10b-5p in a time-dependent manner one hour (2 \times) and six hours (6 \times) post irradiation, returning to control levels after 24 hours. Moreover, the data show that IR strongly reduces the growth rate (Fig. 7C), with a consistent decrease in the number of viable cells (Fig. 7D) of the irradiated cells in

comparison with paired non-exposed cells (control). Therefore, these results indicate that irradiated FRTL KiKi cells recapitulate the IR-induced behavior of FRTL-5 CL2 cells transfected with miR-10b-5p precursor oligonucleotide.

Next, miR-10b-5p expression (anti-miR-10b-5p) was inhibited in irradiated FRTL KiKi cells in order to assess its role on cell proliferation and viability. Interestingly, the transfection of anti-miR-10b-5p stimulated the growth rate of irradiated FRTL KiKi cells in comparison with scramble (Fig. 7E). In agreement with that, the inhibition of miR-10b-5p consistently increased the relative number of viable cells compared to scramble (around 30%) (Fig. 7F). Taken together, these results indicate that miR-10b-5p sensitizes FRTL KiKi cells to IR.

MiR-10b-5p promotes radiosensitivity in human ATC cell line (8505c)

ATCs exhibit an aggressive behavior and are refractory to most cancer therapies, including radiotherapy (14). Thus, the

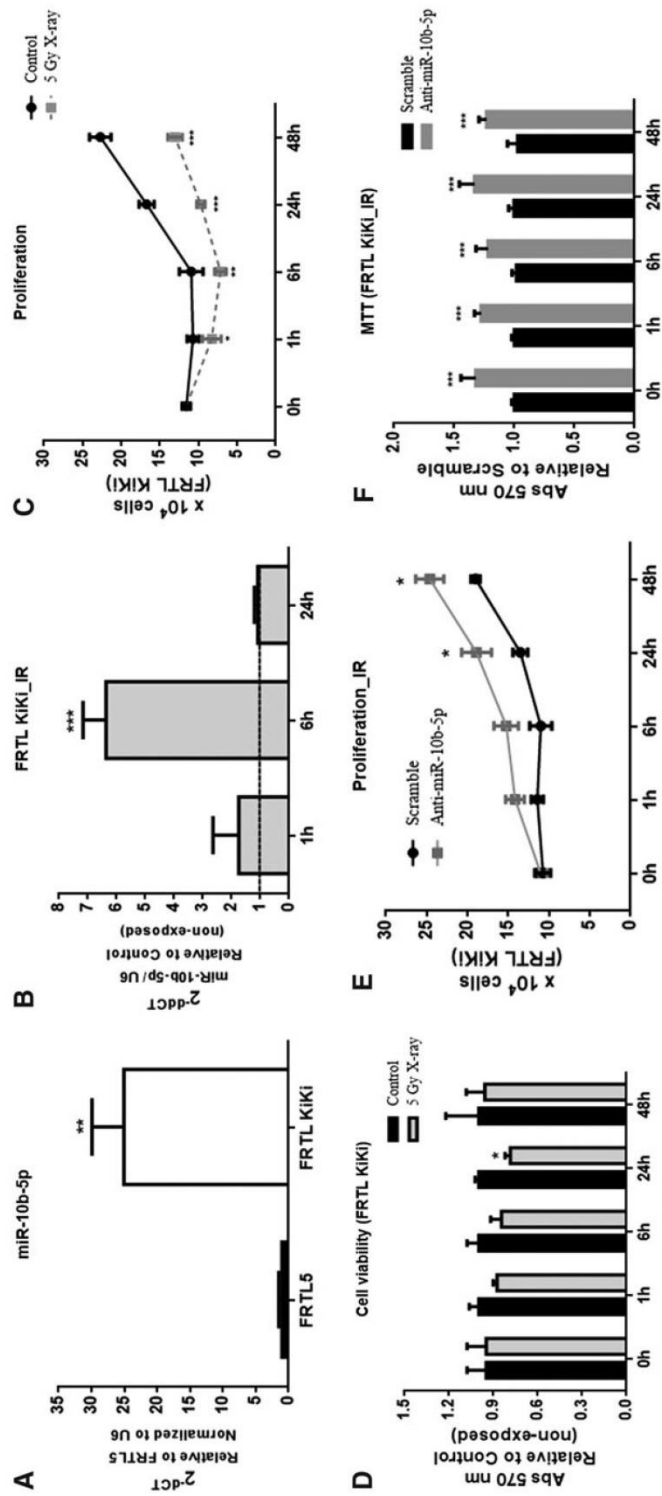


FIG. 7. Effects of miR-10b-5p on Kras-transformed FRTL5 cells (FRTL KiKi). (A) Basal expression of miR-10b-5p was assessed in FRTL-5 CL2 and FRTL KiKi cells by qRT-PCR. Results are relative to miR-10b-5p expression levels in FRTL-5 CL2 cells. (B) FRTL KiKi cells were exposed to 5 Gy X-ray (IR), and the expression of miR-10b-5p was evaluated at a time course of 0, 1, 6, 24, and 48 hours. (C) Growth curve of paired non-exposed cells (control). (D) Cell viability of control and irradiated FRTL KiKi cells was assessed by MTT assay in the same conditions. (E) FRTL KiKi cells were transfected with miR-10b-5p inhibitor (anti-miR-10b-5p) or non-targeting scramble, and 24 hours after transfection, cells were exposed to 5 Gy X-ray and counted using trypan blue at 0, 1, 6, 24, and 48 hours post irradiation. (F) Cell viability was assessed by the MTT assay in the same conditions. Results are expressed as relative to paired control. Results are expressed as the mean value \pm SD from three independent experiments. * $p < 0.05$; ** $p < 0.01$; *** $p < 0.001$.

study considered whether miR-10b-5p could also sensitize ATC cells to IR. First, the expression of miR-10b-5p was screened in a panel of human thyroid carcinoma cell lines. The 8505c cell line was chosen because (i) these cells are derived from human ATC, and (ii) they express the lowest levels of miR-10b-5p in comparison with all tested human thyroid carcinoma cell lines (Fig. 8A). Therefore, miR-10b-5p was overexpressed in these cells (Fig. 8B). It was observed that miR-10b-5p increases the proliferation rate of 8505c cells (Fig. 8C). Subsequently, it was found that miR-10b-5p attenuates the growth rate (Fig. 8D) and viability (16%) (Fig. 8E) of irradiated 8505c cells in comparison with cells transfected with SC. Therefore, these data clearly indicate that miR-10b-5p induces radiosensitivity in the 8505c cell line.

Discussion

Epigenetic mechanisms such as miRNA expression profiles have been reported as stress sensors involved in radiation-induced responses (13). In this context, this study investigated the influence of IR, a well-known risk factor for PTC development (6) (7), on differential global expression miRNA in the differentiated thyroid cell line FRTL-5 CL2 (21). This analysis revealed the induction or the repression of distinct miRNAs in irradiated FRTL-5 CL2 cells, depending on the exposure time. It was found that seven miRNAs downregulated one hour post irradiation, when FRTL-5 CL2 cells have a peak of γ H2AX modification, as previously demonstrated (25), whereas 10 miRNAs were significantly upregulated by IR after six hours, when most of the DSB lesions were repaired (25). Consistently, gene ontology analysis demonstrates that most of the altered miRNAs belong to a class of "cellular response to stress" or "gene silencing by miRNA," targeting DSB repair genes. Then, the study focused on miR-10b-5p and miR-199a-3p because these miRNAs were deregulated by IR at both one and six hours after irradiation and are described to have an oncogenic (23) and a tumor suppressor (26) activity in thyroid cancer, respectively.

Since the HR pathway is critical for DSB repair in thyroid cells, preventing *RET/PTC* rearrangement (35), the role of these miRNAs in DSB repair was investigated. It was found that miR-199a-3p and miR-10b-5p increase IR-induced DSB, indirectly measured by γ H2AX levels (34). Since HMGA2 activates ATR in cancer cell lines (36), basal lower protein levels of ATR might be related to the delayed DSB repair in miR-199a-3p-overexpressing cells. Conversely, the downregulation of *Dicer1* could account for the reduced levels of activated ATM and ATR, as well as the increased γ H2AX levels in FRTL-5 CL2 cells transfected with miR-10b-5p precursor oligonucleotide. Indeed, *DICER1* plays a central miRNA biogenesis (31), and it is also crucial for DSB repair signaling and ATM phosphorylation in eukaryotes (37–39).

Interestingly, it has also been reported that defects in HR are related to radiosensitivity in cancer cells, predisposing them to accumulate unrepaired DSB, a lethal type of DNA lesion (40). Accordingly, the overexpression of miR-10b-5p slightly attenuated cell viability and compromised the growth of normal and neoplastic irradiated thyroid cell lines. These effects are likely due to the deficiency in HR activation after IR exposure, resulting in DSB accumulation, even though a role of the increased growth rate induced by miR-10b-5p

overexpression cannot be excluded. Apart from that, IR exposure independently affects mitochondrial function and DNA. Although the MTT assay has classically been used to measure cell survival after irradiation (41), it has been reported that high doses of radiation (>1 Gy) impacts the MTT assay by affecting the dehydrogenase activity, and thus the results obtained with MTT assays are less reliable than those obtained by using cell counting after trypan blue staining (42,43). These results appear in contrast with the radioresistance promoted by miR-10b-5p in glioblastoma cells (44), suggesting that the effects of miR-10b-5p on cell sensitivity to IR is dependent on the cellular context, as already reported for other miRNAs (45), such as miR-205 that induces radioresistance in nasopharyngeal carcinoma cell lines (46) but sensitizes breast cancer cells to IR (47).

It is noteworthy that some of the findings might have clinical relevance in the understanding of the mechanisms involved in thyroid carcinogenesis, and also for the development of new strategies for the therapy of ATC. The findings highlight the targets of the miR-199a-3p (*Lin28b*) and miR-10b-5p (*Dicer1*) that are upregulated and downregulated, respectively, in human thyroid carcinomas. The study demonstrates that miR-199a-3p targets *Lin28b*, leading to a reduced expression of HMGA2, and it is speculated that the overexpression of *let-7b* could be involved in this phenomenon. Accordingly, this study reports that *let-7* decreases *RAS* expression and thus compromises MAPK activation, which is fundamental for thyroid cell proliferation (48). Therefore, miR-199a-3p downregulation in thyroid carcinomas would lead to an increased expression of HMGA2, thereby contributing to cancer progression. Similarly, the study reports that miR-10b-5p targets the 3'-UTR region of *Dicer1* mRNA, repressing its translation, resulting in a reduction of its protein levels, a mechanism that has already been associated with thyroid cell transformation (32,33). Moreover, the ability of both miRNAs to modulate IR-induced DSB may account for the reduced ability of thyroid cancer cells in DSB repair when these miRNAs are deregulated. Furthermore, the study reports an interesting role of miR-10b-5p in promoting the radiosensitivity of thyroid cancer cells, and thus it is hypothesized that the induction of miR-10b-5p-overexpression in malignant thyroid neoplasias, in particular ATCs, which are refractory to radiotherapy, might result in a better response to radiotherapy. Interestingly, recent studies provide reasonable perspectives of a therapy based on miRNA restoration. Indeed, liposomal encapsulation technology and biodegradable polymers delivery systems are used to deliver therapeutic miRNAs *in vivo* (49). For example, intranasal administration of *let-7* inhibited lung tumor growth in *Kras*-mutant mice (50). Moreover, the restoration of miR-34 by infusion and the intravenous administration of miR-16 are in a Phase I clinical trial with patients with advanced solid tumors (49). The results of miR-10b-5p-overexpressing ATC cells are in agreement with the biphasic expression levels of miR-10b-5p in irradiated FRTL5 cells. Since miR-10b-5p stimulates thyroid cell proliferation, it is expected that miR-10b-5p expression levels are reduced at the first hour after irradiation, when cells stop proliferating in order to repair DNA damage. Once the DNA damage is repaired, six hours after irradiation, miR-10b-5p is upregulated in order to recover their proliferation. Since miR-10b-5p overexpression stimulates

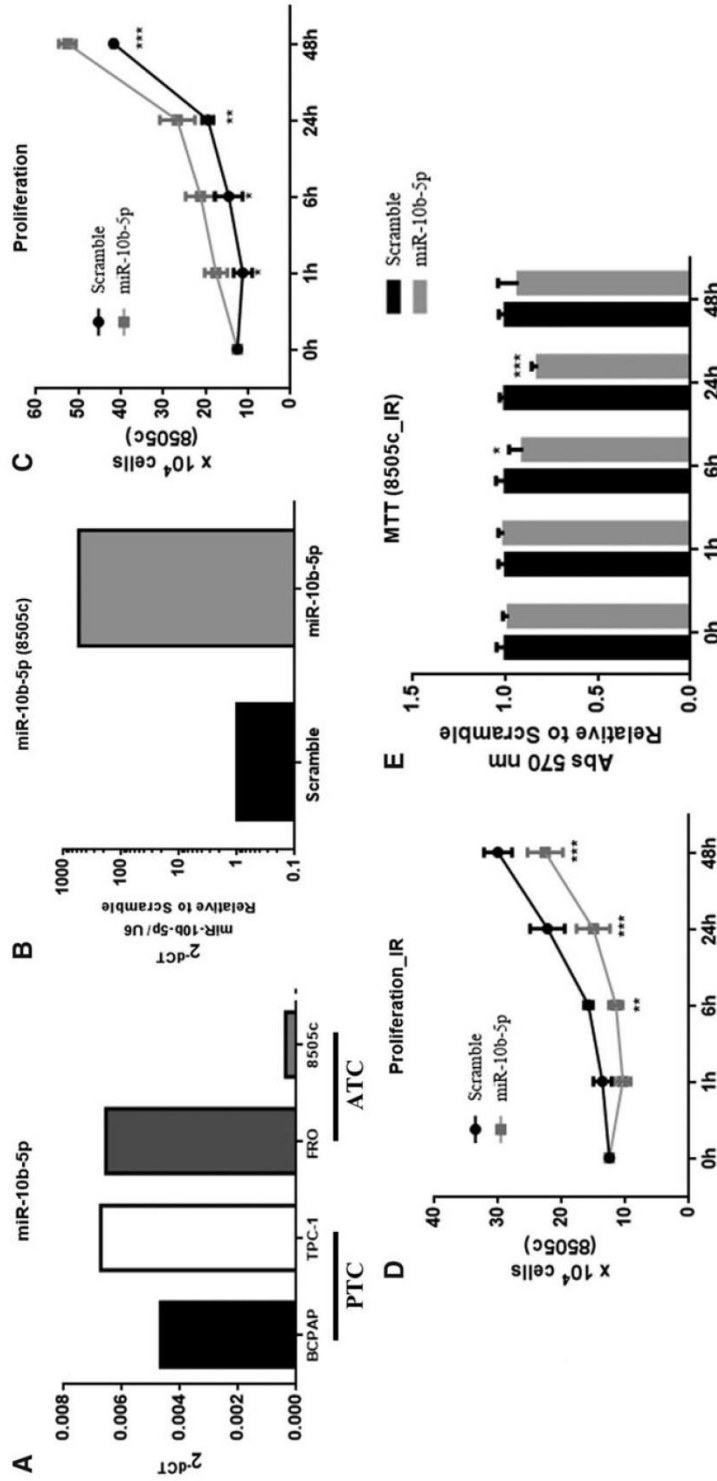


FIG. 8. miR-10b-5p increases proliferation and sensitizes the human anaplastic thyroid carcinoma cell line 8505c to IR. (A) Basal expression of miR-10b-5p among human thyroid carcinoma cell lines (BCPAP, TPC-1, FRO, and 8505c) by qRT-PCR. (B) The transient overexpression of miR-10b-5p or no-targeting scramble (scramble) 8505c cell line. Results are relative to scramble. (C) Growth curve of non-irradiated 8505c cells transfected with miR-10b-5p or no-targeting scramble (scramble) oligonucleotide precursors was performed at a time course of 0, 1, 6, 24, and 48 hours. (D) The 8505c cells were transfected with the mentioned miRNA oligonucleotide precursors and, 24 hours later, cells were exposed to 5 Gy X-ray (IR), and the growth curve was performed at 0, 1, 6, 24, and 48 hours post irradiation. (E) Cell viability was assessed by the MTT in the same conditions. Data are relative to scramble. Results are expressed as the mean value \pm SD from three independent experiments. * $p < 0.05$; ** $p < 0.01$; *** $p < 0.001$.

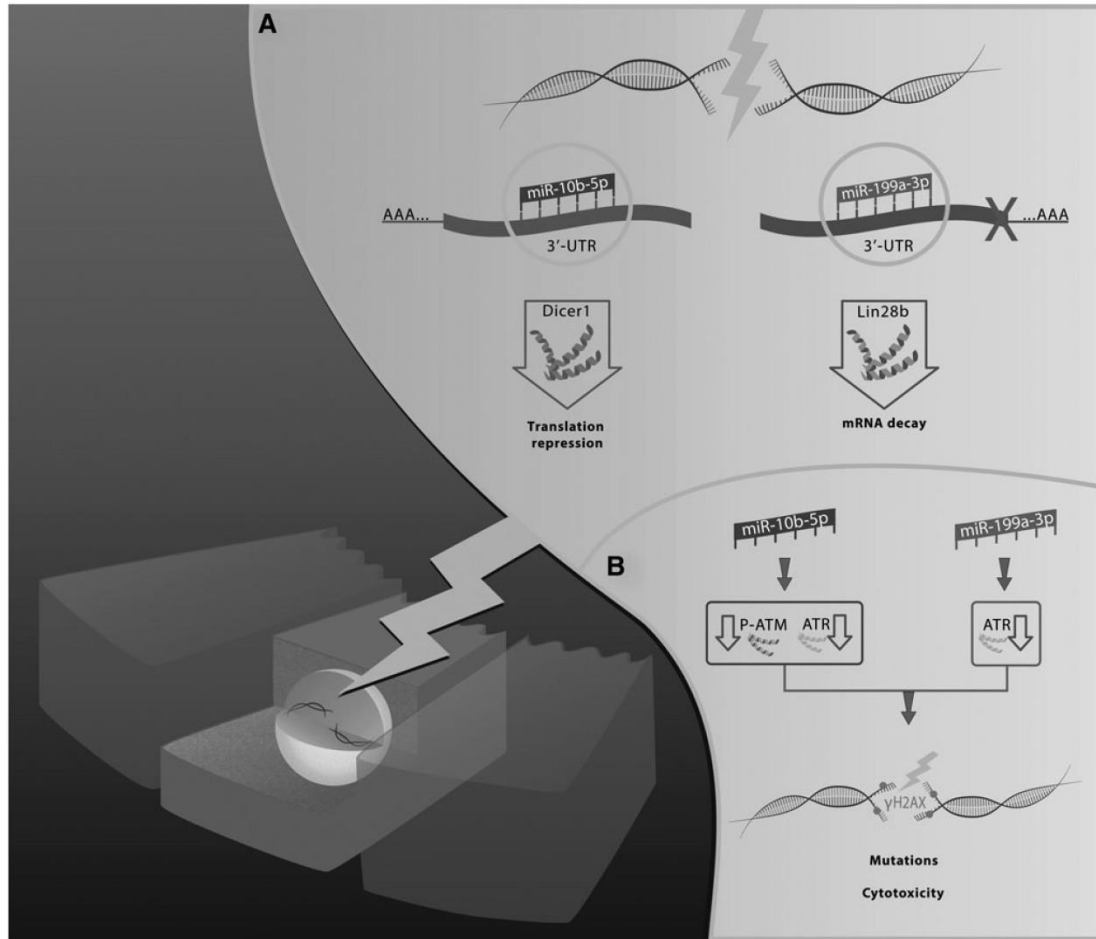


FIG. 9. Schematic representation of the findings in this study. (A) In the nucleus of the thyrocytes, ionizing radiation (yellow arrow) induces double-strand DNA breaks (DSB) and deregulates the expression of miR-10b-5p and miR-199a-3p. These radiation-induced miRNAs, in turn, bind to *Dicer1* and *Lin28b* 3'-UTR regions, respectively, leading to repression of translation of *Dicer1* and degradation of mRNA of *Lin28b* and, consequently, reduced protein levels. (B) MiR-10b-5p overexpression decreases the phosphorylation of ATM (p-ATM) and the expression of ATR, while miR-199a-3p attenuates the expression of ATR in irradiated thyroid cells, which contributes to the accumulation of DSB, indirectly measured by γ H2AX modification. γ H2AX flanks the DSB damage sites, amplifies DSB repair signaling, and recruits the SWI/SNF chromatin remodeling complex that facilitates the access of the DSB repair machinery. Therefore, deficient response to DSB prones cells to mutations and/or cytotoxic damage. 3'-UTR, untranslated region at the 3' end of mRNA; ATM, kinase ataxia-telangiectasia mutated; ATR, ataxia telangiectasia and Rad3-related protein; γ H2AX, histone variant H2AX phosphorylated on serine 139.

thyroid cell proliferation and negatively affects DNA repair efficiency, cells that overexpress this microRNA might be more susceptible to IR.

In conclusion, the results reported here demonstrate that miR-199a-3p and miR-10b-5p, that respectively target *Dicer1* and *Lin28b*, are deregulated by IR and compromise DSB repair efficiency of thyroid cells by affecting the activation of ATM and ATR, hence predisposing cells to accumulate DSB after X-ray exposure (Fig. 9). Moreover, the data indicate that miR-10b-5p promotes radiosensitivity in a cell line, derived from ATC known to be refractory to

radiotherapy, suggesting that the restoration of miR-10b-5p expression could form a new approach in the treatment of ATC.

Acknowledgments

This study has been supported by grants from CNR Flagship Projects (Epigenomics-EPIGEN) and the Associazione Italiana per la Ricerca sul Cancro (AIRC IG 11477). R.C.C.P. was the recipient of a fellowship CAPES for the program "Ciencias sem Fronteiras." A.F. was granted with a Special

Downloaded by Mary Ann Liebert, Inc., publishers from www.liebertpub.com at 03/20/18. For personal use only.

Visiting Researcher (PVE) fellowship sponsored by CAPES. Thanks to Simone Eboli for the graphic art.

Author Disclosure Statement

The authors have declared no conflict of interest.

References

- Pasquinelli AE 2012 MicroRNAs and their targets: recognition, regulation and an emerging reciprocal relationship. *Nat Rev Genet* **13**:271–282.
- Santarpia L, Nicoloso M, Calin GA 2010 MicroRNAs: a complex regulatory network drives the acquisition of malignant cell phenotype. *Endocr Relat Cancer* **17**:F51–75.
- Pallante P, Visone R, Croce CM, Fusco A 2010 Deregulation of microRNA expression in follicular cell-derived human thyroid carcinomas. *Endocr Relat Cancer* **17**:F91–104.
- Pallante P, Battista S, Pierantoni GM, Fusco A 2014 Deregulation of microRNA expression in thyroid neoplasias. *Nat Rev Endocrinol* **10**:88–101.
- Leone V, D'Angelo D, Ferraro A, Pallante P, Rubio I, Santoro M, Croce CM, Fusco A 2011 A TSH-CREB1-microRNA loop is required for thyroid cell growth. *Mol Endocrinol* **25**:1819–1830.
- Ron E, Lubin JH, Shore RE, Mabuchi K, Modan B, Potterm LM, Schneider AB, Tucker MA, Boice JD Jr 1995 Thyroid cancer after exposure to external radiation: a pooled analysis of seven studies. *Radiat Res* **141**:259–277.
- Pacini F, Vorontsova T, Demidchik EP, Molinaro E, Agate L, Romei C, Shavrova E, Cherstvoy ED, Ivashkevitch Y, Kuchinskaya E, Schlumberger M, Ronga G, Filesi M, Pinchera A 1997 Post-Chernobyl thyroid carcinoma in Belarus children and adolescents: comparison with naturally occurring thyroid carcinoma in Italy and France. *J Clin Endocrinol Metab* **82**:3563–3569.
- Cardis E, Howe G, Ron E, Bebesko V, Bogdanova T, Bouville A, Carr Z, Chumak V, Davis S, Demidchik Y, Drozdovitch V, Gentner N, Gudzenko N, Hatch M, Ivanov V, Jacob P, Kapitonova E, Kenigsberg Y, Kesminiene A, Kopecky KJ, Kryuchkov V, Loos A, Pinchera A, Reiners C, Repacholi M, Shibata Y, Shore RE, Thomas G, Tirmarche M, Yamashita S, Zvonova I 2006 Cancer consequences of the Chernobyl accident: 20 years on. *J Radiol Prot* **26**:127–140.
- Mizuno T, Iwamoto KS, Kyoizumi S, Nagamura H, Shinohara T, Koyama K, Seyama T, Hamatani K 2000 Preferential induction of RET/PTC1 rearrangement by X-ray irradiation. *Oncogene* **19**:438–443.
- Caudill CM, Zhu Z, Ciampi R, Stringer JR, Nikiforov YE 2005 Dose-dependent generation of RET/PTC in human thyroid cells after *in vitro* exposure to gamma-radiation: a model of carcinogenic chromosomal rearrangement induced by ionizing radiation. *J Clin Endocrinol Metab* **90**:2364–2369.
- Kondo T, Ezzat S, Asa SL 2006 Pathogenetic mechanisms in thyroid follicular-cell neoplasia. *Nat Rev Cancer* **6**:292–306.
- Bohgaki T, Bohgaki M, Hakem R 2010 DNA double-strand break signaling and human disorders. *Genome Integr* **1**:15.
- Metheerairut C, Slack FJ 2013 MicroRNAs in the ionizing radiation response and in radiotherapy. *Curr Opin Genet Dev* **23**:12–19.
- Molinaro E, Romei C, Biagini A, Sabini E, Agate L, Mazzeo S, Materazzi G, Sellari-Franceschini S, Ribecchini A, Torregrossa L, Basolo F, Vitti P, Elisei R 2017 Anaplastic thyroid carcinoma: from clinicopathology to genetics and advanced therapies. *Nat Rev Endocrinol* **13**:644–660.
- Zhang R, Hardin H, Chen J, Guo Z, Lloyd RV 2016 Non-coding RNAs in thyroid cancer. *Endocr Pathol* **27**:12–20.
- Garcia AI, Buisson M, Bertrand P, Rimokh R, Rouleau E, Lopez BS, Lidereau R, Mikaélian I, Mazoyer S 2011 Down-regulation of *BRCA1* expression by miR-146a and miR-146b-5p in triple negative sporadic breast cancers. *EMBO Mol Med* **3**:279–290.
- Chan LW, Wang F, Meng F, Wang L, Wong SC, Au JS, Yang S, Cho WC 2017 MiR-30 family potentially targeting PI3K-SIAH2 predicted interaction network represents a novel putative theranostic panel in non-small cell lung cancer. *Front Genet* **8**:8.
- Fuziwara CS, Kimura ET 2014 MicroRNA deregulation in anaplastic thyroid cancer biology. *Int J Endocrinol* **2014**:743450.
- Rueda A, Barturen G, Lebrón R, Gómez-Martín C, Alganza Á, Oliver JL, Hackenberg M 2015 sRNAtoolbox: an integrated collection of small RNA research tools. *Nucleic Acids Res* **43**:W467–473.
- Tarazona S, García-Alcalde F, Dopazo J, Ferrer A, Conesa A 2011 Differential expression in RNA-seq: a matter of depth. *Genome Res* **21**:2213–2223.
- Ambesi-Impombato FS, Parks LA, Coon HG 1980 Culture of hormone-dependent functional epithelial cells from rat thyroids. *Proc Natl Acad Sci U S A* **77**:3455–3459.
- Fusco A, Berlingieri MT, Di Fiore PP, Portella G, Grieco M, Vecchio G 1987 One- and two-step transformations of rat thyroid epithelial cells by retroviral oncogenes. *Mol Cell Biol* **7**:3365–3370.
- Mussnich P, D'Angelo D, Leone V, Croce CM, Fusco A 2013 The high mobility group A proteins contribute to thyroid cell transformation by regulating miR-603 and miR-10b expression. *Mol Oncol* **7**:531–542.
- Schmittgen TD, Livak KJ 2008 Analyzing real-time PCR data by the comparative C(T) method. *Nat Protoc* **3**:1101–1108.
- Penha RCC, Lima SCS, Boroni M, Ramalho-Oliveira R, Viola JPB, de Carvalho DP, Fusco A, Pinto LFR 2017 Intrinsic LINE-1 hypomethylation and decreased Brcal expression are associated with DNA repair delay in irradiated thyroid cells. *Radiat Res* **188**:144–155.
- Minna E, Romeo P, De Cecco L, Dugo M, Cassinelli G, Pilotti S, Degl'Innocenti D, Lanzi C, Casalini P, Pierotti MA, Greco A, Borrello MG 2014 miR-199a-3p displays tumor suppressor functions in papillary thyroid carcinoma. *Oncotarget* **5**:2513–2528.
- Piskounova E, Polytarchou C, Thornton JE, LaPierre RJ, Pothoulakis C, Hagan JP, Iliopoulos D, Gregory RI 2011 Lin28A and Lin28B inhibit let-7 microRNA biogenesis by distinct mechanisms. *Cell* **147**:1066–1079.
- Chiappetta G, Ferraro A, Vuttariello E, Monaco M, Galdiero F, De Simone V, Califano D, Pallante P, Botti G, Pezzullo L, Pierantoni GM, Santoro M, Fusco A 2008 HMGA2 mRNA expression correlates with the malignant phenotype in human thyroid neoplasias. *Eur J Cancer* **44**:1015–1021.
- Li T, Yang XD, Ye CX, Shen ZL, Yang Y, Wang B, Guo P, Gao ZD, Ye YJ, Jiang KW, Wang S 2017 Long noncoding RNA HIT00218960 promotes papillary thyroid cancer oncogenesis and tumor progression by upregulating the expression of high mobility group AT-hook 2 (HMGA2) gene. *Cell Cycle* **16**:224–231.

30. Agarwal V, Bell GW, Nam JW, Bartel DP 2015 Predicting effective microRNA target sites in mammalian mRNAs. *eLife* **4**:e05005.
31. Kurzynska-Kokorniak A, Koralewska N, Pokornowska M, Urbanowicz A, Tworak A, Mickiewicz A, Figlerowicz M 2015 The many faces of Dicer: the complexity of the mechanisms regulating Dicer gene expression and enzyme activities. *Nucleic Acid Res* **43**:4365–4380.
32. Frezzetti D, Reale C, Cali G, Nitsch L, Fagman H, Nilsson O, Scarfò M, De Vita G, Di Lauro R 2011 The microRNA-processing enzyme Dicer is essential for thyroid function. *PLoS One* **6**:e27648.
33. Penha RCC, Sepe R, De Martino M, Esposito F, Pellicchia S, Raia M, Vecchio LD, Decaussin-Petrucci M, De Vita G, Pinto LFR, Fusco A 2017 Role of Dicer1 in thyroid cell proliferation and differentiation. *Cell Cycle* **16**:2282–2289.
34. Grabarz A, Barascu A, Guirouilh-Barbat J, Lopez BS 2012 Initiation of DNA double strand break repair: signaling and single-stranded resection dictate the choice between homologous recombination, non-homologous end-joining and alternative end-joining. *Am J Cancer Res* **2**:249–268.
35. Gandhi M, Evdokimova V, Nikiforov YE 2010 Mechanisms of chromosomal rearrangements in solid tumors: the model of papillary thyroid carcinoma. *Mol Cell Endocrinol* **321**:36–43.
36. Natarajan S, Hombach-Klonisch S, Dröge P, Klonisch T 2013 HMG2A2 inhibits apoptosis through interaction with ATR-CHK1 signaling complex in human cancer cells. *Neoplasia* **15**:263–280.
37. Francia S, Micheli F, Saxena A, Tang D, de Hoon M, Anelli V, Mione M, Carninci P, d'Adda di Fagnana F 2012 Site-specific DICER and DROSHA RNA products control the DNA-damage response. *Nature* **488**:231–235.
38. Wei W, Ba Z, Gao M, Wu Y, Ma Y, Amiard S, White CI, Rendtlew Danielsen JM, Yang YG, Qi Y 2012 A role for small RNAs in DNA double-strand break repair. *Cell* **149**:101–112.
39. Gao M, Wei W, Li MM, Wu YS, Ba Z, Jin KX, Li MM, Liao YQ, Adhikari S, Chong Z, Zhang T, Guo CX, Tang TS, Zhu BT, Xu XZ, Mailand N, Yang YG, Qi Y, Rendtlew Danielsen JM 2014 Ago2 facilitates Rad51 recruitment and DNA double-strand break repair by homologous recombination. *Cell Res* **24**:532–541.
40. Choudhury A, Zhao H, Jalali F, Al Rashid S, Ran J, Supiot S, Kiltie AE, Bristow RG 2009 Targeting homologous recombination using imatinib results in enhanced tumor cell chemosensitivity and radiosensitivity. *Mol Cancer Ther* **8**:203–213.
41. Slavotinek A, McMillan TJ, Steel CM 1994 Measurement of radiation survival using the MTT assay. *Eur J Cancer* **30A**:1376–1382.
42. Buch K, Peters T, Nawroth T, Sängler M, Schmidberger H, Langguth P 2012 Determination of cell survival after irradiation via clonogenic assay versus multiple MTT assay—a comparative study. *Radiat Oncol* **7**:1.
43. Chung DM, Kim JH, Kim JK 2015 Evaluation of MTT and Trypan Blue assays for radiation-induced cell viability test in HepG2 cells. *Int J Radiat Res* **13**:331–335.
44. Zhen L, Li J, Zhang M, Yang K 2016 MiR-10b decreases sensitivity of glioblastoma cells to radiation by targeting AKT. *J Biol Res (Thessalon)* **23**:14.
45. Czochoch JR, Glazer PM 2014 MicroRNAs in cancer cell response to ionizing radiation. *Antioxid Redox Signal* **21**:293–312.
46. Qu C, Liang Z, Huang J, Zhao R, Su C, Wang S, Wang X, Zhang R, Lee MH, Yang H 2012 MiR-205 determines the radioresistance of human nasopharyngeal carcinoma by directly targeting PTEN. *Cell Cycle* **11**:785–796.
47. Zhang P, Wang L, Rodriguez-Aguayo C, Yuan Y, Debeb BG, Chen D, Sun Y, You MJ, Liu Y, Dean DC, Woodward WA, Liang H, Yang X, Lopez-Berestein G, Sood AK, Hu Y, Ang KK, Chen J, Ma L 2014 miR-205 acts as a tumour radiosensitizer by targeting ZEB1 and Ubc13. *Nat Commun* **5**:5671.
48. Perdas E, Stawski R, Nowak D, Zubrzycka M 2016 The role of miRNA in papillary thyroid cancer in the context of miRNA let-7 family. *Int J Mol Sci* **17**:E909.
49. Shah MY, Ferrajoli A, Sood AK, Lopez-Berestein G, Calin GA 2016 microRNA therapeutics in cancer—an emerging concept. *EBioMedicine* **12**:34–42.
50. Trang P, Medina PP, Wiggins JF, Ruffino L, Kelnar K, Omotola M, Homer R, Brown D, Bader AG, Weidhaas JB, Slack FJ 2010 Regression of murine lung tumors by the let-7 microRNA. *Oncogene* **29**:1580–1587.

Address correspondence to:

Alfredo Fusco, MD

Istituto di Endocrinologia ed Oncologia

Sperimentale del CNR

Dipartimento di Medicina Molecolare e Biotecnologie

Mediche

Università degli Studi di Napoli “Federico II”

via Pansini 5

80131 Naples

Italy

E-mail: alfusco@unina.it

4.2.1 DADOS NÃO PUBLICADOS DO CAPÍTULO II

MATERIAL E MÉTODOS

CULTURA DE CÉLULAS, IRRADIAÇÃO E TRANSFECCÃO

A linhagem de tireócito normal de rato FRTL-5 CL2 foi cultivada em meio Ham's F-12 modificado de Coon (Euroclone, Itália), suplementados com tireotrofina 1 mU/ml, insulina 10 µg/ml, transferrina 5 µg/ml, hidrocortisona 10 nM, somatostatina 10 ng/ml, glicil-histidina 10 ng/ml, 5% de soro fetal bovino e antibiótico (Sigma Aldrich, EUA) (Fusco e cols., 1987). A linhagem de tireócito de rato FRTL-5 CL2 transformada com o oncogene *v-Ras-Ki* (FRTL KiKi) foi cultivada em meio Ham's F-12 modificado de Coon (Euroclone, Itália), suplementado com 10% de soro fetal bovino e antibiótico, sem a presença dos seis hormônios (Fusco e cols., 1987). As linhagens humanas de CPT (TPC-1 e BCPAP), as de CAT (FRO e 8505c), a de câncer cervical (HeLa) e a embrionária de rim humano (HEK293) foram cultivadas em meio DMEM (Life Technologies, EUA), suplementadas com 10% de soro fetal bovino, 1% de glutamina 10 mM e 1% de penicilina/estreptomicina (Life Technologies, EUA).

As células confluentes foram expostas a doses únicas de 5 Gy de raio-X (1 Gy/minuto a 320KV, 12.5mA, 50 cm de distância da fonte; X-RAD 320, Precision X-Ray, EUA) e coletadas 1, 6, 12, 24 e 48 horas após à exposição para os experimentos subsequentes. Para os experimentos de superexpressão transiente, as células foram transfectadas com o controle negativo #1 (AM17110), os oligonucleotídeos precursores de miR-10b-5p (PM10133) e de miR-199a-3p (PM11779) na concentração final de 50 nM, usando o reagente Lipofectamina 2000 (Life Technologies, EUA), seguindo as recomendações do fabricantes.

qRT-PCR

O RNA total das linhagens celulares de tireoide foi extraído usando o reagente Trizol (Invitrogen, EUA), seguindo as instruções do fabricante. Para avaliar a expressão dos miRNAs, foi utilizado 1µg do RNA total, usando miScript reverse transcription Kit (Qiagen, Alemanha). Basicamente, os miRNAs maduros são poliadenilados pela enzima polimerase poli(A) e

convertidos a cDNA pela ação de uma transcriptase reversa com oligonucleotídeos que reconhecem a cauda poli(A). A reação de qRT-PCR foi realizada com miScript System Kits (Qiagen, Alemanha), de acordo com as instruções do fabricante, no termociclador CFX96 (Bio-Rad, EUA), numa placa de 96 poços e volume final de 20 µl. Para cada reação, utilizou-se um o miScript Universal Primer (oligonucleotídeo antissenso), o QuantiTect SYBR Green PCR Master e um conjunto de oligonucleotídeos específicos para cada miRNA maduro (oligonucleotídeo senso) (miScript Primer Sets; Qiagen, Alemanha): miR-10b-5p (MS00033194); miR-199a-3p (MS00013195). O pseudogene RNU6 (MS00033740) foi utilizado como normalizador dos níveis de RNA. A expressão gênica relativa foi determinada a partir da subtração do CT do gene de interesse e do normalizador, calculado usando o método ddCT (Schmittgen & Livak, 2008) e, expresso como relativo ao controle.

WESTERN BLOT

O extrato total proteico foi obtido pela lise das células com o tampão RIPA (Tris-HCl 20 mM pH 7.5; EDTA 5 mM, NaCl 150 mM, NP40 1% e inibidores de fosfatase e protease) e centrifugado a 13000 rpm a 4°C por 10 minutos. As proteínas (50 µg) foram separadas por um gel desnaturante de poliacrilamida de 6-10% (SDS-PAGE) e depois transferidas para uma membrana Immobilon-P (Millipore, EUA). O bloqueio de ligações não específicas foi feito com leite desnatado 5% em Tween 0,1 % por 1 hora e, posteriormente, incubadas com os anticorpos primários específicos para γ -tubulin (1:1000; sc-8035, Santa Cruz Biotechnology, EUA), vinculina (1:1000; sc-7649, Santa Cruz Biotechnology, EUA), p-ATM (1:1000; Rockland, EUA), ATM (1:1000; ab91, Abcam, EUA), ATR (1:2000; Novus Biological, Canadá) e γ H2AX (1:1000; #05-636, Upstate, EUA). A detecção do sinal foi feita com o ECL (Thermo Scientific, EUA).

ENSAIO TRANSIENTE DE RECOMBINAÇÃO HOMÓLOGA (HR)

Como previamente descrito por Morra e cols. (2015), as células HeLa ($2,5 \times 10^5$ células) foram plaqueadas em placas de 60 cm^2 e, 24 horas após, cotransfectadas com 50 nM de precursores dos miRNAs (pre-miR-10b-5p, pre-miR-199a-3p ou controle/scramble) e o vetor DR-GFP sozinho (controle negativo) ou na presença do vetor SceI (codifica uma endonuclease que promove a quebra-dupla do DNA), usando o reagente de transfecção Fugene HD (Promega, EUA), de acordo com as recomendações do fabricante. O vetor DR-GFP é um plasmídeo repórter baseado numa construto desenvolvido por Jasin (1996), contendo duas sequências codificantes de GFP mutados, separados pelo gene que codifica o marcador de seleção puromicina. O vetor que expressa GFP selvagem foi usado para o controle da eficiência de transfecção. Após 48 horas, as células foram coletadas e a porcentagem de células GFP positivas em relação ao controle foi avaliada no citometro de fluxo BD Accuri C6 Flow Cytometer (Becton Dickinson, EUA).

ENSAIO DE FORMAÇÃO DE COLÔNIAS

Para o ensaio de formação de colônias, as células 8505c foram transfectadas com o precursor de miR-10b-5p ou controle (Scramble) e, após 48 horas, foram tripsinizadas e replaqueadas (1×10^4 células/ poço) nas placas de 6 poços. Após 24 horas, as células foram irradiadas nas doses de 0, 2, 4, 6, 8 Gy de radiação X. Uma semana após a irradiação, as colônias de células foram coradas com cristal violeta 0,01% e as imagens foram capturadas. A quantificação relativa do número de colônias formadas foi realizada no programa ImageJ versão 1.51.

RESULTADOS

Os miR-10b-5p e miR-199a-3p afetam negativamente a eficiência do reparo por recombinação homóloga

Inicialmente, investigamos quais eram as vias de sinalização, alvo dos miRNAs alterados pela radiação X, usando o programa mirPath v.3 (Vlachos e cols., 2015). Como esperado, as vias de biossíntese de aminoácidos, a de PI3K-Akt e às relacionadas ao câncer compartilham alvos desses miRNAs (Tabela 1), que impactam diretamente ou indiretamente na maquinaria de reparo do DNA e na resposta à RI. Sobretudo, os miR-10b-5p e miR-199a-3p, os miRNAs mais desregulados pela radiação X em todos os tempos analisados, possuem como alvos preditos, genes que participam em todas as vias de sinalização citadas acima.

Tabela 1. Vias de sinalização alvo dos miRNAs alterados pela radiação X na linhagem FRTL-5 CL2

Vias de sinalização (KEGG)	p-value	#genes	#miRNAs
Biossíntese de aminoácidos	0.0242	11	2
Glioma	0.0242	8	2
Via de sinalização de prolactina	0.0242	7	3
Carcinogênese viral	0.0242	18	4
Via de sinalização de PI3K-Akt	0.0253	24	4
Degradação de lisinas	0.0276	5	2
Câncer de pulmão	0.0276	7	2
Metabolismo do ácido 2-Oxocarboxílico	0.0439	3	2
Melanoma	0.0439	8	2
Metabolismo do carbono central no câncer	0.0449	7	3
Processamento de proteínas no retículo endoplasmático	0.0490	13	3

Em seguida, analisamos a expressão basal de miR-10b-5p e miR-199a-3p nas linhagens FRTL-5 CL2 e FRTL KiKi. Os nossos dados revelam a superexpressão de miR-10b-5p (25x) e miR-199a-3p (600x) na linhagem transformada com o oncogene *v-Ras-Ki* em relação à linhagem normal de tireoide (Figura 5A), sugerindo que a desregulação desses miRNAs ocorra em etapas precoces da carcinogênese tireóidea e seja mediada por *RAS*.

Dado que as proteínas p-ATM, ATR e γ H2AX foram reguladas por miR-10b-5p e miR-199a-3p nas células FRTL-5 CL2 irradiadas, avaliamos esse efeito nas células FRTL KiKi, que superexpressam basalmente ambos os miRNAs. Como podemos observar na figura 5B, ATM não é ativado/ fosforilado nas células FRTL KiKi irradiadas. Além disso, a expressão proteica de ATR encontra-se reduzida nas células FRTL KiKi na primeira hora após a irradiação. Os níveis de γ H2AX foram induzidos pela RI em ambas as linhagens celulares. Desse modo, nos dados indicam que as células FRTL KiKi apresentam uma maquinaria de reparo do DNA por HR deficiente em comparação às células FRTL-5 CL2.

Em seguida, nos perguntamos se a eficiência do reparo por HR seria afetado pelos miR-10b-5p e miR-199a-3p (Figura 5C). Para tanto, utilizamos o sistema repórter DR-GFP (Jasin,1996) e o plasmídeo que codifica a enzima SceI, responsável por provocar lesões do tipo DSB, usando o sistema heterólogo celular HeLa, como previamente descrito por Morra e cols. (2015). Nossos resultados revelaram que os miR-10b-5p e miR-199a-3p diminuem a atividade de reparo do DNA por HR em 9 % e 10 %, respectivamente, em relação ao Scramble. Assim, os nossos achados demonstram que os miR-10b-5p e miR-199a-3p diminuem a eficiência do reparo das DSB ao afetar a via de reparo do DNA por HR.

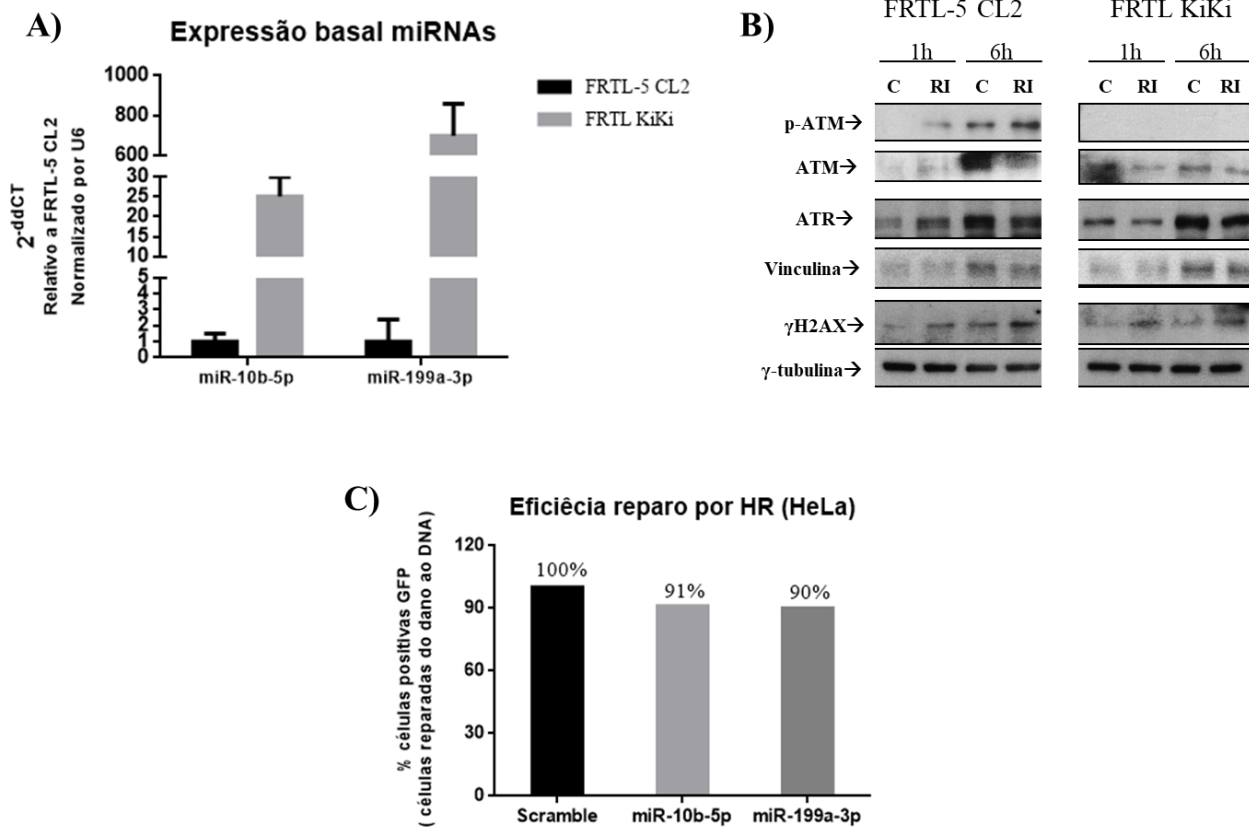


Figura 5 Expressão basal dos miR-10b-5p e miR-199a-3p nas linhagens celulares de tireoide e os seus efeitos sobre a maquinaria de reparo por recombinação homóloga (HR). (A) Comparação da expressão basal dos miR-10b-5p e miR-199a-3p nas células FRTL KiKi e FRTL-5 CL2 por qRT-PCR. Os valores de expressão dos miRNAs são relativos aos das células FRTL-5 CL2. O pseudogene RNU6 foi utilizado como normalizador dos níveis de miRNA. (B) Western blot representativo das proteínas envolvidas no reparo de quebras duplas do DNA, p-ATM, ATM, ATR e γ H2AX, nos tempos 1 e 6 horas após a irradiação (RI) nas células FRTL-5 CL2 e FRTL KiKi. (C) Para avaliar a atividade do reparo por HR, as células HeLa foram co-transfectadas com os vetores DR-GFP e SceI na presença dos oligonucleotídeos precursores de miR-10b-5p, miR-199a-3p ou Scramble. Os resultados foram expressos pela porcentagem de células GFP positivas em relação ao Scramble. Os resultados foram representados pelos valores das médias \pm SD de dois experimentos independentes.

O miR-10b-5p promove radiosensibilidade na linhagem celular de CAT (8505c)

Os carcinomas anaplásicos de tireoide (CAT) exibem um comportamento agressivo e são refratários à maioria das terapias de câncer, incluindo radioterapia (Molinaro e cols., 2017). Assim, nos perguntamos se a superexpressão de miR-10b-5p, mesmo que transitória, poderia sensibilizar as células tumorais de CAT à RI. Para tal, realizamos o ensaio de formação de colônias nas células 8505c transfectadas transitoriamente com os oligonucleotídeos precursores de miR-10b-5p ou Scramble (Figura 6A). Como podemos observar na figura 6.3B, a superexpressão de miR-10b-5p aumentou em 2,2 x o número de colônias das células 8505c não irradiadas (0 Gy). Por outro lado, o número de colônias formadas, relativo aos controles pareados, foi menor nas células 8505c irradiadas que superexpressam miR-10b-5p do que o Scramble (SC) e, tal efeito foi dependente da dose de radiação X. Este fenômeno foi mais evidente na maior dose de 8 Gy, quando observou-se uma redução de 50% no número de colônias formadas das células transfectadas com o miR-10b-5p em relação ao Scramble (Figura 6B). Portanto, nossos dados indicam claramente que miR-10b-5p induz radiosensibilidade na linhagem celular 8505c.

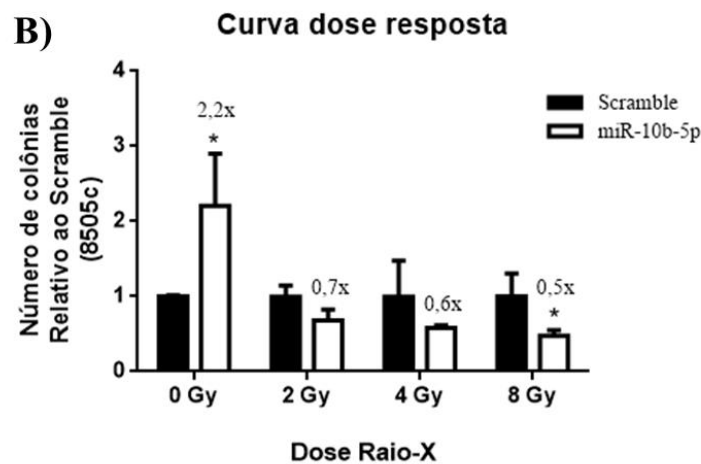
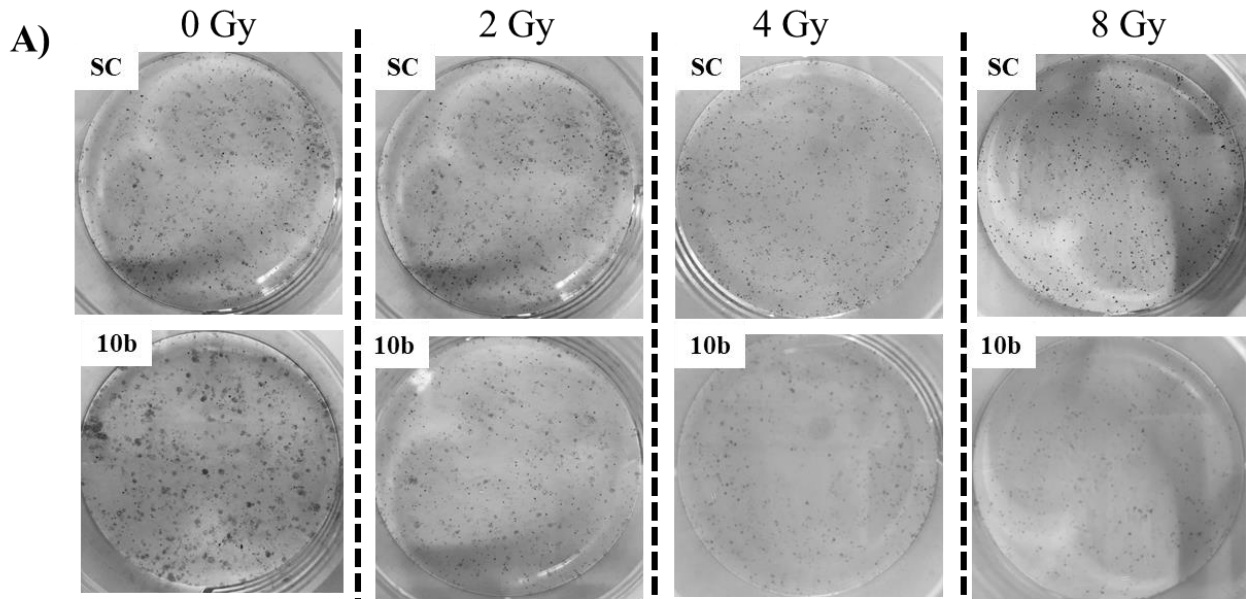


Figura 6 O miR-10b-5p sensibiliza a linhagem de CAT, 8505c, à RI. (A) As células 8505c, transfectadas com os oligonucleotídeos precursores de miR-10b-5p (10b) ou Scramble (SC), foram expostas à dose de 0, 2, 4 e 8 Gy de radiação X. Uma semana após a exposição à RI, as colônias de células foram coradas e quantificadas. Imagem representativa de três experimentos independentes. (B) Quantificação do número de colônias em resposta às doses de radiação X, usando as células 8505c. Os resultados são relativos aos seus respectivos controles em cada dose (Scramble) e, representados pela média de três experimentos independentes \pm SD. * $p < 0.05$.

4.3 CAPÍTULO III

O papel de *Dicer1* na proliferação e diferenciação de células da tireoide

A endonuclease *DICER1* desempenha um papel central na biogênese dos miRNAs, sendo fundamental para a ontogenia e homeostasia celular em vertebrados. A expressão alterada dos miRNAs e a desregulação de *DICER1* tem sido descrita em vários tipos de tumor, incluindo os da tireoide. Recentemente, o nosso grupo identificou uma nova mutação somática no gene de *DICER1* (c.5438A>G; E1813G) nas amostras de CPT com função desconhecida para a carcinogênese da tireoide. Nesse capítulo, foi observada a superexpressão de *DICER1*, no nível de RNAm (fold-change ≥ 1), em um número significativo de amostras de carcinoma papilífero da tireoide (CPT, 70%) e carcinoma anaplásico da tireoide (CAT, 42%) embora os seus níveis estejam drasticamente diminuídos nas linhagens humanas de carcinoma da tireoide (TPC-1, BCPAP, FRO e 8505c) em comparação às amostras de tireoide saudável. Por outro lado, os níveis proteicos de *DICER1* estão reduzidos em todas as amostras de CPT em relação à tireoide saudável ou ao tecido normal adjacente pareado. Em seguida, foram realizados ensaios funcionais para determinar a importância de *DICER1* para células normais e de câncer da tireoide. O silenciamento parcial da expressão de *DICER1* na linhagem de tireócito normal (PCCl 3) levou à: 1) atenuação da expressão/ processamento de miRNAs (miR-21-5p, miR-125-5p) regulados por *DICER1*; 2) redução da viabilidade e proliferação celular; 3) diminuição da expressão das ciclinas E e B1, bem como à parada das células na fase S do ciclo celular; 4) perda dos marcadores de diferenciação da tireoide (*Ttf-1*, *Pax8*, *Tg*, *Tpo* e *Nis*). Esses dados foram reproduzidos na linhagem de tireócito transformada com o oncogene v-*RAS*-Ki. Para determinar o significado biológico da mutação c.5438A>G; E1813G no gene de *DICER1*, as linhagens humanas de CPT (TPC-1 e BCPAP) foram transfectadas com os plasmídeos que codificam *DICER1* selvagem ou mutada. A superexpressão de *DICER1* selvagem induziu: 1) o processamento dos miRNAs; 2) o aumento da viabilidade e proliferação celular; 3) a expressão das ciclinas D e E, assim como o número de células na fase S do ciclo celular. A presença da mutação c.5438A>G; E1813G afetou negativamente todos os efeitos mediados por *DICER1* selvagem e induziu a expressão dos níveis endógenos de *DICER1*. A introdução desta mutação nas células PCCl 3 não alterou nenhum dos parâmetros avaliados. Por outro lado, a superexpressão de *DICER1* parece ter efeito inibitório sobre o processamento dos miRNAs nas

células PCCI 3, sugerindo que a regulação fina dos níveis de expressão de *DICER1* seja importante para a homeostasia celular. Em suma, a mutação c.5438A>G; E1813G parece antagonizar os efeitos da *DICER1* selvagem e, juntamente com outras mutações somáticas e germinativas nesse gene, poderiam contribuir para carcinogênese da tireoide, particularmente nos portadores da síndrome DICER.

Role of *Dicer1* in thyroid cell proliferation and differentiation

Ricardo Cortez Cardoso Penha^{a,b}, Romina Sepe^a, Marco De Martino^a, Francesco Esposito^a, Simona Pellecchia^a, Maddalena Raia^c, Luigi del Vecchio^{c,d}, Myriam Decaussin-Petrucci^{ib,e}, Gabriella De Vita^{ib,d}, Luis Felipe Ribeiro Pinto^b, and Alfredo Fusco^{ib,a,b}

^aIstituto per l'Endocrinologia e l'Oncologia Sperimentale (IEOS) "G. Salvatore", Consiglio Nazionale delle Ricerche (CNR), c/o Dipartimento di Medicina Molecolare e Biotecnologie Mediche, Università degli Studi di Napoli "Federico II", Naples, Italy; ^bInstituto Nacional de Câncer - INCA, Centro de Pesquisas (CPQ), Rio de Janeiro, RJ, Brazil; ^cCEINGE-Biotecnologie Avanzate, Università di Napoli Federico II, Naples, Italy; ^dDepartment of Molecular Medicine and Medical Biotechnologies, University of Naples Federico II, Naples, Italy; ^eCentre de Pathologie Sud, Centre Hospitalier Lyon Sud, Pierre Bénite, France

ABSTRACT

DICER1 plays a central role in the biogenesis of microRNAs and it is important for normal development. Altered microRNA expression and *DICER1* dysregulation have been described in several types of tumors, including thyroid carcinomas. Recently, our group identified a new somatic mutation (c.5438A>G; E1813G) within *DICER1* gene of an unknown function. Herein, we show that *DICER1* is overexpressed, at mRNA level, in a significant relative number of papillary (70%) and anaplastic (42%) thyroid carcinoma samples, whereas is drastically downregulated in all the analyzed human thyroid carcinoma cell lines (TPC-1, BCPAP, FRO and 8505c) in comparison with normal thyroid tissue samples. Conversely, *DICER1* is downregulated, at protein level, in PTC in comparison with normal thyroid tissues. Our data also reveals that *DICER1* overexpression positively regulates thyroid cell proliferation, whereas its silencing impairs thyroid cell differentiation. The expression of *DICER1* gene mutation (c.5438A>G; E1813G) negatively affects the microRNA machinery and cell proliferation as well as upregulates *DICER1* protein levels of thyroid cells but has no impact on thyroid differentiation. In conclusion, *DICER1* protein is downregulated in papillary thyroid carcinomas and affects thyroid proliferation and differentiation, while *DICER1* gene mutation (c.5438A>G; E1813G) compromises the *DICER1* wild-type-mediated microRNA processing and cell proliferation.

ARTICLE HISTORY

Received 14 June 2017
Revised 8 September 2017
Accepted 11 September 2017

KEYWORDS

Dicer1; microRNA; papillary thyroid carcinoma; thyroid cells

Introduction



Mature microRNAs (miRNAs or miRs) are small regulatory RNAs of 21–24 nucleotides (nt) in length that exert a crucial role on a variety of biological processes such as differentiation, proliferation, apoptosis, survival, growth, senescence and migration in vertebrates.¹ They lead to decreased protein levels *via* repression of translation and/ or mRNA decay *via* deadenylation when miRNA pairs with target mRNA.² A central role in the biogenesis of miRNAs is played by *DICER1* that recognizes and cleaves the miRNAs precursors (50–70 nt) into mature miRNAs.²


Therefore, *DICER1* gene is fundamental for normal development. Indeed, conditional *DICER1* knockout models unraveled its importance for normal cerebellar³ and female reproductive system⁴ development as well as thyroid organogenesis and function.⁵

Moreover, recent studies have already demonstrated the dysregulation of *DICER1* gene expression and/or mutations in human cancer. In fact, the downregulation of *DICER1* expression has been associated to lung,⁶ breast⁷ and ovarian⁸ cancer progression and worse patient prognosis. Conversely, its overexpression has been described in prostate,⁹ colorectal¹⁰ and

thyroid cancer.¹¹ Somatic mutations in the metal-binding sites within the RNase IIIb catalytic domain (c.5438A>G, c.5429A>T and c.5429A>G) have been also described in human carcinomas. In particular, the mutation c.5438A>G (E1813G) has been reported in several human neoplasias, including non-epithelial ovarian,¹² childhood cystic nephroma¹³ and thyroid cancer¹⁴ as well as Wilms tumors:¹⁵ it is predicted to impair the RNase IIIb function, critical for miRNA interaction and cleavage. Interestingly, this mutation has been also identified by our group in papillary thyroid carcinoma (PTC) samples¹⁶ and then further confirmed by Yoo et al. (2016)¹¹ and associated with *DICER1* overexpression. Noteworthy, the germline *DICER1* mutations, concerning the coding sequence, have also been identified.¹⁷ They result in truncated protein nearby RNase III domain (i.e. c.3579_3580delCA), with an increased risk of multinodular thyroid hyperplasia and differentiated thyroid carcinoma for the patients carrying these mutations.¹⁴

In this study, we aimed at evaluating the role of *DICER1* on thyroid proliferation and differentiation using rat normal and

CONTACT Alfredo Fusco  alfusco@unina.it  Istituto di Endocrinologia ed Oncologia Sperimentale del CNR, Dipartimento di Medicina Molecolare e Biotecnologie Mediche, Università degli Studi di Napoli "Federico II", via Pansini 5, 80131 Naples, Italy.

 Supplemental data for this article can be accessed on the publisher's website.

© 2017 Taylor & Francis

human carcinoma thyroid cell lines. Our data reveals that *DICER1* overexpression positively regulates thyroid cell proliferation, whereas its silencing impairs thyroid cell differentiation. Finally, the expression of *DICER1* gene mutation c.5438A>G (E1813G) in thyroid cells negatively affects miRNA processing and also thyroid cell proliferation.

Material and methods

Human thyroid samples

The human thyroid biopsies – 7 normal thyroid tissues (NT), 31 papillary thyroid carcinomas (PTC) and 14 anaplastic thyroid carcinomas (ATC) – were provided by the service of Pathological Anatomy of the Centre Hospitalier Lyon Sud, Pierre Bénite, France. Informed written consent was obtained from the patients.

Cell culture and transfection

PCCl 3 rat thyroid cells, derived from 18-month-old Fisher rats, were grown in Coon's modified Ham's F-12 medium (Euroclone), supplemented with 5% calf-serum and a six-hormone mixture (1 mU/ml TSH, 10 µg/ml insulin, 5 µg/ml transferrin, 10 nM hydrocortisone, 10 ng/ml somatostatin, and 10 ng/ml glycyl-L-histidyl-L-lysine acetate).¹⁸ Kras-transformed PCCl 3 (kiki) were cultured in Ham's F12 medium (Euroclone), supplemented with 10% calf serum.¹⁸ The human papillary thyroid carcinoma cell lines TPC-1 (RET/PTC) and BCPAP (*BRAFV600E*) were grown in DMEM medium (Life Technologies), supplemented with 10% fetal bovine serum.

For the inhibition of *DICER1* expression in PCCl 3 and PCCl 3 kiki, cells were transfected with a short interfering RNA (siRNA) specific for *DICER1* (NM_001195573-1/2, Ribox life science) and Nonsilencing Control siRNA (IBONI control N3, Ribox life science) using Lipofectamine RNAi MAX (Life Technologies), according to the manufacturer's recommendations. The siRNAs were used at a final concentration of 50 nM.

For overexpression of *DICER1*, transfections procedures were performed using Fugene HD reagent (Promega) for TPC-1 and BCPAP cells and, Lipofectamine 2000 (Life Technologies) for PCCl 3, following manufacturer's instructions.

Plasmids

The plasmid pFRT/TO/FLAG/HA-DEST *DICER1*¹⁹ (pDI-CER1wt; #19881; Addgene) encodes human *DICER1* protein (5772 bp; NM_177438) fused to the epitope of FLAG/HA in the N-terminal region. The vector containing the c.5438A>G (E1813G) mutation was constructed by excising the 788 bp fragment, flanking the mutation site, using the restriction enzymes XmaI (#R0180S; New England BioLabs) and PspXI (#R0656L; New England BioLabs) and, further, inserting the synthesized fragment containing the c.5438A>G (E1813G) mutation (Integrated DNA Technologies) into the linearized pDI-CER1wt, generating a plasmid encoding human mutated *DICER1* (pDI-CER1mut). The plasmid was sequenced (Eurofins

Genomics) and *DICER1* expression was validated by q-RT-PCR and western blot analysis.

Cell proliferation

Cells were counted 48 hours post transfection using trypan blue. In parallel, as an index of cell viability, we used the commercially available MTT assay (Sigma-Aldrich). MTT reagent was diluted at final concentration of 0.5 mg/mL in cell medium and then, solubilized in DMSO. Measures were performed at 570 nm using ELx800 microplate Reader (BIO-TEK).

Flow cytometry

Cell cycle profile was evaluated using propidium iodide (2 µg/mL) on FACScan flow cytometer (Becton Dickinson) and analyzed on CELL-FIT software (Becton Dickinson).

q-RT-PCR

Total RNA was extracted from thyroid cell lines using the Trizol reagent (Life Technologies) according to the manufacturer's instruction. 1 µg of total RNA of each sample was used to obtain single strand cDNA with the QuantiTect Reverse Transcription Kit (Qiagen) using an optimized blend of oligo-dT and random primers according to the manufacturer's instruction.

Quantitative Real-Time PCR (q-RT-PCR) was performed with the CFX96 thermocycler (Bio-Rad) in 96-well plates using a final volume of 20 µl. For each of the PCR reaction, it was used 10 µl of 2X Sybr Green (Bio-Rad), 200 nM of each primer, and 20 ng of the cDNA previously generated. The oligonucleotides for q-RT-PCR, comprising exon-exon junctions, were purchased from Integrated DNA Technologies and designed with Primer-BLAST software,²⁰ are listed in Table 1. Relative gene expression was determined using comparative C(T) method.²¹ *RP18S* and *Rpl4* were used as housekeeping gene for human and rat samples, respectively.

To assess miRNA expression, 1 µg of total RNA of each sample was reverse transcribed with the miScript reverse transcription Kit (Qiagen), according to the manufacturer's

Table 1. Sequences of the primers used for q-RT-PCR.

Target	Sequences
hs/rno_Dicer1	F: CACATGCCTCTACCACTACAAT R: TGCTTGGTTATGAGGTAGTCCA
hs_RP18S	F: TGCGAGTACTCAACACCAA R: TTGGTGAAGTCAATGTCTGC
rno_Rpl4	F: GATGAATTGTACGGCACTTGG R: TCTTTGGATCTCGGGCTTTTTC
rno-Ttf1	F: CTA CTGCAACGGCAACCTG R: CCCATGCCATCATATATTCAT
rno_Pax8	F: GCCATGGCTGTGAAGCAAGA R: GCTTGGAGCCCTATCACT
rno_Tg	F: CATGGAATCTAATGCCAAGAAGT R: TCCCTGTGAGCTTTTGGAAATG
rno_Tpo	F: CAAAGGCTGGAACCTAATTTCT R: AACTTGAATGAGGTGCTTGCA
rno_Nis	F: TCCACAGGAATCATCTGCACC R: CCACGGCTTCATACCACC

instruction. For q-RT-PCR analysis, it was used miScript System Kits (Qiagen) and the following specific primers for mature miR (miScript Primer Sets; Qiagen): miR-21-5p (5'UAGCUUA UCAGACUGAUGUUGA); miR-33-5p (5'GUGCAUUGUAG UUGCAUUGCA); miR-125b-1-5p (5'UCCUGAGACCCUA ACUUGUGA); miR-296-5p (5'AGGGCCCCCUCAAUCUGU); miR-362 (5'AAUCCUUGGAACCUAGGUGUGA AU). RNU6 (MS00033740) was used for normalization.

Western blot

Cells were homogenized in RIPA buffer lysis (20 mM Tris-HCl pH 7.5, 5 mM EDTA, 150 mM NaCl, 1% Nonidet P40, and a mix of protease inhibitors) and then centrifuged at 13000 rpm at 4°C for 10 min. Cell lysate proteins (50–100 µg) were then subjected to SDS/PAGE electrophoresis, transferred onto Immobilon-P Transfer membranes (Millipore), membranes were blocked with 5% non-fat milk proteins and probed with the indicated antibodies at the appropriate dilutions: DICER1 (1:1000; sc-136981), Cyclin D1 (1:1000; sc-718), Cyclin E (1:1000; sc-248), Cyclin B1 (1:1000; sc-254), Vinculin (1:1000; sc-7649) and γ -tubulin (1:1000; sc-8035), all from Santa Cruz Biotechnology. Thyroglobulin (1:5000), TTF-1 (1:500) and PAX8 (1:5000) are rabbit polyclonal antibodies and described elsewhere.⁵ Membranes were then incubated with horseradish peroxidase-conjugated secondary antibody (1:3000) for 60 min at room temperature and the signals were detected by western blotting detection system (ECL) (Thermo Scientific).

Statistical analysis

All results were expressed as mean \pm SD. Data were analyzed by non-parametric Mann Whitney's test (when comparing two groups) or by the non-parametric Kruskal-Wallis test followed by Dunn's multiple comparison test (when comparing three or

more groups). Statistical analyses were performed using the software Graphpad Prism (Version 5, Graphpad Software Inc.) and the difference was considered significant when $p < 0.05$.

Results

DICER1 expression in human thyroid carcinoma cell lines and tissues

First, we analyzed the expression of *DICER1* in human thyroid carcinoma tissues and cell lines. The results shown in Fig. 1A demonstrate that *DICER1* mRNA levels are increased in 22 out of 31 PTC and 6 out of 14 anaplastic thyroid carcinoma (ATC) samples when compared to normal thyroid tissue (NT) ($p < 0.05$) (fold-change ≥ 2), exhibiting a heterogeneous expression profile among thyroid carcinomas. Interestingly, *DICER1* is drastically downregulated in all the analyzed thyroid carcinoma cell lines (TPC-1, BCPAP, FRO and 8505c; $p < 0.001$). Conversely, *DICER1* protein levels were reduced in PTC in comparison with NT (0.31 ± 0.2) (Fig. 1B, C).

Silencing of Dicer1 affects proliferation and differentiation of normal thyroid cell line PCC13

Then, we investigated whether *Dicer1* has a role in thyroid cell proliferation and differentiation using the normal rat thyroid cell line PCC13. This cell line is not tumorigenic and keeps *in vitro* all the markers of thyroid differentiation, i.e. thyroglobulin synthesis and secretion, ability to trap iodide and the dependency on thyrotropin for the growth.¹⁸ We knocked down (KD) *Dicer1* expression by transfecting the PCC13 cells with *Dicer1* siRNAs. First, we validated the silencing of *Dicer1* mRNA (Fig. 2A) and protein levels (Fig. 2B) by q-RT-PCR and western blot analysis, respectively. Accordingly, decreased expression levels of miR-21-5p and miR-125-5p (Fig. 2C),

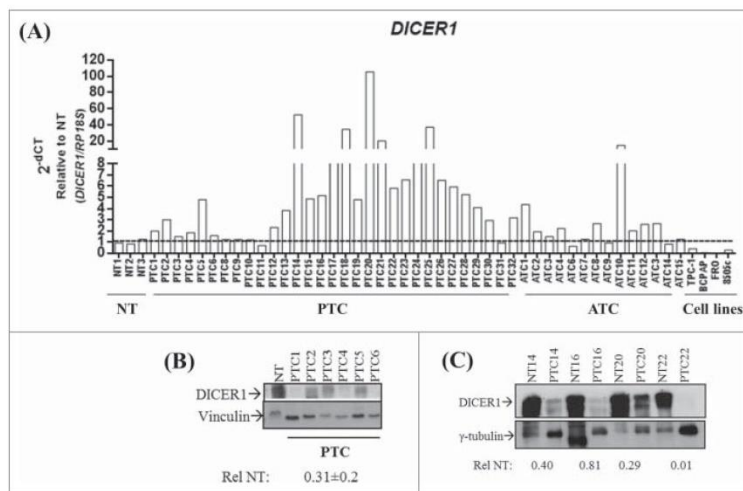


Figure 1. Expression of *DICER1* in human thyroid carcinoma tissues and cell lines. (A) Expression of *DICER1* was evaluated by q-RT-PCR in normal thyroid tissues (NT, $n = 3$), papillary thyroid carcinomas (PTC, $n = 31$), anaplastic thyroid carcinomas (ATC, $n = 14$) and human thyroid carcinoma cell lines (TPC-1, BCPAP, FRO, 8505c). *RP18S* was used as housekeeping gene. Expression levels were relative to NT. (PTC vs. NT, $p = 0.049$; ATC vs. NT, $p = 0.048$; cell lines vs. NT, $p = 0.002$). The *DICER1* protein levels were assessed by western blot in (B) NT (1) and PTC (6) samples and, (C) four normal/PTC paired samples. The results of the densitometric analysis were normalized by vinculin and γ -tubulin levels and relative to NT \pm SD.

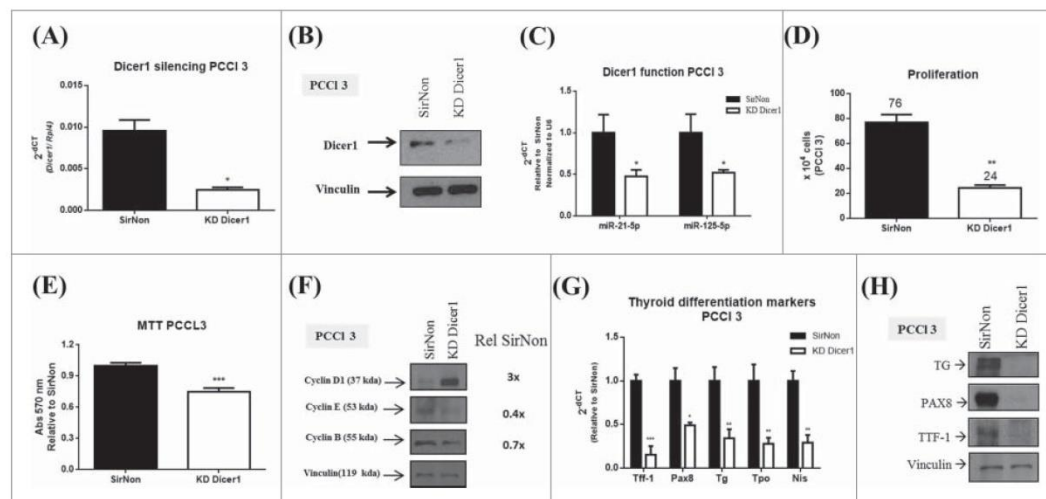


Figure 2. Silencing of *Dicer1* in PCCl 3 cells. Cells were transfected with nonsilencing control siRNA (SirNon) or specific *Dicer1* siRNA (KD *Dicer1*) and (A) *Dicer1* mRNA and (B) protein levels were assessed by q-RT-PCR and western blot, respectively. (C) Expression of miR-21-5p and miR-125-5p to evaluate *Dicer1* function. (D) Number of PCCl 3 cells was counted using trypan blue 48 hours post transfection with SirNon or specific *Dicer1* siRNA. (E) In parallel, cell viability was assessed using MTT assay in the same conditions. (F) Expression of cyclin D1, E and B by western blot 48 hours after the transfection of PCCl 3 cells with SirNon or specific *Dicer1* siRNA. Densitometry intensity quantification was calculated as ratio target: vinculin and relative to SirNon. (G) mRNA levels of the thyroid differentiation markers *Ttf-1*, *Pax8*, *Tg*, *Tpo* and *Nis* 48 hours after the transfection of PCCl 3 cells with SirNon or specific *Dicer1* siRNA were evaluated by q-RT-PCR. (H) Protein levels of thyroglobulin (TG), PAX8 and TTF-1 were assessed by western blot in the same conditions. Data were relative to SirNon. Vinculin was used as loading control for western blot. Rpl4 and pseudogene U6 were used as housekeeping for q-RT-PCR of mRNA and miR levels, respectively. $p < 0.05$, $p < 0.01$; $p < 0.001$.

previously shown to be modulated by *Dicer1*,²² in comparison with the control transfected PCCl 3 cells were observed. The *Dicer1* downregulation results in a decreased number of cells (76 vs. 24, $p < 0.01$) (Fig. 2D) and a reduction of cell viability (25%) with respect to the control cells (Fig. 2E). Consistently, the analysis of cyclin expression reveals decreased levels of cyclin E and cyclin B1 in *Dicer1*-silenced PCCl 3 cells in comparison with the control cells (Fig. 2F). Unexpectedly, an increased cyclin D1 expression was found in *Dicer1*-silenced PCCl 3 cells. However, a recent study showed that the cyclin D1 expression in breast cancer cells does not influence cell proliferation in absence of *Dicer1* expression.²³

Since *Dicer1* has been previously reported to have a critical role in thyroid organogenesis,⁵ we next investigated the expression of thyroid differentiation markers in the *Dicer1*-silenced PCCl 3 cells. As shown in Fig. 2G, the *Ttf-1*, *Pax8*, *Tg*, *Tpo* and *Nis* mRNA levels were drastically downregulated by silencing of *Dicer1* expression and, further confirmed by western blot analysis for *Ttf-1*, *Pax8* and *Tg* protein levels (Fig. 2H). These results suggest that *Dicer1* and, consequently miRNA maturation, plays a critical role in the regulation of thyroid cell proliferation and differentiation.

Silencing of *Dicer1* inhibits also the growth of *Kras*-transformed PCCl 3 cells (PCCl 3 kiki cells)

Subsequently, we silenced *Dicer1* expression in the PCCl 3 cells transformed by the Kirsten murine sarcoma virus carrying the *Kras* oncogene. The q-RT-PCR (Fig. 3A) and western blot (Fig. 3B) analysis confirmed the silencing of *Dicer1* expression at mRNA and protein level, respectively. In order to assess *Dicer1* function, we analyzed the expression of miR-21-5p and

miR-125-5p. As shown in Fig. 3C, the inhibition of *Dicer1* expression results in a reduction of these miRNA levels. As shown above for the normal PCCl 3 cells, the number of cells diminished in comparison to SirNon (44 vs. 129, $p < 0.05$) (Fig. 3D) as well as attenuated the number of viable cells (20%) (Fig. 3E). Accordingly, both of the expression of cyclin D1 and E was downregulated in *Dicer1*-silenced cells (Fig. 3F). These data evidence that suppression of *Dicer1* expression may also affect transformed thyroid cell proliferation.

The mutation c.5438A>G (E1813G) within DICER1 gene affects DICER1 activity

In order to investigate the role of the *DICER1* mutation c.5438A>G (E1813G), that was previously identified in PTC samples,^{11,14,16} we transfected two human thyroid papillary carcinomas cell lines, BCPAP and TPC-1, with the expressing vectors, containing the wild-type (pDICER1wt) and the mutated *DICER1* (pDICER1mut) cDNAs. Firstly, we validated the overexpression of both expressing vectors by q-RT-PCR (Fig. 4A, D) and western blot (Fig. 4B, E) in comparison with the empty vector (EV). Since the expression of miR-21-5p and miR-125-5p was not regulated by pDICER1wt or pDICER1mut with respect to EV in BCPAP cells (data not shown), we searched for miRNA involved in thyroid differentiation and cancer: miR-33-5p and miR-296 target several thyroid differentiation markers such as NIS, thyroglobulin and TSH receptor.²² MiR-362 is downregulated in variant papillary thyroid carcinomas.²⁴ Interestingly, the overexpression of pDICER1wt resulted in an increased expression of the miR-33-5p and miR-362 in BCPAP (Fig. 4C) and miR-21-5p and miR-296-5p in TPC-1 cells

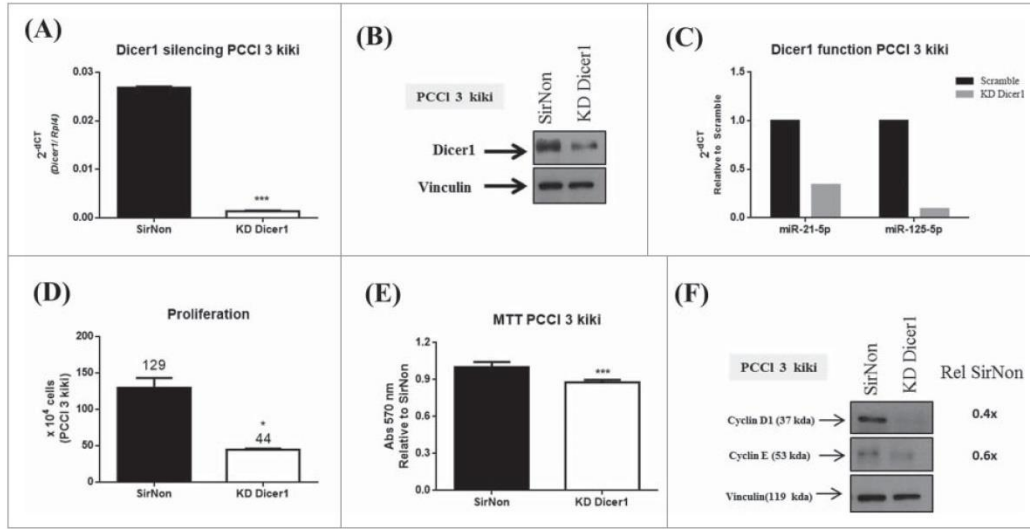


Figure 3. *Dicer1* impacts the proliferation of *KRAS*-transformed PCC1 3 cells (PCC1 3 kiki). Cells were transfected with SirNon or *Dicer1* specific siRNAs and (A) *Dicer1* mRNA and (B) protein levels were assessed by q-RT-PCR and western blot, respectively. (C) To assess *Dicer1* function, miR-21-5p and miR-125-5p expression were evaluated by q-RT-PCR in the same conditions. (D) Number of PCC1 3 kiki cells was counted using trypan blue 48 hours post transfection with SirNon or specific *Dicer1* siRNAs. (E) Cell viability was assessed using MTT assay in the same conditions. (F) Expression of cyclin D1 and E by western blot 48 hours after the transfection of PCC1 3 kiki cells with SirNon or specific *Dicer1* siRNA. Densitometry intensity quantification was calculated as ratio target: vinculin and relative to SirNon. Vinculin was used as loading control for western blot. *Rpl4* was used as housekeeping gene. * $p < 0.05$; *** $p < 0.001$.

(Fig. 4F) and, the expression of the mutated *DICER1* (p*DICER1*mut) reversed these phenomena, suggesting that this mutation might affect miRNA machinery.

Then, we wondered whether the growth rate of thyroid cells was affected by p*DICER1*wt and p*DICER1*mut. As shown in Fig. 5, when BCPAP and TPC-1 cells were transfected with p*DICER1*wt construct, but not with the

p*DICER1*mut, they displayed a higher growth rate (80%, BCPAP, $p < 0.001$; 30%, TPC-1, $p < 0.01$) in comparison with the empty vector transfected cells (Fig. 5A, D). Moreover, p*DICER1*wt construct increased cell viability (13%, BCPAP, $p < 0.001$; 42%, TPC-1, $p < 0.05$) with respect to p*DICER1*mut (Fig. 5B, E). In agreement with that, an increment of the cyclins D1 and E levels was observed when cells

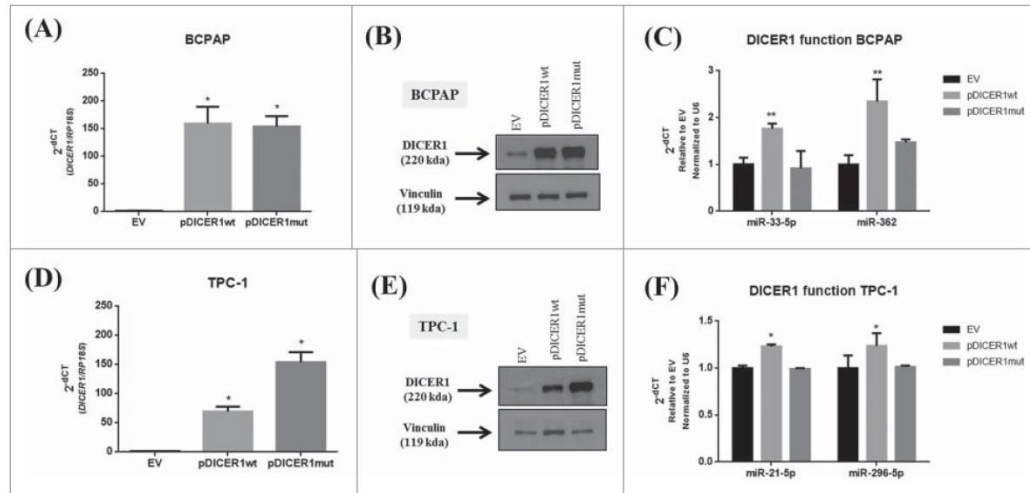


Figure 4. Effect of wild-type and mutated c.5438A>G (E1813G) *DICER1* function in BCPAP and TPC-1 cells. Cells were transfected with empty vector (EV) and constructs expressing *DICER1* wild-type (p*DICER1*wt) or mutated c.5438A>G (E1813G) (p*DICER1*mut) and 48 hours after transfection: (A) *DICER1* mRNA and (B) protein levels were assessed in BCPAP cells by q-RT-PCR and western blot, respectively. (C) Expression of miR-33-5p and miR-362 to evaluate *DICER1* function 48 hours post transfection in BCPAP cells. (D) mRNA and (E) protein levels of *DICER1* in TPC-1 cells 48 hours after transfection with EV, p*DICER1*wt or p*DICER1*mut. (F) Expression of miR-21-5p and miR-296-5p to evaluate *DICER1* function 48 hours post transfection in TPC-1 cells. Vinculin was used as loading control for western blot. *RP18S* and pseudogene *U6* were used as housekeeping for q-RT-PCR of gene and miR expression, respectively. * $p < 0.05$, ** $p < 0.01$.

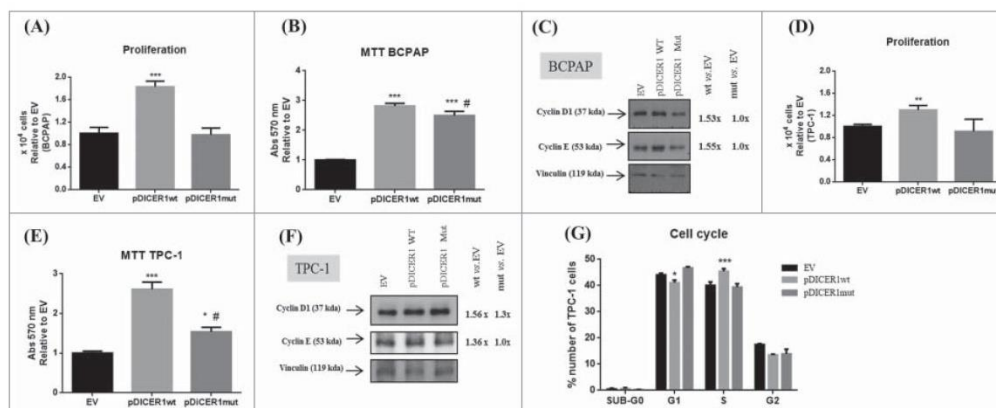


Figure 5. Effect of wild-type and mutated c.5438A>G (E1813G) *DICER1* on BCPAP and TPC-1 cell proliferation. Cells were transfected with empty vector (EV) and *DICER1*-overexpression vectors, containing *DICER1* wild-type (pDICER1wt) or mutated c.5438A>G (E1813G) *DICER1* (pDICER1mut) cDNA and, 48 hours post transfection: (A) the number of BCPAP cells were counted using trypan blue and the results were relative to EV; (B) cell viability was evaluated using the MTT assay in BCPAP cells; (C) expression of cyclins D1 and E by western blot. Densitometry analyses were performed in comparison with EV in BCPAP cells. The same assays and conditions were performed for TPC-1 cells. (D) the number of TPC-1 cells were counted using trypan blue and the results were relative to EV; (E) cell viability was evaluated using the MTT assay in TPC-1 cells; (F) expression of cyclins D1 and E. Densitometry analyses were performed in comparison with EV; (G) cell cycle by flow cytometry using propidium iodide and data were represented as the percentage of cells in each phase of the cell cycle. Vinculin was used as loading control for western blot. * $p < 0.05$; ** $p < 0.01$; *** $p < 0.001$ compared to EV. # $p < 0.05$, compared to pDICER1wt.

were transfected with pDICER1wt construct, in comparison with pDICER1mut or EV (Fig. 5C, F). Cell cycle analysis unraveled that *DICER1*-overexpressing vectors induced in pDICER1wt-transfected TPC-1 cells, but not pDICER1mut, a decreased cell number in G1 (40% vs. 45%, $p < 0.05$) and an increased one in S phase (45% vs. 40%, $p < 0.05$) of the cell cycle in comparison to EV (Fig. 5G).

These data suggest that *DICER1* wild-type overexpression induces human thyroid carcinoma cell line proliferation and enhances miRNA processing, while the mutated *DICER1* form negatively impacts on these parameters.

Dicer1 overexpression increases the proliferation rate of the PCC1 3 cells, but does not affect thyroid differentiation

To investigate the role of the mutated *DICER1* in normal thyroid cells, we transfected the PCC1 3 cells with pDICER1wt or pDICER1mut. We confirmed the overexpression of both constructs by q-RT-PCR (Fig. S1A) and western blot (Fig. S1B) analysis, forty-eight hours post transfection. Unexpectedly, the expression of miR-21-5p and miR-125-5p were downregulated by pDICER1wt with respect to EV and a weak or no effect was observed after the transfection with pDICER1mut (Fig. S1C). Then, we observed that pDICER1wt slightly increased the cell growth rate in comparison with EV (63 vs. 45, $p < 0.001$) and pDICER1mut reversed this effect (Fig. S1D). Accordingly, pDICER1wt weakly increased the number of viable cells in comparison with EV (27%, $p < 0.001$) and pDICER1mut reversed it (Fig. S1E). Above all, the transfection of *DICER1*-overexpressing vectors had no effect on the expression of the thyroid differentiation markers (*Ttf-1*, *Pax8*, *Tg*, *Tpo* and *Nis*) (Fig. S1F),

suggesting that basal *Dicer1* levels are important to maintain thyroid differentiation.

Discussion

DICER1 is a key player in miRNA processing and its role on development and cancer has been widely explored. Herein, we assess *DICER1* expression in thyroid carcinoma samples and then, we focused on *DICER1* impact on proliferation and differentiation of normal and cancer thyroid cell lines as well as the function of the mutation c.5438A>G (E1813G) on these parameters.

DICER1 dysregulation has been reported in thyroid cancer^{11,14,16} and its upregulation was associated with aggressive behavior (i.e. extrathyroidal extension and distant metastasis) of PTC.²⁵ Our results demonstrate that *DICER1* mRNA levels are upregulated in almost 70% of PTC and 42% of ATC analyzed. The limited sample number might account for the differences found at *DICER1* mRNA levels of thyroid carcinoma samples between our results and those present in the TCGA database²⁶ as well as the different technical approaches to assess *DICER1* expression might account for the magnitude of its mRNA levels. Conversely, *DICER1* protein levels were reduced in PTC samples. The downregulation of *DICER1*, at least at protein level, is in accordance with TCGA database.²⁶ The discrepancy between mRNA and protein levels of *DICER1* has been already reported by several studies,^{25,27} indicating that post-transcriptional mechanisms regulate *DICER1* protein levels in neoplastic tissues.

Interestingly, a drastic *DICER1* downregulation was found in all thyroid carcinoma cell lines. This result may be associated to the critical role of miRNA and, consequently, *DICER1* on

thyroid differentiation.⁵ Besides, thyroid carcinoma cell lines exhibit a dedifferentiated phenotype when compared to their original *in vivo* thyroid tumors²⁸ or may be simply due to the very high number of passages of these cell lines in culture.

The effect of *DICER1* on cell proliferation is still controversial. Our data point out that *DICER1* stimulates thyrocyte proliferation. These results are in accordance with knockout *DICER1* mice models, in which the loss of *DICER1* led to a smaller sized thyroid gland.^{5,29} Paradoxically, in the same model the authors observed an increased BrdU positive cells,²⁹ a proliferation marker,³⁰ which could be partially explained by the severe hypothyroidism and increased TSH plasma levels induced by *DICER1* loss. Moreover, it has been reported that the monoallelic but not biallelic loss of *DICER1* promotes tumorigenesis *in vivo*, which means that the effect of *DICER1* on cell proliferation depends on its levels.^{31,32} Thus, while the partial loss is advantageous to tumors, the massive decrease of *DICER1* expression could compromise thyroid cell viability and proliferation. Accordingly, our results are in agreement with those reported by Frezzetti *et al.*,⁵ in which the thyroid glands of *Dicer1* knockout mice were smaller than control and heterozygous mice. Interestingly, miR-21-5p and miR-125-5p, previously shown to target thyroid differentiation markers and to be modulated by *DICER1*,²² are downregulated in *DICER1*-silenced PCCL 3 cells, however, they are also downregulated in *DICER1*-overexpressing PCCL 3 cells, suggesting that the tight regulation of *DICER1* levels are important to maintain miRNA processing machinery.

Noteworthy, *DICER1*-silencing PCCL 3 cells exhibit a dedifferentiated phenotype, whereas the differentiation markers do not show any change in their expression when *DICER1* wild-type or mutated is overexpressed, indicating that basal expression of *DICER1* is important to the maintenance of thyroid differentiation. In fact, *DICER1* expression is crucial to thyroid homeostasis and its loss has been reported to disturb thyroid organogenesis and differentiation and might prompt cells to acquire cancer-like features.^{5,29}

The RNase IIIb domain of *DICER1* is a mutational hotspot in non-epithelial gonadal³³ and endometrial tumors.³⁴ The mutation E1813G of *DICER1*, located within RNase IIIb domain, has been consistently identified in thyroid carcinoma (5–8% of the cases) by several studies.^{11,14,16} Our data point out that the mutation E1813G of *DICER1* negatively affects the proliferation and miRNA processing machinery of thyroid cells. Indeed, this mutation could partially reduce *DICER1* activity since it is predicted to impair the RNase IIIb function, failing to cleave miRNAs from the 5'-arm of pre-miRNA hairpins,² which is in agreement with the inability of mutated *DICER1* form to induce the miRNA expression in comparison with the *DICER1* wild-type. Moreover, we could not exclude the contribution of other mutations within *DICER1* gene for cell transformation. In fact, the presence of *DICER1* germline mutations and additional somatic mutations such as E1813G were associated to well-differentiated thyroid carcinoma development in *DICER1* syndrome patients.¹⁴

In summary, *DICER1* protein is downregulated in papillary thyroid carcinomas and its basal expression is fundamental to thyroid differentiation. Moreover, the mutation E1813G within *DICER1* gene affects *DICER1* wild-type-mediated proliferation and activity.

Disclosure of interest

The authors report no conflict of interest.


Funding

This study has been supported by grants from: PNR-CNR Aging Program 2012–2014, CNR Flagship Projects (Epigenomics-EPIGEN), Associazione Italiana per la Ricerca sul Cancro (AIRC IG 11477). AF and RCCP have a scholarship from CAPES (Brazil).

ORCID

Myriam Decaussin-Petrucci  <http://orcid.org/0000-0002-6065-0756>

Gabriella De Vita  <http://orcid.org/0000-0002-7302-1174>

Alfredo Fusco  <http://orcid.org/0000-0003-3332-5197>

References

- Wahid F, Shehzad A, Khan T, Kim YY. MicroRNAs: synthesis, mechanism, function, and recent clinical trials. *Biochim Biophys Acta*. 2010;1803(11):1231–43. doi:10.1016/j.bbamer.2010.06.013. PMID:20619301
- Kurzynska-Kokorniak A, Koralewska N, Pokornowska M, Urbanowicz A, Tworak A, Mickiewicz A, Figlerowicz M. The many faces of Dicer: the complexity of the mechanisms regulating Dicer gene expression and enzyme activities. *Nucleic Acids Res*. 2015;43(9):4365–80. doi:10.1093/nar/gkv328. PMID:25883138
- Zindy F, Lee Y, Kawachi D, Ayrault O, Merzoug LB, Li Y, McKinnon PJ, Roussel MF. Dicer is required for normal cerebellar development and to restrain medulloblastoma formation. *PLoS One*. 2015;10(6):e0129642. doi:10.1371/journal.pone.0129642. PMID:26091048
- Hong X, Luense LJ, McGinnis LK, Nothnick WB, Christenson LK. Dicer1 is essential for female fertility and normal development of the female reproductive system. *Endocrinology*. 2008;149(12):6207–12. doi:10.1210/en.2008-0294. PMID:18703631
- Frezzetti D, Reale C, Cali G, Nitsch L, Fagman H, Nilsson O, Scarfò M, De Vita G, Di Lauro R. The microRNA-processing enzyme Dicer is essential for thyroid function. *PLoS One*. 2011;6(11):e27648. doi:10.1371/journal.pone.0027648. PMID:22132122
- Karube Y, Tanaka H, Osada H, Tomida S, Tatematsu Y, Yanagisawa K, Yatabe Y, Takamizawa J, Miyoshi S, Mitsudomi T, et al. Reduced expression of Dicer associated with poor prognosis in lung cancer patients. *Cancer Sci*. 2005;96(2):111–5. doi:10.1111/j.1349-7006.2005.00015.x. PMID:15723655
- Khoshnaw SM, Rakha EA, Abdel-Fatah TM, Nolan CC, Hodi Z, Macmillan DR, Ellis IO, Green AR. Loss of Dicer expression is associated with breast cancer progression and recurrence. *Breast Cancer Res Treat*. 2012;135(2):403–13. doi:10.1007/s10549-012-2169-3. PMID:22821364
- Faggad A, Budczies J, Tchernitsa O, Darb-Esfahani S, Sehoulji J, Müller BM, Wirtz R, Chekerov R, Weichert W, Sinn B, et al. Prognostic significance of Dicer expression in ovarian cancer-link to global microRNA changes and oestrogen receptor expression. *J Pathol*. 2010;220(3):382–91. PMID:19960504
- Ambs S, Prueitt RL, Yi M, Hudson RS, Howe TM, Petrocca F, Wallace TA, Liu CG, Volinia S, Calin GA, et al. Genomic profiling of microRNA and messenger RNA reveals deregulated microRNA expression in prostate cancer. *Cancer Res*. 2008;68(15):6162–70. doi:10.1158/0008-5472.CAN-08-0144. PMID:18676839
- Faber C, Horst D, Hlubek F, Kirchner T. Overexpression of Dicer predicts poor survival in colorectal cancer. *Eur J Cancer*. 2011;47(9):1414–9. doi:10.1016/j.ejca.2011.01.006. PMID:21345667
- Yoo SK, Lee S, Kim SJ, Jee HG, Kim BA, Cho H, Song YS, Cho SW, Won JK, Shin JY, et al. Comprehensive analysis of the transcriptional and mutational landscape of follicular and papillary

- thyroid cancers. *PLoS Genet.* 2016;12(8):e1006239. doi:10.1371/journal.pgen.1006239. PMID:27494611
- [12] Heravi-Moussavi A, Anglesio MS, Cheng SW, Senz J, Yang W, Prentice L, Fejes AP, Chow C, Tone A, Kalloger SE, et al. Recurrent somatic DICER1 mutations in nonepithelial ovarian cancers. *N Engl J Med.* 2012;366(3):234-42. doi:10.1056/NEJMoa1102903. PMID:22187960
- [13] Doros LA, Rossi CT, Yang J, Field A, Williams GM, Messinger Y, Cajaiba MM, Perlman EJ, A Schultz K, Cathro HP, et al. DICER1 mutations in childhood cystic nephroma and its relationship to DICER1-renal sarcoma. *Mod Pathol.* 2014;27(9):1267-80. doi:10.1038/modpathol.2013.242. PMID:24481001
- [14] de Kock L, Sabbaghian N, Soglio DB, Guillerman RP, Park BK, Chami R, Deal CL, Priest JR, Foulkes WD. Exploring the association Between DICER1 mutations and differentiated thyroid carcinoma. *J Clin Endocrinol Metab.* 2014;99(6):E1072-7. doi:10.1210/jc.2013-4206. PMID:24617712
- [15] Wu MK, Sabbaghian N, Xu B, Addidou-Kalucki S, Bernard C, Zou D, Reeve AE, Eccles MR, Cole C, Choong CS, et al. Biallelic DICER1 mutations occur in Wilms tumours. *J Pathol.* 2013;230(2):154-64. doi:10.1002/path.4196. PMID:23620094
- [16] Costa V, Esposito R, Ziviello C, Sepe R, Bim LV, Cacciola NA, Decaussin-Petrucci M, Pallante P, Fusco A, Ciccodicola A. New somatic mutations and WNK1-B4GALNT3 gene fusion in papillary thyroid carcinoma. *Oncotarget.* 2015;6(13):11242-51. doi:10.18632/oncotarget.3593. PMID:25803323
- [17] Foulkes WD, Priest JR, Duchaine TF. DICER1: mutations, microRNAs and mechanisms. *Nat Rev Cancer.* 2014;14(10):662-72. doi:10.1038/nrc3802. PMID:25176334
- [18] Fusco A, Berlingieri MT, Di Fiore PP, Portella G, Grieco M, Vecchio G. One- and two-step transformations of rat thyroid epithelial cells by retroviral oncogenes. *Mol Cell Biol.* 1987;7(9):3365-70. doi:10.1128/MCB.7.9.3365. PMID:3670314
- [19] Landthaler M, Gaidatzis D, Rothballer A, Chen PY, Soll SJ, Dinic L, Ojo T, Hafner M, Zavolan M, Tuschl T. Molecular characterization of human Argonaute-containing ribonucleoprotein complexes and their bound target mRNAs. *RNA.* 2008;14(12):2580-96. doi:10.1261/rna.1351608. PMID:18978028
- [20] Ye J, Coulouris G, Zaretskaya I, Cutcutache I, Rozen S, Madden TL. Primer-BLAST: a tool to design target-specific primers for polymerase chain reaction. *BMC Bioinformatics.* 2012;13:134. doi:10.1186/1471-2105-13-134. PMID:22708584
- [21] Schmittgen TD, Livak KJ. Analyzing real-time PCR data by the comparative C(T) method. *Nat Protoc.* 2008;3(6):1101-8. doi:10.1038/nprot.2008.73. PMID:18546601
- [22] Fuziwara CS, Kimura ET. MicroRNAs in thyroid development, function and tumorigenesis. *Mol Cell Endocrinol.* 2017;456:44-50. doi:10.1016/j.mce.2016.12.017.
- [23] Yu Z, Wang L, Wang C, Ju X, Wang M, Chen K, Loro E, Li Z, Zhang Y, Wu K, et al. Cyclin D1 induction of Dicer governs microRNA processing and expression in breast cancer. *Nat Commun.* 2013;4:2812. doi:10.1038/ncomms3812. PMID:24287487
- [24] Borrelli N, Denaro M, Ugolini C, Poma AM, Miccoli M, Vitti P, Miccoli P, Basolo F. miRNA expression profiling of 'noninvasive follicular thyroid neoplasms with papillary-like nuclear features' compared with adenomas and infiltrative follicular variants of papillary thyroid carcinomas. *Modern Pathology.* 2016;30(1):39-51. doi:10.1038/modpathol.2016.157.
- [25] Erler P, Keutgen XM, Crowley MJ, Zetoune T, Kundel A, Kleiman D, Beninato T, Scognamiglio T, Elemento O, Zarnegar R, et al. Dicer expression and microRNA dysregulation associate with aggressive features in thyroid cancer. *Surgery.* 2014;156(6):1342-50. doi:10.1016/j.surg.2014.08.007. PMID:25456905
- [26] Cancer Genome Atlas Research Network. Integrated genomic characterization of papillary thyroid carcinoma. *Cell.* 2014;159(3):676-90. doi:10.1016/j.cell.2014.09.050. PMID:25417114
- [27] Jakymiw A, Patel RS, Deming N, Bhattacharyya I, Shah P, Lamont RJ, Stewart CM, Cohen DM, Chan EK. Overexpression of dicer as a result of reduced let-7 MicroRNA levels contributes to increased cell proliferation of oral cancer cells. *Genes Chromosomes Cancer.* 2010;49(6):549-59. doi:10.1002/gcc.20765. PMID:20232482
- [28] Saiselet M, Floor S, Tarabichi M, Dom G, Hébrant A, van Staveren WC, Maenhaut C. Thyroid cancer cell lines: an overview. *Front Endocrinol (Lausanne).* 2012;3:133. PMID:23162534
- [29] Rodriguez W, Jin L, Janssens V, Pierreux C, Hick AC, Urizar E, Costagliola S. Deletion of the RNaseIII enzyme dicer in thyroid follicular cells causes hypothyroidism with signs of neoplastic alterations. *PLoS One.* 2012;7(1):e29929. doi:10.1371/journal.pone.0029929. PMID:22242190
- [30] Muskhelishvili L, Latendresse JR, Kodell RL, Henderson EB. Evaluation of cell proliferation in rat tissues with BrdU, PCNA, Ki-67(MIB-5) immunohistochemistry and in situ hybridization for histone mRNA. *J Histochem Cytochem.* 2003;51(12):1681-8. doi:10.1177/002215540305101212. PMID:14623936
- [31] Kumar MS, Pester RE, Chen CY, Lane K, Chin C, Lu J, Kirsch DG, Golub TR, Jacks T. Dicer1 functions as a haploinsufficient tumor suppressor. *Genes Dev.* 2009;23(23):2700-4. doi:10.1101/gad.1848209. PMID:19903759
- [32] Lambertz I, Nittner D, Mestdagh P, Denecker G, Vandesompele J, Dyer MA, Marine JC. Monoallelic but not biallelic loss of Dicer1 promotes tumorigenesis in vivo. *Cell Death Differ.* 2010;17(4):633-41. doi:10.1038/cdd.2009.202. PMID:20019750
- [33] Witkowski L, Mattina J, Schönberger S, Murray MJ, Choong CS, Huntsman DG, Reis-Filho JS, McCluggage WG, Nicholson JC, Coleman N, et al. DICER1 hotspot mutations in non-epithelial gonadal tumours. *Br J Cancer.* 2013;109(10):2744-50. doi:10.1038/bjc.2013.637. PMID:24136150
- [34] Chen J, Wang Y, McMonechy MK, Anglesio MS, Yang W, Senz J, Maines-Bandiera S, Rosner J, Trigo-Gonzalez G, Grace Cheng SW, et al. Recurrent DICER1 hotspot mutations in endometrial tumours and their impact on microRNA biogenesis. *J Pathol.* 2015;237(2):215-25. doi:10.1002/path.4569. PMID:26033159

4.3.1 DADOS SUPLEMENTARES DO ARTIGO 3

(PENHA *ET AL.* CELL CYCLE, V. 16, N. 23, P. 2282-2289, DEC 2017)

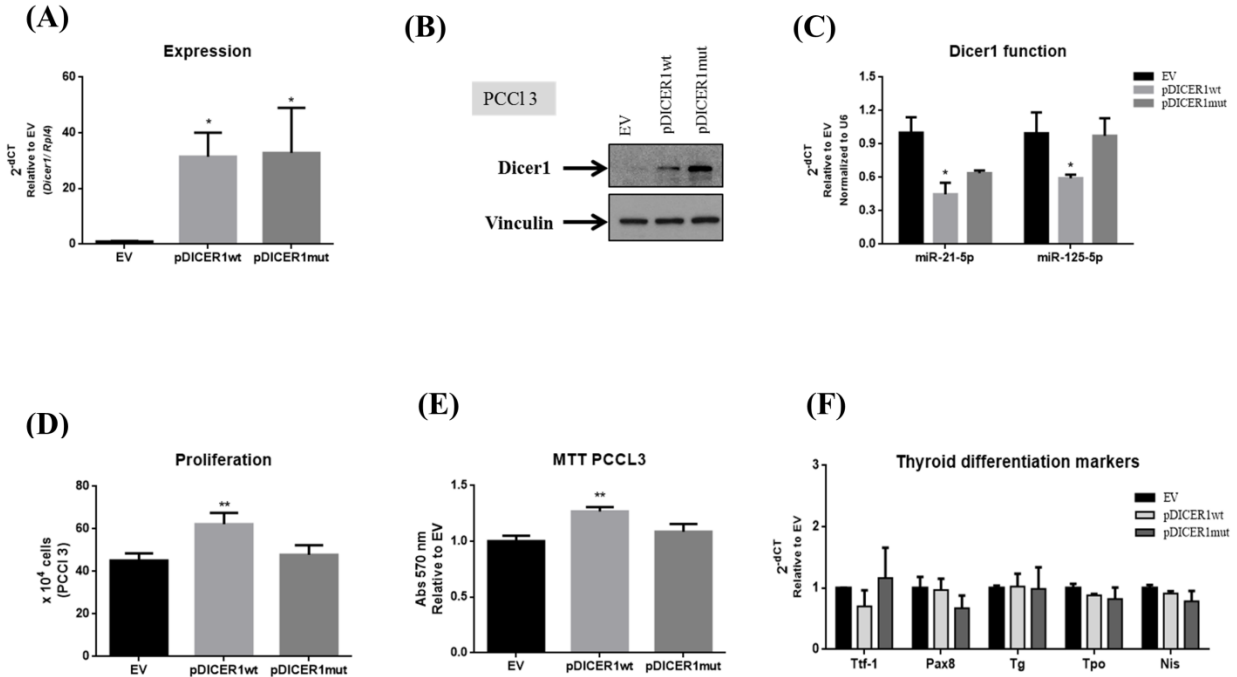


Figure S1. The effect of the mutation c.5438A>G (E1813G) of *DICER1* in PCCl 3 cells. Cells were transfected with empty vector (EV) and *DICER1*-overexpression vectors, containing *DICER1* wild-type (pDICER1wt) or mutated c.5438A>G (E1813G) *DICER1* (pDICER1mut) cDNA and, 48 hours post transfection: (A) mRNA and (B) protein levels of *Dicer1* were validated by q-RT-PCR and western blot, respectively; (C) Expression of miR-21-5p and miR-125-5p to evaluate *Dicer1* function; (D) The number of PCCl 3 cells were counted using trypan blue and the results were relative to EV; (E) Cell viability was evaluated using the MTT assay in the same conditions; (F) Expression of thyroid differentiation markers *Ttf-1*, *Pax8*, *Tg*, *Tpo* and *Nis* and data were expressed as relative to EV. *Rpl4* and pseudogene *U6* were used as housekeeping for q-RT-PCR of gene and miR expression, respectively. Vinculin was used as loading control for western blot. *p < 0.05, **p < 0.01, ***p < 0.001.

4.3.2 DADOS NÃO PUBLICADOS DO CAPÍTULO III

MATERIAL E MÉTODOS

CITOMETRIA DE FLUXO

As células PCCI 3 (2×10^5 células/ poço) foram plaqueadas na placa de 6 poços e, 24 horas depois, as células foram transfectadas com o siRNA não-específico controle (SirNon) ou siRNAs específicos para *DICER1* (KD Dicer1) usando o reagente de transfecção Lipofectamina RNAi MAX (Life Technologies, EUA), seguindo as recomendações do fabricante. Após 48 horas, o *pellet* celular foi ressuspenso em 500 μ L da solução contendo PBS, Triton X-100 0,1%, RNase 0,1% e iodeto de propideo 2 μ g/mL e incubado em gelo por 5 minutos. A análise do ciclo celular foi conduzida no citômetro de fluxo FACScan flow (Becton Dickinson, EUA) e analisado no programa CELL-FIT (Becton Dickinson, EUA).

RESULTADOS

O efeito da perda de DICER1 sobre o ciclo celular das células PCCI 3

Para avaliar o efeito do silenciamento de *DICER1* sobre o ciclo celular das células PCCI 3, a inibição da expressão de *DICER1* e a citometria de fluxo usando o iodeto de propideo foram realizados, como descritos acima. Nossos resultados mostram que a perda parcial da expressão de *DICER1* (KD Dicer1) promove a diminuição da porcentagem do número de células na fase G1 (72% vs. 82%) e o acúmulo de células na fase S (24% vs. 14%) do ciclo celular, quando comparados ao controle (Scramble) (Figura 7).

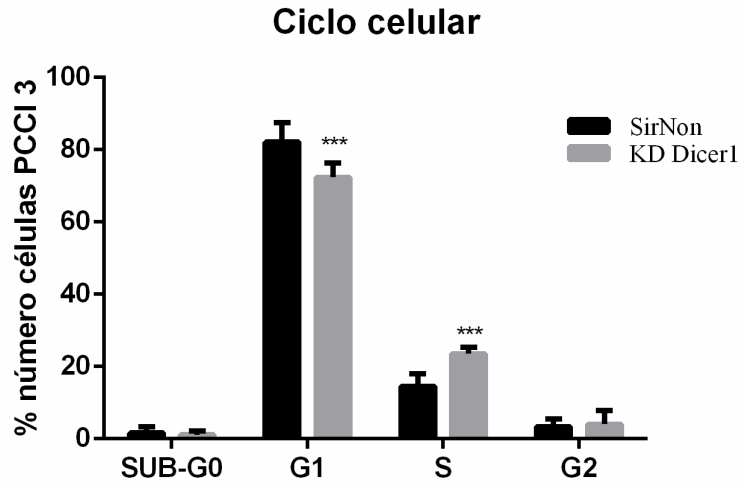


Figura 7 Efeito de *DICER1* sobre o ciclo celular das células PCCl 3. As células PCCl 3 foram transfectadas com os siRNA não-específico controle (SirNon) ou siRNAs específicos para *DICER1* (KD Dicer1) e, após 48 horas, o ciclo celular foi avaliado. Os resultados são representados pela porcentagem de células em cada fase do ciclo celular (SUB-G0, G1, S e G2) de três experimentos independentes. ***, $p < 0.001$.

4.4 CAPÍTULO IV

Artigo submetido à *Cancer Epidemiology, Biomarkers & Prevention*

A RI é o fator de risco mais bem estabelecido para o desenvolvimento do CPT. Os miRNAs são regulados pela RI e as alterações no seu perfil de expressão foram descritas como uma ferramenta valiosa no diagnóstico das neoplasias da tireoide. Portanto, a hipótese do nosso trabalho seria a de que os miRNAs, regulados pela RI em etapas iniciais da carcinogênese da tireoide, poderiam ser usados como biomarcadores de exposição em amostras de CPT. Para tal, avaliamos a expressão dos miRNAs alterados pela RI em células diferenciadas da tireoide, previamente analisados no capítulo II desta tese (15) e por outro grupo (16), em 398 amostras de CPT do banco de dados TCGA. As análises foram conduzidas a partir de dois critérios para a seleção dos pacientes. No primeiro, os pacientes com histórico confirmado de exposição à RI (n=15; Grupo exposto) foram comparados aqueles sem exposição (n=331; Grupo não exposto). Para a segunda análise, os 18 pacientes que foram detectados com as fusões gênicas relacionadas à RI - 10 *RET/PTC1*, 3 *RET/PTC3* e 5 *ETV6-NTRK3*- foram comparados aos 380 pacientes negativos para essas fusões gênicas. A expressão dos miRNAs regulados pela RI foi avaliada entre os grupos e os diferencialmente expressos ($p < 0,05$) foram selecionados para as análises subsequentes. O desempenho dos modelos de classificação foi avaliado pelas curvas ROC. Todas as análises foram conduzidas no software R e as do enriquecimento das vias de sinalização na ferramenta online DIANA-miRPathway. Como resultado, a combinação da expressão dos hsa-miR-34a e hsa-miR-1249 foi capaz de prever o status de exposição à RI (sensibilidade=73.3%, especificidade=75.5%, AUC=77.6%). Além disso, foi realizada a otimização do modelo para a classificação dos casos para a identificação das fusões gênicas relacionadas à RI, baseando-se na expressão dos hsa-let-7c, hsa-let-7d, hsa-miR-127 e hsa-miR-377) (sensibilidade=88.9%, especificidade=77.6%, AUC=84.2%). A maioria dos miRNAs analisados nos modelos propostos tem como alvo vias de sinalização oncogênicas, frequentemente desreguladas em diversos tipos de tumores, incluindo o da tireoide, como as vias de PI3K-Akt, p53 e ciclo celular ($p < 0,05$). Os nossos achados podem ajudar na identificação dos CPT relacionados à RI e que provavelmente poderão evoluir para uma doença mais agressiva. Contudo, estudos confirmatórios em coortes independentes são necessários.

MicroRNA expression as potential thyroid radiation exposure biomarker and a tool for radiation-related fusion gene identification

Short title: microRNAs as radiation biomarkers in PTC

Authors: Ricardo Cortez Cardoso Penha^{1*}, Mariana Severo Ramundo^{1*}, Alfredo Fusco^{1,2}, Luis Felipe Ribeiro Pinto¹

*These authors equally contributed to this work

Affiliations: ¹ Instituto Nacional de Câncer - INCA, CPQ, Rio de Janeiro, Brazil; ² Istituto di Endocrinologia ed Oncologia Sperimentale - CNR c/o Dipartimento di Medicina Molecolare e Biotecnologie Mediche, Università degli Studi di Napoli “Federico II”, Naples, Italy.

Corresponding author:

Luis Felipe Ribeiro Pinto
Instituto Nacional de Câncer - INCA,
Rua André Cavalcanti, 37-Centro,
Rio de Janeiro, CEP 20231-050 RJ, Brazil.
tel. +55 21 32076598
fax. +55 21 32076536
e mail: lfrpinto@inca.gov.br

Disclosures: The authors have no potential conflicts to disclose

Financial Information: This work was supported by the Swiss Bridge Foundation, “National Counsel of Technological and Scientific Development” (CNPq), “Superior Education Personnel Improvement Coordination” (CAPES) and “Foundation for Research of the State of Rio de Janeiro” (FAPERJ) grants.

Word count: 2,088; **Tables:** 3; **Figures:** 3

Abstract

Background: Ionizing radiation (IR) is a well-known risk factor for papillary thyroid carcinoma (PTC). IR can cause several molecular alterations in thyroid, including *RET/PTC* and other fusions, and differential expression of microRNAs (miRNAs). Thus, we evaluated whether IR-regulated miRNAs could be used as radiation exposure biomarker, and to predict IR-related fusions genes in PTC. **Methods:** The PTC-TCGA database (n=398) were analyzed and the differential expression analysis of IR-regulated miRNAs were assessed between radiation-exposed and non-exposed PTC patients or IR-related fusion gene positive (*RET/PTC1*, *RET/PTC3* and *ETV6-NTRK3*) and negative groups. The classification model's performance was evaluated using ROC (Receiver Operating Characteristics) curves. All analyses were performed using R software. Enrichment analysis was carried out with the online DIANA-miRPathway tool. **Results:** The combined expression of hsa-miR-34a and hsa-miR-1249 could predict radiation exposure status (sensitivity=73.3%, specificity=75.5%, AUC=77.6%). Our proposed model was also able to identify IR-related fusion genes in PTC samples using the expression of four miRNAs (hsa-let-7c, hsa-let-7d, hsa-miR-127 and hsa-miR-377) (sensitivity=88.9%, specificity=77.6%, AUC=84.2%). Most of the IR-regulated miRNAs targets oncogenic pathways deregulated in several types of cancers, including thyroid cancer, such as PI3K-Akt, p53 signaling and cell cycle ($p < 0.05$). **Conclusions:** The predictive miRNA-based models were able to accurately classify radiation exposure status and radiation-related fusion genes in PTC samples. **Impact:** Our findings might help screening PTC patients with radiation history background and, eventually, the early identification of PTC patients who will probably evolve with a more aggressive disease.

Keywords: microRNAs, ionizing radiation, papillary thyroid carcinoma, biomarkers, *RET/PTC*

Introduction

Ionizing radiation (IR) is the main risk factor for papillary thyroid carcinoma (PTC), especially when individuals are exposed at younger ages (< 5 years old), with a relative risk of 3,7 per Gy¹. The radiation-related PTC display greater aggressiveness at presentation when compared with non-related PTC, with a higher frequency of extrathyroidal extension (49% vs. 25%), lymph node dissemination (64% vs. 53%) and often associated with thyroid autoimmunity². Therefore, the search for radiation exposure biomarkers is the key for better comprehension of thyroid carcinogenesis, targets for diagnosis and therapy, as well as radiation emergencies.

The major genetic alteration in radiation-related PTC is *RET/PTC* rearrangements, mostly *RET/PTC1 (RET_CCCDC6)* and *RET/PTC3 (RET_NCOA4)*, reported in atomic bomb survivors in Japan (22%)³, post-Chernobyl tumors (63.8%)⁴, and external radiation for benign or malignant conditions (84%)⁵. Moreover, *RET/PTC* rearrangement formation is induced by IR in a dose-dependent manner⁶, directly linking *RET/PTC* event and radiation exposure. Recently, the gene fusion *ETV6/ NTRK3* has also been identified in 14.5% of post-Chernobyl tumors and its formation was directly induced by IR exposure⁷. Apart from chromosomal aberrations, other molecular alterations may also be associated with radiation exposure. Dom *et al.*⁸ identified a 403-gene signature to classify cases with low accuracy (67%), while Ugolin *et al.*⁹ pointed out an extensive 227-gene expression signature to discriminate post-Chernobyl thyroid tumors from sporadic ones.

MiRNAs are small non-coding RNA sequences (20-22 nucleotides), that mediated gene expression silencing by direct binding to target mRNA¹⁰. They exert pleiotropic role in cell biology and cancer, including DNA damage response (DDR)¹¹. In the thyroid context, we have previously identified the miRNA expression profile of irradiated normal thyroid cells (i.e., miR-10b-5p and miR-199a-3p) and their relevance to DDR by targeting DNA homologous recombination repair genes¹². In agreement with that, a previous work has also described miRNAs that target DNA repair and *TP53* pathways in normal thyroid cells exposed to IR¹³, suggesting that deregulation of miRNA expression might be important at initial steps of IR-related thyroid tumors. Furthermore, a differential expression of miRNA subsets is able to

classify thyroid tumor histotypes and contribute to onset and progression of tumors¹⁴. Thus, miRNA expression could be a promising approach to identify radiation-related thyroid tumors.

The aim of the present study is to evaluate whether IR-regulated miRNAs could predict IR exposure and IR-related fusion genes in PTC samples. To this end, we proposed models based on the differential expression of the 31 miRNAs, previously demonstrated by our group¹² and other colleagues¹³ to be regulated by IR in normal thyroid cells, using PTC data from a well-characterized TCGA database cohort¹⁵.

Methods

PTC samples from TCGA database

The workflow of the study was as follow (Figure 1). The Genomic Data Commons Data Portal (<https://portal.gdc.cancer.gov/>) was used to obtain miRNA quantification and clinical data from PTC-TCGA database¹⁵. The total number of PTC samples with miRNA expression was 398. We performed the analysis using two different criteria to select the patients. First, the patients who had a confirmed history of radiation exposure (n=15; radiation exposed group) were compared with those without exposure (n=331; non-exposed group). For this analysis, patients with unknown radiation exposure (n=13) or not available (n=39) were excluded. On the second analysis, we compared 18 patients who were positive for radiation-related gene fusions¹⁶: 13 *RET/PTC* rearrangements (10 *RET/PTC1* and 3 *RET/PTC3*) and 5 *ETV6-NTRK3*, with the 380 remaining patients without radiation-related gene fusions. The information about the fusion genes at TCGA dataset was gathered in The Tumor Fusion Gene Data Portal (<http://www.tumorfusions.org/>)¹⁷.

Selection of miRNAs

The selection of the miRNAs for the present study was based on two studies in which miRNAs regulated by IR (1-10 Gy) were identified in normal thyroid cells^{12, 13}. The differential miRNA expression analysis between groups was performed with R package DESeq2 1.22.2¹⁸. MiRNAs were considered to be differentially expressed when *p*-value < 0.05.

Performance of the miRNA-based models

To assess the classification model's performances, the expressions of the selected miRNAs that were obtained by the analyses were combined into models to better classify exposure radiation status and the presence of radiation-related fusion genes. ROC (Receiver Operating Characteristics) curves were performed using the R EPI package v2.32¹⁹. A good classification model was considered when accuracy, sensitivity and specificity were > 0.75.

MiRNA target pathways

To identify miRNA target pathways, it was used the DIANA-miRPath v3.0 tool²⁰. This predictive algorithm clusters miRNAs into similar functional categories and enables the identification of miRNA specific pathways controlled by similar miRNAs and ranks them according to their enrichment P-values ($p < 0.05$).

Results

Study population

We identified 398 PTC patients with miRNA quantification in the TCGA database¹⁵. Table 1 shows that most of them were white (71%), female (73%) and ≤ 55 years old (70%). Classical PTC was the most common variant histotype (90%), mostly without extrathyroidal extension (62%) and diagnosed at an early stage (TNM1/2, 65%). Distant metastasis was scarce (1%), while lymph nodes dissemination was frequent (53%). As far as morbidity outcome is concerned, the majority of the patients was PTC-free (87%), and 4% died of PTC. Moreover, 15 PTC patients had a confirmed history of radiation exposure, whereas 18 were positive for IR-related fusion genes (10 *RET/PTC1*, 3 *RET/PTC3* and 5 *ETV6/NTRK3*). Only one patient had a confirmed history of radiation exposure and was positive for *ETV6-NTRK3*.

The miRNA expression model to classify radiation exposure status

To investigate whether miRNA expression could be used as IR exposure biomarker, we evaluated the expression of the 31 miRNAs (Table 2), previously demonstrated to be regulated

by IR in normal thyroid cells^{12, 13}, between radiation-exposed (n=15) vs. non-exposed groups (n=331) at PTC-TGCA database. The analysis demonstrated that only two miRNAs were differentially expressed (p-value adjusted < 0.05) between groups, hsa-miR-34a, identified by Nikiforova *et al.*¹³, and hsa-miR-1249, identified by Penha *et al.*¹² (Table 2). The combined expression of these two miRNAs was able to accurately discriminate the IR exposure status of the PTC samples (sensitivity=73.3%, specificity=75.5%, AUC=77.6%) (Figure 2a). Of note, when analyzed individually, the expressions of these two miRNAs displayed low accuracy at classifying cases (<70%) (*data not shown*).

The miRNA expression models to identify radiation-related fusion genes

Then, we wondered whether the IR-regulated miRNAs could identify radiation-related fusion genes in PTC samples, including *RET/PTC* rearrangements, the major genetic event in radiation-related PTC³⁻⁵. Among the 31 previously selected miRNAs, nine were differentially expressed between radiation-related fusion gene positive and negative groups (p-value < 0.05) (Table 2). The co-expression of these miRNAs (hsa-let-7c, hsa-let-7d, hsa-miR-127, hsa-miR-128-2, hsa-miR-203b, hsa-miR-203a, hsa-miR-296, hsa-miR-34a and hsa-miR-377) accurately classified cases (sensitivity=77.8%, specificity=86.6%, AUC=87.6%) (Figure 2b). In order to optimize the proposed model, we have performed a combinatory analyzes with all nine miRNAs, so that we had the best accuracy with the lowest number of miRNAs included in the model (Supplementary Table 1). The optimized model contained four miRNAs (hsa-let-7c, hsa-let-7d, hsa-miR-127, hsa-miR-377) (sensitivity=88.9%, specificity=77.6%, AUC=85.4%) (Figure 2c).

Signaling pathways regulated by model 3-based miRNAs

To assess biological relevance of the miRNAs differentially expressed among groups, we have performed miRNA pathway analyses using the *in silico* DIANA-mirPath tool²⁰ (Figure 3). Each miRNA was clustered into controlled signaling pathways. The hsa-miR-34a was the only miRNA shared among groups and target pathways involved on onset and progression of several types of tumors, including thyroid cancer, as well as cell cycle and p53 signaling (p<0.05). Moreover, our data pointed out the involvement of hsa-miR-377, hsa-let-7 and hsa-let-7d, that

were differentially expressed between radiation-related fusion gene groups, in PI3K-Akt pathway ($p < 0.05$) (Figure 3B).

Discussion

In this study, for the first time, it was proposed a model to classify radiation exposure status in PTC samples based on miRNA expression. The main advantage of our study is that we have analyzed the expression of miRNAs that had been previously demonstrated to be regulated by IR (1-10 Gy) in normal thyroid cells at initial steps of thyroid carcinogenesis^{12, 13}. This point was critical for subsequent analyses because IR is a strong initiator and promoter of thyroid carcinogenesis⁶. In a total of 31 previously identified miRNAs, only two were differentially expressed between radiation-exposed and non-exposed groups. Since miRNAs are involved in DDR¹¹, it is expected that a significant part of these miRNAs was transiently regulated in response to IR and remained unaffected during thyroid carcinogenesis process. The expression of hsa-miR-34a and hsa-miR-1249 allowed us to accurately predict radiation-exposed PTC patients. Indeed, miR-34a is upregulated after IR in normal and cancer cells, or *in vivo*, no matter cell or tissue types²¹. Interestingly, miR-34a induction by IR was shown to be much higher in young than adult mice²², which is in accordance with thyroid radiosensitivity at younger ages². The fact that miR-34a could also be detected in serum after irradiation²² highlights the possibility of its usage as a promising radiation injury biomarker.

Among all fusion genes reported in IR-related PTC¹⁶, only *RET/PTC1*, *RET/PTC3* and *ETV6/NTRK3* were detected in our study population. Even though these fusion genes are frequently associated with IR, only one case was positive for these alterations that also had a confirmed radiation history exposure, suggesting that other factors could be involved on their generation. Moreover, the radiation-related fusion genes, especially *RET/PTC1* and *RET/PTC3*, are associated with worse clinical course of PTC patients when compared with the negative ones, exhibiting higher frequency of advanced disease (pT3/pT4) and lymph node dissemination at the time of diagnosis⁴. Accordingly, our proposed miRNA-based model (hsa-let-7c, hsa-let-7d, hsa-miR-127, hsa-miR-377) was also able to identify these alterations at PTC samples from TCGA

cohort with high accuracy. In fact, some of these miRNAs, such as let-7d and miR-127, had already been associated with *RET/PTC* rearrangements²³.

In line with its importance to IR response²¹, our findings pointed out that hsa-miR-34a target DNA replication, cell cycle, P53 and PI3K-Akt pathways, which are commonly deregulated in several types of tumors, including PTC¹⁵. Moreover, hsa-let-7c and hsa-let-7, which are involved on DDR²⁴, shared with hsa-miR-34a almost all of the target pathways. Let-7 miRNAs act as tumor suppressors in PTC by reducing *RAS* expression, negatively affecting MAPK activation and proliferation^{25, 26}. Collectively, these IR- regulated miRNAs impact on pathways that are fundamental to thyroid growth and function, response to genotoxic stress, as well as to neoplastic transformation and tumor progression¹⁵.

The main advantages of our proposed model are that miRNAs are stable and their expression could be assessed in formalin-fixed, paraffin-embedded tissues²⁷; the identification of radiation exposure status of PTC patients, even without the presence of radiation-related fusion genes; and the potential translation to clinical practice due to low cost and high accuracy, specificity and sensitivity. Nevertheless, our study presented some limitations such as the lack of information about type and absorbed radiation dose at TCGA samples¹⁵.

In conclusion, we proposed models based on the expression of IR-regulated miRNAs to accurately classify radiation exposure and IR-related fusion genes in PTC samples. Our findings might help screening PTC patients with radiation history background, as well as the early identification of PTC patients who will probably evolve with a more aggressive disease. However, further validation studies in independent PTC cohorts are needed.

Acknowledgments: We thank the Molecular Carcinogenesis Program for the support with the bioinformatic analyses and helpful discussions on this work.

References

1. Veiga LH, Holmberg E, Anderson H, Pottern L, Sadetzki S, Adams MJ, *et al.* Thyroid Cancer after Childhood Exposure to External Radiation: An Updated Pooled Analysis of 12 Studies. *Radiat Res* 2016; 185: 473-84.
2. Pacini F, Vorontsova T, Demidchik EP, Molinaro E, Agate L, Romei C, *et al.* Post-Chernobyl thyroid carcinoma in Belarus children and adolescents: comparison with naturally occurring thyroid carcinoma in Italy and France. *J Clin Endocrinol Metab* 1997; 82: 3563-9.
3. Hamatani K, Eguchi H, Ito R, Mukai M, Takahashi K, Taga M, *et al.* RET/PTC rearrangements preferentially occurred in papillary thyroid cancer among atomic bomb survivors exposed to high radiation dose. *Cancer Res* 2008; 68: 7176-82.
4. Rabes HM, Demidchik EP, Sidorow JD, Lengfelder E, Beimfohr C, Hoelzel D, *et al.* Pattern of radiation-induced RET and NTRK1 rearrangements in 191 post- Chernobyl papillary thyroid carcinomas: biological, phenotypic, and clinical implications. *Clin Cancer Res* 2000; 6: 1093-103.
5. Bounacer A, Wicker R, Caillou B, Cailleux AF, Sarasin A, Schlumberger M, *et al.* High prevalence of activating ret proto-oncogene rearrangements, in thyroid tumors from patients who had received external radiation. *Oncogene* 1997; 15: 1263-73.
6. Caudill CM, Zhu Z, Ciampi R, Stringer JR, Nikiforov YE. Dose-dependent generation of RET/PTC in human thyroid cells after in vitro exposure to gamma-radiation: a model of carcinogenic chromosomal rearrangement induced by ionizing radiation. *J Clin Endocrinol Metab* 2005; 90: 2364-9.
7. Leeman-Neill RJ, Kelly LM, Liu P, Brenner AV, Little MP, Bogdanova TI, *et al.* ETV6-NTRK3 is a common chromosomal rearrangement in radiation-associated thyroid cancer. *Cancer* 2014; 120: 799-807.

8. Dom G, Tarabichi M, Unger K, Thomas G, Oczko-Wojciechowska M, Bogdanova T, *et al.* A gene expression signature distinguishes normal tissues of sporadic and radiation-induced papillary thyroid carcinomas. *Br J Cancer* 2012;107: 994-1000.
9. Ugolin N, Ory C, Lefevre E, Benhabiles N, Hofman P, Schlumberger M, *et al.* Strategy to find molecular signatures in a small series of rare cancers: validation for radiation-induced breast and thyroid tumors. *PLoS One* 2011; 6: e23581.
10. Gebert LFR, MacRae IJ. Regulation of microRNA function in animals. *Nat Rev Mol Cell Biol* 2018; Epub ahead of print.
11. Majidinia M, Yousefi B. DNA damage response regulation by microRNAs as a therapeutic target in cancer. *DNA Repair (Amst)* 2016; 47: 1-11.
12. Penha RCC, Pellicchia S, Pacelli R, Pinto LFR, Fusco A. Ionizing Radiation Deregulates the MicroRNA Expression Profile in Differentiated Thyroid Cells. *Thyroid* 2018; 28: 407-21.
13. Nikiforova MN, Gandhi M, Kelly L, Nikiforov YE. MicroRNA dysregulation in human thyroid cells following exposure to ionizing radiation. *Thyroid* 2011; 21: 261-6.
14. Pallante P, Battista S, Pierantoni GM, Fusco A. Deregulation of microRNA expression in thyroid neoplasias. *Nat Rev Endocrinol* 2014; 10: 88-101.
15. Cancer Genome Atlas Research Network. Integrated genomic characterization of papillary thyroid carcinoma. *Cell* 2014; 159: 676-90.
16. Ricarte-Filho JC, Li S, Garcia-Rendueles ME, Montero-Conde C, Voza F, Knauf JA, *et al.* Identification of kinase fusion oncogenes in post-Chernobyl radiation-induced thyroid cancers. *J Clin Invest* 2013; 123: 4935-44.
17. Yoshihara K, Wang Q, Torres-Garcia W, Zheng S, Vegesna R, Kim H, *et al.* The landscape and therapeutic relevance of cancer-associated transcript fusions. *Oncogene* 2015; 34: 4845-54.
18. Anders S, Huber W. Differential expression analysis for sequence count data. *Genome Biol* 2010; 11: R106.

19. Carstensen B, Plummer M, Laara E, Hills M. Epi: A Package for Statistical Analysis in Epidemiology. R package version 2.32. 2018; URL=<https://CRAN.R-project.org/package=Epi>.
20. Vlachos IS, Zagganas K, Paraskevopoulou MD, Georgakilas G, Karagkouni D, Vergoulis T, *et al.* DIANA-miRPath v3.0: deciphering microRNA function with experimental support. *Nucleic Acids Res* 2015; 43: W460-6.
21. Lacombe J, Zenhausern F. Emergence of miR-34a in radiation therapy. *Crit Rev Oncol Hematol* 2017; 109: 69-78.
22. Liu C, Zhou C, Gao F, Cai S, Zhang C, Zhao L, *et al.* MiR-34a in age and tissue related radio-sensitivity and serum miR-34a as a novel indicator of radiation injury. *Int J Biol Sci* 2011; 7(2): 221-33.
23. Cahill S, Smyth P, Finn SP, Denning K, Flavin R, O'Regan EM, *et al.* Effect of ret/PTC 1 rearrangement on transcription and post-transcriptional regulation in a papillary thyroid carcinoma model. *Mol Cancer* 2006; 5:70.
24. Metheetrairut C, Slack FJ. MicroRNAs in the ionizing radiation response and in radiotherapy. *Curr Opin Genet Dev* 2013; 23(1): 12-19.
25. Johnson CD, Esquela-Kerscher A, Stefani G, Byrom M, Kelnar K, Ovcharenko D, *et al.* The let-7 microRNA represses cell proliferation pathways in human cells. *Cancer Res* 2007; 67: 7713-22.
26. Ricarte-Filho JC, Fuziwara CS, Yamashita AS, Rezende E, da-Silva MJ, Kimura ET. Effects of let-7 microRNA on Cell Growth and Differentiation of Papillary Thyroid Cancer. *Transl Oncol* 2009; 2: 236-41.
27. Liu A, Xu X. MicroRNA isolation from formalin-fixed, paraffin-embedded tissues. *Methods Mol Biol* 2011; 724: 259-67.

Tables

Table 1. Clinical and pathology data summary of papillary thyroid carcinoma (PTC) patients from TCGA cohort with miRNA expression data (n=398)

Variable	Category	No. of cases	% of cases
Ethnicity	White	283	71
	Asian	47	12
	African American	21	5
	Unknown	47	12
Gender	Male	108	27
	Female	290	73
Age	>55 years	118	30
	≤55 years	280	70
Histologic type	Classical	358	90
	Tall cell	37	9
	Other (columnar/follicular)	3	1
Extrathyroidal extension	Yes	137	34
	No	245	62
	Unknown	16	4
Lymph node dissemination	Yes	209	53
	No	164	41
	Unknown	25	6
Distant metastasis	Yes	4	1
	No	248	62
	Unknown	146	37
Disease stage	I	226	57
	II	29	8
	III	94	23
	IVa/b/c	49	12
Disease free status	Yes	346	87
	No	40	10
	Unknown	12	3
Overall Survival Status	Alive	383	96
	Deceased	15	4
Radiation exposure	Yes	15	4
	No	331	83
	Unknown/ NA	52	13
Radiation fusion genes	<i>RET/PTC1</i>	10	2.5
	<i>RET/PTC3</i>	3	0.7
	<i>ETV6-NTRK3</i>	5	1.3
	Negative	380	95.5

Table 2. MicroRNAs selected for this study and their differential expression between groups

miRNA	Log2FoldChange (radiation exposed vs. non-exposed group)	p-value	Log2FoldChange (radiation fusion positive vs. negative group)	p-value
<i>Nikiforova et al., 2011</i>				
hsa-miR-34a^{*#}	-0.68	0.00	-0.72	0.00
hsa-let-7c[#]	0.24	0.15	0.51	0.00
hsa-miR-203b[#]	-0.45	0.13	-0.62	0.02
hsa-miR-203a[#]	-0.44	0.09	-0.61	0.01
hsa-miR-377[#]	-0.11	0.81	-1.22	0.01
hsa-miR-188	-0.23	0.26	-0.35	0.06
hsa-let-7d[#]	-0.05	0.62	-0.24	0.02
hsa-miR-409	-0.11	0.77	-0.65	0.07
hsa-miR-122	-1.25	0.13	-1.00	0.35
hsa-miR-34b	-0.61	0.06	-0.04	0.87
hsa-miR-365a	0.24	0.79	0.16	0.36
hsa-miR-365b	0.23	0.24	0.16	0.36
hsa-miR-146a	0.19	0.53	0.08	0.75
hsa-let-7g	0.15	0.34	0.05	0.71
hsa-miR-452	0.30	0.12	-0.09	0.60
hsa-miR-96	-0.43	0.07	0.40	0.06
hsa-miR-520a	-1.42	0.26	-0.30	0.79
hsa-miR-489	-0.13	0.78	-0.26	0.55
hsa-miR-527	-0.10	0.94	-0.28	0.85
<i>Penha et al., 2018</i>				
hsa-miR-296[#]	-0.16	0.29	-0.36	0.008
hsa-miR-1249[*]	0.64	0.01	0.14	0.59
hsa-miR-127[#]	-0.09	0.81	-0.84	0.02
hsa-miR-128-2[#]	0.04	0.73	0.26	0.04
hsa-miR-411	-0.01	0.96	-0.45	0.27
hsa-miR-328	-0.23	0.23	-0.16	0.37
hsa-miR-10a	0.15	0.48	0.21	0.32
hsa-miR-33a	-0.11	0.64	-0.33	0.13
hsa-miR-128-1	0.06	0.60	0.16	0.13
hsa-miR-30c-1	-0.32	0.052	0.0007	0.99
hsa-miR-30c-2	-0.13	0.40	-0.015	0.91
hsa-miR-541	0.006	0.99	-0.78	0.28
hsa-miR-199a-1	-0.14	0.64	-0.09	0.75
hsa-miR-199a-2	-0.09	0.76	-0.09	0.74
hsa-miR-33b	-0.44	0.13	0.001	0.99
hsa-miR-451a	0.21	0.51	-0.25	0.41
hsa-miR-10b	-0.11	0.61	-0.03	0.85

Present in both works				
hsa-miR-193b	0.29	0.29	-0.26	0.29

miRNAs in bold were selected for further analysis ($p < 0.05$). (*) miRNAs differentially expressed between radiation exposed and non-exposed groups. (#) miRNAs differentially expressed between radiation fusion positive and negative groups. hsa= Homo sapiens; miR=microRNA.

Figure legends

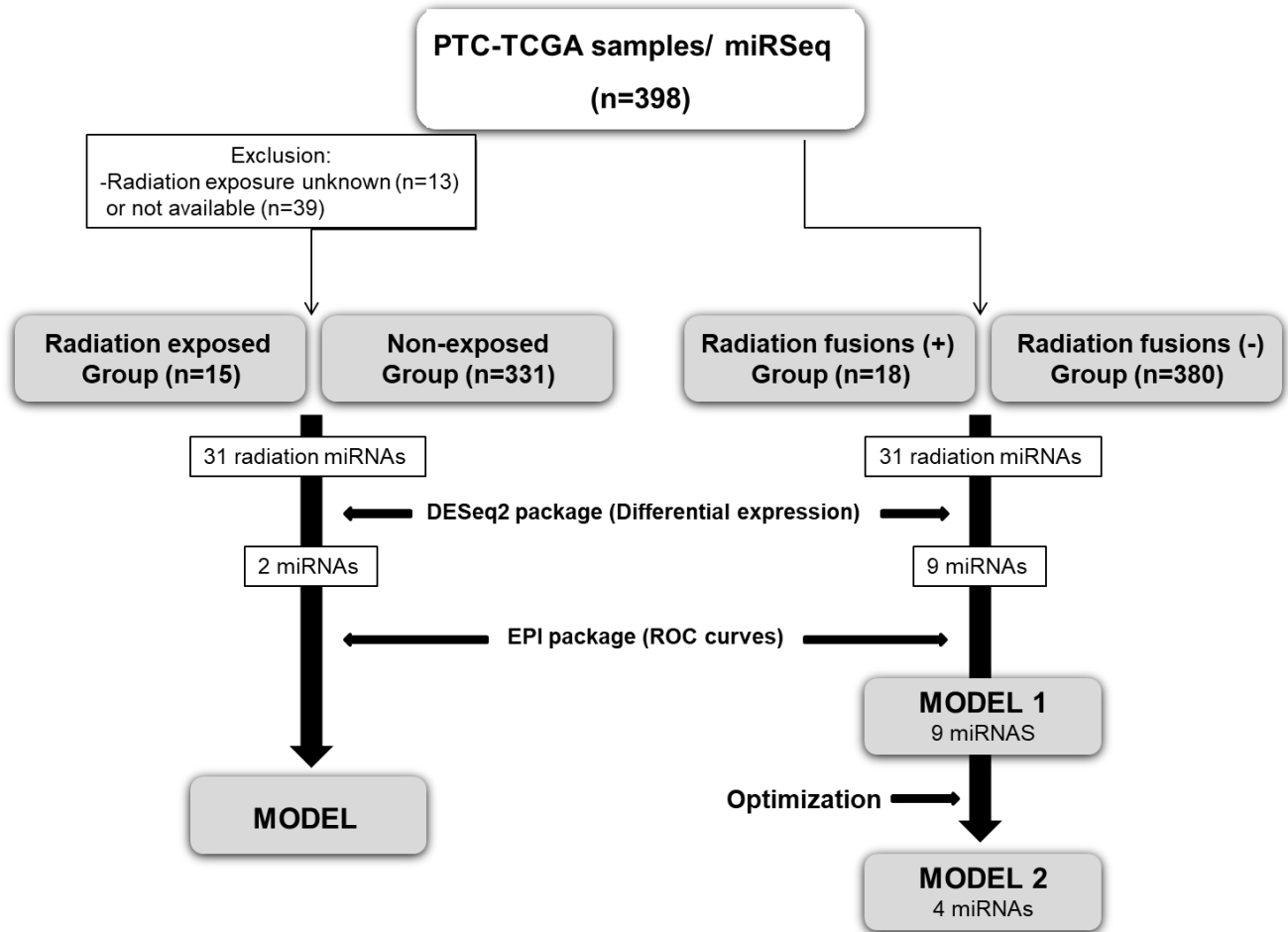


Figure 1. Workflow of the study. *Top:* Extracting data from Genomic Data Commons Data Portal to obtain miRNA quantification and clinical data from PTC-TCGA database, as well as the criteria to form groups. *Center:* Filtering ionizing radiation- miRNAs used in the subsequent analyses based on the differential expression between groups. *Bottom:* Performance of the classification models (ROC curves) to classify cases based on miRNA expression.

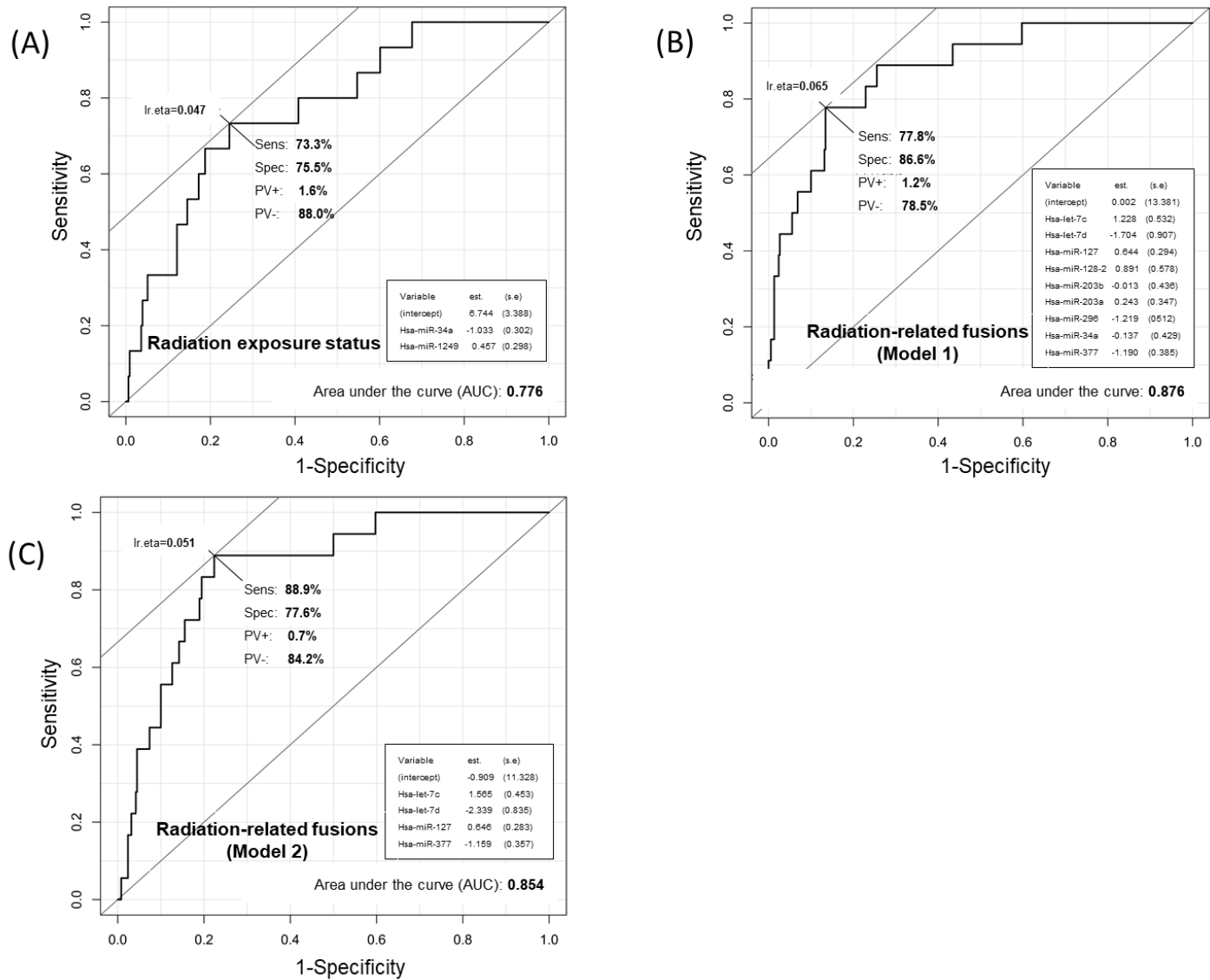


Figure 2. ROC curves for the radiation exposure status and radiation-related fusion genes identification using the expression of radiation-regulated miRNAs at TCGA-PTC samples (n=398). Plots of sensitivity (y coordinate) *versus* 1-specificity (false positive rate; x coordinate) were performed to obtain optimal cutoff points. (A) Model for radiation exposure status (hsa-miR-34a and hsa-miR-1249); (B) Model 1 for radiation-related fusion genes (*RET/PTC1*, *RET/PTC3* and *ETV6-NTRK3*) (hsa-let-7c, hsa-let-7d, hsa-miR-127, hsa-miR128-2, hsa-miR-203a, hsa-miR-203b, hsa-miR-296, hsa-miR-34a and hsa-miR-377) (C) Model 2 for radiation-related fusion genes (hsa-let-7c, hsa-let-7d, hsa-miR-127 and hsa-miR-377). Sens=sensitivity;

Spec=specificity; PV+=Positive Predicted Value; PV-=Negative Predicted Value, lr.eta= linear predictor (logistic regression) from fitted model.

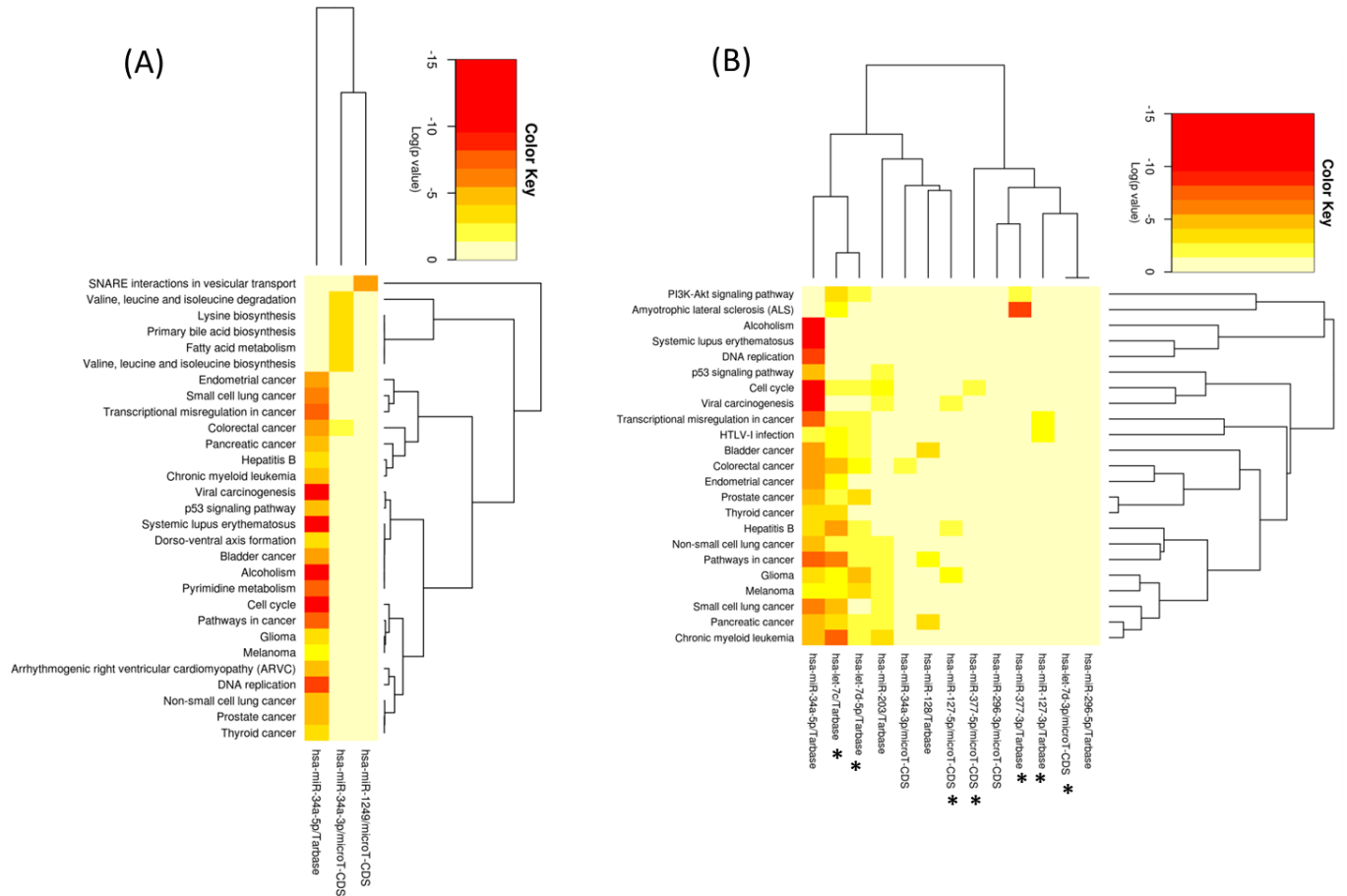


Figure 3. The miRNA target pathways. The miRNAs from models to predict (A) radiation exposure status (hsa-miR-34a and hsa-miR-1249) and (B) radiation-related fusion genes (hsa-let-7c, hsa-let-7d, hsa-miR-127, hsa-miR128-2, hsa-miR-203a, hsa-miR-203b, hsa-miR-296, hsa-miR-34a and hsa-miR-377) were clustered into functional categories and the controlled pathways were identified and ranked according to p-value score. All analyses were performed using mature miRNAs. (*) miRNAs selected for the optimized model to predict radiation-related fusion genes in B.

Supplementary information

Supplementary table 1. Combinatory analysis of 9 miRNAs expressions between positive and negative groups for radiation-related fusion genes to optimize the predictive model

miRNAs combination	Sensitivity	Specificity	Accuracy
hsa.let.7c + hsa.let.7d + hsa.mir.127 + hsa.mir.128.2 + hsa.mir.203a + hsa.mir.203b + hsa.mir.296 + hsa.mir.34a + hsa.mir.377	77.80%	86.60%	87.60%
hsa.let.7c + hsa.let.7d + hsa.mir.127 + hsa.mir.128.2 + hsa.mir.203b + hsa.mir.296 + hsa.mir.34a + hsa.mir.377	77.80%	86.60%	87.60%
hsa.let.7c + hsa.let.7d + hsa.mir.127 + hsa.mir.128.2 + hsa.mir.296 + hsa.mir.34a + hsa.mir.377	83.30%	80.80%	87.90%
hsa.let.7c + hsa.let.7d + hsa.mir.127 + hsa.mir.128.2 + hsa.mir.296 + hsa.mir.377	83.30%	79.50%	87.40%
hsa.let.7c + hsa.let.7d + hsa.mir.127 + hsa.mir.296 + hsa.mir.377	83.30%	82.60%	86.40%
hsa.let.7c + hsa.let.7d + hsa.mir.127 + hsa.mir.377	88.90%	77.60%	85.40%
hsa.let.7c + hsa.let.7d + hsa.mir.377	88.90%	70.80%	81.80%

miRNAs in bold were selected for the optimized model 2

5 DISCUSSÃO

No primeiro capítulo da tese, caracterizamos os modelos celulares que foram utilizados em todas as etapas do trabalho, as linhagens celulares de tireócitos normais FRTL-5 CL2 e PCCI 3. Demonstramos que a RI promove a parada do ciclo celular na fase G₂/M, como previamente reportado por Green e cols. (2001). De maneira interessante, a parada do ciclo celular induzida pela RI foi mais pronunciada nas células FRTL-5 CL2 do que nas PCCI 3, o que poderia ser justificado pela maior taxa de proliferação destas células (Kimura e cols., 2001). Além disso, nossos resultados demonstram que as células da tireoide respondem rapidamente aos insultos causados pela RI, 5 minutos após a exposição, como também observado na cultura primária de tireócitos humanos (Galleani e cols., 2009). Assim, as linhagens celulares FRTL-5 CL2 e PCCI 3 são modelos robustos para entender o reparo do DNA na tireoide. Acima de tudo, as células FRTL-5 CL2 demoram mais tempo para reparar as DSB do que as PCCI 3 e, como resultado, estas células seriam mais susceptíveis a acumular danos no DNA.

Em relação às proteínas envolvidas no reparo das DSB, a expressão de ATR e ATM ativado (p-ATM) revelaram diferenças significativas na capacidade de reparo do DNA entre as duas linhagens celulares. A fosforilação de ATM é maior nas células FRTL-5 CL2 do que nas PCCI 3 enquanto o oposto ocorre com a expressão de ATR 1-6 horas após a irradiação. Ambas as quinases exercem papéis fundamentais para a manutenção da integridade genômica, assim como atuam como uma barreira nas etapas precoces da tumorigênese (Maréchal e cols., 2013). Apesar de ATM e ATR compartilharem diversos efetores na cascata de sinalização, elas são ativadas em resposta a diferentes tipos de lesões (Maréchal e cols., 2013). Enquanto ATM está envolvida primariamente no reparo das DSB, ATR responde a um amplo espectro de danos ao DNA, especialmente aqueles que interferem na replicação. Desse modo, a cinética de ativação dessas quinases poderia estar associada ao reparo tardio das DSB nas células FRTL-5 CL2 e à expressão diferencial de *BRCA1* nas linhagens celulares da tireoide.

Outro achado importante do nosso estudo é que as células FRTL-5 CL2 exibem menores níveis de metilação de *LINE-1* do que as PCCI 3 e a tireoide normal de rato. A metilação de *LINE-1* vem sendo amplamente utilizada como um marcador do perfil de metilação global devido à sua abundância no genoma (aproximadamente 18%) e também pela capacidade de

distinguir o tecido normal do tumoral (Nüsgen e cols., 2015). Além disso, a diminuição dos níveis de metilação de *LINE-1* pode ser observada já nas etapas precoces da tumorigênese (Park e cols., 2014) e, esta característica foi associada ao aumento do risco do desenvolvimento de câncer (Kamiyama e cols., 2012). A hipometilação global é comumente relacionada à instabilidade genômica e à transformação neoplásica (Weidman e cols., 2007; Kovalchuk & Baulch, 2008), sendo importante para a progressão do câncer da tireoide (Smith e cols., 2007, Cancer Genome Atlas Research Network, 2014). Portanto, as células FRTL-5 CL2 seriam mais susceptíveis à instabilidade genômica e à transformação neoplásica, como previamente descrita por Fusco e cols. (1987). Dado que a exposição à RI não foi capaz de modular os níveis de metilação de *LINE-1* nas linhagens FRTL-5 CL2 e PCCI 3, mesmo quando sincronizadas pela privação do hormônio TSH, podemos hipotetizar que a hipometilação global não seria um evento importante nas etapas iniciais da carcinogênese tireóidea e que este seria um mecanismo protetor para a manutenção da viabilidade celular. De fato, o tratamento com o composto desmetilante 5-desoxicidina compromete a viabilidade das células de câncer da tireoide (Dom e cols., 2013). Por outro lado, a expressão de *BRCA1* é menor nas células FRTL-5 CL2 do que as PCCI 3 e, a exposição à RI promoveu uma drástica diminuição da expressão deste gene em ambas as linhagens celulares. Fenotipicamente, a perda da expressão de *BRCA1*, ainda que transiente nas células de câncer de mama MCF7 causa a inativação precoce do ponto de checagem mitótico que, por sua vez, exerce um papel importante na integridade genômica (Chabalier e cols., 2006). Levando em consideração que *BRCA1* é fundamental para o reparo por HR (Caestecker & Van de Walle, 2013) e que a redução da expressão deste gene, mediada pela RI, foi mais acentuada nas células FRTL-5 CL2, esperamos que estas células reparem as DSB de maneira menos eficiente. De fato, a diminuição gradual da expressão dos genes de reparo do DNA e o acúmulo de danos ao mesmo estão presentes em etapas iniciais do processo da tumorigênese de diversos tipos de tumores (Bartkova e cols., 2005), incluindo o CPT (Leprat e cols., 1998).

A hipermetilação das regiões promotoras dos genes supressores de tumor como *ATM* e *MLH1*, assim como os envolvidos na diferenciação celular como *NIS* e *TSHR* e, logo, o silenciamento destes genes, são eventos comuns na progressão do CPT (Smith cols., 2007; Cancer Genome Atlas Research Network, 2014). Todavia, a RI, que atua tanto na iniciação quanto na promoção do CPT (Ron e cols., 1995), não foi capaz de modular o perfil de metilação

da região promotora dos genes de reparo do DNA (*ATM*, *MRE11*, *BRCA1*, *RAD50*, *XRCC1*, *XRCC4*, *PRKDC/DNA-PK*, *XRCC6*, *LIG4*, *MLH1*) nas linhagens celulares de tireócitos normais. Assim, nossos dados sugerem que outros mecanismos estejam envolvidos na perda desses genes nas etapas iniciais da carcinogênese tireóidea, como descrito previamente (Cancer Genome Atlas Research Network, 2014). Vale ressaltar que o nível basal de metilação da região promotora dos genes de reparo do DNA analisados é extremamente baixa (0-9%) o que vai ao encontro da maior expressão desses genes na tireoide quando comparado a outros tecidos (mama, fígado, pulmão, rins), indicando a relevância da expressão desses genes no contexto da tireoide.

Posteriormente, estabelecemos o modelo de exposição crônica à RI usando as células FRTL-5 CL2. Diferente do observado na exposição aguda, a transcrição dos genes de reparo do DNA é induzida durante a exposição crônica à RI nas células FRTL-5 CL2. A principal diferença entre os dois modelos é que no primeiro as células mantêm a capacidade de proliferar, enquanto no último tornam-se senescentes. De fato, o acúmulo de danos não reparados e, conseqüentemente, a sinalização persistente do reparo do DNA resultam em senescência celular (Klement & Goodarzi, 2014). A evasão da senescência, por sua vez, pode dar origem às células transformadas pós-senescentes e células mutadas pré-neoplásicas (Nassour e cols., 2016). Uma vez que a exposição à RI é o fator de risco mais importante para o desenvolvimento do CPT (Ron e cols., 1995), podemos especular que a indução da maquinaria de reparo de DSB contribui para a manutenção da viabilidade celular das células senescentes da tireoide, favorecendo, portanto, o acúmulo de mutações e predispondo à evasão da senescência e transformação neoplásica.

Outro mecanismo importante para a carcinogênese da tireoide é a desregulação da expressão dos miRNAs, estudado no segundo capítulo da tese. Neste capítulo, identificamos os miRNAs regulados pela RI, bem como validamos seus alvos moleculares e funções biológicas nas células normais e de carcinoma da tireoide. Os mecanismos epigenéticos como o perfil de expressão dos miRNAs vem sendo apontado na literatura como um sensor de estresse, envolvido na resposta induzida pela RI (Metheetraitut & Slack, 2013). Nesse contexto, escolhemos estudar a influência da RI sobre a expressão diferencial dos miRNAs, usando a linhagem celular de tireócito normal de rato FRTL-5 CL2 (Ambesi-Impiombato e cols., 1980). A nossa análise

revelou a indução e repressão da expressão de populações distintas de miRNAs, de maneira tempo-dependente. Encontramos 7 miRNAs subexpressos 1 hora após a irradiação, quando ocorre o maior acúmulo das DSB nas células FRTL-5 CL2, como previamente relatado na tese. Em contrapartida, a RI induz a expressão de 10 miRNAs, 6 horas após à exposição, quando grande parte das DSB já foram reparadas. As análises de bioinformática usando os algoritmos do Gene Ontology e do programa mirPath v.3 (Vlachos e cols., 2015) revelaram que a maioria dos miRNAs desregulados pela RI pertence à classe dos “resposta ao estresse celular” ou “silenciamento gênico por miRNA”, tendo como alvos moleculares genes envolvidos diretamente ou indiretamente nas vias de MAPK, proteoglicanas, ácidos graxos, às relacionadas ao câncer e ao reparo do DNA. O miR-541, o miRNA mais alterado pela RI após a primeira hora de exposição, atua como supressor de tumor no câncer de pulmão ao inibir a proliferação e a migração celular pela regulação negativa do repressor da transcrição de genes responsivos ao TGFB, o TGIF2 (Lu e cols., 2016). O miR-33-5p inibe diretamente a expressão da glicosilase 8-oxoguanina, enzima importante para o reparo de danos oxidativos no DNA (Tumurkhuu e cols., 2016). O miR-328 têm como alvo a variante de H2AX e sensibiliza as células de adenocarcinoma de pulmão (A549) à radioterapia (Ma e cols., 2016). Os membros da família do miR-30 estão subexpressos no CAT e a reintrodução desses miRNAs inibe a transição epitélio-mesênquimal (Braun e cols., 2010) e sensibiliza células do CAT ao tratamento com cisplatina (Zhang e cols., 2014). A superexpressão de miR-128 é frequentemente encontrada nas neoplasias da tireoide e correlaciona-se com a presença do rearranjo *RET/PTC* (Pallante e cols., 2014). Decidimos concentrar nossa atenção nos miR-199a-3p e miR-10b-5p porque esses miRNAs foram profundamente alterados pela RI em todos os tempos analisados e são descritos com atividades supressora de tumor (Minna e cols., 2014) e oncogênica (Mussnich e cols., 2013) no câncer de tireoide, respectivamente.

Validamos os novos alvos de miR-199a-3p (*LIN28B*) e miR-10b-5p (*DICER1*) que, por sua vez, são superexpressos e subexpressos, respectivamente, no câncer da tireoide. Demonstramos que *LIN28B* é o alvo de miR-199a-3p, levando à diminuição da expressão de HMGA2 e, desse modo, especulamos que a superexpressão de *let-7b* poderia estar envolvida nesse fenômeno. Os membros da família *let-7* regulam diretamente a expressão do oncogene *RAS* e, conseqüentemente, diminuem a ativação da via de MAPK, fundamental para a

proliferação dos tireócitos (Perdas e cols., 2016). Portanto, a subexpressão de miR-199a-3p no câncer da tireoide poderia levar ao aumento da expressão de *HMGA2* e ao crescimento celular, contribuindo para a progressão tumoral. Por outro lado, reportamos que miR-10b-5p interage com a região 3' não-traduzida do RNAm de *DICER1*, reprimindo sua tradução e, resultando na redução dos seus níveis proteicos, o que já foi associado à transformação celular da tireoide (Frezza e cols., 2011; Rodriguez e cols., 2012). Dado que o miR-10 encontra-se superexpresso nos CFT (Jikuzono e cols., 2013) e CMT (Nikiforova e cols., 2008), além de ser regulado diretamente pelo oncogene *HMGA1* (Mussnich e cols., 2013), a regulação de *DICER1* por miR-10 poderia ser um mecanismo plausível nas células neoplásicas da tireoide.

Uma vez que a eficiência da via de reparo do DNA por HR e a resolução das DSB são fundamentais para prevenir a formação do rearranjo *RET/PTC* nas células da tireoide (Gandhi e cols., 2010), investigamos o papel dos miR-199a-3p e miR-10b-5p nesse contexto. Nossos dados revelam que ambos os miRNAs aumentam a formação de DSB induzidas pela RI, indiretamente quantificada pelos níveis de γ H2AX (Grabarz e cols., 2012). Visto que a proteína HMGA2 pode ativar ATR nas linhagens de câncer (Natarajan e cols., 2013), os menores níveis proteicos basais de ATR poderiam estar relacionados ao retardo do reparo das DSB nas células que superexpressam miR-199a-3p. Por outro lado, a redução da expressão de *DICER1* poderia contribuir para os menores níveis de ATM ativado e ATR, assim como o acúmulo de γ H2AX nas células FRTL-5 CL2 transfectadas com o oligonucleotídeo precursor de miR-10b-5p. De fato, além de desempenhar um papel central na biogênese dos miRNAs (Kurzynska-Kokorniak e cols., 2015), *DICER1* também é crucial para a sinalização do reparo das DSB e fosforilação de ATM em eucariotos (Francia e cols., 2012; Wei e cols., 2012; Gao e cols., 2014). Esses resultados estão de acordo com o comportamento bifásico da expressão de miR-10b-5p nas células FRTL-5 CL2 irradiadas. Desse modo, a desregulação dos miR-199a-3p e miR-10b-5p diminui a eficiência do reparo das DSB pela via de HR nas células da tireoide. Além disso, as células FRTL KiKi, que expressam altos níveis de miR-10b-5p e miR-199a-3p, possuem uma maquinaria de reparo do DNA deficiente, sugerindo que a desregulação desses miRNAs poderiam contribuir para a perda da expressão e/ ou atividade dos genes de reparo do DNA em etapas iniciais da carcinogênese tireóidea. De fato, já foi descrito que ocorre a perda gradual dos genes de reparo de DNA ao longo da progressão do câncer da tireoide (Hu e cols., 2015).

Os defeitos na via de HR estão relacionados à radiosensibilidade nas células neoplásicas, predispondo-as a acumular DSB não reparadas, um tipo letal de dano do DNA (Choudhury e cols., 2009). A superexpressão de miR-10b-5p atenua a viabilidade celular e compromete a proliferação das células normais e neoplásicas da tireoide após serem irradiadas. Dessa maneira, esses efeitos podem ser devido à deficiência da ativação da via de HR após a irradiação, resultando no acúmulo de DSB, embora o efeito estimulatório de miR-10b-5p sobre a proliferação dos tireócitos não possa ser excluído. Dado que miR-10b-5p estimula a proliferação do tireócito, é esperado que os níveis de expressão desse miRNA estejam diminuídos na primeira hora após a irradiação, quando as células param de proliferar para reparar os danos no DNA. Uma vez reparados os danos no DNA, seis horas após o insulto no caso das células FRTL-5 CL2, a expressão de miR-10b-5p é induzida para recuperar a proliferação celular. Além disso, a RI afeta independentemente a função mitocondrial e o DNA. Portanto, uma vez que miR-10b-5p estimula a proliferação e afeta negativamente o reparo pela via de HR, as células que superexpressam esse miRNA são mais susceptíveis à RI. Apesar do ensaio de viabilidade MTT ser a metodologia mais usada para aferir a sobrevivência celular após a irradiação (Slavotinek e cols., 1994), foi descrito que altas doses de radiação (> 1 Gy) impactam na eficiência do ensaio ao afetar a atividade da desidrogenase mitocondrial e, portanto, os resultados obtidos com esse ensaio são menos pronunciados do que aqueles observados usando a contagem do número de células com azul de tripan (Buch e cols., 2012, Chung e cols., 2015). Nossos resultados contrastam com os encontrados nas células de glioblastoma, cujo papel do miR-10b foi o de promover a radiorresistência (Zhen e cols., 2016), sugerindo que o efeito do miR-10b-5p sobre a sensibilidade à RI seja dependente do contexto celular, como já reportado para outros miRNAs (Czochor & Glazer, 2014). Um bom exemplo é o miR-205, que induz a radiorresistência nas células de carcinoma de nasofaringe (Qu e cols., 2012), porém, sensibiliza as células de câncer de mama à RI (Zhang e cols., 2014).

No terceiro capítulo da tese, caracterizamos o papel de *DICER1* na proliferação e diferenciação da tireoide, um assunto ainda muito controverso na literatura. *DICER1* é uma enzima chave no processamento dos miRNAs e as suas funções no desenvolvimento e câncer vêm sendo exploradas amplamente. A desregulação de *DICER1* tem sido descrita no câncer da tireoide (de Kock e cols., 2014; Costa e cols., 2015; Yoo e cols., 2016) e a sua superexpressão

foi associada ao comportamento mais agressivo do CPT (por exemplo, extensão extratireoidiana e metástase à distância) (Erlér e cols., 2014). Nossos resultados mostram que os níveis de RNAm de *DICER1* estão aumentados em 70% dos CPT e 42% dos CAT analisados em comparação às tireoides saudáveis. O número limitado de amostras pode contribuir para as diferenças encontradas nos nossos resultados e os depositados no banco de dados do TGCA (Cancer Genome Atlas Research Network, 2014), bem como as diferentes metodologias empregadas para avaliar a expressão gênica de *DICER1* podem contar para a magnitude dos níveis de RNAm. Em contrapartida, os níveis proteicos de *DICER1* estão reduzidos nas amostras de CPT, como depositado no banco de dados TGCA (Cancer Genome Atlas Research Network, 2014). A discrepância entre os níveis de RNAm e proteína de *DICER1* já foi descrita em diversos trabalhos (Jakymiw e cols., 2010; Erlér e cols., 2014), indicando que mecanismos pós-transcricionais poderiam regular os níveis proteicos de *DICER1* nos tecidos neoplásicos. De forma interessante, *DICER1* é subexpressa em todas as linhagens de câncer de tireoide testadas. Esses resultados podem ser associados ao papel crítico dos miRNAs e, conseqüentemente, de *DICER1* para a diferenciação da tireoide (Frezza e cols., 2011; Rodriguez e cols., 2012). Além disso, as linhagens de câncer da tireoide exibem um fenótipo desdiferenciado quando comparado aos tumores *in vivo* das quais são originárias (Saiselet e cols., 2012) ou simplesmente devido ao elevado número de passagens celulares em cultura.

O efeito de *DICER1* sobre a proliferação celular ainda é controverso. Nossos dados apontam que *DICER1* estimula a proliferação dos tireócitos e, portanto, está de acordo com os resultados encontrados nos modelos de camundongo *knockout* para *DICER1*, cuja perda leva à diminuição do tamanho da glândula tireoide (Frezza e cols., 2011; Rodriguez e cols., 2012). Paradoxalmente, os autores relataram o aumento do número de células positivas (Rodriguez e cols., 2012) para o marcador de divisão celular BrdU (Muskhelishvili e cols., 2003), o que poderia ser explicado parcialmente pelo hipotireoidismo severo e o aumento dos níveis séricos de TSH induzidos pela perda de *DICER1* nesse modelo. Inesperadamente, observamos o aumento da porcentagem de células PCC1 3 na fase S do ciclo celular após o silenciamento de *DICER1*, indo no sentido oposto dos dados de proliferação, da expressão das ciclinas e viabilidade celular encontrados nas mesmas condições. A nossa hipótese é a que a perda de *DICER1* interfira com a replicação do DNA e promova a parada ciclo celular na fase S. Esta é

uma hipótese plausível, uma vez que *DICER1* é importante para o reparo do DNA (Tang & Ren, 2012) e, em condições fisiológicas, os tireócitos produzem grandes quantidades de espécies reativas de oxigênio e nitrogênio (Song e cols., 2007) e, logo, são mais sujeitos aos danos no DNA. Sobretudo, foi descrito que a perda monoalélica e não bialélica de *DICER1* tem efeito tumorigênico *in vivo* e, portanto, os níveis de expressão de *DICER1* são determinantes para o seu efeito sobre a proliferação celular (Kumar e cols., 2009; Lambertz e cols., 2010). Desse modo, enquanto a perda parcial de *DICER1* seria vantajosa para o tumor, a perda massiva de sua expressão poderia comprometer a viabilidade e proliferação do tireócito. De fato, o tamanho da glândula tireoide dos camundongos *knockout* para *DICER1* é menor do que os heterozigotos para esse gene (Frezzetti e cols., 2011), corroborando os nossos dados de silenciamento de *DICER1* (*knockdown*) na linhagem celular PCC1 3.

De maneira interessante, os miRNAs miR-21-5p e miR-125-5p, que têm como alvos genes envolvidos na diferenciação e proliferação da tireoide, além de serem modulados por *DICER1* (Fuziwara & Kimura, 2016), estão regulados negativamente nos modelos celulares de inibição e superexpressão de *DICER1* utilizados no nosso estudo. Estes dados sugerem que a regulação fina da expressão de *DICER1* seja fundamental para a manutenção do processamento dos miRNAs. Além disso, a perda da expressão de *DICER1* induziu o fenótipo desdiferenciado nas células PCC1 3 apesar da superexpressão da mesma não causar qualquer modificação na expressão dos marcadores de diferenciação tireóideos, indicando que a expressão basal de *DICER1* seja importante para a manutenção da diferenciação da tireoide. Nossos dados corroboram os publicados previamente, nos quais a perda da expressão gênica de *DICER1* afetou a arquitetura tecidual da tireoide, bem como a função e diferenciação tireoidiana, levando à aquisição de características semelhantes às encontradas nas células neoplásicas (Frezzetti e cols., 2011; Rodriguez e cols., 2012).

O domínio RNase IIIb de *DICER1* é frequentemente mutado nos tumores de ovário não-epitelial (Witkowski e cols., 2013) e endométrio (Chen e cols., 2015). A mutação E1813G, localizada no domínio IIIb de *DICER1*, foi identificada consistentemente em 5-8% dos casos de câncer da tireoide (de Kock e cols., 2014; Costa e cols., 2015; Yoo e cols., 2016). Nossos achados mostram que esta mutação impacta negativamente na proliferação e no processamento

dos miRNAs mediados por *DICER1*. De fato, essa mutação pode reduzir parcialmente a atividade enzimática de *DICER1*, uma vez que é predita como deletéria ao inibir a função do domínio RNase IIIb, o que levaria à falha da clivagem dos miRNAs no braço 5' dos pré-miRNAs (Kurzynska-Kokorniak e cols., 2015). Tal efeito vai ao encontro da incapacidade de *DICER1* mutada de processar os miRNAs miR-21-5p, miR-33-5p, miR-125-5p e miR-296-5p, quando comparado à *DICER1* selvagem nas linhagens de câncer da tireoide selecionadas para este estudo. Além disso, não podemos excluir a contribuição de outras mutações somáticas e germinativas no gene de *DICER1* para a transformação celular. De fato, mutações germinativas no gene que codifica *DICER1* predisõem o indivíduo à síndrome de DICER1, uma doença rara associada ao desenvolvimento pleiotrópico de tumores, como blastoma pleuropulmonar familiar, nefroma quístico multilocular, tumores de células Sertoli-Leydig no ovário, além de diversas anormalidades tireoidianas, como o bócio multinodular e o CDT (Slade e cols., 2011, de Kock e cols., 2014).

No quarto capítulo da tese, propusemos, pela primeira vez, um modelo baseado na expressão dos miRNAs para classificar o status de exposição à RI em amostras de CPT usando o banco de dados TCGA. A principal vantagem do nosso estudo foi a de analisar a expressão de miRNAs, previamente descritos no capítulo 2 dessa tese e num trabalho prévio (Nikiforova e cols., 2011), que eram regulados pela RI (1-10 Gy) em células normais de tireoide em etapas iniciais da carcinogênese. A escolha do conjunto de miRNA a ser avaliado foi fundamental para análises posteriores porque a RI atua tanto como iniciadora quanto promotora da carcinogênese da tireoide (Caudill e cols., 2005). Dos 31 miRNAs selecionados para o estudo, apenas dois foram diferencialmente expressos entre os grupos exposto e não exposto à RI. Dado que os miRNAs estão envolvidos na resposta ao dano no DNA (Majidinia & Yousefi, 2016), é esperado que uma parte desses miRNAs fossem regulados de maneira transiente em resposta à RI e se mantivessem inalterados durante o processo de carcinogênese da glândula. A expressão dos hsa-miR-34a e hsa-miR-1249 nos permitiu prever de maneira acurada se o paciente com CPT havia sido exposto à RI. De fato, miR-34a é induzido pela RI em células normais e tumorais em experimentos *in vitro* e *in vivo*, independente do tipo celular (Lacombe & Zenhausern, 2017). De maneira, a indução da expressão de miR-34 pela RI é mais acentuada em camundongos jovens do que nos adultos (Liu e cols., 2011), o que vai ao encontro da maior radiosensibilidade

observada em indivíduos jovens (<5 anos) descrita a partir de estudos epidemiológicos com sobreviventes do acidente nuclear de Chernobyl em 1986 (Pacini e cols., 1997). O fato do miR-34a também ser detectado no sangue de pacientes irradiados (Liu e cols., 2011) acende a possibilidade do seu potencial uso clínico como biomarcador de exposição à RI.

Dentre todas as fusões gênicas relacionadas à RI no CPT (Ricarte-Filho e cols., 2013), apenas *RET/PTC1*, *RET/PTC3* e *ETV6/NTRK3* foram detectadas na nossa população de estudo. Apesar dessas alterações moleculares serem frequentemente associadas à RI, somente um caso foi positivo para *ETV6/NTRK3* e havia o histórico confirmado de exposição à RI, sugerindo que outros fatores poderiam estar envolvidos nas formações destas fusões gênicas. Além disso, tais alterações moleculares, especialmente os rearranjos *RET/PTC1* e *RET/PTC3*, estão associadas à pior evolução clínica dos pacientes com CPT quando comparado aos negativos para esses rearranjos cromossômicos, sendo descritas maiores frequências de doença avançada (pT3/pT4) e disseminação para linfonodos ao diagnóstico com rápida progressão da doença nesses pacientes (Rabes e cols., 2000). Nesse sentido, o modelo otimizado proposto no capítulo 4, baseado na expressão dos quatro miRNAs (hsa-let-7c, hsa-let-7d, hsa-miR-127 e hsa-miR-377) diferencialmente expressos entre os grupos positivo e negativo para tais fusões gênicas relacionadas à RI, foi capaz de identificá-las em amostras de CPT com alta acurácia, sensibilidade e especificidade. De fato, parte desses miRNAs, como let-7d e miR-127 já haviam sido associados aos rearranjos RET/PTC (Cahill e cols., 2006).

Em concordância com a sua importância para a resposta à RI (Lacombe & Zenhausern, 2017), nossos achados apontam que o hsa-miR-34a tem como alvo as vias de replicação do DNA, ciclo celular, P53 e PI3K-Akt que, por sua vez, são comumente desreguladas em diversos tipos de tumores, incluindo os da tireoide (Cancer Genome Atlas Research Network, 2014). Além disso, os miRNAs hsa-let-7c e hsa-let-7, cuja função na DDR já foi relatada anteriormente (Metheetraitut & Slack, 2013), compartilham das mesmas vias de sinalização alvo do hsa-miR-34a. A família let-7 atua como supressora de tumor no CPT ao reduzir a expressão do oncogene *RAS*, afetando negativamente à ativação da via de MAPK e, conseqüentemente, à proliferação celular (Johnson e cols., 2007; Ricarte-Filho e cols., 2009). A função do miR-1249 no contexto da tireoide ainda é desconhecido. Têm sido relatado que o miR-1249 atua como oncogene nos

hepatocarcinoma (Ye e cols., 2017) e glioma (Fang e cols., 2018). Tomados em conjunto, os miRNAs regulados pela RI e selecionados para este estudo impactam em vias de sinalização fundamentais para o crescimento e função da tireoide, resposta ao estresse genotóxico, assim como na transformação neoplásica e progressão tumoral (Cancer Genome Atlas Research Network, 2014).

As maiores vantagens do nosso modelo são: os miRNAs são relativamente estáveis e a sua expressão poderia ser avaliada em tecidos fixados em formalina e embebidos em parafina (Liu & Xu, 2011); a identificação dos CPT relacionados à RI independente da presença dos rearranjos cromossômicos ligados à RI; potencial de ser inserido na prática clínica devido ao seu baixo custo e maior acurácia, especificidade e sensibilidade. Por outro lado, as limitações do nosso trabalho são a falta de informação sobre o tipo e dose absorvida de radiação nas amostras do TCGA e estudos confirmatórios em coortes independentes são necessários para validar os nossos achados.

6 CONCLUSÕES

Em suma, a exposição à RI afeta a eficiência da maquinaria de reparo das DSB pela via de reparo do DNA por recombinação homóloga, refletindo no reparo tardio e acúmulo dessas lesões nas células normais da tireoide. Embora a alteração do perfil de metilação do DNA seja importante para a progressão do câncer da tireoide, esse mecanismo epigenético parece não estar envolvido diretamente na regulação da expressão gênica e eficiência da maquinaria de reparo do DNA e dos níveis globais de metilação do DNA das células tireoidianas irradiadas. Sobretudo, nossos resultados revelam que a regulação do perfil de expressão dos miRNAs parece ser importante na resposta à RI, particularmente os miR-199a-3p e miR-10b-5p que, por sua vez, regulam genes relevantes para a fisiopatologia da tireoide, como *LIN28b* e *DICER1*, respectivamente. Nossos dados demonstram que *DICER1* está subexpressa no CPT e apontam a repressão da tradução de *DICER1* por miR-10b-5p como um novo mecanismo de regulação pós-transcricional de *DICER1* nas células neoplásicas. Além disso, foi demonstrado que a regulação fina de *DICER1* e, logo, o processamento dos miRNAs é fundamental para a manutenção da diferenciação e proliferação do tireócito. Nossos achados podem ter relevância clínica para a compreensão de alguns mecanismos envolvidos na carcinogênese da tireoide, bem como para novas perspectivas de estratégias terapêuticas para o tratamento do CAT. O papel de miR-10b-5p de promover radiosensibilidade nas células normais e de câncer da tireoide nos leva a hipotetizar que a sua superexpressão nas neoplasias malignas tireoidianas, especialmente os CAT, poderia melhorar a resposta à radioterapia. Por fim, os modelos preditivos baseados na expressão dos miRNAs regulados pela RI foram capazes de classificar de forma acurada os pacientes com CPT expostos à RI e as fusões relacionadas à RI em amostras do banco de dados TCGA. Nossos resultados, podem ajudar na identificação de pacientes com histórico de exposição à RI, que podem evoluir com uma doença mais agressiva. Contudo, são necessários estudos confirmatórios em coortes independentes de CPT.

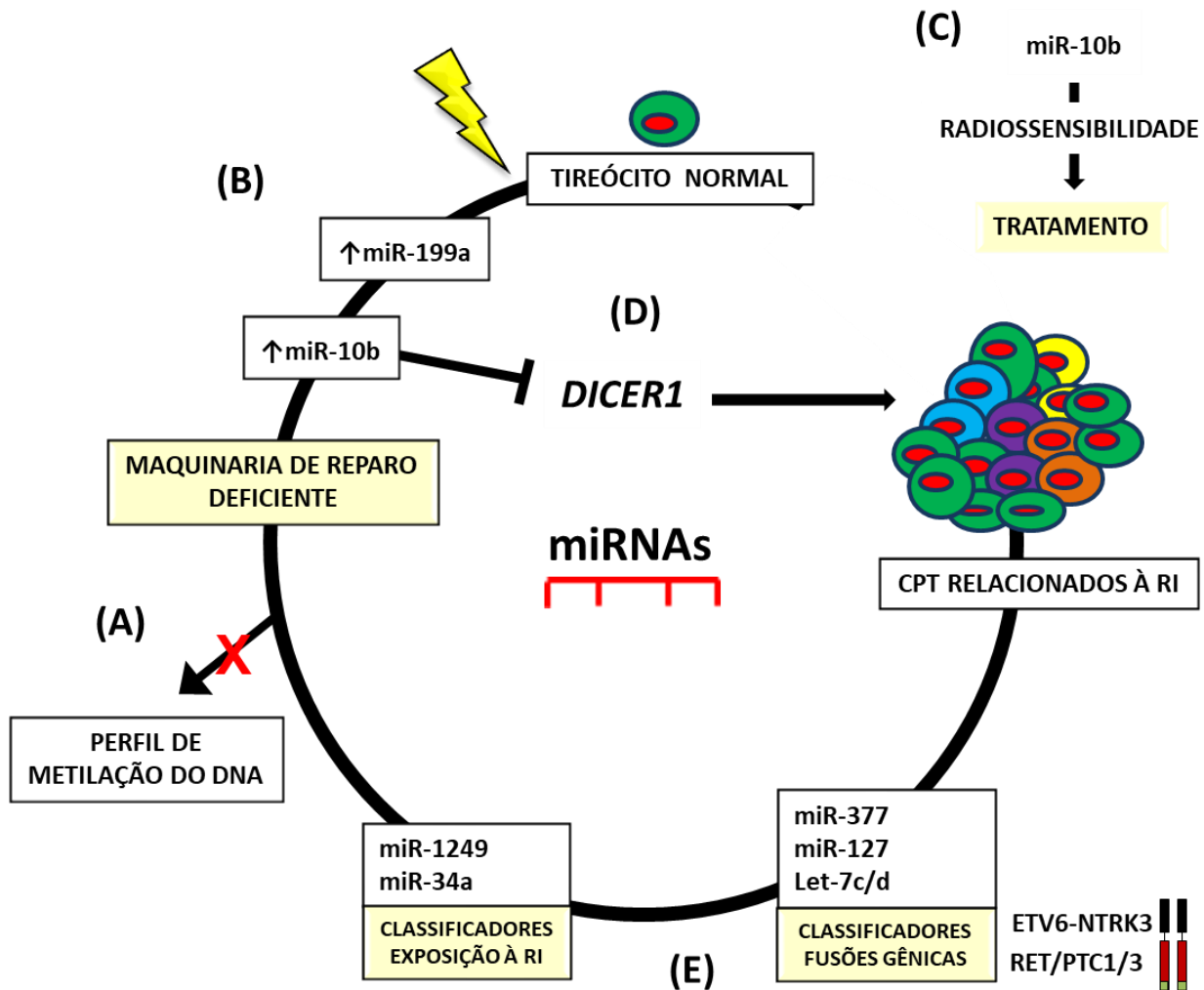


Figura 8. Principais achados da tese de doutorado. (A) A desregulação da metilação do DNA não parece ser mecanismo epigenético envolvido na regulação da expressão gênica e eficiência da maquinaria de reparo do DNA das células tireoidianas irradiadas; (B) Os miR-10b-5p e miR-199a-3p, regulados pela RI, afetam negativamente o reparo das quebras duplas do DNA por recombinação homóloga nas células da tireoide; (C) A indução de miR-10b-5p promove radiosensibilidade nas células da tireoide irradiadas, incluindo as células oriundas de tumores anaplásicos (8505c), refratário a todas as terapias convencionais, incluindo a radioterapia; (D) O miR-10b-5p inibe a expressão de *DICER1* pela repressão da tradução do RNA mensageiro que, por sua vez, está subexpressa nos CPT, o que poderia contribuir para a perda de diferenciação e o aumento da proliferação celular no processo de carcinogênese da tireoide; (E) Os miRNAs, regulados pela RI, são capazes de classificar de

forma acurada os pacientes com CPT expostos à RI e as fusões relacionadas à RI em amostras do banco de dados TCGA.

7 REFERÊNCIA BIBLIOGRÁFICA

ABOU-EL-ARDAT, K. *et al.* Low dose irradiation of thyroid cells reveals a unique transcriptomic and epigenetic signature in RET/PTC-positive cells. **Mutat Res**, v. 731, n. 1-2, p. 27-40, Mar 2012.

ADAMS, R.L. *et al.* Mouse DNA methylase: methylation of native DNA. **Biochim Biophys Acta**, v. 561, n. 2, p. 345-357, Feb 1979.

AKHTAR, A.; BECKER, P.B. Activation of transcription through histone H4 acetylation by MOF, an acetyltransferase essential for dosage compensation in *Drosophila*. **Mol Cell**, v. 5, n. 2, p. 367-375, Feb 2000.

AL-BRAHIM, N.; ASA, S.L. Papillary thyroid carcinoma: an overview. **Arch Pathol Lab Med**, v. 130, n. 7, p. 1057-62, Jul 2006.

ALLIS, C.D.; JENUWEIN, T. The molecular hallmarks of epigenetic control. **Nat Rev Genet**, v. 17, n. 8, p. 487-500, Aug 2016.

AMBESI-IMPIOMBATO, F.S., PARKS, L.A., COON, H.G. Culture of hormone-dependent functional epithelial cells from rat thyroids. **Proc Natl Acad Sci U S A**, v. 77, n. 6, p. 3455-3459, Jun 1980.

AMBROS, V.; CHEN, X. The regulation of genes and genomes by small RNAs. **Development**, v. 134, n. 9, p. 1635-1641, May 2007.

AMBS, S. *et al.* Genomic profiling of microRNA and mRNA reveals deregulated microRNA expression in prostate cancer. **Cancer Res**, v. 68, n. 15, p. 6162-6170, Aug 2008.

ANDERS, S.; HUBER, W. Differential expression analysis for sequence count data. **Genome Biol**, v. 11, n. 10, p. R106, Oct 2010.

ANTWIH, D.A. *et al.* Radiation-induced epigenetic DNA methylation modification of radiation-response pathways. **Epigenetics**, v. 8, n. 8, p. 839-848, Aug 2013.

BALL, D.W. Medullary thyroid cancer: monitoring and therapy. **Endocrinol Metab Clin North Am**, v. 36, n. 3, p. 823-837, Sep 2007.

BARTKOVA, J. *et al.* DNA damage response as a candidate anti-cancer barrier in early human tumorigenesis. **Nature**, v. 434, n. 7035, p. 864-870, Apr 2005.

BAYLIN, S.B.; JONES, P.A. A decade of exploring the cancer epigenome - biological and translational implications. **Nat Rev Cancer**, v. 11, n. 10, p. 726-734, Sep 2011.

BAYLIN, S.B.; OHM, J.E. Epigenetic gene silencing in cancer - a mechanism for early oncogenic pathway addiction? **Nat Rev Cancer**, v. 6, n. 2, p. 107-116, Feb 2006.

BRAY, F. *et al.* Global cancer statistics 2018: GLOBOCAN estimates of incidence and mortality worldwide for 36 cancers in 185 countries. **CA Cancer J Clin**, Sep 2018.

BEROUKHIM, R. *et al.* The landscape of somatic copy-number alteration across human cancers. **Nature**, v. 463, n. 7283, p. 899-905, Feb 2010.

BIRD, A. DNA methylation patterns and epigenetic memory. **Genes Dev**, v. 16, n. 1, p. 6-21, Jan 2002.

BLOT, W.J. *et al.* Thyroid cancer in the Pacific. **J Natl Cancer Inst**, v. 89, n. 1, p. 90-91, Jan 1997.

BOICE, J.D. JR. Radiation epidemiology and recent paediatric computed tomography studies. **Ann ICRP**, v. 44, n. 1 Suppl, p. 236-248, Mar 2015.

BOLTZE, C. *et al.* Sporadic and radiation-associated papillary thyroid cancers can be distinguished using routine immunohistochemistry. **Oncol Rep**, v. 22, n. 3, p. 459-467, Sep 2009.

BORBONE E, E. *et al.* Enhancer of Zeste Homolog 2 Overexpression Has a Role in the Development of Anaplastic Thyroid Carcinomas. **J Clin Endocrinol Metab**, v. 96, n. 4, p. 1029-1038, Apr 2011.

BORBONE E, E. *et al.* Histone deacetylase inhibitors induce thyroid cancer-specific apoptosis through proteasome-dependent inhibition of TRAIL degradation. **Oncogene**, v. 29, n. 1, p. 105-116, Jan 2010.

BOUNACER, A. *et al.* High prevalence of activating ret proto-oncogene rearrangements, in thyroid tumors from patients who had received external radiation. **Oncogene**, v. 15, n. 11, p. 1263-1273, Sep 1997.

BOVERI, T.; BOVERI, M. The Origin of Malignant Tumors. **Williams and Wilkins, Baltimore**, 1929.

BRAUN, J. *et al.* Downregulation of microRNAs directs the EMT and invasive potential of anaplastic thyroid carcinomas. **Oncogene**, v. 29, n. 29, p. 4237-4244, Jul 2010.

BRUECKNER, B. *et al.* The human let-7a-3 locus contains an epigenetically regulated microRNA gene with oncogenic function. **Cancer Res**, v. 67, n. 4, p. 1419-1423, Feb 2007.

BUCH, K. *et al.* Determination of cell survival after irradiation via clonogenic assay versus multiple MTT Assay - a comparative study. **Radiat Oncol**, v. 7, p. 1, Jan 2012.

BUNZ, F. **Principles of Cancer Genetics**, 1 ed. Baltimore (USA): Springer Science + Business Media B.V, 2008.

BUSCAGLIA, L.E.; LI, Y. Apoptosis and the target genes of microRNA-21. **Chin J Cancer**, v. 30, n. 6, p. 371-380, Jun 2011.

CAHILL, S. *et al.* Effect of ret/PTC 1 rearrangement on transcription and post-transcriptional regulation in a papillary thyroid carcinoma model. **Mol Cancer**, v. 5, p. 70, Dec 2006.

CALIN, G.A.; CROCE, C.M. MicroRNA signatures in human cancers. **Nat Rev Cancer**, v. 6, n. 11, p. 857-866, Nov 2006.

CANCER GENOME ATLAS RESEARCH NETWORK. Integrated genomic characterization of papillary thyroid carcinoma. **Cell**, v. 159, n. 3, p. 676-690, Oct 2014.

CARDIS, E. *et al.* Cancer consequences of the Chernobyl accident: 20 years on. **J Radiol Prot**, v. 26, n. 2, p. 127-140, Jun 2006.

CAUDILL, C.M. *et al.* Dose-dependent generation of RET/PTC in human thyroid cells after in vitro exposure to gamma-radiation: a model of carcinogenic chromosomal rearrangement induced by ionizing radiation. **J Clin Endocrinol Metab**, v. 90, n. 4, p. 2364-2369, Apr 2005.

CHABALIER, C. *et al.* BRCA1 downregulation leads to premature inactivation of spindle checkpoint and confers paclitaxel resistance. **Cell Cycle**, v. 5, n. 9, p. 1001-1007, May 2006.

CHEN, Y.; VERFAILLIE, C.M. MicroRNAs: the fine modulators of liver development and function. **Liver Int**, v. 34, n. 7, p. 976-990, Aug 2014.

CHOUDHURY, A. *et al.* Targeting homologous recombination using imatinib results in enhanced tumor cell chemosensitivity and radiosensitivity. **Mol Cancer Ther**, v. 8, n. 1, p. 203-213, Jan 2009.

CHU, J.Y. *et al.* Dicer function is required in the metanephric mesenchyme for early kidney development. **Am J Physiol Renal Physiol**, v. 306, n. 7, p. F764-F772, Apr 2014.

CHUNG, D.M., KIM, J.H., KIM, J.K. Evaluation of MTT and Trypan Blue assays for radiation-induced cell viability test in HepG2 cells. **Int. J. Radiat. Res**, v. 13, n. 4, p. 331-335, Oct 2015.

CIAMPI, R. *et al.* Oncogenic AKAP9-BRAF fusion is a novel mechanism of MAPK pathway activation in thyroid cancer. **J Clin Invest**, v. 115, n. 1, p. 94-101, Jan 2005.

CLÉRO, É. *et al.* Pooled analysis of two case-control studies in New Caledonia and French Polynesia of body mass index and differentiated thyroid cancer: the importance of body surface area. **Thyroid**, v. 20, n. 11, p. 1285-1293, Nov 2010.

CLÉRO, É. *et al.* Dietary iodine and thyroid cancer risk in French Polynesia: a case-control study. **Thyroid**, v. 22, n. 4, p. 422-429, Apr 2012.

COSTA, V. *et al.* New somatic mutations and WNK1-B4GALNT3 gene fusion in papillary thyroid carcinoma. **Oncotarget**, v. 6, n. 13, p. 11242-11251, May 2015.

CRAMER, J.D. *et al.* Analysis of the rising incidence of thyroid cancer using the Surveillance, Epidemiology and End Results national cancer data registry. **Surgery**, v. 148, n. 6, p.1147-52, Dec 2010.

CZOCHOR, J.R., GLAZER, P.M. MicroRNAs in Cancer Cell Response to Ionizing Radiation. **Antioxid Redox Signal**, v. 21, n. 2, p. 293-312, Jul 2014.

DE CASTRO, T.P. *et al.* Predictors for papillary thyroid cancer persistence and recurrence: a retrospective analysis with a 10-year follow-up cohort study. **Clin Endocrinol (Oxf)**, v. 85, n. 3, p. 466-74, Sep 2016.

DE FELICE, M; DI LAURO, R. Thyroid development and its disorders: genetics and molecular mechanisms. **Endocr Rev**, v. 25, n. 5, p. 722-46, Oct 2004.

DE KOCK, L. *et al.* Exploring the association Between DICER1 mutations and differentiated thyroid carcinoma. **J Clin Endocrinol Metab**, v. 99, n. 6, p. E1072-7, Jun 2014.

DE LELLIS, R.A.; LLOYD, R.V.; HEITZ, P.U. World Health Organization Classification of Tumours. **Pathology and Genetics of Tumours of Endocrine Organs**. Lyon (France): WHO/IARC Press. 3. ed.: v. 8, 2004.

DE MARTINO, I. *et al.* Regulation of microRNA expression by HMGA1 proteins. **Oncogene**, v. 28, n. 11, p. 1432-1442, Mar 2009.

DE SOUSA, G.R. *et al.* Low DICER1 expression is associated with poor clinical outcome in adrenocortical carcinoma. **Oncotarget**, v. 6, n. 26, p. 22724-22733, Sep 2015.

DENIS, H.; NDLOVU, M.N.; FUKS, F. Regulation of mammalian DNA methyltransferases: a route to new mechanisms. **EMBO Rep**, v. 12, n. 7, p. 647-656, Jul 2011.

DENT, P. *et al.* MAPK pathways in radiation response. **Oncogene**, v. 22, n. 37, p. 5885-5896, Sep 2003.

DI COSMO, C. *et al.* Mice deficient in MCT8 reveal a mechanism regulating thyroid hormone secretion. **J Clin Invest**, v. 120, n. 9, p. 3377-88, Aug 2010.

DOHÁN, O. *et al.* The sodium/iodide Symporter (NIS): characterization, regulation, and medical significance. **Endocr Rev**, v. 24, n. 1, p. 48-77, Feb 2003.

DOM, G. *et al.* 5-aza-2'-deoxycytidine has minor effects on differentiation in human thyroid cancer cell lines, but modulates genes that are involved in adaptation in vitro. **Thyroid**, v. 23, n. 3, p. 317-328, Mar 2013.

DOM, G. *et al.* A gene expression signature distinguishes normal tissues of sporadic and radiation-induced papillary thyroid carcinomas. **Br J Cancer**, v. 107, n. 6, p. 994-1000, Sep 2012.

DURANTE, C. *et al.* BRAF mutations in papillary thyroid carcinomas inhibit genes involved in iodine metabolism. **J Clin Endocrinol Metab**, v. 92, n. 7, p. 2840-3, May 2007.

ELLIS, R.J. *et al.* Genome-wide methylation patterns in papillary thyroid cancer are distinct based on histological subtype and tumor genotype. **J Clin Endocrinol Metab**, v. 99, n. 2, p. E329-E337, Feb 2014.

ERLER, P. *et al.* Dicer expression and microRNA dysregulation associate with aggressive features in thyroid cancer. **Surgery**, v. 156, n. 6, p. 1342-1350, Dec 2014.

FABER, C. *et al.* Overexpression of Dicer predicts poor survival in colorectal cancer. **Eur J Cancer**, v. 47, n. 9, p. 1414-1419, Jun 2011.

FANG, B. *et al.* MicroRNA miR-1249 downregulates adenomatous polyposis coli 2 expression and promotes glioma cells proliferation. **Am J Transl Res**, v. 10, n. 5, p. 1324-1336, May 2018.

FAGGAD, A. *et al.* Prognostic significance of Dicer expression in ovarian cancer-link to global microRNA changes and oestrogen receptor expression. **J Pathol**, v. 220, n. 3, p. 382-391, Feb 2010.

FEINBERG, A.P.; TYCKO, B. The history of cancer epigenetics. **Nat Rev Cancer**, v. 4, n. 2, p. 143-153, Feb 2004.

FOULKES, W.D.; PRIEST, J.R.; DUCHAINE, T.F. DICER1: mutations, microRNAs and mechanisms. **Nat Rev Cancer**, v. 14, n. 10, p. 662-672, Oct 2014.

FRANCIA, S. *et al.* Site-specific DICER and DROSHA RNA products control the DNA-damage response. **Nature**, v. 488, n. 7410, p. 231-235, Aug 2012.

FREZZETTI, D. *et al.* The microRNA-processing enzyme Dicer is essential for thyroid function. **PLoS One**, v. 6, n. 11, p. e27648, Nov 2011.

FRIEDMAN, R.C. *et al.* Most mammalian mRNAs are conserved targets of microRNAs. **Genome Res**, v. 19, n. 1, p. 92-105, Jan 2009.

FUSCO, A. *et al.* A new oncogene in human thyroid papillary carcinomas and their lymph-nodal metastases. **Nature**, v. 328, n. 6126, p. 170-172, Jul 1987.

FUSCO, A., SANTORO, M. 20 years of RET/PTC in thyroid cancer: clinico-pathological correlations. **Arq Bras Endocrinol Metabol**, v. 51, n. 5, p. 731-5, Jul 2007.

FUZIWARA, C.S.; KIMURA, E.T. MicroRNAs in thyroid development, function and tumorigenesis. **Mol Cell Endocrinol**, v. 456, p. 44-50, Nov 2017.

GALLEANI, J. *et al.* H2AX phosphorylation and kinetics of radiation-induced DNA double strand break repair in human primary thyrocytes. **Thyroid**, v. 19, n. 3, p. 257-264, Mar 2009.

GANDHI, M., EVDOKIMOVA, V., NIKIFOROV, Y.E. Mechanisms of chromosomal rearrangements in solid tumors: the model of papillary thyroid carcinoma. **Mol Cell Endocrinol**, v. 321, n. 1, p. 36-43, May 2010.

GAO, C. *et al.* Up-regulated expression of Dicer reveals poor prognosis in laryngeal squamous cell carcinoma. **Acta Otolaryngol**, v. 134, n. 9, p. 959-963, Sep 2014.

GAO, M. *et al.* Ago2 facilitates Rad51 recruitment and DNA double-strand break repair by homologous recombination. **Cell Res**, v. 24, n. 5, p. 532-541, May 2014.

GEBERT, L.F.R.; MACRAE, I.J. Regulation of microRNA function in animals. **Nat Rev Mol Cell Biol**, v. 20, n. 1, p. 21-37, Jan 2019.

GRABARZ, A. *et al.* Initiation of DNA double strand break repair: signaling and single-stranded resection dictate the choice between homologous recombination, non-homologous end-joining and alternative end-joining. **Am J Cancer Res**, v. 2, n. 3, p. 249-268, Apr 2012.

GREAVES, M.; MALEY, C.C. Clonal evolution in cancer. **Nature**, v. 481, n. 7381, p. 306-313, Jan 2012.

GREEN, L.M. *et al.* Response of thyroid follicular cells to gamma irradiation compared to proton irradiation. I. Initial characterization of DNA damage, micronucleus formation, apoptosis, cell survival, and cell cycle phase redistribution. **Radiat Res**, v. 155, n. 1, p. 32-42, Jan 2001.

GUAN, H. *et al.* Hypermethylation of the DNA mismatch repair gene hMLH1 and its association with lymph node metastasis and T1799A BRAF mutation in patients with papillary thyroid cancer. **Cancer**, v. 113, n. 2, p. 247-255, Jul 2008.

GUO, K.; WANG, Z. Risk factors influencing the recurrence of papillary thyroid carcinoma: a systematic review and meta-analysis. **Int J Clin Exp Pathol**, v. 7, n. 9, p. 5393-403, Aug 2014.

HAMATANI, K. *et al.* RET/PTC rearrangements preferentially occurred in papillary thyroid cancer among atomic bomb survivors exposed to high radiation dose. **Cancer Res**, v. 68, n. 17, p. 7176-82, Sep 2008.

HANLY, E.K. *et al.* Disruption of mutated BRAF signaling modulates thyroid cancer phenotype. **BMC Res Notes**, v. 7, p. 187, Mar 2014.

HE, H. *et al.* The role of microRNA genes in papillary thyroid carcinoma. **Proc Natl Acad Sci U S A**, v. 102, n. 52, p. 19075-80, Dec 2005.

HERCEG, Z. Epigenetics and cancer: towards an evaluation of the impact of environmental and dietary factors. **Mutagenesis**, v. 22, n. 2, p. 91-103, Mar 2007.

HOLLIDAY, R. Epigenetics: a historical overview. **Epigenetics**, v. 1, n. 2, p. 76-80, Abril 2006.

HONG, X. *et al.* Dicer1 is essential for female fertility and normal development of the female reproductive system. **Endocrinology**, v. 149, n. 12, p. 6207-6212, Dec 2008.

HU, B. *et al.* miR-21-mediated Radioresistance Occurs via Promoting Repair of DNA Double Strand Breaks. **J Biol Chem**, v. 292, n. 8, p. 3531-3540, Feb 2017.

HU, J.L. *et al.* Abnormal Expression of DNA Double-Strand Breaks Related Genes, ATM and GammaH2AX, in Thyroid Carcinoma. **Int J Endocrinol**, v. 2015, p. 136810, Mar 2015.

ILIOPOULOS, D. *et al.* STAT3 activation of miR-21 and miR-181b-1 via PTEN and CYLD are part of the epigenetic switch linking inflammation to cancer. **Mol Cell**, v. 39, n. 4, p. 493-506, Aug 2010.

INCA. Estimativa 2018: incidência de câncer no Brasil. **Instituto Nacional de Câncer José Alencar Gomes da Silva**, Ministério da Saúde, 2017.

JAKYMIW, A. *et al.* Overexpression of dicer as a result of reduced let-7 MicroRNA levels contributes to increased cell proliferation of oral cancer cells. **Genes Chromosomes Cancer**, v. 49, n. 6, p. 549-559, Jun 2010.

JIKUZONO, T. *et al.* The miR-221/222 cluster, miR-10b and miR-92a are highly upregulated in metastatic minimally invasive follicular thyroid carcinoma. **Int J Oncol**, v. 42, n. 6, p. 1858-1868, Jun 2013.

JOHNSON, C.D. *et al.* The let-7 microRNA represses cell proliferation pathways in human cells. **Cancer Res**, v. 67, n. 16, p. 7713-22, Aug 2007.

KAMIYAMA, H. *et al.* DNA demethylation in normal colon tissue predicts predisposition to multiple cancers. **Oncogene**, v. 31, n. 48, p. 5029-5037, Nov 2012.

KARUBE, Y. *et al.* Reduced expression of Dicer associated with poor prognosis in lung cancer patients. **Cancer Sci**, v. 96, n. 2, p. 111-115, Feb 2005.

KEUTGEN, X.M. *et al.* Management of anaplastic thyroid cancer. **Gland Surg**, v. 4, n. 1, p. 44-51, Feb 2015.

KHOSHNAW, S.M. *et al.* Loss of Dicer expression is associated with breast cancer progression and recurrence. **Breast Cancer Res Treat**, v. 135, n. 2, p. 403-413, Sep 2012.

KIMURA, T. *et al.* Regulation of thyroid cell proliferation by TSH and other factors: a critical evaluation of in vitro models. **Endocr Rev**, v. 22, n. 5, p. 631-656, Oct 2001.

KITAHARA, C.M. *et al.* Obesity and thyroid cancer risk among U.S. men and women: a pooled analysis of five prospective studies. **Cancer Epidemiol Biomarkers Prev**, v. 20, n. 3, p. 464-472, Mar 2011.

KLEMENT, K., GOODARZI, A.A. DNA double strand break responses and chromatin alterations within the aging cell. **Exp Cell Res**, v. 329, n. 1, p. 42-52, Nov 2014.

KONDO, T.; EZZAT, S.; ASA, S.L. Pathogenetic mechanisms in thyroid follicular-cell neoplasia. **Nat Rev Cancer**, v. 6, n. 4, p. 292-306, Apr 2006.

KOVALCHUK, O., BAULCH, J.E. Epigenetic changes and non-targeted radiation effects – is there a link? **Environmental and Molecular Mutagenesis**, v. 49, n. 1, p. 16-25, Jan 2008.

KOZAKI, K. *et al.* Exploration of tumor-suppressive microRNAs silenced by DNA hypermethylation in oral cancer. **Cancer Res**, v. 68, n. 7, p. 2094-2105, Apr 2008.

KUMAR, M.S. *et al.* Dicer1 functions as a haploinsufficient tumor suppressor. **Genes Dev**, v. 23, n. 23, p. 2700-2704, Dec 2009.

KURZYNSKA-KOKORNIK, A. *et al.* The many faces of Dicer: the complexity of the mechanisms regulating Dicer gene expression and enzyme activities. **Nucleic Acids Res**, v. 43, n. 9, p. 4365-4380, May 2015.

LACOMBE, J., ZENHAUSERN, F. Emergence of miR-34a in radiation therapy. **Crit Rev Oncol Hematol**, v. 109, p. 69-78, Jan 2017.

LAMBERTZ, I. *et al.* Monoallelic but not biallelic loss of Dicer1 promotes tumorigenesis in vivo. **Cell Death Differ**, v. 17, n. 4, p. 633-641, Apr 2010.

LAND, C.E. *et al.* Projected lifetime cancer risks from exposure to regional radioactive fallout in the Marshall Islands. **Health Phys**, v. 99, n. 2, p. 201-215, Aug 2010.

LARSEN, P.R. *et al.* Thyroid physiology and diagnostic evaluation of patients with thyroid disorders. In: KRONENBERG, H.M. *et al.* **Williams Textbook of Endocrinology**. 11. ed. Philadelphia (USA): Saunders Elsevier, 2008. p. 299-332.

LAWRENCE, M.; DAUJAT, S.; SCHNEIDER, R. Lateral Thinking: How Histone Modifications Regulate Gene Expression. **Trends Genet**, v. 32, n. 1, p. 42-56, Jan 2016.

LEEMAN-NEILL, R.J. *et al.* ETV6-NTRK3 is a common chromosomal rearrangement in radiation-associated thyroid cancer. **Cancer**, v. 120, n. 6, p. 799-807, Mar 2014.

LEONE, V. *et al.* A TSH-CREB1-microRNA loop is required for thyroid cell growth. **Mol Endocrinol**, v. 25, n. 10, p. 1819-1830, Oct 2011.

LEPRAT, F. *et al.* Impaired DNA repair as assessed by the "comet" assay in patients with thyroid tumors after a history of radiation therapy: a preliminary study. **Int J Radiat Oncol Biol Phys**, v. 40, n. 5, p. 1019-1026, Mar 1998.

LHAKHANG, T.W.; CHAUDHRY, M.A. Interactome of Radiation-Induced microRNA-Predicted Target Genes. **Comp Funct Genomics**, v. 2012, p. 569731, Jun 2012.

LIMA, J. *et al.* BRAF mutations are not a major event in post-Chernobyl childhood thyroid carcinomas. **J Clin Endocrinol Metab**, v. 89, n. 9, p. 4267-4271, Sep 2004.

LIMA, S.C. *et al.* Identification of a DNA methylome signature of esophageal squamous cell carcinoma and potential epigenetic biomarkers. **Epigenetics**, v. 6, n. 10, p. 1217-1227, Oct 2011.

LITTLE, J.B. Radiation carcinogenesis. **Carcinogenesis**, v. 21, n. 3, p. 397-404, Mar 2000.

LIU, A.; XU, X. MicroRNA isolation from formalin-fixed, paraffin-embedded tissues. **Methods Mol Biol**, v. 724, p. 259-67, Aug 2011.

LIU, C. *et al.* MiR-34a in age and tissue related radio-sensitivity and serum miR-34a as a novel indicator of radiation injury. **Int J Biol Sci**, v. 7, n. 2, p. 221-33, Mar 2011.

LIVOLSI, V.A. Papillary thyroid carcinoma: an update. **Mod Pathol**, v. 2 Suppl, p. S1-9, Apr 2011.

LLOYD, R.V.; BUEHLER, D.; KHANAFSHAR, E. Papillary thyroid carcinoma variants. **Head Neck Pathol**, v. 5, n. 1, p. 51-56, Mar 2011.

LOPEZ, J. *et al.* The context and potential of epigenetics in oncology. **Br J Cancer**, v. 100, n. 4, p. 571-577, Feb 2009.

LU, X. *et al.* The effect of H3K79 dimethylation and H4K20 trimethylation on nucleosome and chromatin structure. **Nat Struct Mol Biol**, v. 15, n. 10, p. 1122-1124, Oct 2008.

LU, Y.J. *et al.* MiR-541-3p reverses cancer progression by directly targeting TGIF2 in non-small cell lung cancer. **Tumour Biol**, v. 37, n. 9, p. 12685-12695, Sep 2016.

MAJIDINIA, M.; YOUSEFI, B. DNA damage response regulation by microRNAs as a therapeutic target in cancer. **DNA Repair (Amst)**, v. 47, p. 1-11, Nov 2016.

MARÉCHAL, A., ZOU, L. DNA damage sensing by the ATM and ATR kinases. **Cold Spring Harb Perspect Biol**, v. 5, n 9, p. a012716, Sep 2013.

MAZZAFERRI, E.L. An overview of the management of papillary and follicular thyroid carcinoma. **Thyroid**, v. 9, n. 5, p. 421-427, May 1999.

METHEETRAIRUT, C.; SLACK, F.J. MicroRNAs in the ionizing radiation response and in radiotherapy. **Curr Opin Genet Dev**, v. 23, n. 1, p. 12-19, Feb 2013.

MIZUNO, T. *et al.* Preferential induction of RET/PTC1 rearrangement by X-ray irradiation. **Oncogene**, v. 19, n. 3, p. 438-443, Jan 2000.

MOLLOY, P.L.; WATT, F. DNA methylation and specific protein-DNA interactions. **Philos Trans R Soc Lond B Biol Sci**, v. 326, n. 1235, p. 267-275, Jan 1990.

MUKHERJEE, S. **O imperador de todos os males: Uma biografia do câncer**. 1. ed. São Paulo: Companhia das Letras, 2012.

MUSKHELISHVILI, L. *et al.* Evaluation of cell proliferation in rat tissues with BrdU, PCNA, Ki-67(MIB-5) immunohistochemistry and in situ hybridization for histone mRNA. **J Histochem Cytochem**, v. 51, n. 12, p. 1681-1688, Dec 2003.

NAN, X. *et al.* Transcriptional repression by the methyl-CpG-binding protein MeCP2 involves a histone deacetylase complex. **Nature**, v. 393, n. 6683, p. 386-389, May 1998.

NASSOUR, J. *et al.* Defective DNA single-strand break repair is responsible for senescence and neoplastic escape of epithelial cells. **Nat Commun**, v. 7, p. 10399, Jan 2016.

NATARAJAN, S. *et al.* HMGA2 inhibits apoptosis through interaction with ATR-CHK1 signaling complex in human cancer cells. **Neoplasia**, v. 15, n. 3, p. 263-280, Mar 2013.

NIKIFOROVA, M.N. *et al.* MicroRNA expression profiling of thyroid tumors: biological significance and diagnostic utility. **J Clin Endocrinol Metab**, v. 93, n. 5, p. 1600-1608, May 2008.

NIKIFOROVA, M.N. *et al.* MicroRNA dysregulation in human thyroid cells following exposure to ionizing radiation. **Thyroid**, v. 21, n. 3, p. 261-6, Mar 2011.

NIKIFOROV, Y.E., NIKIFOROVA, M.N. Molecular genetics and diagnosis of thyroid cancer. **Nat Rev Endocrinol**, v. 7, n. 10, p. 569-80, Aug 2011.

NOSÉ, V. Familial thyroid cancer: a review. **Mod Pathol**, v. 2 Suppl, p. S19-33, Abril 2011.

NUNES, M.T.; UBIRATAN, F.M.; KIMURA, E.T. Fisiologia Endócrina. In: De Mello Aires, M. *et al.* **FISIOLOGIA**. 3. ed. Rio de Janeiro: Guanabara Koogan, 2008. p. 919-91.

NÜSGEN, N. *et al.* Inter-locus as well as intra-locus heterogeneity in LINE-1 promoter methylation in common human cancers suggests selective demethylation pressure at specific CpGs. **Clin Epigenetics**, v. 7, p. 17, Mar 2015.

OKUNO, E.; YOSHIMURA, E. M. **Física das radiações**. 1. ed. São Paulo: Oficina de Textos, 2010.

O'NEILL, J.P.; SHAHA, A.R. Anaplastic thyroid cancer. **Oral Oncol**, v. 49, n. 7, p. 702-706, Jul 2013.

PACINI, F. *et al.* Medullary thyroid carcinoma. **Clin Oncol (R Coll Radiol)**, v. 22, n. 6, p. 475-488, Aug 2010.

PACINI, F. *et al.* Post-Chernobyl thyroid carcinoma in Belarus children and adolescents: comparison with naturally occurring thyroid carcinoma in Italy and France. **J Clin Endocrinol Metab**, v. 82, n. 11, p. 3563-3569, Nov 1997.

PAI, C.C. *et al.* A histone H3K36 chromatin switch coordinates DNA double-strand break repair pathway choice. **Nat Commun**, v. 5, p. 4091, Jun 2014.

PALLANTE, P. *et al.* Deregulation of microRNA expression in follicular-cell-derived human thyroid carcinomas. **Endocr Relat Cancer**, v. 17, n. 1, p. F91-F104, Jan 2010.

PALLANTE, P. *et al.* Deregulation of microRNA expression in thyroid neoplasias. **Nat Rev Endocrinol**, v. 10, n. 2, p. 88-101, Feb 2014.

PARAMESWARAN, R.; BROOKS, S.; SADLER, G.P. Molecular pathogenesis of follicular cell derived thyroid cancers. **Int J Surg**, v. 8, n. 3, p. 186-193, Jan 2010.

PARK, S.Y. *et al.* Alu and LINE-1 hypomethylation is associated with HER2 enriched subtype of breast cancer. **PLoS One**, v. 9, n. 6, p. e100429, Jun 2014.

PASSLER, C. *et al.* Prognostic factors of papillary and follicular thyroid cancer: differences in an iodine-replete endemic goiter region. **Endocr Relat Cancer**, v. 11, n. 1, p. 131-139, Mar 2004.

PELLEGRITI, G. *et al.* Worldwide Increasing Incidence of Thyroid Cancer: Update on Epidemiology and Risk Factors. **J Cancer Epidemiol**, v. 2013, p. 965212, May 2013.

PENG, Y.; CROCE, C.M. The role of MicroRNAs in human cancer. **Signal Transduct Target Ther**, v. 1, p. 15004, Jan 2016.

PENHA, R.C.C. *et al.* Ionizing Radiation Deregulates the MicroRNA Expression Profile in Differentiated Thyroid Cells. **Thyroid**, v. 28, n. 3, p. 407-21, Mar 2018.

PERDAS, E. *et al.* The Role of miRNA in Papillary Thyroid Cancer in the Context of miRNA Let-7 Family. **Int J Mol Sci**, v. 17, n. 6, p. E909, Jun 2016.

QU, C. *et al.* MiR-205 determines the radioresistance of human nasopharyngeal carcinoma by directly targeting PTEN. **Cell Cycle**, v. 11, n. 4, p. 785-796, Feb 2012.

RABES, H.M. *et al.* Pattern of radiation-induced RET and NTRK1 rearrangements in 191 post-Chernobyl papillary thyroid carcinomas: biological, phenotypic, and clinical implications. **Clin Cancer Res**, v. 6, n. 3, p. 1093-103, Mar 2000.

REPPLINGER, D. *et al.* Is Hashimoto's thyroiditis a risk factor for papillary thyroid cancer? **J Surg Res**, v. 150, n. 1, p. 49-52, Nov 2008.

RICARTE-FILHO, J.C. *et al.* Effects of let-7 microRNA on Cell Growth and Differentiation of Papillary Thyroid Cancer. **Transl Oncol**, v. 2, n. 4, p. 236-241, Dec 2009.

RICARTE-FILHO, J.C. *et al.* Identification of kinase fusion oncogenes in post-Chernobyl radiation-induced thyroid cancers. **J Clin Invest**, v. 123, n. 11, p. 4935-44, Nov 2013.

RODRIGUEZ, W. *et al.* Deletion of the RNaseIII enzyme dicer in thyroid follicular cells causes hypothyroidism with signs of neoplastic alterations. **PLoS One**, v. 7, n. 1, p. e29929, Jan 2012.

ROMAN, S.; LIN, R.; SOSA, J.A. Prognosis of medullary thyroid carcinoma: demographic, clinical, and pathologic predictors of survival in 1252 cases. **Cancer**, v. 107, n. 9, p. 2134-2142, Nov 2006.

RON, E. *et al.* Thyroid cancer after exposure to external radiation: a pooled analysis of seven studies. **Radiat Res**, v. 141, n. 3, p. 259-277, Mar 1995.

ROSSING, M.A.; SCHWARTZ, S.M.; WEISS, N.S. Thyroid cancer incidence in Asian migrants to the United States and their descendants. **Cancer Causes Control**, v. 6, n. 5, p. 439-444, Sep 1995.

ROY, M.; CHEN, H.; SIPPEL, R.S. Current understanding and management of medullary thyroid cancer. **Oncologist**, v. 18, n. 10, p. 1093-1100, Oct 2013.

RUDQVIST, N. *et al.* Dose-specific transcriptional responses in thyroid tissue in mice after (131)I administration. **Nucl Med Biol**, v. 42, n. 3, p. 263-268, Mar 2015.

RUEDA, A. *et al.* sRNAtoolbox: an integrated collection of small RNA research tools. **Nucleic Acids Res**, v. 43, n. 1, p. 467-473, Jul 2015.

RUEGEMER, J.J. *et al.* Distant metastases in differentiated thyroid carcinoma: a multivariate analysis of prognostic variables. **J Clin Endocrinol Metab**, v. 67, n. 3, p. 501-508, Sep 1988.

SAISELET, M. *et al.* Thyroid cancer cell lines: an overview. **Front Endocrinol (Lausanne)**, v. 3, p. 133, Nov 2012.

SALZMAN, D.W. *et al.* miR-34 activity is modulated through 5'-end phosphorylation in response to DNA damage. **Nat Commun**, v. 7, p. 10954, Mar 2016.

SANTARPIA, L.; NICOLOSO, M.; CALIN, G.A. MicroRNAs: a complex regulatory network drives the acquisition of malignant cell phenotype. **Endocr Relat Cancer**, v. 17, n. 1, p. F51-F75, Jan 2010.

SANTORO, M.; CARLOMAGNO, F. Central role of RET in thyroid cancer. **Cold Spring Harb Perspect Biol**, v. 5, n. 12, p. a009233, Dec 2013.

SARASIN, A. *et al.* Mechanisms of mutagenesis in mammalian cells. Application to human thyroid tumours. **Comptes Rendus de L'Academie des Sciences III**, v. 322, n. 2-3, p. 143-149, Feb 1999.

SCHMIDBAUER, B. *et al.* Differentiated Thyroid Cancer-Treatment: State of the Art. **Int J Mol Sci**, v. 18, n. 6, p. E1292, Jun 2017.

SCHONFELD, S.J. *et al.* Medical exposure to radiation and thyroid cancer. **Clin Oncol (R Coll Radiol)**, v. 23, n. 4, p. 244-250, May 2011.

SEO, D. *et al.* Evaluation based on Monte Carlo simulation of lifetime attributable risk of cancer after neck X-ray radiography. **Radiol Med**, v. 120, n. 11, p. 1043-1049, Nov 2015.

SHI, R.L. *et al.* The Trend of Age-Group Effect on Prognosis in Differentiated Thyroid Cancer. **Sci Rep**, v. 6, p. 27086, Jun 2016.

SHILOH, Y. ATM and related protein kinases: safeguarding genome integrity. **Nat Rev Cancer**, v. 3, n. 3, p. 155-168, Mar 2003.

SCHMITTGEN, T.D., LIVAK, K.J. Analyzing real-time PCR data by the comparative C(T) method. **Nat Protoc**, v. 3, n. 6, p. 1101-1108, 2008.

SLADE, I. *et al.* DICER1 syndrome: clarifying the diagnosis, clinical features and management implications of a pleiotropic tumour predisposition syndrome. **J Med Genet**, v. 48, n. 4, p. 273-278, Apr 2011.

SLAVOTINEK, A., MCMILLAN, T.J., STEEL, C.M. Measurement of radiation survival using the MTT assay. **Eur J Cancer**, v. 30, n. 9, p. 1376-1382, 1994.

SMITH, J.A. *et al.* Methylation status of genes in papillary thyroid carcinoma. **Arch Otolaryngol Head Neck Surg**, v. 133, n. 10, p. 1006-1011, Oct 2007.

SMITH, J.A. *et al.* Methylation status of genes in papillary thyroid carcinoma. **Arch Otolaryngol Head Neck Surg**, v. 133, n. 10, p. 1006-1011, Oct 2007.

SOBRINHO-SIMÕES, M. *et al.* Follicular thyroid carcinoma. **Mod Pathol**, v. 2 Suppl, p. S10-18, Apr 2011.

SONG, Y. *et al.* Roles of hydrogen peroxide in thyroid physiology and disease. **J Clin Endocrinol Metab**, v. 92, n. 10, p. 3764-73, Oct 2007.

SPIZZO, R. *et al.* SnapShot: MicroRNAs in Cancer. **Cell**, v. 137, n. 3, p. 586, May 2009.

STRATTON, M.R.; CAMPBELL, P.J.; FUTREAL, P.A. The cancer genome. **Nature**, v. 458, n. 7239, p. 719-724, Apr 2009.

SU, Y.P. *et al.* Radiation dose in the thyroid and the thyroid cancer risk attributable to CT scans for pediatric patients in one general hospital of China. **Int J Environ Res Public Health**, v. 11, n. 3, p. 2793-2803, Mar 2014.

SUGITANI, I. *et al.* Prognostic factors and treatment outcomes for anaplastic thyroid carcinoma: ATC Research Consortium of Japan cohort study of 677 patients. **World J Surg**, v. 36, n. 6, p. 1247-1254, Jun 2012.

SUGITANI, I.; FUJIMOTO, Y.; YAMAMOTO, N. Papillary thyroid carcinoma with distant metastases: survival predictors and the importance of local control. **Surgery**, v. 143, n. 1, p. 35-42, Jan 2008.

SUZUKI, K.; YAMASHITA, S. Low-dose radiation exposure and carcinogenesis. **Jpn J Clin Oncol**, v. 42, n. 7, p. 563-568, Jul 2012.

TAKANO, T. Fetal cell carcinogenesis of the thyroid: a modified theory based on recent evidence. **Endocr J**, v. 61, n. 4, p. 311-320, Feb 2014.

TAKANO, T.; AMINO, N. Fetal cell carcinogenesis: a new hypothesis for better understanding of thyroid carcinoma. **Thyroid**, v. 15, n. 5, p. 432-438, Maio 2005.

TANG, K. F., REN, H. The Role of Dicer in DNA Damage Repair. **Int J Mol Sci**, v. 12, n. 12, p. 16769–16778, Dec 2012.

TARAZONA, S. *et al.* Differential expression in RNA-seq: a matter of depth. **Genome Res**, v. 21, n. 12, p. 2213-2223, Dec 2011.

TRONKO, M. *et al.* Radiation induced thyroid cancer: fundamental and applied aspects. **Exp Oncol**, v. 32, n. 3, p. 200-204, Sep 2010.

TRUONG, T. *et al.* Role of dietary iodine and cruciferous vegetables in thyroid cancer: a countrywide case-control study in New Caledonia. **Cancer Causes Control**, v. 21, n. 8, p. 1183-1192, Aug 2010.

TUMURKHUU, G. *et al.* Ogg1-Dependent DNA Repair Regulates NLRP3 Inflammasome and Prevents Atherosclerosis. **Circ Res**, v. 119, n. 6, p. 76-90, Sep 2016.

TUTTLE, R.M.; HAUGEN, B.; PERRIER, N.D. Updated American Joint Committee on Cancer/Tumor-Node-Metastasis Staging System for Differentiated and Anaplastic Thyroid Cancer (Eighth Edition): What Changed and Why? **Thyroid**, v. 27, n. 6, p. 751-56, Jun 2017.

UGOLIN, N. *et al.* Strategy to find molecular signatures in a small series of rare cancers: validation for radiation-induced breast and thyroid tumors. **PLoS One**, v. 6, n. 8, p. e23581, Aug 2011.

UNITED NATIONS SCIENTIFIC COMMITTEE ON THE EFFECTS OF ATOMIC RADIATION (UNSCEAR). Sources, Effects and Risks of Ionizing Radiation. **UNSCEAR Report**, 2016.

VEIGA, L.H. *et al.* Thyroid Cancer after Childhood Exposure to External Radiation: An Updated Pooled Analysis of 12 Studies. **Radiat Res**, v. 185, n. 5, p. 473-84, Apr 2016.

VISONE, R. *et al.* Specific microRNAs are downregulated in human thyroid anaplastic carcinomas. **Oncogene**, v. 26, n. 54, p. 7590-7595, Nov 2007.

VLACHOS, I.S. *et al.* DIANA-miRPath v3.0: deciphering microRNA function with experimental support. **Nucleic Acids Res**, v. 43, n. 1, p. 460-466, Jul 2015.

WAHID, F. *et al.* MicroRNAs: synthesis, mechanism, function, and recent clinical trials. **Biochim Biophys Acta**, v. 1803, n. 11, p. 1231-1243, Nov 2010.

WARD, J.F. DNA damage as the cause of ionizing radiation-induced gene activation. **Radiat Res**, v. 138, n. 1 Suppl, p. S85-88, Apr 1994.

WATANABE, R. *et al.* Possible involvement of BRAFV600E in altered gene expression in papillary thyroid cancer. **Endocr J**, v. 56, n. 3, p. 407-14, Feb 2009.

WEBER, M.; SCHÜBELER, D. Genomic patterns of DNA methylation: targets and function of an epigenetic mark. **Curr Opin Cell Biol**, v. 19, n. 3, p. 273-280, Jun 2007.

WEI, W. *et al.* A role for small RNAs in DNA double-strand break repair. **Cell**, v. 149, n. 1, p. 101-112, Mar 2012.

WEIDMAN, J.R. *et al.* Cancer susceptibility: epigenetic manifestation of environmental exposures. **Cancer**, v. 13, n. 1, p. 9-16, Jan 2007.

WETERINGS, E.; CHEN, D.J. DNA-dependent protein kinase in nonhomologous end joining: a lock with multiple keys? **J Cell Biol**, v. 179, n. 2, p. 183-186, Oct 2007.

WHO. Latest global cancer data: Cancer burden rises to 18.1 million new cases and 9.6 million cancer deaths in 2018. **World Health Organization**, 2018.

WILLERS, H.; HELD, K.D. Introduction to clinical radiation biology. **Hematol Oncol Clin North Am**, v. 20, n. 1, p. 1-24, Feb 2006.

XING, M. *et al.* Early occurrence of RASSF1A hypermethylation and its mutual exclusion with BRAF mutation in thyroid tumorigenesis. **Cancer Res**, v. 64, n. 5, p. 1664-1668, Mar 2004.

XING, M. Genetic alterations in the phosphatidylinositol-3 kinase/Akt pathway in thyroid cancer. **Thyroid**, v. 20, n. 7, p. 697-706, Jul 2010.

YAMASHITA, S. *et al.* Lessons from Fukushima: Latest Findings of Thyroid Cancer After the Fukushima Nuclear Power Plant Accident. **Thyroid**, v. 28, n. 1, p. 11-22, Jan 2018.

YAN, S.; SORRELL, M.; BERMAN, Z. Functional interplay between ATM/ATR-mediated DNA damage response and DNA repair pathways in oxidative stress. **Cell Mol Life Sci**, v. 71, n. 20, p. 3951-3967, Oct 2014.

YE, J. *et al.* Primer-BLAST: a tool to design target-specific primers for polymerase chain reaction. **BMC Bioinformatics**, v. 13, p. 134, Jun 2012.

YE, Y. *et al.* Induced MiR-1249 expression by aberrant activation of Hedgehog signaling pathway in hepatocellular carcinoma. **Exp Cell Res**, v. 355, v. 1, p. 9-17, Jun 2017.

YOO, S.K. *et al.* Comprehensive Analysis of the Transcriptional and Mutational Landscape of Follicular and Papillary Thyroid Cancers. **PLoS Genet**, v. 12, n. 8, p. e1006239, Aug 2016.

YOSHIHARA, K. *et al.* The landscape and therapeutic relevance of cancer-associated transcript fusions. **Oncogene**, v. 34, n. 37, p. 4845-54, Sep 2015.

ZHANG, P. *et al.* MiR-205 acts as a tumour radiosensitizer by targeting ZEB1 and Ubc13. **Nat Commun**, v. 5, p. 5671, Dec 2014.

ZHANG, Y. *et al.* Regulation of autophagy by miR-30d impacts sensitivity of anaplastic thyroid carcinoma to cisplatin. **Biochem Pharmacol**, v. 87, n. 4, p. 562-570, Feb 2014.

ZHAO, H. *et al.* Down-regulation of Dicer expression in cervical cancer tissues. **Med Oncol**, v. 31, n. 5, p. 937, May 2014.

ZHEN, L. *et al.* MiR-10b decreases sensitivity of glioblastoma cells to radiation by targeting AKT. **J Biol Res (Thessalon)**, v. 23, p. 14, Jun 2016.

ZIMMERMANN, M.B.; GALETTI, V. Iodine intake as a risk factor for thyroid cancer: a comprehensive review of animal and human studies. **Thyroid Res**, v. 8, p. 8, Jun 2015.

ZINDY, F. *et al.* Dicer Is Required for Normal Cerebellar Development and to Restrain Medulloblastoma Formation. **PLoS One**, v. 10, n. 6, p. e0129642, Jun 2015.

8 ANEXOS

8.1 ANEXO I- REVISÃO SISTEMÁTICA SOBRE RADIAÇÃO IONIZANTE

PAJAR 2015 volume 3 number 1 pages 29-35
<http://revistaseletronicas.pucrio.br/ojs/index.php/pajar/>

Pontifical Catholic University of Rio Grande do Sul
Institute of Geriatrics and Gerontology
Biomedical Gerontology Graduate Program

 <http://dx.doi.org/10.15448/2357-9641.2015.1.21138>



REVIEW ARTICLE

Open Access

Radiation-induced senescence and thyroid cancer: a barrier or a driving force

*Senescência e câncer de tireóide induzido por radiação:
uma barreira ou uma força motriz*

Ricardo Cortez Cardoso Penha^a, Sheila Coelho Soares Lima^b,
Luis Felipe Ribeiro Pinto^c, Alfredo Fusco^d

^a Instituto Nacional de Câncer – INCA, Rio de Janeiro, RJ, Brazil. <ricardocortezcardoso@gmail.com>.

^b Instituto Nacional de Câncer – INCA, Rio de Janeiro, RJ, Brazil. <sheilacoelho@gmail.com>.

^c Instituto Nacional de Câncer – INCA, Rio de Janeiro, RJ, Brazil. <lfrpinto@inca.gov.br>.

^d Instituto Nacional de Câncer – INCA, Rio de Janeiro, RJ, Brazil. Istituto di Endocrinologia ed Oncologia Sperimentale del CNR c/o Dipartimento di Medicina Molecolare e Biotechnologie Mediche, Università degli Studi di Napoli "Federico II", Napoli, Italy. <alfusco@unina.it>.

ARTICLE INFO

Article history

Received: 24/06/2015

Accepted: 12/10/2015

Correspondent Author

Alfredo Fusco

Istituto di Endocrinologia e Oncologia
Sperimentale del CNR
Dipartimento di Medicina Molecolare e
Biotechnologie Mediche
Università degli Studi di Napoli "Federico II"
Via Sergio Pansini, 5
80131 Napoli, Italy
<alfusco@unina.it>

© 2015 All rights reserved

Editors

Alfredo Cataldo Neto
Irenio Gomes

ABSTRACT

Aims: The main goal of this review-article was to shed light on the impact of senescence on thyroid carcinogenesis, a promising but still neglected field. **Source of data:** PubMed database and Google Scholar search was performed for English language articles with terms: ionizing radiation exposure, thyroid cancer, radiation signature, RET/PTC, senescence and radiation-induced senescence. We have no date restrictions. **Summary of findings:** Ionizing radiation (IR) is undoubtedly the most well-characterized risk factor for thyroid cancer of the papillary histotype and its pivotal role as senescence inducer has been proposed. A paradoxical role of senescence on carcinogenesis – a barrier to cancer cell proliferation in early steps and a driving force to cancer progression by secreting proinflammatory cytokines and matrix degrading enzymes – is the heart of the matter of age-related cancer and bring to light new insights to thyroid cancer research field. This review-article briefly points out the major findings that link ionizing radiation to thyroid carcinogenesis, highlighting the molecular alterations mediated by acute and chronic radiation exposure in thyroid cells. **Conclusions:** Evidences provided by our group and other few reports suggest that, like other oncogenic stimuli in different cell types, IR induces a senescent phenotype in thyroid cells, what could represent an initial barrier to transformation. However, how senescence could contribute to tumor progression still remains elusive. The comprehension of these mechanisms could not only help elucidating thyroid cancer initiation and progression, but could also indicate new therapeutical targets.

KEYWORDS: Ionizing radiation; Thyroid cancer; Senescence; DNA damage; RET/PTC.

RESUMO

Objetivos: O principal objetivo deste artigo de revisão foi lançar luz sobre o impacto da senescência na carcinogênese da tireoide, um campo promissor, mas ainda negligenciado. **Fonte dos dados:** pesquisa nos bancos de dados PubMed e Google Scholar realizada para artigos em inglês com os termos: exposição à radiação ionizante, câncer de tireoide, radiação assinatura, RET/PTC, senescência e senescência induzida por radiação. Não houve restrições quanto a data. **Resumo das constatações:** radiação ionizante (IR) é, sem dúvida, o fator de risco mais bem caracterizado para o câncer de tireoide de histotipo papilar e seu papel central como indutor de senescência tem sido proposto. Um papel paradoxal da senescência na carcinogênese – uma barreira a proliferação celular cancerígena em etapas precoces e uma força motriz para a progressão do câncer através de secreção de citocinas pró-inflamatórias e enzimas matriz degradantes – é o foco principal sobre o câncer relacionado à idade e trazem à vida novos insights para a investigação do câncer de tireoide. Este artigo de revisão mostra brevemente as principais conclusões que apontam a radiação ionizante à carcinogênese de tireoide, destacando as alterações moleculares mediadas pela exposição aguda e crônica à radiação em células da tireoide. **Conclusões:** Evidências fornecidas por nosso grupo e outros poucos relatos sugerem que, tal como outros estímulos oncogênicos em diferentes tipos de células, IR induz um fenótipo senescente em células da tireoide, o que poderia representar uma barreira inicial a transformação. No entanto, como a senescência poderia contribuir para a progressão do tumor ainda permanece indefinida. A compreensão destes mecanismos não só poderia ajudar a elucidar a iniciação e progressão do câncer de tireoide, mas também pode indicar novos alvos terapêuticos.

DESCRIPTORIOS: Radiação ionizante; Câncer de tireoide; Senescência; Danos no ADN; RET/PTC.



This work is licensed under a Creative Commons – Attribution 4.0 International.
<http://creativecommons.org/licenses/by/4.0/>

THYROID CANCER AND IONIZING RADIATION

Thyroid cancer is one of the most common endocrine-related neoplasia.¹ Its incidence rates have been continuously growing among developed countries, and also in developing countries, which includes Brazil, where 9,200 new cases are estimated in 2014,² mainly due to the increase in papillary thyroid carcinoma (PTC) (Cramer et al. 2010) and the availability of diagnostic tools. The vast majority of differentiated thyroid carcinomas are PTC (80%),³ that in almost all the cases retain the ability to uptake iodine and express differentiation markers, as thyroglobulin, essentials for thyroid normal function.⁴ Therefore, most PTC are highly curable and have good prognosis with an overall 5-year relative survival rate of about 90%.⁵

Ionizing radiation (IR) is a well-established risk factor for thyroid cancer.⁵ This finding was reinforced by Ron et al. (1995)⁶ that performed a pooled analysis based on several reports and observed an increase in thyroid tumor rates, mostly PTC, in populations exposed to IR – atomic bomb survivors in Japan (1945) and patients irradiated during childhood for tonsil, tinea capitis, and cancer – and found a 7.7 excess relative risk per Gy (ERR/Gy) through linear dose-response models, previously applied to a Japanese A-bomb survivors life span study. In addition to that, nuclear test detonations in Marshall islands (1946-1958) significantly contributed to higher thyroid cancer rates in populations living around the archipelago (cumulative 0.1-10 Gy thyroid mean radiation dose).⁷ Above all, these data highlighted that thyroid is more susceptible to the carcinogenic action of IR during childhood, especially in infants up to 5 years old, observed after Chernobyl accident (1987).^{8,9} Currently, the main sources of radiation exposure are medical procedures (20%, 0.62 mSv) and environmental (80%, 2.4 mSv).¹⁰

MOLECULAR MECHANISMS UNDERLYING RADIATION-RELATED THYROID CARCINOMAS

Radiation-related carcinogenesis could be attributed to DNA base damages (3,000/Gy), DNA single strand breaks (1,000/Gy) and to a larger extent, DNA double strand breaks (DSB) (40/Gy),^{11,12} that might lead to mutations, deletions and chromosomal rearrangements.¹³ DSB formation is particularly associated to chromosomal rearrangements involved in PTC induction.^{4,14}

Sporadic or radiation-related PTC have distinct molecular etiology and radiation seems to confer a specific gene expression signature to thyroid carcinomas.¹⁵ Post-Chernobyl childhood PTC have higher frequency of RET/PTC1 and RET/PTC3 (50-90%) than PTC cases with no radiation-exposure background (13-43%).^{4,16,17} In fact, gamma-radiation exposure can induce RET rearrangements in a dose-dependent manner in human thyroid cells.¹⁴ RET/PTC, which is a fusion product of RET tyrosine kinase domain sequence with heterologous genes, was originally demonstrated in PTC DNA extracted samples, with transforming activity.¹⁸ Sporadic PTC harbor BRAF_{V600E} mutation (46% vs. 12%)¹⁹ while chromosomal translocation AKAP9-BRAF occurs in radiation-related PTC (11% vs. 1%).²⁰ Thus, these data revealed that MAPK pathway activation plays an important role in thyroid carcinogenesis, regardless of specific known driver mutations or rearrangements. Apart from that, radiation-induced PTC behave aggressively (extrathyroid and lymph node extensions) when compared to sporadic PTC.⁸ Indeed, radiation-related PTC expressed higher protein levels of matrix metalloproteinases (MMP-1, MMP-9, MMP13), often correlated to tumor aggressiveness.²¹

ACUTE EFFECTS OF IONIZATION RADIATION ON THYROID CELLS

In this review, acute effects are defined as the phenotype following hours or few days after single radiation dose exposure. Radiation responses vary according to tissue or cell type, dose and time. Abou-El-Ardat et al. (2012)²² reported that RET/PTC-positive thyroid cell line (TPC-1), derived from PTC, and normal thyroid cells distinctly respond to radiation. At low dose (62 mGy), X-ray enhanced normal thyroid cells proliferation and the opposite effect was observed in RET/PTC-positive cells. At high doses (0.5, 4 Gy), the latter activated P53 pathway while the former triggered TGFβ. In accordance to that, TGFβ and SMAD (canonical TGFβ pathway) were also regulated in normal thyroid gland after ¹³¹I administration in mice²³ and the profound diversity of biological responses to radiation doses were also recapitulated *in vivo*. So far, the main limitations of these models are: 1) the lack of temporal points; 2) most of the approaches have been conducted in immortalized cells; 3) Species-specific molecular alterations in response to radiation (i.e, RET/PTC only detected in humans). Accordingly, Mizuno et al. (1997)²⁴ proposed a new model to investigate radiation effects that basically consists of

human thyroid tissue engraftment into severe combined immunodeficiency (scid) mice. This model allowed subsequent studies to elucidate the properties and role of RET/PTC on thyroid carcinogenesis in humans. Gandhi and Nikiforov (2011)²⁵ brought to life that rodents and humans do not share common nuclear architecture. The authors demonstrated that RET and fusion genes have spatial positioning differences between both species, which might explain the absence of human RET/PTC orthologs in rodents. Mizuno et al. (2000)²⁶ also revealed that X-ray induces RET/PTC1 rather than RET/PTC3, in a time and dose-dependent manner.

CHRONIC EFFECTS OF IONIZING RADIATION ON THYROID CELLS

Herein, chronic effects are defined as the consequences of radiation exposure after a short or long period. First, chronic low (≤ 100 mSv) and high doses (>100 mSv)¹⁰ have different impacts on thyroid cells. Concerning low doses, linear-non-threshold (LNT) model – assumes that cancer risk is linearly proportional to radiation dose – fails to predict risks for cancer incidence due to its fluctuations in low radiation doses, which limit statistical significance^{27,28}. However, LNT optimization using Monte Carlo method – computational algorithm based on mathematical probability that calculates the organ and effective doses from interactions due to the Compton effect in the human body – indicated that, after cervical X-ray, effective dose of thyroid is 1.48 mSv, and that, even minor doses potentially increase lifetime risk for developing thyroid cancer.²⁹ Based on these findings, one aspect to consider is the worldwide increase in medical radiation exposure³⁰ and the influence of these low-doses in radiosensitive organs as thyroid. Several studies successfully correlated number and radiation dose of CT Scans for infants and adolescents to a greater thyroid cancer risk,^{29,31,32} especially in females. Another relevant question is whether genetic alterations could predispose to radiation carcinogenic actions. Missense single nucleotide polymorphisms (SNP) of DNA damage response genes (*ATM* and *TP53*) were specifically associated to an increased thyroid cancer risk in sporadic and radiation-related PTC.³³ Moreover, post-Chernobyl PTC cases often carry a SNP in the DNA repair gene *XRCC1* that potentially conferred a greater risk for thyroid cancer.³⁴ Until now, literature is sparse about low-dose radiation. For example, acute exposure to 100 mSv induces four DSB per cell while chronic exposure to 100 mSv during the year promotes one DSB in one cell

of 2400 cells per hour (Suzuki and Yamashita, 2012), so that further studies are necessary to understand its biological relevance.

Concerning chronic doses > 100 mSv, extensive data are available on literature. The vast majority of clinical and epidemiological studies are addressed above and most of them fitted LNT model to explain lifetime risk to thyroid cancer. A classic example of chronic radiation exposure is observed in population nearby Marshall islands that although nuclear test ceased in 1958, they were chronically affected by radiation due to fallout deposited on the ground until 1970, which reflected in one of the greatest female thyroid cancer rates in the world, 19.28 per 100,000 per year, age-adjusted.⁷

SENESCENCE AND THYROID CELLS

The concept that “cell division is not everlasting but finite” was originally proposed by the German August Weismann.³⁵ After 80 years, Leonard Hayflick and Paul Moorhead (1961)³⁶ revisited this concept and published the timeless work in which they fully characterized that normal human cell strains have finite replicative capacity and suggested that this phenomenon as ageing at cellular level or, more precisely, senescence. Later on, researchers established that normal human cells telomeres shorten as they reached Hayflick limit,³⁷ replicative senescence, and it might determinate cell longevity.³⁸

Senescent cells are mainly characterized by morphological and molecular features.³⁹ During senescence, cells undergo multiple changes that distinguish them from quiescent or terminal differentiated cells: 1) morphology: flattened, elongated and enlarged cell shape; 2) metabolism: display high lysosomal β -D-galactosidase activity at pH 6 due to increased numbers of lysosomes; 3) chromatin organization: irreversible RB-dependent heterochromatin structures, named as Senescence-Associated Heterochromatin Foci (SAHF); 4) The senescence-associated secretory phenotype (SASP): proinflammatory cytokines, chemokines and extracellular matrix metalloproteinases; 5) cell cycle arrest in early G1 mediated by p53, p21 and p16.

The paradoxical behavior of senescent cells in tumorigenesis is still an enigma to be clarified. The concept of senescence providing a barrier to cell proliferation is well-accepted, although its contribution on different stages of carcinogenesis is yet to be elucidated. The key to understand this phenomenon rely on the crosstalk between the stromal and tumor cells, and how SASP might originate an altered micro-environment that promotes tumor progression.⁴⁰

However, these questions remain unanswered for thyroid carcinoma.

Senescence itself is not necessarily induced by the physical presence of shortened telomeres or DSB in eroded telomeres, but rather as a result of the signaling pathways triggered in response to them.⁴¹ In fact, stress-inducible senescence, which encompasses oncogene activation and exogenous stimuli (i.e., ionizing radiation), often occurs in a telomere-independent manner. The first strong evidence came from Serrano et al. (1997)⁴² in which RAS activation promoted permanent arrest in early G1 mediated by p53 and p16, a senescence-like phenotype. Similar results were obtained in primary thyrocytes, in which the proinflammatory cytokine

IL-8 and its receptor CXCR2 support growth arrest triggered by oncogenic RAS, in agreement with the notion that senescence is intrinsically associated with inflammation.⁴³ Recently, Cisowski et al. (2015)⁴⁴ demonstrated that RAS and BRAF_{V600E} coactivation in early carcinogenesis induced senescence in lung cancer cells, leading to a negative clonal selection, which might be a plausible explanation for the reason why mutated RAS and BRAF_{V600E} are mutually exclusive in thyroid carcinoma.

Radiation plays a pleotropic role in cellular biological process. Several works proposed IR as a senescence inducer in human diploid cells through P53 activation without telomere shortening.⁴⁵⁻⁴⁷ In thyroid context, to our knowledge, one article

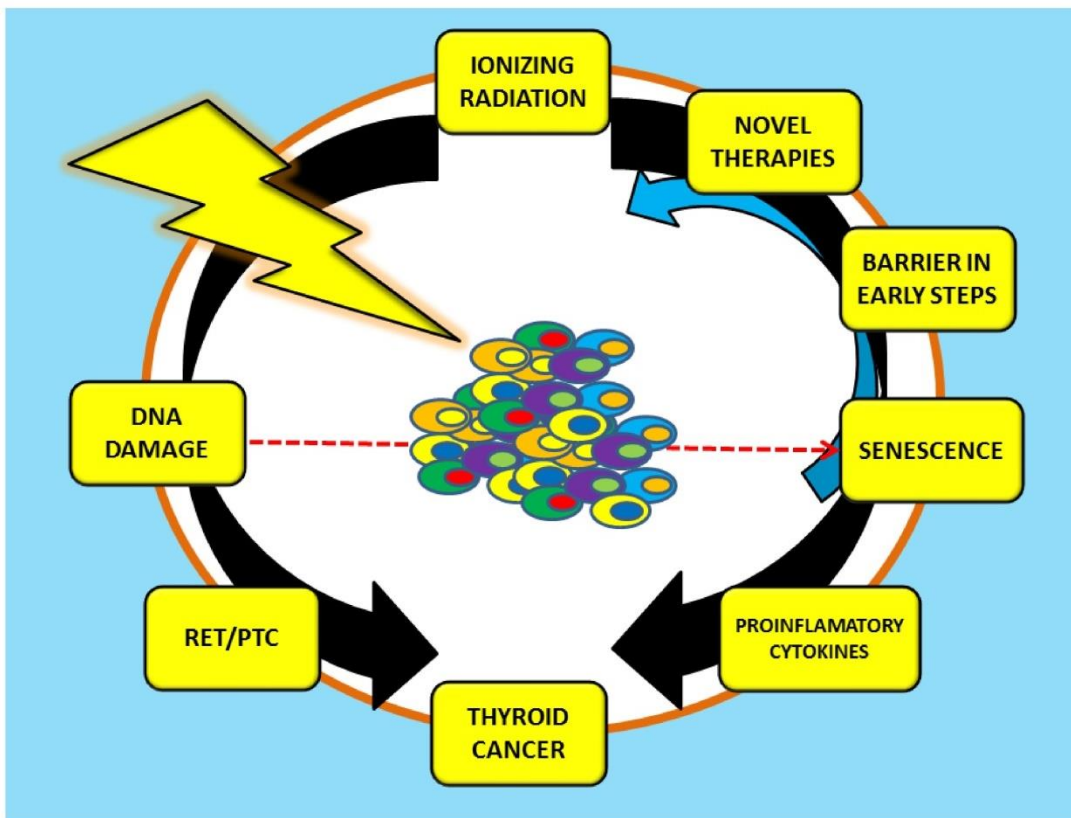


Figure 1. Schematic physical thyroid carcinogenesis overview. Ionizing radiation induces DNA damages, especially DNA double-strand breaks, often correlated to RET/PTC generation. RET/PTC oncogenic activity leads normal follicular cells to acquire malignant phenotype (anticlockwise black arrow; pro-oncogenic pathway). Ionizing radiation could also induce premature senescence that represents a barrier to cancer cells in early steps of thyroid carcinogenesis (anticlockwise blue arrow; anti-oncogenic pathway) and/or promotes senescence-associated secretory phenotype and releasing of proinflammatory cytokines (i.e., IL-8), that contribute to cancer progression (clockwise black arrow; pro-oncogenic pathway). Rather than DNA damages, signaling pathways triggered in response to them induce senescence (dashed red line; crosstalk).

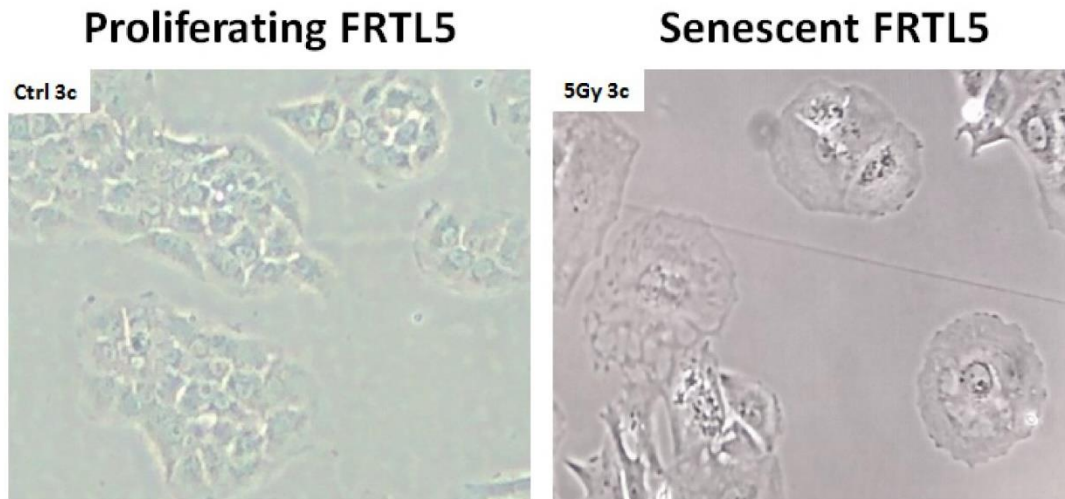


Figure 2. X-ray promotes senescence in normal thyroid cells (FRTL5). Normal rat thyroid cell line (FRTL5) was chronically exposed to X-ray, 3 cycles of 5 Gy, with an accumulative radiation dose of 15 Gy and senescence morphology was observed in irradiated cells: flattened, elongated and enlarged cell shape. CTRL 3c = non-exposed cells; 5Gy 3c = irradiated cells after an accumulative radiation dose (15 Gy).

reported that radiation induced premature senescence in synergism with thyroid hormone receptor beta,⁴⁸ a suppressor gene proposed as a novel inducer of cellular senescence in thyroid cells.⁴⁹ Thus, one of our research interests is to investigate the parallel between thyroid carcinogenesis and premature senescence related to ionizing radiation, focusing on the turning point in which radiation might lead a normal thyroid cell to gain proliferative advantages among surrounding cells in early thyroid carcinogenesis or senescence. To this end, the normal rat thyroid FRTL5 cell line were chronically exposed to X-ray, based on the mean radiation dose (25 Gy) for childhood cancer treatment⁶ and senescence morphology were observed after three cycles of 5 Gy (Figure 2) (*unpublished data*). Once the senescence model was established, the future steps consist of full molecular characterization of each time point in order to identify molecular alterations that might guide us to a better understanding of thyroid carcinogenesis.

CONCLUSIONS

DNA damage induced by ionizing radiation could lead normal thyroid cells to acquire a malignant phenotype, mediated by oncogenic activity of RET/PTC-MAPK pathway. Dose and time of radiation

exposure dictates different molecular responses and, as a matter of fact, only a full characterization of the molecular alterations will bring light to the genesis of thyroid cancer. LNT model fits high acute or chronic radiation doses to explain lifetime attributable risk for thyroid cancer while LNT model combined with Monte Carlo simulations predict low doses exposure. Pathways triggered by unrepaired DNA damage rather than damage itself activate senescence that act as a barrier to cancer progression. Taking into account the irreversible state of senescence, novel therapy-induced senescence is a promising approach that might induce a persistent growth inhibitory response in both early- and late steps of carcinogenesis while reducing toxicity,⁵⁰ and thus, could be an alternative treatment to iodine-refractory thyroid tumors.

ACKNOWLEDGMENTS

The study was supported by P.O.R. Campania FSE 2007-2013, CUP B25B09000050007, PNR-CNR Aging “Program 2012-2014” and Grant IG-11477 from the Associazione Italiana Ricerca sul Cancro (AIRC – Italy). AF was granted with a Special Visiting Researcher (PVE) fellowship sponsored by CAPES.

REFERENCES

1. DeLellis RA, Lloyd RV, Heitz PU. World Health Organization Classification of Tumours. Pathology and Genetics of Tumours of Endocrine Organs. IARC Press: Lyon (France); 2004.
2. Instituto Nacional do Câncer (INCA). Estimativa 2014 de Incidência de Câncer no Brasil. Rio de Janeiro (Brazil): INCA; 2014.
3. Albores-Saavedra J, Henson DE, Glazer E, et al. Changing patterns in the incidence and survival of thyroid cancer with follicular phenotype-papillary, follicular, and anaplastic: a morphological and epidemiological study. *Endocr Pathol.* 2007;18:1-7.
4. Kondo T, Ezzat S, Asa SL. Pathogenetic mechanisms in thyroid follicular-cell neoplasia. *Nat Rev Cancer* 2006;6: 292-306.
5. American Cancer Society. Cancer Facts & Figures 2014. Atlanta (US): American Cancer Society; 2014.
6. Ron E, Lubin JH, Shore RE, et al. Thyroid Cancer after Exposure to External Radiation: A Pooled Analysis of Seven Studies. *Radiat. Res.* 1995;141:259-277.
7. Land CE, Bouville A, Apostoaei I, et al. Projected lifetime cancer risks from exposure to regional radioactive fallout in the Marshall Islands. *Health Phys.* 2010;99:201-15.
8. Pacini F, Vorontsova T, Demidchik EP, et al. Post-Chernobyl thyroid carcinoma in Belarus children and adolescents: comparison with naturally occurring thyroid carcinoma in Italy and France. *J Clin Endocrinol Metab.* 1997;82:3563-9.
9. Cardis E, Howe G, Ron E, et al. Cancer consequences of the Chernobyl accident: 20 years on. *J Radiol Prot.* 2006;26: 127-40.
10. United Nations Scientific Committee on the Effects of Atomic Radiation (UNSCEAR). Sources and effects of ionizing radiation. New York (US): 2008 Report; Sales No. E.10.XI.3.
11. Ward J. DNA damage as the cause of ionizing radiation-induced gene activation. *Radiat. Res.* 1994;138:S85-S88.
12. Sarasin A, Bounacer A, Lepage F, et al. Mechanisms of mutagenesis in mammalian cells. Application to human thyroid tumours. *C R Acad Sci III.* 1999;322:143-9.
13. Little JB. Radiation carcinogenesis. *Carcinogenesis.* 2000; 21:397-404.
14. Caudill CM, Zhu Z, Ciampi R, et al. Dose-dependent generation of RET/PTC in human thyroid cells after in vitro exposure to γ -radiation: a model of carcinogenic chromosomal rearrangement induced by ionizing radiation. *J Clin Endocrinol Metab* 2005;90:2364-9.
15. Port M, Boltze C, Wang Y, et al. A radiation-induced gene signature distinguishes post-Chernobyl from sporadic papillary thyroid cancers. *Radiat Res.* 2007;168: 639-49.
16. Bounacer A, Wicker R, Caillou B, et al. High prevalence of activating ret proto-oncogene rearrangements, in thyroid tumors from patients who had received external radiation. *Oncogene* 1997;15:1263-73.
17. Tronko M, Bogdanova T, Voskoboynik L, et al. Radiation induced thyroid cancer: fundamental and applied aspects. *Exp Oncol.* 2010;32:200-204.
18. Fusco A, Grieco M, Santoro M, et al. A new oncogene in human thyroid papillary carcinomas and their lymph-nodal metastases. *Nature.* 1987;328:170-2.
19. Lima J, Trovisco V, Soares P, et al. BRAF mutations are not a major event in post-Chernobyl childhood thyroid carcinomas. *J Clin Endocrinol Metab.* 2004;89:4267-71.
20. Ciampi R, Knauf JA, Kerler R, et al. Oncogenic AKAP9-BRAF fusion is a novel mechanism of MAPK pathway activation in thyroid cancer. *J Clin Invest.* 2005;115: 94-101.
21. Boltze C, Riecke A, Ruf CG, et al. Sporadic and radiation-associated papillary thyroid cancers can be distinguished using routine immunohistochemistry. *Oncol Rep.* 2009;22:459-67.
22. Abou-El-Ardat K, Monsieurs P, Anastasov N, et al. Low dose irradiation of thyroid cells reveals a unique transcriptomic and epigenetic signature in RET/PTC-positive cells. *Mutat Res.* 2012;731:27-40.
23. Rudqvist N, Schüller E, Parris TZ, et al. Dose-specific transcriptional responses in thyroid tissue in mice after (131) I administration. *Nucl Med Biol.* 2015;42:263-8.
24. Mizuno T, Kyoizumi S, Suzuki T, et al. Continued expression of a tissue specific activated oncogene in the early steps of radiation-induced human thyroid carcinogenesis. *Oncogene.* 1997;15:1455-60.
25. Gandhi M, Nikiforov YE. Suitability of animal models for studying radiation-induced thyroid cancer in humans: evidence from nuclear architecture. *Thyroid.* 2011;21: 1331-7.
26. Mizuno T, Iwamoto KS, Kyoizumi S, et al. Preferential induction of RET/PTC1 rearrangement by X-ray irradiation. *Oncogene.* 2000;19:438-43.
27. Trosko JE, Chang CC, Upham BL, et al. Low-dose ionizing radiation: induction of differential intracellular signalling possibly affecting intercellular communication. *adiat Environ Biophys.* 2005;44:3-9.
28. Suzuki K, Yamashita S. Low-dose radiation exposure and carcinogenesis. *Jpn J Clin Oncol.* 2012;42:563-8.
29. Seo D, Han S, Kim KH, et al. Evaluation based on Monte Carlo simulation of lifetime attributable risk of cancer after neck X-ray radiography. *Radiol Med.* 2015; Epub ahead of print.
30. Schonfeld SJ, Lee C, Berrington de González A. Medical exposure to radiation and thyroid cancer. *Clin Oncol (R Coll Radiol)* 2011;23:244-50.
31. Su YP, Niu HW, Chen JB, et al. Radiation dose in the thyroid and the thyroid cancer risk attributable to CT scans for pediatric patients in one general hospital of China. *Int J Environ Res Public Health.* 2014;11:2793-803.
32. Boice JD Jr. Radiation epidemiology and recent paediatric computed tomography studies. *Ann ICRP.* 2015;44:236-48.
33. Akulevich NM, Saenko VA, Rogounovitch TI, et al. Polymorphisms of DNA damage response genes in radiation-related and sporadic papillary thyroid carcinoma. *Endocr Relat Cancer.* 2009;16:491-503.
34. Shkarupa VM, Henyk-Berezovska SO, Neumerzhyska LV, et al. Allelic polymorphism of DNA repair gene XRCC1 in patients with thyroid cancer who were exposed to ionizing radiation as a result of the Chernobyl accident. *Probl Radiac Med Radiobiol.* 2014;19:377-388.
35. Weismann, A. Collected Essays upon Heredity and Kindred Biological Problems (ed. Poulton, E. B.) (Clarendon, Oxford, 1889).
36. Hayflick L, Moorhead PS. The serial cultivation of human diploid cell strains. *Exp. Cell Res.* 1961;25:585-621.

37. Harley CB, Futcher AB, Greider CW. Telomeres shorten during ageing of human fibroblasts. *Nature* 1990;345:458-60.
38. Hayflick, L. A brief overview of the discovery of cell mortality and immortality and of its influence on concepts about ageing and cancer. *Pathol. Biol.* 1999;47:1094-104.
39. Kuilman T, Michaloglou C, Mooi WJ, et al. The essence of senescence. *Genes Dev.* 2010;24:2463-79.
40. Coppé JF, Desprez PY, Krtolica A, et al. The senescence-associated secretory phenotype: the dark side of tumor suppression. *Annu Rev Pathol.* 2010;5:99-118.
41. Klement K, Goodarzi AA. DNA double strand break responses and chromatin alterations within the aging cell. *Exp Cell Res.* 2014;329:42-52.
42. Serrano M, Lin AW, McCurrach ME, et al. Oncogenic ras provokes premature cell senescence associated with accumulation of p53 and p16INK4a. *Cell.* 1997;88:593-602.
43. Vizioli MG, Possik PA, Tarantino E, et al. Evidence of oncogene-induced senescence in thyroid carcinogenesis. *Endocr Relat Cancer.* 2011;18:743-57.
44. Cisowski J, Sayin VI, Liu M, et al. Oncogene-induced senescence underlies the mutual exclusive nature of oncogenic KRAS and BRAF. *Oncogene.* 2015; Epub ahead of print.
45. Suzuki K, Mori I, Nakayama Y, et al. Radiation-induced senescence-like growth arrest requires TP53 function but not telomere shortening. *Radiat Res.* 2001;155:248-253.
46. Meng A, Wang Y, Van Zant G, et al. Ionizing radiation and busulfan induce premature senescence in murine bone marrow hematopoietic cells. *Cancer Res.* 2003;63:5414-9.
47. Mirzayans R, Andrais B, Scott A, et al. Ionizing radiation-induced responses in human cells with differing TP53 status. *Int J Mol Sci.* 2013;14:22409-35.
48. Matsuse M, Saenko V, Sedliarou I, et al. A novel role for thyroid hormone receptor beta in cellular radiosensitivity. *J Radiat Res.* 2008;49:17-27.
49. Zambrano A, Garcia-Carpizo V, Gallardo ME, et al. The thyroid hormone receptor β induces DNA damage and premature senescence. *J Cell Biol.* 2014;204:129-46.
50. Ewald JA, Desotelle JA, Wilding G, et al. Therapy-Induced Senescence in Cancer. *Natl Cancer Inst.* 2010;102:1536-46.

8.2 ANEXO II- ARTIGO SOBRE OS RNAS LONGOS NÃO CODIFICANTES NO CPT



cancers



Article

The Long Non-Coding RNA *RP5-1024C24.1* and Its Associated-Gene *MPPED2* Are Down-Regulated in Human Thyroid Neoplasias and Act as Tumour Suppressors

Romina Sepe^{1,2} , Simona Pellecchia^{1,2}, Pierre Serra³, Daniela D'Angelo^{1,2} , Antonella Federico^{1,2}, Maddalena Raia^{2,4}, Ricardo Cortez Cardoso Penha^{1,2,5}, Myriam Decaussin-Petrucci³ , Luigi Del Vecchio^{2,4}, Alfredo Fusco^{1,2,*} and Pierlorenzo Pallante^{1,2,*}

¹ Institute of Experimental Endocrinology and Oncology (IEOS) "G. Salvatore", National Research Council (CNR), Via Sergio Pansini 5, 80131 Naples, Italy; romina.sepe@unina.it (R.S.); simona.pellecchia@unina.it (S.P.); daniela.dangelo@unina.it (D.D.); anfederi@unina.it (A.F.); ricardocortezcardoso@gmail.com (R.C.C.P.)

² Department of Molecular Medicine and Medical Biotechnology (DMMBM), University of Naples "Federico II", Via Sergio Pansini 5, 80131 Naples, Italy; raia@ceinge.unina.it (M.R.); luigi.delvecchio@unina.it (L.D.V.)

³ Service d'Anatomie et Cytologie Pathologiques, Centre de Biologie Sud, Groupement Hospitalier Lyon Sud, 69495 Pierre Bénite, France; pserra54@gmail.com (P.S.); myriam.decaussin-petrucci@chu-lyon.fr (M.D.-P.)

⁴ CEINGE-Biotechnologie Avanzate, Via Gaetano Salvatore 486, 80145 Naples, Italy

⁵ Instituto Nacional de Cancer, Laboratorio de Carcinogénesis Molecular, Rua Andre Cavalcanti 37, Centro, Rio de Janeiro 20231-050, Brazil

* Correspondence: alfusco@unina.it (A.F.); pallante@ieos.cnr.it (P.P.); Tel.: +39-081-7463749 (A.F.); +39-081-7463347 (P.P.); Fax: +39-081-2296674 (A.F. & P.P.)

Received: 3 May 2018; Accepted: 15 May 2018; Published: 18 May 2018



Abstract: *Background:* Well-differentiated papillary thyroid carcinoma (PTC) represents the thyroid neoplasia with the highest incidence. Long non-coding RNAs (lncRNAs) have been found deregulated in several human carcinomas, and hence, proposed as potential diagnostic and prognostic markers. Therefore, the aim of our study was to investigate their role in thyroid carcinogenesis. *Methods:* We analysed the lncRNA expression profile of 12 PTC and four normal thyroid tissues through a lncRNA microarray. *Results:* We identified 669 up- and 2470 down-regulated lncRNAs with a fold change >2. Among them, we focused on the down-regulated *RP5-1024C24.1* located in an antisense position with respect to the *MPPED2* gene which codes for a metallophosphoesterase with tumour suppressor activity. Both these genes are down-regulated in benign and malignant thyroid neoplasias. The restoration of *RP5-1024C24.1* expression in thyroid carcinoma cell lines reduced cell proliferation and migration by modulating the PTEN/Akt pathway. Inhibition of thyroid carcinoma cell growth and cell migration ability was also achieved by the *MPPED2* restoration. Interestingly, *RP5-1024C24.1* over-expression is able to increase *MPPED2* expression. *Conclusions:* Taken together, these results demonstrate that *RP5-1024C24.1* and *MPPED2* might be considered as novel tumour suppressor genes whose loss of expression contributes to thyroid carcinogenesis.

Keywords: long non-coding RNA; *MPPED2*; thyroid carcinoma; tumour suppressor; carcinogenesis

1. Introduction

Thyroid carcinomas are moderately rare, constituting 1% of all human carcinomas, but represent the highest percentage of all malignancies derived from the endocrine system [1]. Neoplasias resulting

from thyroid follicular cells consist of a wide spectrum of lesions with increasing degree of malignancies going from benign follicular thyroid adenomas (FTA), to differentiated carcinomas (papillary thyroid carcinomas, PTC, and follicular thyroid carcinomas, FTC), to completely undifferentiated carcinomas (anaplastic thyroid carcinomas, ATC) that are always fatal [2]. Among thyroid carcinomas, PTC is the most frequent histotype representing about 80% of all diagnosed thyroid carcinomas. Some genetic mutations are already known to be involved in PTC development, such as *RET/PTC* rearrangement [3–5], *BRAF* and *RAS* mutations [6–9]. Moreover, microRNA (miRNA) deregulated expression has been frequently described in human thyroid carcinomas [10]. However, most of the molecular mechanisms underlying thyroid carcinogenesis have not been completely elucidated yet.

In order to better understand the basic mechanisms involved in thyroid carcinogenesis, a great interest has been recently raised by long non-coding RNAs (lncRNAs), single-strand RNA molecules with a length that varies between 200 and 100,000 nucleotides. They are classified in five different groups on the basis of their position in the genome (sense, antisense, bidirectional, intronic, intergenic) [11,12].

Currently, their molecular action mechanisms and their role played in gene expression regulation have not been clarified, but it has been demonstrated that they can modulate gene expression by inducing histonic epigenetic modifications or acting as “sponge” for miRNAs, thus playing a role in both normal biological processes and diseases, including cancer [13–17]. Moreover, recent evidence has shown that lncRNAs are deregulated in several neoplasias depending on the tumour histotype, proposing their detection as an important tool in cancer diagnosis and prognosis [18–20].

Therefore, in order to identify deregulated lncRNAs in thyroid neoplasias and unveil their role in thyroid carcinogenesis, we analysed the expression profile of 12 PTC versus four normal thyroid tissues. Several lncRNAs differentially expressed in PTC compared to normal thyroid tissues were identified. Then, we focused on the lncRNA *RP5-1024C24.1* that was also down-regulated in FTA, FTC and ATC. Interestingly, the expression of *MPPED2*, its associated gene, was significantly decreased in the thyroid carcinoma samples analysed, suggesting a role of both these genes in thyroid carcinogenesis. Accordingly, the stable restoration of both *RP5-1024C24.1* and *MPPED2* expression was able to attenuate proliferation and migration rate of thyroid cancer cell lines, suggesting a role of both these genes in thyroid cancer progression.

2. Results

2.1. Identification of LncRNAs Deregulated in Human PTC

In order to identify the lncRNAs deregulated in PTC, we analysed the lncRNA expression profile of 12 PTC and four normal thyroid tissues (see Supplementary Material, Table S1) by hybridizing the RNA extracted from these samples to the Human LncRNA Microarray Version 3.0 (Arraystar, Rockville, MD, USA). After hybridization and normalization of the raw data, we obtained through bioinformatic analysis a list of 669 and 2470 lncRNAs that resulted up- and down-regulated, respectively, in the PTC tissues analysed compared to normal thyroid samples with fold change >2 and *p*-value < 0.05. The complete list of up- and down-regulated lncRNAs is provided in Supplementary Material (Table S2). A representative partial list of deregulated lncRNAs is shown in Table 1.

Table 1. Representative list of lncRNAs deregulated in papillary thyroid carcinomas (PTC) vs. normal thyroid tissues (NT) ¹.

Up-Regulated lncRNAs (PTC vs. NT)							
Gene Symbol	Seqname	Fold Change	p-Value	Chr.	Strand	Relationship	Associated Gene
<i>XLOC_010052</i>	TCONS_00020760	44.796062	0.011679098	chr12	–	intergenic	
<i>EGFEM1P</i>	ENST00000488647	29.21525	0.003039263	chr3	+	intergenic	
<i>RP11-230G5.2</i>	ENST00000538294	16.403324	0.003381364	chr12	–	natural antisense	<i>MSRB3</i>
<i>AC008079.9</i>	ENST00000434390	15.255612	0.017524553	chr22	–	intergenic	
<i>RP11-353N14.2</i>	ENST00000576963	14.603789	6.1×10^{-5}	chr17	+	intergenic	
<i>AC079630.2</i>	ENST00000457989	12.705946	0.00535464	chr12	+	intergenic	<i>LRRK2</i>
<i>CTC-255N20.1</i>	ENST00000504297	6.02792	0.001935031	chr5	–	bidirectional	<i>STK32A</i>
<i>AC003102.3</i>	ENST00000453562	5.626362	7.34×10^{-4}	chr17	–	natural antisense	<i>RUNDC3A</i>
<i>DLEU2</i>	uc001vdo.1	4.361354	9.4×10^{-4}	chr13	–	natural antisense	<i>TRIM13</i>
<i>RP11-4C20.4</i>	ENST00000433110	3.8502407	0.035742607	chr10	+	intron sense-overlapping	<i>PTPRE</i>
Down-Regulated lncRNAs (PTC vs. NT)							
Gene Symbol	Seqname	Fold Change	p-Value	Chr.	Strand	Relationship	Associated Gene
<i>CTB-85P21.2</i>	ENST00000566630	72.72284	6.38×10^{-7}	chr5	+	intergenic	
<i>SLC26A4-AS1</i>	NR_028137	27.245485	0.006468582	chr7	–	natural antisense	<i>SLC26A4</i>
<i>RP11-317P15.5</i>	ENST00000570153	20.019192	0.007198248	chr1	–	intergenic	
<i>RP1-240B8.3</i>	ENST00000511849	17.767982	0.001431982	chr6	–	exon sense-overlapping	<i>KHDRBS2</i>
<i>ZFY-AS1</i>	ENST00000417305	14.560697	0.017612867	chrY	–	natural antisense	<i>ZFY</i>
<i>LA16c-329F2.1</i>	ENST00000570022	12.498036	0.031231718	chr16	–	intronic antisense	<i>MAPK3IP3</i>
<i>RP5-1024C24.1</i>	ENST00000531002	10.285704	7.4×10^{-6}	chr11	+	intronic antisense	<i>MPPED2</i>
<i>AC002066.1</i>	ENST00000439070	9.467349	8.22×10^{-4}	chr7	–	intergenic	
<i>ST7-AS1</i>	NR_002330	8.9516325	1.38×10^{-4}	chr7	–	natural antisense	<i>ST7</i>
<i>RP11-121G22.3</i>	ENST00000553197	8.723473	5.89×10^{-6}	chr12	+	intronic antisense	<i>PPF1A2</i>

¹ For each lncRNA we report the gene symbol, accession number, the fold change expression compared to normal thyroid tissues, the p-value of the analysis, the chromosome and the DNA strand in which they are located, their classification and the name of their associated gene on the genome.

To validate the results obtained by the microarray analysis, we selected six up- (*EGFEM1P*, *RP11-230G5.2*, *AC008079.9*, *RP11-353N14.2*, *AC079630.2* and *DLEU2*) and six down-regulated lncRNAs (*SLC26A4-AS1*, *RP1-240B8.3*, *ZFY-AS1*, *RP5-1024C24.1*, *AC002066.1* and *ST7-AS1*) with respect to normal thyroid tissues. Then, we evaluated their expression by qRT-PCR in the same PTC and normal thyroid samples previously used for the lncRNA microarray thus confirming the results obtained. In fact, as shown in Figure 1A,B, we found that the expression of *EGFEM1P*, *RP11-230G5.2*, *AC008079.9*, *RP11-353N14.2*, *AC079630.2* and *DLEU2* was up-regulated in PTC, while the expression of *SLC26A4-AS1*, *RP1-240B8.3*, *ZFY-AS1*, *RP5-1024C24.1*, *AC002066.1* and *ST7-AS1* resulted down-regulated. Moreover, we selected the lncRNAs *RP11-230G5.2*, *DLEU2* and *SCL26A4-AS1* and analysed their expression levels in additional 12 PTC comparing them to the mean of three normal thyroid tissues (three out of the four normal thyroid samples used for microarray hybridization and validation, see Materials and Methods section). By qRT-PCR, we observed also in this case an up-regulation of *RP11-230G5.2* and *DLEU2*, and a down-regulation of *SCL26A4-AS1*, thus supporting the lncRNA microarray analysis (see Supplementary Material, Figure S1).

As shown in Table S2, the lncRNAs identified were classified on the basis of their genomic orientation with respect to their neighbouring genes in exon-sense overlapping, intron-sense overlapping, intronic antisense, natural antisense, bidirectional and intergenic [11,12]. Since several studies have recently demonstrated that lncRNAs frequently act through the modulation of their associated neighbouring gene expression [21–26], we focused our attention on the antisense class of lncRNAs for further investigations. By the lncRNA microarray analysis, we observed the following association between lncRNAs and related genes: *RP11-230G5.2*, antisense with respect to the *MSRB3* gene; *AC079630.2*, intergenic with respect to the *LRRK2* gene; *DLEU2*, antisense with respect to the *TRIM13* gene; *SLC26A4-AS1*, antisense with respect to the *SLC26A4* gene; *RP1-240B8.3* antisense with respect to the *KHDRBS2* gene; *ZFY-AS1*, antisense with respect to the *ZFY* gene; *RP5-1024C24.1*, antisense with respect the *MPPED2* gene; *ST7-AS1*, antisense with respect to the *ST7* gene (Table 1 and Table S2). Therefore, we evaluated, by qRT-PCR, the expression of the selected lncRNA-associated genes in the same PTC and normal thyroid microarray samples. Interestingly, we found a positive association between the lncRNAs and their related gene expression in six out of eight lncRNA/neighbouring-gene pairs analysed (Figure 1A,B). Conversely, a negative association was

observed between *RP11-230G5.2* and *MSRB3* expression, and no association was observed between *DLEU2* and *TRIM13* expression (Figure 1A).

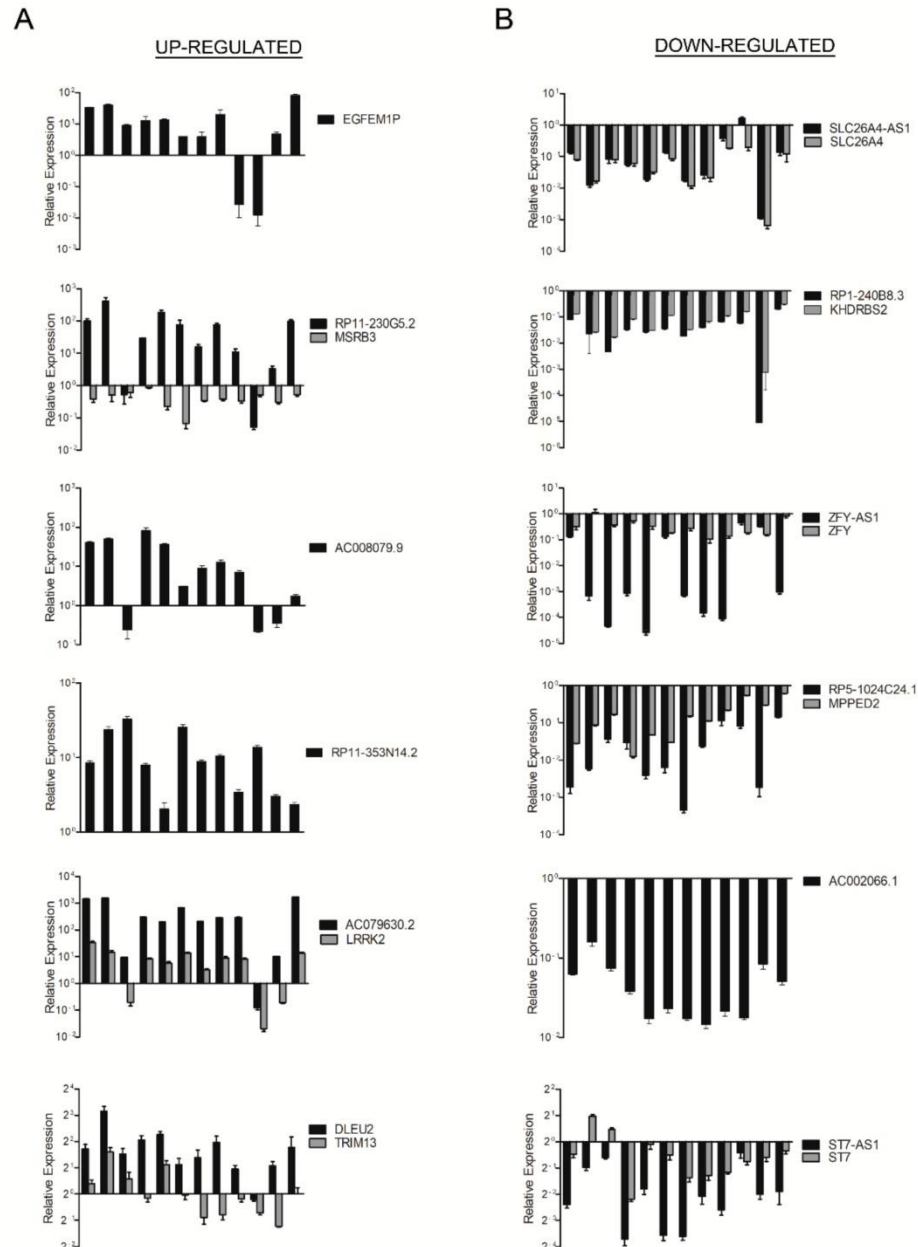


Figure 1. Analysis of lncRNA and gene expression in papillary thyroid carcinoma (PTC). Total RNA extracted from 12 PTC and four normal thyroid samples was hybridized to a lncRNA microarray. qRT-PCR analysis was performed to evaluate the expression of up-regulated (A) and down-regulated (B) lncRNAs and their associated genes. Results are reported as relative expression \pm SEM compared to the mean of four normal thyroid samples set equal to 1.

2.2. Analysis of *RP5-1024C24.1* and *MPPED2* Expression in Neoplastic Thyroid Diseases

To characterize the role of lncRNAs in thyroid carcinogenesis, we decided to focus our study on the lncRNA *RP5-1024C24.1*, located on chromosome 11 in antisense position with respect to the *MPPED2* gene encoding a metallophosphoesterase protein. We made this choice since both of them were drastically down-regulated in all the PTC samples analysed by the lncRNA microarray, and then by qRT-PCR. Moreover, *MPPED2* gene has been already reported to play an important anti-oncogenic role in oral squamous cell carcinoma [27], cervical cancer [28] and neuroblastoma [29]. Therefore, we decided to further investigate the functional role of the lncRNA *RP5-1024C24.1* and its associated *MPPED2* gene in human thyroid carcinomas and their possible relationship in thyroid cancer.

To this aim, we analysed by qRT-PCR the expression levels of both *RP5-1024C24.1* and *MPPED2* in a set of nine FTA samples, additional 12 PTC samples, six FTC and 12 ATC and compared them to the mean of three normal thyroid tissues (three out of the four normal thyroid samples used for microarray hybridization and validation, see Materials and Methods section). As shown in Figure 2A, we observed a reduced expression of both genes with respect to normal thyroid tissues in all the thyroid neoplastic histotypes analysed, including the FTA samples. Moreover, we found a significant ($p = 0.0444$) positive correlation between their expression in the whole neoplasm set analysed, suggesting that both *RP5-1024C24.1* and *MPPED2* are co-regulated during the process of thyroid carcinogenesis (Figure 2B, left panel). The positive correlation between *RP5-1024C24.1* and *MPPED2* expression was still significant when we consider only the thyroid malignant samples (PTC, FTC, ATC) ($p = 0.0381$) (Figure 2B, right panel). These results were then confirmed at the protein level by immunohistochemical analysis using an anti-MPPED2 antibody. In fact, reduced MPPED2 protein levels were found in 37% of FTA (7 out of 19 cases), 79% of PTC (116 out of 147 cases), 77% of FTC (23 out of 30 cases), 86% of PDC (32 out of 37 cases) and 53% of ATC (8 out of 15 cases) in comparison to normal matched thyroid tissue (Table 2).

Representative results are shown in Figure 2C. The signal corresponding to MPPED2 was strong (Score = 3) with a granular cytoplasmic expression in the normal tissues. Conversely, in the paired PTC, FTC and ATC samples shown in the same figure, the signal corresponding to MPPED2 was completely absent (Score = 0) or mild and non-granular (Score = 1) (see Materials and Methods section). Statistical analyses of MPPED2 expression in thyroid carcinoma samples compared to their adjacent normal tissue reveal significant differences between tumours and their corresponding normal tissue in the following categories: whole cohort ($p < 0.001$), PTC ($p < 0.001$), FTC ($p < 0.001$), PDC ($p < 0.001$), ATC ($p = 0.003$) (Table 2). We did not observe any significant differences of MPPED2 expression levels between the different histological groups. Moreover, as far as the association of differential MPPED2 expression between tumour and normal matched samples with clinico-pathological information is concerned, we did not find any significant correlation with the TNM stage, morphological tumour characteristics and the mutational status of specific thyroid cancer-related genes (data not shown).

Table 2. Expression of MPPED2 protein levels in thyroid neoplasias analysed by immunohistochemistry.

Histotype (n)	Reduced Expression ¹ (n, %)	
FTA ² (n = 19)	n = 7 (37%)	
PTC ³ (n = 147)	n = 116 (79%)	p < 0.001
FTC ⁴ (n = 30)	n = 23 (77%)	p < 0.001
PDC ⁵ (n = 37)	n = 32 (86%)	p < 0.001
ATC ⁶ (n = 15)	n = 8 (53%)	p = 0.003
Whole cohort p < 0.001		

¹ MPPED2 protein expression in thyroid carcinoma vs. the adjacent corresponding normal thyroid tissue; ² FTA, follicular thyroid adenoma; ³ PTC, papillary thyroid carcinoma; ⁴ FTC, follicular thyroid carcinoma; ⁵ PDC, poorly differentiated carcinoma; ⁶ ATC, anaplastic thyroid carcinoma.

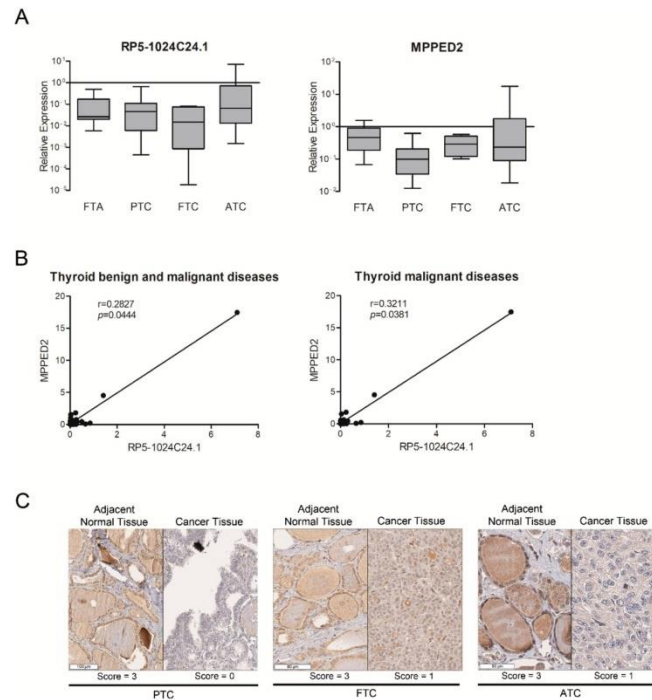


Figure 2. Analysis of *RP5-1024C24.1* and *MPPED2* expression in thyroid neoplastic diseases. (A) qRT-PCR analysis performed on FTA ($n = 9$), PTC ($n = 12$ previously used for lncRNA microarray hybridization and $n = 12$ additional samples), FTC ($n = 6$), ATC ($n = 12$) to evaluate the expression of *RP5-1024C24.1* (left panel) and *MPPED2* (right panel). Results are reported as relative expression compared to the mean of normal thyroid samples, set equal to 1 (box and whiskers, min to max). (B) Correlation scatterplot (Spearman test) of *RP5-1024C24.1* and *MPPED2* mRNA levels (relative expression) in thyroid benign and malignant diseases (FTA, PTC, FTC, ATC) (left panel). Correlation scatterplot (Spearman test) of *RP5-1024C24.1* and *MPPED2* mRNA levels (relative expression) in thyroid carcinomas (PTC, FTC, ATC) (right panel). (C) Representative immunohistochemical staining of *MPPED2* protein in thyroid carcinoma samples (PTC, FTC, ATC) and in their corresponding adjacent normal tissue. The *MPPED2* signal is strong in normal thyroid tissues (Score = 3) and mild (Score = 1) or absent (Score = 0) in thyroid carcinoma tissues (magnification 40 \times).

2.3. Down-Regulation of *RP5-1024C24.1* Expression Contributes to Thyroid Carcinogenesis by Affecting the *PTEN/Akt* Pathway

Subsequently, to better define the role of *RP5-1024C24.1* in thyroid carcinogenesis, we modulated its expression in thyroid carcinoma cell lines. To achieve this aim, we first analysed the expression of this gene by qRT-PCR in a panel of thyroid carcinoma cell lines, including TPC-1 and B-CPAP (PTC-derived cell lines), WRO (FTC-derived cell line) and FB-1 and FRO (ATC-derived cell lines). As shown in Figure S2, the expression of *RP5-1024C24.1* was much lower in all the cell lines analysed in comparison with three normal thyroid samples used as control (see Materials and Methods section).

Then, we restored the expression of *RP5-1024C24.1* in TPC-1 and FRO cell lines by transfecting them with a vector expressing the lncRNA and selected the transfected cells in a G418-containing medium. Next, we confirmed by qRT-PCR the restoration of *RP5-1024C24.1* expression in the selected cells (Figure 3A and Figure S3A) and evaluated its effects on cell proliferation. As shown in Figure 3B, both TPC-1 and FRO cells expressing *RP5-1024C24.1* displayed a significant reduction in the cell growth rate compared to the respective empty vector transfected cells. Consistently, cell colony-forming assays evidenced that

RP5-1024C24.1 reduces the number of colonies compared to the control cells (Figure 3C), thus confirming that *RP5-1024C24.1* is able to negatively modulate the cell proliferation of both PTC and ATC cells.

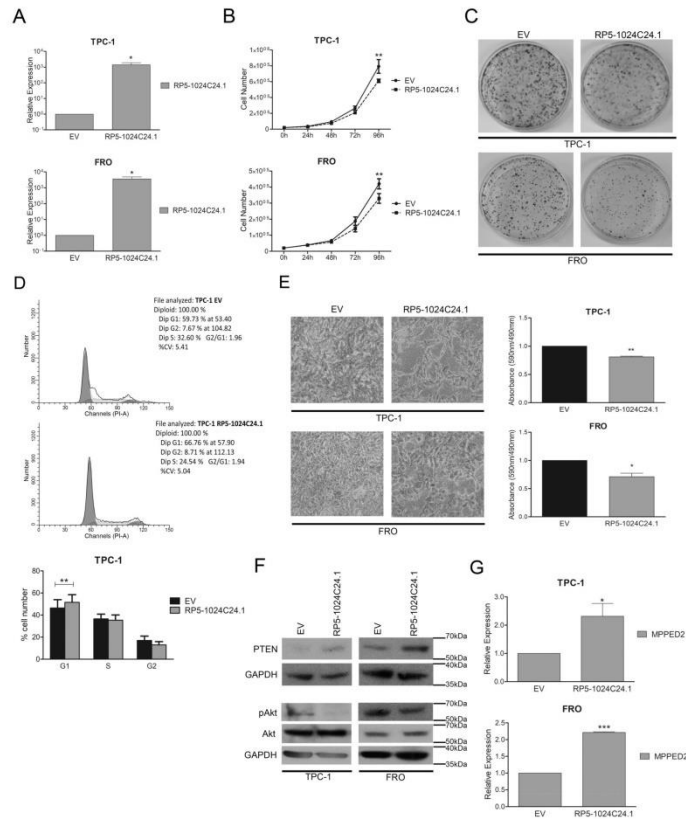


Figure 3. *RP5-1024C24.1* reduces cell migration and proliferation of thyroid carcinoma cell lines. (A) qRT-PCR analysis performed on TPC-1 and FRO cell lines stably carrying *RP5-1024C24.1* or the corresponding empty vector (EV). Results were obtained from four independent experiments. Data were compared to EV, set equal to 1, and reported as relative expression \pm SEM. *t*-test; * $p < 0.05$. (B) Cell growth analysis of TPC-1 and FRO stably carrying *RP5-1024C24.1* or EV. Cell number was evaluated at 24 h, 48 h, 72 h and 96 h after seeding. Values were obtained from three independent experiments performed in duplicate. Data were reported as mean \pm SEM. 2-way Anova-test followed by Bonferroni post-test; ** $p < 0.01$. (C) Representative colony assay performed on TPC-1 and FRO cell lines stably carrying *RP5-1024C24.1* or EV. (D) Representative cell cycle analysis of TPC-1 cell lines stably carrying *RP5-1024C24.1* or EV. Cell number was reported on the *y*-axis while the percentage of propidium iodide (PI) incorporated was reported on the *x*-axis (upper panel). Values shown in the lower panel were obtained from five independent experiments. *t*-test; ** $p < 0.01$ compared to EV cells. (E) Representative acquisition of migration assays performed on TPC-1 and FRO stably carrying *RP5-1024C24.1* or EV (magnification 40 \times) (left panel). Data obtained from three (TPC-1) or four (FRO) independent experiments are shown in the right panel. Values were reported as mean value \pm SEM and compared to the EV, set equal to 1. *t*-test; * $p < 0.05$; ** $p < 0.01$. (F) Immunoblot analysis performed on TPC-1 and FRO cell lines stably carrying *RP5-1024C24.1* or EV to analyze the protein level of PTEN, Akt and pAkt. GAPDH was used to normalize the amount of loaded protein. (G) *MPPED2* expression evaluated by qRT-PCR in TPC-1 and FRO stably expressing *RP5-1024C24.1*. Data were obtained from five (TPC-1) or three (FRO) independent experiments. Values were reported as relative expression \pm SEM and were compared to the EV, set equal to 1. *t*-test; * $p < 0.05$; *** $p < 0.001$.

Cell cycle analysis performed by flow cytometry showed that *RP5-1024C24.1* increased the number of TPC-1 cells in the G1 phase compared to the empty vector (TPC-1-EV, G1: 59.73%; TPC-1-*RP5-1024C24.1*, G1: 66.76%; $p = 0.0092$) (Figure 3D). Moreover, to verify whether the restoration of *RP5-1024C24.1* has an effect on other cancer-associated processes as well, we analysed the cell migration rate of TPC-1 and FRO stably expressing *RP5-1024C24.1* by transwell assays after inhibiting cell proliferation with mytomicin C. As shown in Figure 3E, we found that the restoration of the lncRNA expression was also able to reduce the migration ability of the selected thyroid carcinoma cell lines.

Next, to characterize the molecular mechanisms by which the lncRNA *RP5-1024C24.1* may act, we evaluated the expression of PTEN, a well-known oncosuppressor protein [30,31], in TPC-1 and FRO cells stably expressing the lncRNA. By western blot analysis, we found that *RP5-1024C24.1* is able to increase PTEN levels (Figure 3F, upper panel). In addition, we analysed the effect of the PTEN induction on its down-stream effector Akt [32,33] and found that cells expressing *RP5-1024C24.1* showed a reduced Akt phosphorylation on Ser473 (Figure 3F, lower panel) resulting in the reduction of its activation [34].

Therefore, these results indicate that *RP5-1024C24.1* can affect cell proliferation and migration through a mechanism that involves the modulation of the PTEN/Akt pathway, further supporting the anti-oncogenic role played by *RP5-1024C24.1* in thyroid carcinogenesis.

2.4. *MPPED2* Is Induced by *RP5-1024C24.1* and Negatively Modulates Cell Proliferation and Migration of Thyroid Carcinoma Cell Lines

To investigate whether *RP5-1024C24.1* modulates the expression of its-associated *MPPED2* gene, we analysed the expression of *MPPED2* by qRT-PCR in TPC-1 and FRO stably expressing *RP5-1024C24.1*. Interestingly, we found that *RP5-1024C24.1* is able to increase the expression of *MPPED2* in both cell lines with respect to the empty vector transfected cells, thus suggesting that the lncRNA may act also through the modulation of the *MPPED2* expression (Figure 3G).

Next, to characterize the role that this gene plays in thyroid carcinogenesis, we analysed by qRT-PCR the expression of *MPPED2* in a panel of thyroid carcinoma cell lines (Figure S2) and then we stably restored its expression in TPC-1 and FRO cell lines. After G418 selection, we confirmed the increased expression of *MPPED2* in the transfected cells (Figure 4A and Figure S3B) and evaluated its functional effects. As displayed in Figure 4B,C, the growth curve and colony formation assays showed that both the *MPPED2*-transfected TPC-1 and FRO cells have a lower proliferation rate than cells carrying the empty vector. Moreover, cell cycle progression analysis performed on TPC-1 cells through flow cytometry confirmed the negative effect of *MPPED2* on cell proliferation by showing an increased percentage of cells in the G1 phase when compared to cells carrying the empty vector (TPC-1-EV, G1: 56.04%; TPC-1-*MPPED2*, G1: 60.07%; $p = 0.0367$) (Figure 4D).

In addition, to evaluate the effects of *MPPED2* on cancer progression, we performed transwell assays on *MPPED2*-expressing TPC-1 and FRO cells treated with mytomicin C. Interestingly, as shown in Figure 4E, we found a significant reduction of migrating cells both in *MPPED2*-TPC-1 and FRO cells, thus demonstrating a role of *MPPED2* in inhibiting also cellular migration.

Noteworthy, through qRT-PCR, we observed no modulation of the *RP5-1024C24.1* expression mediated by *MPPED2*, thus indicating that *RP5-1024C24.1* is able to modulate *MPPED2*, but not vice versa (Figure 4F).

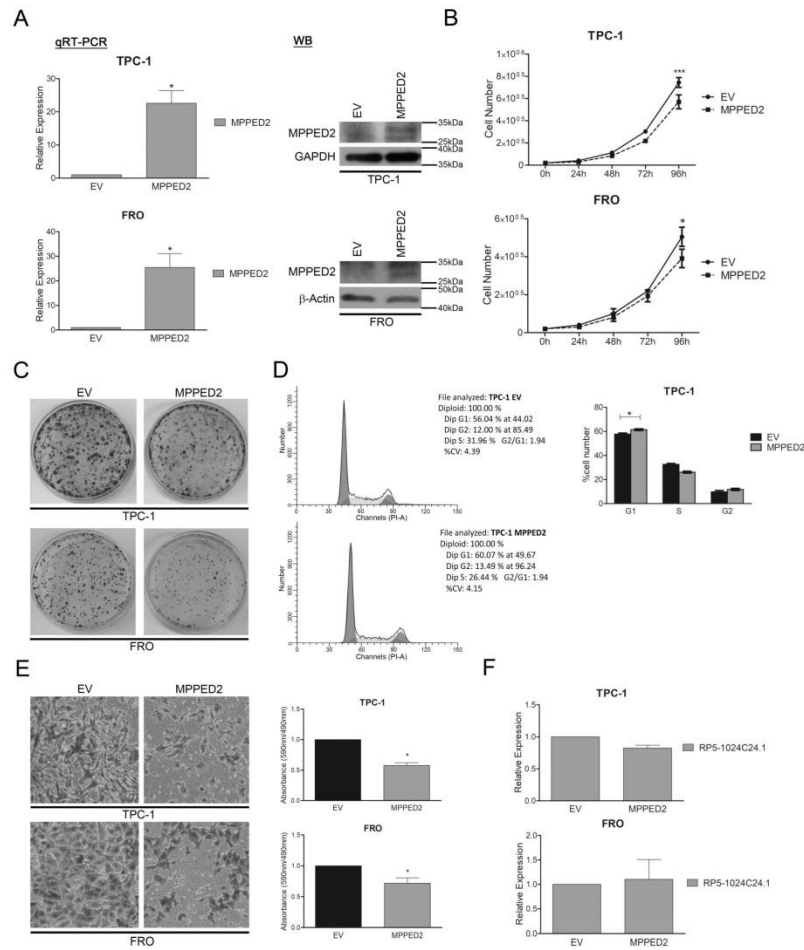


Figure 4. MPPED2 negatively modulates cell proliferation and migration of thyroid carcinoma cell lines. (A) qRT-PCR analysis performed on TPC-1 and FRO cell lines stably carrying *MPPED2* or the corresponding empty vector (*EV*). Values were reported as relative expression \pm SEM and were compared to *EV*, set equal to 1. *t*-test; * $p < 0.05$ (left panel). Immunoblot analysis confirming the expression of MPPED2. GAPDH and β -Actin were used to normalize the amount of loaded protein (right panel). (B) Cell growth analysis of TPC-1 and FRO stably carrying *MPPED2* or *EV*. Cell number was evaluated at 24 h, 48 h, 72 h and 96 h after seeding. Values were obtained from three independent experiments performed in duplicate and data were reported as mean \pm SEM. 2-way Anova-test followed by Bonferroni post-test; * $p < 0.05$; *** $p < 0.001$. (C) Representative colony assay performed on TPC-1 and FRO cell lines stably carrying *MPPED2* or *EV*. (D) Representative cell cycle analysis of TPC-1-*MPPED2* and TPC-1-*EV* cells. Cell number was reported on the *y*-axis while the percentage of propidium iodide (PI) incorporated was reported on the *x*-axis (left panel). Values shown in the right panel were obtained from three independent experiments. *t*-test; * $p < 0.05$ compared to *EV*. (E) Representative acquisition of migration assays performed on *MPPED2* or *EV* transfected TPC-1 and FRO cells (magnification 40 \times) (left panel). Values obtained from three (TPC-1) or four (FRO) independent experiments were reported as mean \pm SEM and compared to the *EV*, set equal to 1 (right panel). *t*-test; * $p < 0.05$. (F) qRT-PCR analysis to evaluate the expression of *RP5-1024C24.1* after *MPPED2* transfection. Data obtained from three (TPC-1) or five (FRO) independent experiments were reported as relative expression \pm SEM and were compared to the *EV*, set equal to 1. *t*-test; $p = ns$.

3. Discussion

The aim of our study was to investigate the role of lncRNAs in thyroid carcinogenesis by evaluating the expression profile of 12 PTC compared to four normal thyroid samples through a human lncRNA microarray approach. This analysis identified a relevant number of lncRNAs deregulated in PTC compared to normal thyroid tissues. The microarray results were confirmed by evaluating the expression of six up- and six down-regulated lncRNAs by qRT-PCR. Subsequently, we focused our attention on the *RP5-1024C24.1* lncRNA, that was drastically down-regulated in all PTC samples analysed with respect to normal thyroid tissues. However, we are currently planning to examine in depth the role of other deregulated lncRNAs in thyroid carcinogenesis.

The next step of our investigation was to evaluate the expression of *RP5-1024C24.1* in thyroid neoplastic samples of different malignant degrees. Interestingly, we observed that the expression levels of this lncRNA are decreased in both differentiated and undifferentiated thyroid carcinomas. Surprisingly, *RP5-1024C24.1* reduction was also observed in benign FTA suggesting a key role of *RP5-1024C24.1* down-regulation even in the early phases of thyroid cell neoplastic transformation.

Bioinformatic analyses (Materials and Methods section) revealed that *RP5-1024C24.1* is located on the genome in an antisense position with respect to *MPPED2*. This gene codes for an enzyme belonging to the III class-family of phosphoesterase in mammals and is highly expressed in foetal brain. Recent studies have demonstrated that the expression of *MPPED2* is drastically down-regulated in several malignant neoplasias originating from different tissues. Moreover, its restoration in cancer cell lines induces apoptosis and negatively modulates cell proliferation [27–29], thus proposing *MPPED2* as a potential candidate tumour suppressor gene. Consequently, we evaluated the expression of the *MPPED2* gene by qRT-PCR in the same set of thyroid neoplastic samples analysed for *RP5-1024C24.1* expression: a reduced expression of this gene was observed in the different histotypes analysed. In addition, we observed a significant positive correlation between *MPPED2* and *RP5-1024C24.1* expression in the thyroid neoplastic samples analysed ($p = 0.0444$).

Noteworthy, immunohistochemical analysis performed on a large number of paraffin-embedded thyroid neoplastic tissues and their adjacent normal thyroid tissue confirmed the results obtained by qRT-PCR. In fact, we observed that *MPPED2* levels were moderately decreased in FTA, and strongly decreased in FTC, PTC and PDC. Surprisingly, while the expression of *MPPED2* was markedly reduced in 86% of PDC samples, in the ATC set only 53% of cases showed reduced expression of *MPPED2*. Additionally, by analysing each thyroid carcinoma histotype, we found significant differences of *MPPED2* expression between neoplastic and normal tissue samples.

Functional studies were performed to define the role of *RP5-1024C24.1* and *MPPED2* down-regulation in thyroid carcinogenesis. Accordingly, we stably restored the expression of *RP5-1024C24.1* in two thyroid carcinoma cell lines by transfecting them with a vector expressing the lncRNA sequence. We observed that *RP5-1024C24.1* was able to reduce the cell proliferation and migration rate, thus indicating that the deregulation of this lncRNA might play a causative role in the modulation of the biological processes leading to thyroid carcinoma development.

Interestingly, in order to clarify the molecular mechanisms by which *RP5-1024C24.1* is able to affect cell growth and migration in thyroid carcinoma cells, we found that the restoration of *RP5-1024C24.1* is able to increase PTEN protein levels and to reduce Akt-Ser473 phosphorylation, thus suggesting that the modulation of this pathway could account for the effects of *RP5-1024C24.1* on cell proliferation and migration [30–34].

However, since we demonstrated that also *MPPED2* restoration is able to inhibit cell proliferation and migration in TPC-1 and FRO cell lines, we suggest that the functional effects of *RP5-1024C24.1* could also be due to the up-regulation of the *MPPED2* gene expression. Interestingly, no *RP5-1024C24.1* modulation was observed in *MPPED2*-expressing cells indicating that the regulation is unidirectional.

As far as the mechanisms by which *RP5-1024C24.1* is able to positively regulate *MPPED2* are concerned, they still need to be clarified, although several pieces of evidence suggest that lncRNAs are able to modulate the expression of their associated genes through epigenetic regulations [21–26].

Consistently, Shen and colleagues have recently indicated miR-448 as a negative regulator of *MPPED2* [27]. Therefore, we have analysed the expression of this miRNA in our thyroid carcinoma cell systems stably expressing *RP5-1024C24.1*. Interestingly, our preliminary data have shown a reduction of the miR-448 expression following the restoration of the lncRNA expression (data not shown), thus suggesting that one of the mechanisms by which *RP5-1024C24.1* might positively regulate *MPPED2* expression could be through the negative modulation of the miR-448.

In conclusion, the results presented here indicate that the down-regulated *RP5-1024C24.1* and its associated-gene *MPPED2*, could represent novel tumour suppressor genes with a considerable role in thyroid cell neoplastic transformation and progression.

4. Materials and Methods

4.1. Human Thyroid Samples

The whole set of human thyroid carcinoma specimens used was provided by the Service d'Anatomie et Cytologie Pathologiques, Centre de Biologie Sud, Groupement Hospitalier Lyon Sud, Pierre Bénite, France. The histotype and TNM characteristics of PTC samples used for lncRNA microarray analysis are reported in Table S1. The activity of biological samples conservation was declared under the number DC-2011-1437 to the ministry of Research, to the committee of people's protection of south-east IV and to the Health Regional Agency. The activity of biological material cession was agreed upon by the ministry of Health under the number AC-2013-1867.

4.2. Long Non-Coding RNA Microarray Analysis

Total RNA extracted from 12 PTC samples and four normal thyroid tissues was hybridized to the Human lncRNA Microarray Version 3.0 of the Arraystar company (Rockville, MD, USA). This system is based on probes able to recognize specific exons or splice junction of each lncRNA. The expression analysis was performed by comparing the average of the expression levels observed in 12 PTC samples with the average of the expression levels observed in four normal thyroid tissues. Bioinformatic analyses were performed by the Arraystar company based on the following databases: Refseq, UCSC, GENCODE, RNADB, NRED, UCR, lincRNA catalogs [35,36] (<https://www.arraystar.com/human-lncrna-expression-microarray-v4-0/>) (Table S2).

4.3. Cell Lines and Transfection

TPC-1 and FRO cell lines were grown in DMEM (Sigma-Aldrich, St. Louis, MO, USA) supplemented with 10% foetal bovine serum (Euroclone, Milan, Italy), 1% L-glutamine, 1% penicillin/streptomycin (Sigma-Aldrich) and were maintained at 37 °C under 5% CO₂ atmosphere.

The authenticity of cell lines has been confirmed through short tandem repeat (STR) profiling.

TPC-1 cells were transfected using Fugene HD reagent (Promega, Fitchburg, WI, USA) while FRO cells were transfected using the Lipofectamine 2000 reagent (Life Technologies, Grand Island, NY, USA), according to the manufacturer's instructions. For stably-expressing cell lines, TPC-1 and FRO were selected by using 1000 µg/mL and 1200 µg/mL of G418 (Life Technologies), respectively.

For cell count number assays, 2×10^4 TPC-1 and FRO stable clones were seeded in a six well plate in duplicate and counted after 24 h, 48 h, 72 h, 96 h using a Burkert chamber.

4.4. Plasmids

The *RP5-1024C24.1* expression vector was obtained by cloning the lncRNA sequence in the pCMV6-AC-GFP vector (Origene Technologies, Rockville, MD, USA) using the HindIII and XhoI restriction sites. The pCMV6-MPPED2-DDK-myc expression vector encoding human MPPED2 (NM_00145399.1) fused to the myc/DDK epitope in the C-terminal region was purchased from Origene Technologies (RC227201).

4.5. RNA Extraction and qRT-PCR

Total RNA was extracted from cell lines and tissues by using Trizol reagent (Life Technologies), according to the manufacturer's instructions. 1 µg of total RNA was used to obtain a double strand cDNA with the QuantiTect Reverse Transcription Kit (Qiagen, Hilden, Germany). qRT-PCR was carried out in a 96 well plate with the CFX 96 thermocycler (Bio-Rad, Hercules, CA, USA) using 20 ng of each cDNA and SYBR Green (Bio-Rad). *G6PD* was used as reference gene for qRT-PCR performed on thyroid neoplasias, while *β-Actin* was used for thyroid carcinoma cell lines. Primers sequences are listed in Table S3.

Relative expression values were calculated according to the $2^{-\Delta\Delta C_t}$ formula as previously described [37].

As far as qRT-PCR analyses are concerned, we used four normal thyroid tissue samples for the validation of the microarray results (lncRNA and associated gene expression in PTC). However, we used only three out of four normal thyroid tissues for further analyses (expression analyses in additional set of thyroid neoplasms and cell lines) since the RNA of one out of the four normal samples ran out.

4.6. Protein Extraction and Western Blot Analysis

Total protein extracts were obtained using the lysis buffer (120 mM NaCl, 20 mM Tris-HCl pH 7.5, 2% Nonidet P40) completed with a mix of proteases and phosphatases inhibitors. 80 µg of extracted proteins were separated by SDS-PAGE and then transferred onto PVDF membranes (Merck Millipore, Darmstadt, Germany). Membranes were blocked with BSA or 5% not-fat milk and then incubated with the following antibodies: anti-myc tag (ab9132, Abcam, Cambridge, UK), anti-MPPED2 (H00000744-D01P, Abnova, Taipei City, Taiwan), anti-PTEN (ab32199, Abcam), anti-phospho-Akt (Ser473) (#4051, Cell Signaling, Danvers, MA, USA), anti-Akt (#92725, Cell Signaling). To normalize the amount of protein loaded, the membranes were incubated with anti-GAPDH (Santa Cruz Biotechnology Inc., Santa Cruz, CA, USA) and anti-β-Actin protein (Sigma-Aldrich). Filters were then incubated with horseradish peroxidase-conjugated secondary antibody (1:3000) for 1 h at room temperature and the signals were detected by western blotting detection system (ECL).

4.7. Cell Migration Assays

Transwell motility assays were performed as previously described [38]. Briefly, cells were first treated with mytomicin C (Sigma-Aldrich) at a final concentration of 0.01 mg/mL for 3 h. Then, 3×10^4 TPC-1 and FRO cells were seeded both in the transwell for migration and in a 96 well plate in triplicate or quadruplicate to normalize the number of cells used for each cell line. The cell titer and the crystal violet de-stained with PBS-0.1% SDS solution were read at 490 nm and 590 nm, respectively, in a microplate reader (LX 800, Universal Microplate Reader, BioTek, Winooski, VT, USA). Results were obtained by normalizing the crystal violet values to cell titer ones.

4.8. Immunohistochemical Analysis

In the IHC analysis, the following set of thyroid neoplasias and the corresponding adjacent normal thyroid tissue was included: FTA, $n = 19$; PTC, $n = 147$ (classical variant, $n = 74$; follicular variant, $n = 73$); FTC, $n = 30$; PDC, $n = 37$; ATC, $n = 15$.

The original Hematoxylin-Eosin-Saffron (HES) stained slides were reviewed. For the PTC cases, the most representative areas of normal and tumoural tissues were circled. Up to two formalin-fixed paraffin-embedded (FFPE) blocks were selected to be sampled in a tissue microarray (TMA). One 0.6 mm normal tissue core and three 0.6 mm tumoural tissue cores were collected and aligned in two TMA blocks, using the tissue arrayer Minicore® 3 (Alphelys, Plaisir, France). The blocks were sectioned at 3 µm. An HES stain of the TMAs was performed to assess the representativeness of the cores. The ATC and FTA cases were processed as whole slides following the same immunohistochemical protocol as the TMAs.

Immunohistochemical staining was performed on a Benchmark Ultra automated staining platform (Ventana, Tucson, AZ, USA) using a rabbit polyclonal MPPED2 antibody (Abnova), with a 1:60 dilution and an UltraView DAB detection kit (Ventana). A hematoxylin counterstain followed.

The level of staining was evaluated in the normal and tumoural tissues following a qualitative scoring method. The expected staining pattern was “cytoplasmic granular”, conforming to what was observed in the positive controls (normal duodenal epithelium). The absence of staining was scored 0, a mild non-granular staining was scored 1, a granular moderate staining was scored 2 and a granular intense staining was scored 3.

The difference of MPPED2 expression between non tumoural and tumoural tissue, in the whole cohort and in each histologic subtype, was analysed using the paired sample *t*-test.

4.9. Flow Cytometry Analysis

For cell cycle analyses, cells were processed as previously described [39]. Briefly, cells were trypsinized and, after washing in PBS, fixed in 70% ethanol. After a centrifugation at 1200 rpm for 10 min at 4 °C, cells were treated with 50 µg/mL propidium iodide and 25 µg/mL ribonuclease A in PBS for 20 min at RT safe of light. For each measurement 10,000 events were analysed using a FACScanto II flow cytometer (Becton Dickinson, San Jose, CA, USA) and then cell cycle data were analysed with the ModFit LT 2.0 software (Verity Software House, Topsham, ME, USA) in a semiautomatic analysis procedure. The ModFit algorithm was finally used to analyse the files obtained, calculating the percentage of cells in each cell cycle phase.

4.10. Statistical Analysis

GraphPad Prism software was used for statistical analyses. *t*-test and Anova tests were used to evaluate the statistical significance of the obtained data, while gene expression correlation was evaluated through non-parametric Spearman’s Rank correlation coefficient. When Anova test was significant ($p < 0.05$), we determined the differences between groups using Bonferroni post-test. In all the experiments, the significance was assessed for $p < 0.05$. Data are reported as mean values \pm standard error of mean (SEM).

5. Conclusions

In this study, we identified several lncRNAs whose expression is deregulated in PTC compared to normal thyroid samples and, among them, we focused on *RP5-1024C24.1* and on its associated-antisense gene *MPPED2* for further investigation. We report that both genes are down-regulated in thyroid neoplasias. Moreover, the restoration of their expression in thyroid cancer cell lines reduces cell proliferation and migration, thus suggesting a tumour suppressor role for *RP5-1024C24.1* and *MPPED2* in the development of thyroid neoplasias.

Supplementary Materials: The following are available online at <http://www.mdpi.com/2072-6694/10/5/146/s1>, Figure S1: lncRNA expression analysis in additional PTC samples. qRT-PCR analysis to evaluate the expression of RP11-230G5.2, DLEU2 and SLC26A4-AS1 in additional PTC samples. Results are reported as relative expression \pm SEM compared to the mean of three normal thyroid samples set equal to 1; Figure S2: Expression analysis of *RP5-1024C24.1* and *MPPED2* in thyroid carcinoma cell lines. qRT-PCR performed on papillary (TPC-1, B-CPAP), follicular (WRO), anaplastic (FB-1 and FRO) thyroid carcinoma cell lines and three normal thyroid tissue samples (NT1, NT2, NT3). Data are reported as $2^{-\Delta Ct}$ values \pm SD; Figure S3: Analysis of *RP5-1024C24.1* and *MPPED2* expression in TPC-1- and FRO-transfected cells. qRT-PCR analysis performed on TPC-1 and FRO cell lines stably expressing *RP5-1024C24.1* (A), *MPPED2* (B) or carrying the corresponding empty vector (EV), and three normal thyroid tissue samples (NT1, NT2, NT3). Data are reported as $2^{-\Delta Ct}$ values \pm SEM; Table S1: PTC samples used for lncRNA microarray; Table S2: Whole list of lncRNAs deregulated in PTC vs. NT; Table S3: List of primer sequences used for qRT-PCR analyses.

Author Contributions: R.S. contributed to the scientific planning and experimental execution, the interpretation and analyses of the data and the manuscript drafting; S.P. contributed to the experimental procedure and analyses of the data; P.S. and M.D.-P. contributed to samples collection and IHC analyses; D.D., A.F. and R.C.C.P. contributed to cloning procedure and migration experiments; M.R. and L.D.V. contributed to cell cycle analyses; P.P. and

A.F. contributed to study design, manuscript writing and final approval. All authors read and approved the final manuscript.

Acknowledgments: This work was supported by grants provided by: “Progetto di Interesse Strategico Invecchiamento (PNR-CNR Aging Program) PNR-CNR 2012–2014” and “CNR Flagship Projects (Epigenomics-EPIGEN)”. Romina Sepe was granted with a fellowship provided by “Fondazione Adriano-Buzzati Traverso”, 2016. We thank Giuseppina Ippolito and Giulia Speranza (IEOS-CNR) for administrative support and Salvatore Sequino (DMMBM, University of Naples “Federico II”) for technical support.

Conflicts of Interest: The authors declare no conflict of interest.

Availability of Data and Materials: All published data and material are available upon request to the corresponding authors.

References

1. Parkin, D.M.; Bray, F.; Ferlay, J.; Pisani, P. Global cancer statistics, 2002. *CA Cancer J. Clin.* **2005**, *55*, 74–108. [[CrossRef](#)] [[PubMed](#)]
2. Hedinger, C.; Williams, E.D.; Sobin, L.H. The who histological classification of thyroid tumors: A commentary on the second edition. *Cancer* **1989**, *63*, 908–911. [[CrossRef](#)]
3. Fusco, A.; Grieco, M.; Santoro, M.; Berlingieri, M.T.; Pilotti, S.; Pierotti, M.A.; Della Porta, G.; Vecchio, G. A new oncogene in human thyroid papillary carcinomas and their lymph-nodal metastases. *Nature* **1987**, *328*, 170–172. [[CrossRef](#)] [[PubMed](#)]
4. Fusco, A.; Santoro, M. 20 years of RET/PTC in thyroid cancer: Clinico-pathological correlations. *Arq. Bras. Endocrinol. Metabol.* **2007**, *51*, 731–735. [[CrossRef](#)] [[PubMed](#)]
5. Grieco, M.; Santoro, M.; Berlingieri, M.T.; Melillo, R.M.; Donghi, R.; Bongarzone, I.; Pierotti, M.A.; Della Porta, G.; Fusco, A.; Vecchio, G. PTC is a novel rearranged form of the ret proto-oncogene and is frequently detected in vivo in human thyroid papillary carcinomas. *Cell* **1990**, *60*, 557–563. [[CrossRef](#)]
6. Jung, C.K.; Little, M.P.; Lubin, J.H.; Brenner, A.V.; Wells, S.A., Jr.; Sigurdson, A.J.; Nikiforov, Y.E. The increase in thyroid cancer incidence during the last four decades is accompanied by a high frequency of BRAF mutations and a sharp increase in RAS mutations. *J. Clin. Endocrinol. Metab.* **2014**, *99*, E276–E285. [[CrossRef](#)] [[PubMed](#)]
7. Ming, J.; Liu, Z.; Zeng, W.; Maimaiti, Y.; Guo, Y.; Nie, X.; Chen, C.; Zhao, X.; Shi, L.; Liu, C.; et al. Association between BRAF and RAS mutations, and ret rearrangements and the clinical features of papillary thyroid cancer. *Int. J. Clin. Exp. Pathol.* **2015**, *8*, 15155–15162. [[PubMed](#)]
8. Penna, G.C.; Vaisman, F.; Vaisman, M.; Sobrinho-Simoes, M.; Soares, P. Molecular markers involved in tumorigenesis of thyroid carcinoma: Focus on aggressive histotypes. *Cytogenet. Genome Res.* **2017**, *150*, 194–207. [[CrossRef](#)] [[PubMed](#)]
9. Melillo, R.M.; Castellone, M.D.; Guarino, V.; De Falco, V.; Cirafici, A.M.; Salvatore, G.; Caiazza, F.; Basolo, F.; Giannini, R.; Kruhoffer, M.; et al. The RET/PTC-RAS-BRAF linear signaling cascade mediates the motile and mitogenic phenotype of thyroid cancer cells. *J. Clin. Investig.* **2005**, *115*, 1068–1081. [[CrossRef](#)] [[PubMed](#)]
10. Pallante, P.; Battista, S.; Pierantoni, G.M.; Fusco, A. Deregulation of microrna expression in thyroid neoplasias. *Nat. Rev. Endocrinol.* **2013**, *10*, 88–101. [[CrossRef](#)] [[PubMed](#)]
11. Derrien, T.; Johnson, R.; Bussotti, G.; Tanzer, A.; Djebali, S.; Tilgner, H.; Guernec, G.; Martin, D.; Merkel, A.; Knowles, D.G.; et al. The GENCODE v7 catalog of human long noncoding RNAs: Analysis of their gene structure, evolution, and expression. *Genome Res.* **2012**, *22*, 1775–1789. [[CrossRef](#)] [[PubMed](#)]
12. Guttman, M.; Amit, I.; Garber, M.; French, C.; Lin, M.F.; Feldser, D.; Huarte, M.; Zuk, O.; Carey, B.W.; Cassady, J.P.; et al. Chromatin signature reveals over a thousand highly conserved large non-coding RNAs in mammals. *Nature* **2009**, *458*, 223–227. [[CrossRef](#)] [[PubMed](#)]
13. Gutschner, T.; Diederichs, S. The hallmarks of cancer: A long non-coding RNA point of view. *RNA Biol.* **2012**, *9*, 703–719. [[CrossRef](#)] [[PubMed](#)]
14. Gupta, R.A.; Shah, N.; Wang, K.C.; Kim, J.; Horlings, H.M.; Wong, D.J.; Tsai, M.C.; Hung, T.; Argani, P.; Rinn, J.L.; et al. Long non-coding RNA HOTAIR reprograms chromatin state to promote cancer metastasis. *Nature* **2010**, *464*, 1071–1076. [[CrossRef](#)] [[PubMed](#)]
15. Tsai, M.C.; Manor, O.; Wan, Y.; Mosammaparast, N.; Wang, J.K.; Lan, F.; Shi, Y.; Segal, E.; Chang, H.Y. Long noncoding RNA as modular scaffold of histone modification complexes. *Science* **2010**, *329*, 689–693. [[CrossRef](#)] [[PubMed](#)]

16. Wapinski, O.; Chang, H.Y. Long noncoding RNAs and human disease. *Trends Cell Biol.* **2011**, *21*, 354–361. [[CrossRef](#)] [[PubMed](#)]
17. Ponting, C.P.; Oliver, P.L.; Reik, W. Evolution and functions of long noncoding RNAs. *Cell* **2009**, *136*, 629–641. [[CrossRef](#)] [[PubMed](#)]
18. Zhang, C.G.; Yin, D.D.; Sun, S.Y.; Han, L. The use of lncRNA analysis for stratification management of prognostic risk in patients with NSCLC. *Eur. Rev. Med. Pharmacol. Sci.* **2017**, *21*, 115–119. [[PubMed](#)]
19. Zhang, J.; Lin, Z.; Gao, Y.; Yao, T. Downregulation of long noncoding RNA MEG3 is associated with poor prognosis and promoter hypermethylation in cervical cancer. *J. Exp. Clin. Cancer Res.* **2017**, *36*, 5. [[CrossRef](#)] [[PubMed](#)]
20. Chen, M.; Liu, B.; Xiao, J.; Yang, Y.; Zhang, Y. A novel seven-long non-coding RNA signature predicts survival in early stage lung adenocarcinoma. *Oncotarget* **2017**, *8*, 14876–14886. [[CrossRef](#)] [[PubMed](#)]
21. Liu, T.; Huang, Y.; Chen, J.; Chi, H.; Yu, Z.; Wang, J.; Chen, C. Attenuated ability of bace1 to cleave the amyloid precursor protein via silencing long noncoding RNA bace1as expression. *Mol. Med. Rep.* **2014**, *10*, 1275–1281. [[CrossRef](#)] [[PubMed](#)]
22. Kotake, Y.; Nakagawa, T.; Kitagawa, K.; Suzuki, S.; Liu, N.; Kitagawa, M.; Xiong, Y. Long non-coding RNA ANRIL is required for the PRC2 recruitment to and silencing of *p15^{INK4B}* tumor suppressor gene. *Oncogene* **2011**, *30*, 1956–1962. [[CrossRef](#)] [[PubMed](#)]
23. Yap, K.L.; Li, S.; Munoz-Cabello, A.M.; Raguz, S.; Zeng, L.; Mujtaba, S.; Gil, J.; Walsh, M.J.; Zhou, M.M. Molecular interplay of the noncoding RNA ANRIL and methylated histone H3 lysine 27 by polycomb CBX7 in transcriptional silencing of INK4a. *Mol. Cell.* **2010**, *38*, 662–674. [[CrossRef](#)] [[PubMed](#)]
24. Beckedorff, F.C.; Ayupe, A.C.; Crocci-Souza, R.; Amaral, M.S.; Nakaya, H.I.; Soltys, D.T.; Menck, C.F.; Reis, E.M.; Verjovski-Almeida, S. The intronic long noncoding RNA ANRASSF1 recruits PRC2 to the RASSF1A promoter, reducing the expression of RASSF1A and increasing cell proliferation. *PLoS Genet.* **2013**, *9*, e1003705. [[CrossRef](#)] [[PubMed](#)]
25. Berghoff, E.G.; Clark, M.F.; Chen, S.; Cajigas, I.; Leib, D.E.; Kohtz, J.D. Evt2 (Dlx6as) lncRNA regulates ultraconserved enhancer methylation and the differential transcriptional control of adjacent genes. *Development* **2013**, *140*, 4407–4416. [[CrossRef](#)] [[PubMed](#)]
26. Da Rocha, S.T.; Boeva, V.; Escamilla-Del-Arenal, M.; Ancelin, K.; Granier, C.; Matias, N.R.; Sanulli, S.; Chow, J.; Schulz, E.; Picard, C.; et al. Jarid2 is implicated in the initial XIST-induced targeting of PRC2 to the inactive X chromosome. *Mol. Cell.* **2014**, *53*, 301–316. [[CrossRef](#)] [[PubMed](#)]
27. Shen, L.; Liu, L.; Ge, L.; Xie, L.; Liu, S.; Sang, L.; Zhan, T.; Li, H. miR-448 downregulates MPPED2 to promote cancer proliferation and inhibit apoptosis in oral squamous cell carcinoma. *Exp. Ther. Med.* **2016**, *12*, 2747–2752. [[CrossRef](#)] [[PubMed](#)]
28. Zhang, R.; Shen, C.; Zhao, L.; Wang, J.; McCrae, M.; Chen, X.; Lu, F. Dysregulation of host cellular genes targeted by human papillomavirus (HPV) integration contributes to HPV-related cervical carcinogenesis. *Int. J. Cancer* **2016**, *138*, 1163–1174. [[CrossRef](#)] [[PubMed](#)]
29. Liguori, L.; Andolfo, I.; de Antonellis, P.; Aglio, V.; di Dato, V.; Marino, N.; Orlotti, N.I.; De Martino, D.; Capasso, M.; Petrosino, G.; et al. The metallophosphodiesterase Mpped2 impairs tumorigenesis in neuroblastoma. *Cell Cycle* **2012**, *11*, 569–581. [[CrossRef](#)] [[PubMed](#)]
30. Tamura, M.; Gu, J.; Matsumoto, K.; Aota, S.; Parsons, R.; Yamada, K.M. Inhibition of cell migration, spreading, and focal adhesions by tumor suppressor PTEN. *Science* **1998**, *280*, 1614–1617. [[CrossRef](#)] [[PubMed](#)]
31. Song, M.S.; Salmena, L.; Pandolfi, P.P. The functions and regulation of the PTEN tumour suppressor. *Nat. Rev. Mol. Cell Biol.* **2012**, *13*, 283–296. [[CrossRef](#)] [[PubMed](#)]
32. Sun, H.; Lesche, R.; Li, D.M.; Liliental, J.; Zhang, H.; Gao, J.; Gavrilo, N.; Mueller, B.; Liu, X.; Wu, H. PTEN modulates cell cycle progression and cell survival by regulating phosphatidylinositol 3,4,5-trisphosphate and AKT/protein kinase B signaling pathway. *Proc. Natl. Acad. Sci. USA* **1999**, *96*, 6199–6204. [[CrossRef](#)] [[PubMed](#)]
33. Stambolic, V.; Suzuki, A.; de la Pompa, J.L.; Brothers, G.M.; Mirtsos, C.; Sasaki, T.; Ruland, J.; Penninger, J.M.; Siderovski, D.P.; Mak, T.W. Negative regulation of PKB/AKT-dependent cell survival by the tumor suppressor PTEN. *Cell* **1998**, *95*, 29–39. [[CrossRef](#)]
34. Xu, N.; Lao, Y.; Zhang, Y.; Gillespie, D.A. AKT: A double-edged sword in cell proliferation and genome stability. *J. Oncol.* **2012**, *2012*, 951724. [[CrossRef](#)] [[PubMed](#)]

35. Cabili, M.N.; Trapnell, C.; Goff, L.; Koziol, M.; Tazon-Vega, B.; Regev, A.; Rinn, J.L. Integrative annotation of human large intergenic noncoding RNAs reveals global properties and specific subclasses. *Genes Dev.* **2011**, *25*, 1915–1927. [[CrossRef](#)] [[PubMed](#)]
36. Khalil, A.M.; Guttman, M.; Huarte, M.; Garber, M.; Raj, A.; Rivea Morales, D.; Thomas, K.; Presser, A.; Bernstein, B.E.; van Oudenaarden, A.; et al. Many human large intergenic noncoding RNAs associate with chromatin-modifying complexes and affect gene expression. *Proc. Natl. Acad. Sci. USA* **2009**, *106*, 11667–11672. [[CrossRef](#)] [[PubMed](#)]
37. Livak, K.J.; Schmittgen, T.D. Analysis of relative gene expression data using real-time quantitative PCR and the 2^{-Delta Delta C(T)} method. *Methods* **2001**, *25*, 402–408. [[CrossRef](#)] [[PubMed](#)]
38. Sepe, R.; Formisano, U.; Federico, A.; Forzati, F.; Bastos, A.U.; D'Angelo, D.; Cacciola, N.A.; Fusco, A.; Pallante, P. CBX7 and hmga1b proteins act in opposite way on the regulation of the SPP1 gene expression. *Oncotarget* **2015**, *6*, 2680–2692. [[CrossRef](#)] [[PubMed](#)]
39. Puca, F.; Colamaio, M.; Federico, A.; Gemei, M.; Tosti, N.; Bastos, A.U.; Del Vecchio, L.; Pece, S.; Battista, S.; Fusco, A. Hmga1 silencing restores normal stem cell characteristics in colon cancer stem cells by increasing p53 levels. *Oncotarget* **2014**, *5*, 3234–3245. [[CrossRef](#)] [[PubMed](#)]



© 2018 by the authors. Licensee MDPI, Basel, Switzerland. This article is an open access article distributed under the terms and conditions of the Creative Commons Attribution (CC BY) license (<http://creativecommons.org/licenses/by/4.0/>).